Ecosystem Development

Vol. 2

Initial development of the artificial catchment ‘Chicken Creek’ – monitoring program and survey 2005-2008

Edited by

W. Schaaf, D. Biemelt, R.F. Hüttl

BTU COTTBUS
Research Center
Landscape Development
and Mining Landscapes

Brandenburg University of Technology Cottbus 2010

Ecosystem Development

Vol. 2

This study is part of the Transregional Collaborative Research Centre 38 (SFB/TRR 38) which is financially supported by the Deutsche Forschungsgemeinschaft (DFG, Bonn), the Brandenburg Ministry of Science, Research and Culture (MWFK, Potsdam) and the Brandenburg University of Technology at Cottbus. The authors also thank Vattenfall Europe Mining AG for providing the research site.

Imprint:

Brandenburg University of Technology Cottbus

Konrad-Wachsmann-Allee 6

D-03046 Cottbus

Germany

This series is edited by: Reinhard F. Hüttl

Wolfgang Schaaf

Detlef Biemelt

Werner Gerwin

ISSN: 1867-7800

published online at http://www.tu-cottbus.de/sfb_trr/ecodev.htm

Ecosystem Development, Vol. 2 (2010)

Initial development of the artificial catchment 'Chicken Creek' – monitoring program and survey 2005 - 2008

Content

1. Introduction

Wolfgang Schaaf[1], Werner Gerwin[2]

[1] Brandenburg University of Technology Cottbus, Chair of Hydrology and Water Resource Management

[2] Brandenburg University of Technology Cottbus, Research Center Landscape Development and Mining Landscapes

The increasing complexity of environmental problems, scientific questions and the demand for answers to politicians and society resulted in large efforts to understand and predict ecosystem functions and services. Studies of terrestrial systems have been carried out in forest, agricultural and natural ecosystems from the plot scale to the scale of landscapes (e.g. Campbell et al. 2007; Ellenberg et al. 1986; Fränzle et al 2008).

The analysis of water and element cycling plays a key role in understanding the functioning, stability, elasticity and resilience of ecosystems. The definition of clearly outlined budget areas is critical for this kind of studies. Catchments and watersheds are therefore frequently used as fundamental spatial landscape units (Liken, 1989) offering the opportunity to quantify input parameters as well as the output from the considered system, and to quantify water and element budgets (Neal et al. 2003; Schleppi et al. 1998). Catchments integrate complex processes over several scales and can be treated as dynamic systems (Kirchner 2009) functioning as ´a mirror of the landscape´ or as an organism (Likens & Borman 1995). However, natural catchments are often characterized by a huge complexity and heterogeneity. Therefore, artificially created watersheds at a landscape scale could be an appropriate alternative to overcome these disadvantages. The artificial watershed 'Chicken Creek' (*Volume 1 of this series*, Gerwin et al. 2009a+b) represents a landscape unit characterized by relatively low complexity and well documented initial structures and boundaries. Within the Transregional Collaborative Research Center (SFB/TRR 38) ´Patterns and processes of initial ecosystem development within an artificial catchment´ an intensive monitoring program was established at the main research site ´Chicken Creek´ (Gerwin et al., 2009c). The objective of the project is to investigate the development of an ecosystem beginning at point zero. The monitoring program is inevitable therefore to identify structures and their interactions with processes. Changes in the behaviour of the system can be detected and different phases of the initial ecosystem development will be derived from this data.

Although ´monitoring does not win glittering prizes´ and ´publication is difficult, infrequent and unread´ (Nisbet 2007) the value of high quality long-term monitoring data has been recognized as essential for understanding the functioning of ecosystems. Long-term monitoring of ecosystems has proven to be an important tool to understand the complex interactions and feedback mechanisms of different processes and patterns within the systems, and to predict their future development (Parr et al. 2002). Lovett et al. (2007) make an argument for environmental monitoring studies and state explicitly the importance of these investigations. They reviewed different long-term observations, such as the Hubbard Brook Experimental Forest, and conclude that "careful, structured observation is as fundamental to science as is hypothesis testing" (p. 254). The International Long-Term Ecological Research (ILTER) Network was established with more than 20 countries contributing a large number of monitoring sites (Waide et al. 1998). Recently, several new networks are emerging such as the National Ecological Oberservatory Network (NEON, Pennisi 2010), the Critical Zone Exploration Network (CZEN, http://www.czen.org/), the WATERS network in the USA (http://www.watersnet.org/) or the Biodiversity Exploratories and the Terrestrial Environmental Observatoria (TERENO, Bogena et al. 2006) in Germany.

Generally, the catchment can be divided into three major sections: (1) the backslope area which covers most of the site, (2) the footslope with a steeper inclination, and (3) the pond basin with the single outlet of the watershed (Fig. 1.1). The site is fenced in completely to avoid disturbance and vandalism particularly by human visitors but also by the abundant game animals of this area.

In a first step the site was subdivided by a regular grid of 20 x 20 m using precise GPS technique. Each grid point was marked by a small flag for a permanent easy orientation within the catchment with rows in NE-SW direction numbered from 1 to 7 and rows in NW-SE direction labeled with A to V (cf. Fig. 1.2).

Within the catchment monitoring of environmental parameters is carried out to measure meteorological (cf. Chapter 2), hydrologic (cf. Chapter 4) and soil conditions (cf. Chapters 5-6) as well as deposition inputs (cf. Chapter 3). As the grid samples proved the Quaternary substrate to be relatively homogenous both spatially and with depth, all installations were oriented along the basic 20x20 m grid. Fig. 1.2 gives an overview of the installations within the catchment.

In addition to these permanent installations other measurements, records and samplings are carried out with respect to vegetation (cf. Chapter 7), soil fauna (cf. Chapter 8) and limnology (cf. Chapters 9+10). These more biological monitoring programmes are summarized in Fig. 1.3.

This report summarizes the monitoring installations and activities, covering various aspects and compartments of the catchment system from meteorology and hydrology, soil and soil solution chemistry, vegetation and soil fauna to limnology and surface patterns, as well as results of the measurements for the period 2005 to 2008. This volume is the beginning of a series with results of the ongoing Chicken Creek monitoring program, which is funded by the Brandenburg Ministry of Science, Research and Culture (MWFK).

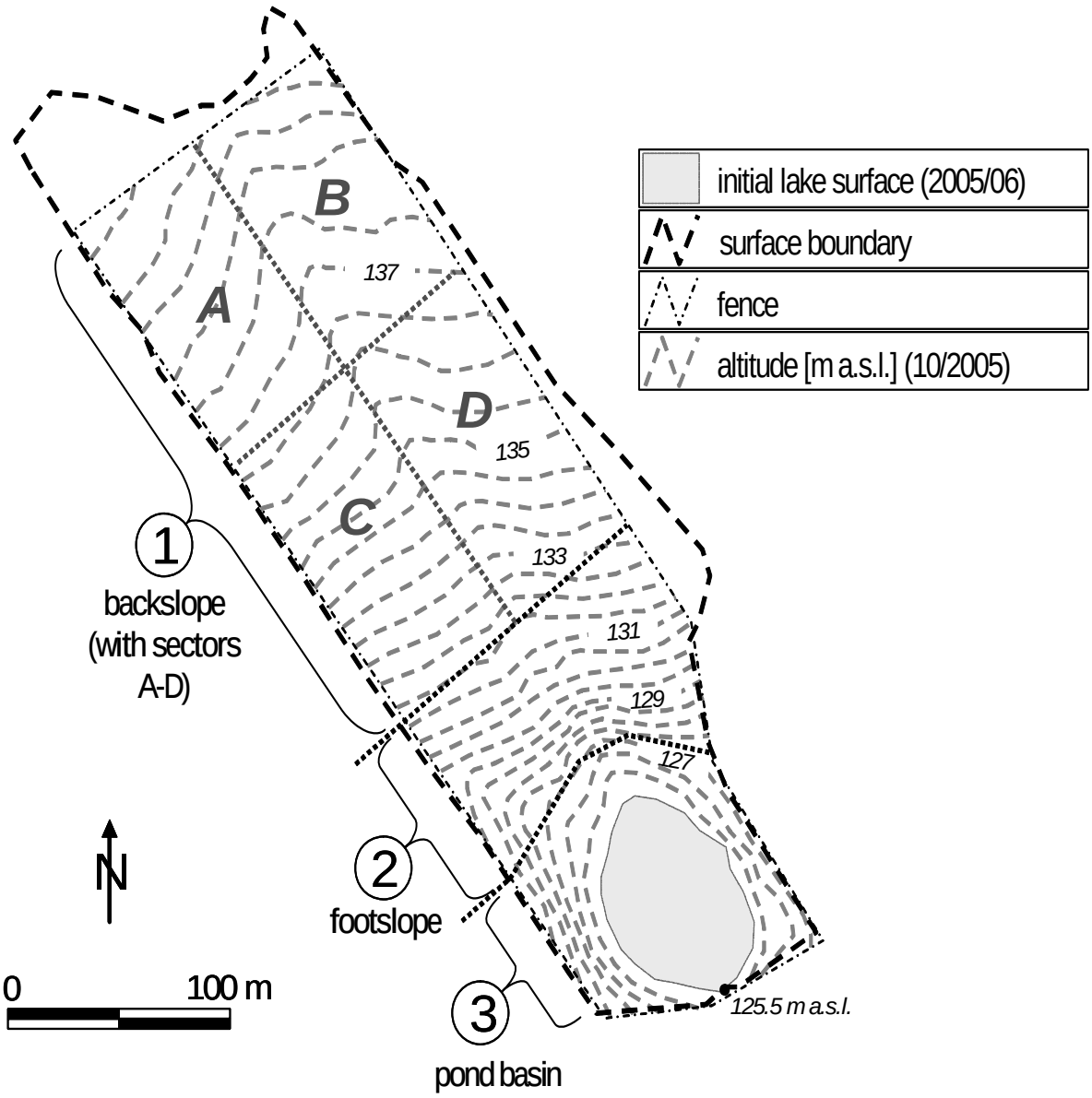

Fig. 1.1: Map of the artificial catchment Chicken Creek.

Fig. 1.2: Overview over grid points and monitoring installations at ´Chicken Creek´.

Fig. 1.3: Overview over the biological monitoring programme at ´Chicken Creek´.

References

Bogena, H., Schulz, K., Vereecken, H., 2006: Towards a network of observatories in terrestrial environmental research. Adv. Geosci. 9, 109-114.

Campbell, J.L., Driscoll, C.T., Eagar, C., Likens, G.E., Siccama, T.G., Johnson, C.E., Fahey, T.J., Hamburg, S.P., Holmes, R.T., Bailey, A.S., Buso, D.C., 2007: Long-term trends from ecosystem research at the Hubbard Brook Experimental Forest. Gen. Tech. Rep. NRS-17. Newtown Square, PA: U.S. Dept. Agriculture, Forest Service, Northern Research Station.

Ellenberg, H., Mayer, R., Schauermann, J., 1986: Ökosystemforschung; Ergebnisse des Sollingprojektes 1966-1986, Ulmer, Stuttgart.

Fränzle, O., Kappen, L., Blume, H.-P., Dierssen, K., (Eds) 2008: Ecosystem Organization of a Complex Landscape; Long-term Research in the Bornhöved Lake District, Germany. Ecological Studies, 202, Springer, Berlin, Heidelberg.

Gerwin, W., Schaaf, W., Biemelt, D., Fischer, Q., Winter, S., Hüttl, R. F., 2009a: The artificial catchment “Chicken Creek” (Lusatia, Germany) - A landscape laboratory for interdisciplinary studies of initial ecosystem development. Ecol. Eng. doi:10.1016/ j.ecoleng.2009.09.003.

Gerwin, W., Raab, T., Biemelt, D., Schaaf, W., Bens, O., Hüttl, R.F., 2009b: The artificial water catchment "Chicken Creek" as an observatory for critical zone processes and structures. Hydrol. Earth Syst. Sci. Discuss., 6, 1769-1795.

Gerwin, W., Schaaf, W., Biemelt, D., Fischer, Q., Winter, S., Veste, M., Hüttl, R. F., 2009c: Ecological monitoring at the artificial watershed Chicken Creek (Germany). Physics and chemistry of the Earth (submitted).

Kirchner, J. W., 2009: Catchments as simple dynamic systems: catchment characterization, rainfall-runoff modelling, and doing hydrology backward. Water Resour. Res. 45. W02429, doi: 10.1029/2008WR006912.

Likens, G. E., 1989: Long-Term Studies in Ecology. New York.

Likens, G. E. and Bormann, F. H., 1995: Biogeochemistry of a forested ecosystem. Springer, New York. 159 p.

Lovett, G.M., Burns, D.A., Driscoll, C.T., Jenkins, J.C., Mitchell, M.J., Rustad, L., Shanley, J.B., Likens, G.E. and Haeuber, R., 2007: Who needs environmental monitoring? Front. Ecol. Environ., 5, 253-260.

Neal, C., Reynolds, B., Neal, M., Hill, L., Wickham, H., Pugh, B., 2003: Nitrogen in rainfall, cloud water, throughfall, stemflow, stream water and groundwater for the Plynlimon catchments of mid-Wales. Sci. Total Enviro., 314-316, 121-151.

Nisbet, E., 2007: Cinderella science. Nature 450, 789-790.

Parr, T.W., Ferretti, M., Simpson, I.C., Forsius, M., Kovacs-Lang, E., 2002: Towards a long-term integrated monitoring programme in Europe: Network design in theory and practice. Environ. Monit. Assess., 78, 253-290.

Pennisi, E., 2010: A groundbreaking observatory to monitor the environment. Science 328, 418-420.

Schleppi, P., Muller, N., Feyern, H., Papritz, A., Bucher, J.B., Flühler, H., 1998: Nitrogen budgets of two small experimental forested catchments at Alptal, Switzerland. Forest Ecol. Manag., 101, 177-185.

Waide, R., French, C., Sprott, P., Williams, L., 1998: The International Long Term Ecological Research Network 1998. US LTER Network, Department of Biology, University of New Mexico.

2. Meteorology

Detlef Biemelt[1], Rossen Nenov[2]

[1]Brandenburg University of Technology Cottbus, Chair of Hydrology and Water Resource Management

[2]Brandenburg University of Technolgy Cottbus, Research Center Landscape Development and Mining Landscapes

2. 1 Introduction

The weather conditions define fundamental fluxes of energy and water at the upper boundary of the Chicken Creek catchment. Weather influences the development of flora and fauna, the fluxes of water and elements, the flow paths and the soil.

The closest climate station of the German Meteorological Service is located in Cottbus, approximately 20 km away from the Chicken Creek catchment. Data from this climate station can be used for the climatologic assessment of separate measurement periods in terms of e.g. warmer or colder than normal and more humid or drier than normal.

Two weather stations operate in the catchment. Weather station 1 is used for the registration of basic data. Weather station 2 provides more detailed data. It also increases the data security with regard to quality of the measured data and the prevention of data loss.

Weather station 2 registers the data in shorter time intervals. Wind speed, air temperature and humidity are measured at 3 elevations above ground. Downward and upward directed as well as short-wave and long-wave radiation components are measured separately. Soil heat flux is also registered. In addition to the measurement at 1 m height above ground, precipitation is also measured at the soil surface.

2. 2 Materials and methods

Weather station 1 (Fig. 2.1) measures basic meteorological parameters with time resolution of 1 hour since September 25th, 2005 and is located in the upper eastern part of the catchment (near grid point C6). The measured parameters are listed in Tab. 2.1. The sensors and the logger are produced by A. Thies GmbH Germany, Göttingen (THIES Klima, www.thiesclima.com). All data are saved on the internal logger and can be transferred manually to the database using a memory card. The data are available in separate files (text-format, “Excel”-format) with hourly, daily and monthly resolution.

Fig. 2.1: Weather station 1.

Fig. 2.2: Weather station 2.

Weather station 2 (Fig. 2.2) measures also specific meteorological parameters with a time resolution of 10 minutes since February 26th, 2008. The weather station is located in the lower part of the catchment. These data are transferred daily by GSM Modem to a data server and they include a webcam photo which is available online on the homepage (http://www.tu-cottbus.de/BTU/Innov/SFB/index.htm).

In addition to the directly measured data daily values of corrected precipitation and potential evapotranspiration are calculated. Richter (1995) suggested a correction factor (P_{cor}) for the measured daily sums of precipitation, which takes into account the wind-induced error and the losses due to evaporation and initial wetting of the rainfall gauge (Eq. 2.1).

$$P_{cor} = P + b \cdot P^{\varepsilon} \tag{2.1}$$

The values of the coefficients ε and b depend on the precipitation type. The coefficient b considers the influence of the wind depending on the distance of the rainfall gauge to obstacles like trees or buildings. If the precipitation type is unknown, it can be defined through air temperature.

Tab.2.1: Explication of weather data sampling

Station	measure	sensor type	measuring hight or depth	frequency f measurement	method / frequency of save	unit
1	wind direction	THIES wind direction transmitter “compact”	2 m	1 min	mean / 1 hour	°
	wind speed	THIES wind transmitter “compact”	2 m	1 min	mean / 1 hour	m s^{-1}
	air temperature	THIES temperature and humidity sensor “compact” with radiation protection case unventilated	2 m	1 min	mean / 1 hour	°C
	humidity		2 m	1 min	mean / 1 hour	%
	global radiation	Pyranometer CM3 0,305-2,8 µm	2 m	1 min	sum / 1 hour	Wh m^{-2} h^{-1}
	precipitation	tipping bucket, 200 cm²	1 m	1 hour	sum / 1 hour	mm h^{-1}
	precipitation	Hellmann precipita-tion sampler, 200 cm²	1 m	manually monthly	sum / sample interval	mm
	soil temperature	Pt 100	-0,05 m	1 min	mean / 1 hour	°C
		Pt 100	-0,10 m	1 min	mean / 1 hour	°C
2	wind speed	THIES wind transmitter “compact”	0,5 m, 2 m, 10 m	1 min	mean / 10-minutes	m s^{-1}
	air temperature	Hydroclip S3 temperature and humidity sensor with radiation protection case unventilated	0,5 m, 2 m, 10 m	1 min	mean / 10-minutes	°C
	humidity		0,5 m, 2 m, 10 m	1 min	mean / 10-minutes	%
	soil temperature	Pt 100	-0,05 m	1 min	mean / 10-minutes	°C
		Pt 100	-0,10 m	1 min	mean / 10-minutes	°C
	soil heat flux	HFP01	-0,2 m	1 min	sum / 10-minutes	Wh m^{-2} h^{-1}
	precipitation	Hellmann precipita-tion sampler, 200 cm²	1 m	manually monthly	sum / sample interval	mm
	snow high/ Pan evaporation	Class A Evaporation tank with UPM-8 ultrasonic level sensor	0 m	1 hour	sum / hour	mm

The potential evapotranspiration in the form of the grass reference evapotranspiration for daily time steps is suggested as a composite climate parameter (Eq. 2.2). This provides a standard measure of the energy available for evaporation (Allen, et al., 1994).

$$PET_{GRASS} = g(T,u) * (\frac{R_n}{L} + f(T) * u_2 (1 - \frac{RH}{100})) , \quad (2.2)$$

where $f(T) = \frac{e_S(T)}{s} * \frac{\gamma * 90}{T + 273}$ and $g(T,u) = \frac{s}{s + \gamma * (1 + 0.34 * u_2)}$.

u_2	daily average wind speed at 2 m height above ground in m/s,
RH	daily average relative air humidity in %.
s	slope of the saturation vapour pressure curve in hPa K^{-1},
γ	psychrometric constant in hPa K^{-1},
L	specific heat of vaporization in W m^{-2} mm^{-1},
R_n	daily average net radiation in W m^{-2}
T	daily average air temperature at 2 m height above ground in K

In order to characterize the water budget of an area, the climatic water balance can be used, which is the difference between the corrected precipitation amount and the potential evapotranspiration. Best results were achieved after a calibration based on discharge measured at a number of water catchments in the Federal State of Brandenburg. The calibration yielded a factor of 1.1 for the grass reference evapotranspiration (Eq. 2.3, Lahmer et al. 2000).

$$KWB = P_{cor} - 1.1 \cdot PET_{Grass} \quad (2.3)$$

The temperature in the soil is additionally measured in the depths 10 cm, 30 cm, 50 cm and 80 cm from the four soil shafts (cf. Capture 7.2) with electrical PT100 resistance thermometers and logged together with the soil water contents and the tensions.

2. 3 Results and discussion

According to Heyer (1993) Germany is located in the temperate seasonal climate in with westerly winds predominate. Böer (1996) and Grosser (1998) assign the region of Lusatia to the continental area of the North German Plain. Heyer (1962) divides the climate of the Federal State of Brandenburg into 5 zones. According to this the research area Chicken Creek belongs to the "Lowland climate of the North and the midaltitudes of the Southwest and the South with annual sums of precipitation amount between 540 and 600 mm".

The average annual air temperature at the climate station Cottbus is 9.3°C and the average annual precipitation amount is 559 mm for the period 1971 – 2000. The average climatic water balance of the hydrologic years from November 1st, 1971 to October 31st, 2000 amounts to -49 mm. According to this there is on average an excess of available energy considering the water supply by precipitation. The fluctuation behaviour of some climate elements is clearly illustrated by the observed extremes (Tab. 2.2).

Tab. 2.2: Weather extremes from Cottbus

	temperature		precipitation highest			precipitation lowest	snow cover
	highest	lowest	Daily	monthly	yearly	yearly	highest
value	39.4 °C	-29.5 °C	130 mm	244 mm	865 mm	335	41 cm
date	Aug 20th, 1943	Feb 11th, 1929	Aug 8th, 1978	Aug, 1948	1974	1976	Mar 4th, 1943

Data from weather station 1 from the beginning of the measurements until 31.12.2008 are used for the following analysis.

Monthly values of air temperature, precipitation amount and climatic water balance are shown for each separate year (Fig. 2.3, 2.4, 2.6) in order to characterize the weather conditions during the ongoing development of the Chicken Creek catchment. The long-standing average values from the climate station Cottbus are added for comparison.

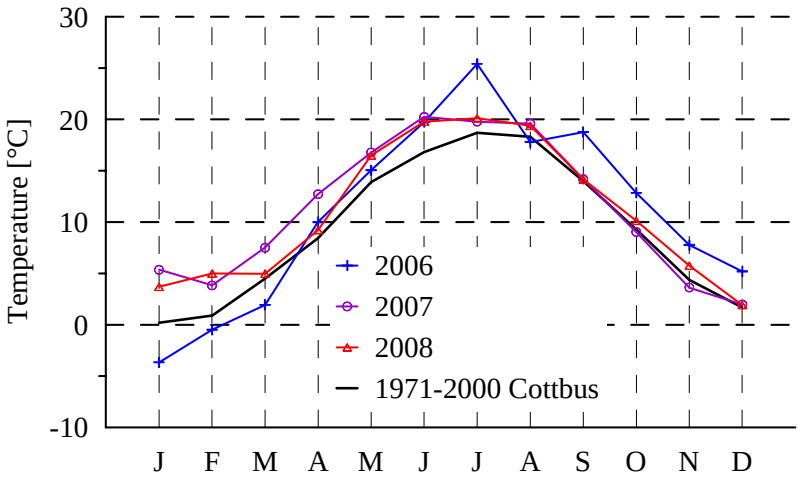

Fig. 2.3: Monthly mean temperatures from the “Chicken Creek” Catchment and long time monthly mean temperatures from Cottbus.

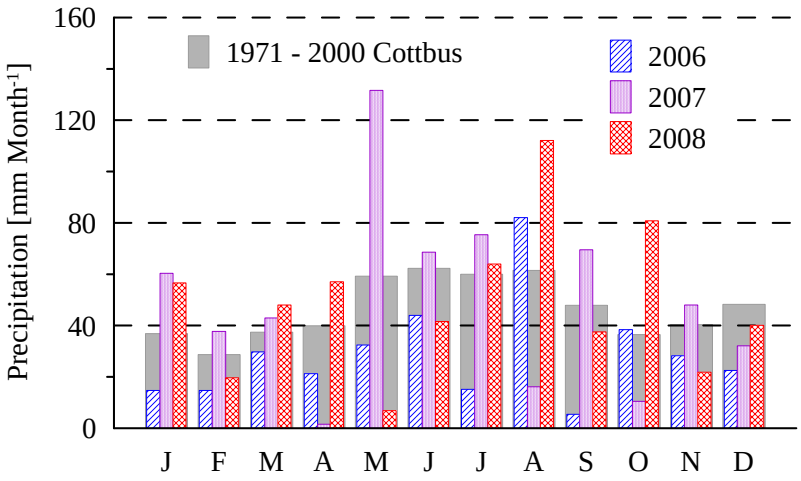

Fig. 2.4: Monthly sums of precipitation from the “Chicken Creek” Catchment and long time monthly mean sums of precipitation from Cottbus.

January, February and March 2006 were relatively cold months (Fig. 2.3), whereas July, September, October, November and December 2006 were relatively warm. The months from January until April 2007 and January and February 2008 were relatively warm. The months from May until December of the years 2007 and 2008 had very similar monthly average temperatures.

The annual average air temperatures of the years 2006, 2007 and 2008 for the Chicken Creek catchment were 10.9 °C, 11.2 °C and 10.9 °C respectively. Based on the comparison of the annual mean air temperatures in Cottbus (9.8 °C, 11.3 °C and 10.3 °C) and the long-term annual average of 9.3 °C, these 3 years classify as relatively warm.

The highest air temperature measured so far in the catchment was 39.4 °C (July 16th, 2007). The lowest air temperature was -19.7 °C (January 23rd, 2007). 2006 had the highest amount of freezing days and, the longest growing period (days with air temperature >5 °C) as well as the longest main growing period (days with air temperature >10 °C) of the 3 years of monitoring until now (Tab. 2.3).

Fig. 2.4 shows the monthly sums of precipitation. Typical of the west-wind-zone is the strong variation from one month to another and from year to year. The smallest monthly sum of precipitation until now (1.6 mm) and the highest monthly sum (132 mm) occurred in two successive months – April and May 2007. The monthly sum of precipitation in April 2007 at the climate station Cottbus was 1.9 mm and in May 2007 it was 185 mm. Thus, April 2007 has been the April with the lowest precipitation since 1961 and May 2007 has been the May with the highest precipitation since 1961 at the climate station Cottbus.

Tab. 2.3: Weather extremes in the „Chicken Creek" catchment

Year	Temperature		Number of days with temperature			Precipitation	
	lowest	highest				highest hourly	highest daily
	[°C]	[°C]	<0 °C	>5 °C	>10 °C	[mm hour^{-1}]	[mm day^{-1}]
2006	-19,7	37,2	79	224	137	14,6	14,8
2007	-9,3	39,4	39	218	133	24,8	32,4
2008	-8,7	34,1	39	220	132	19,1	24,4

The annual sums of precipitation for the Chicken Creek catchment for 2006, 2007 and 2008 were 349 mm, 595 mm and 587 mm respectively. The highest hourly and the highest daily precipitation amount (24.8 mm and 32.4 mm respectively) occurred during a storm event on May 27th, 2007 (Tab. 2.3). The relatively small differences between the maximum hourly and the maximum daily precipitation amounts (Tab. 2.4) suggest that high precipitation amounts are often associated with short precipitation events with high intensity. However, the distribution of the hourly precipitation intensities shows that the intensity is below 1 mm/hour in 84 % of all precipitation hours (Fig. 2.5).

The annual sums of the climatic water balance amounts to -427 mm, -225 mm and -131 mm for the hydrologic years 2006, 2007 and 2008, respectively (Fig. 2.6). This negative or extremely negative balance indicates a clear excess of available energy over available water. In all 3 years the cumulative climatic water balance became negative in June.

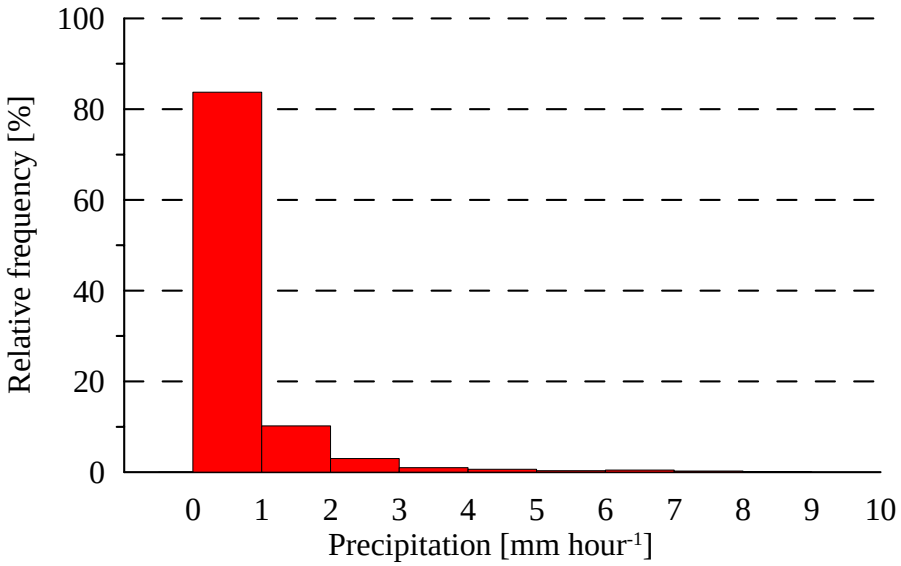

Fig. 2.5: Relative frequency of hourly precipitation intensities from the “Chicken Creek” Catchment.

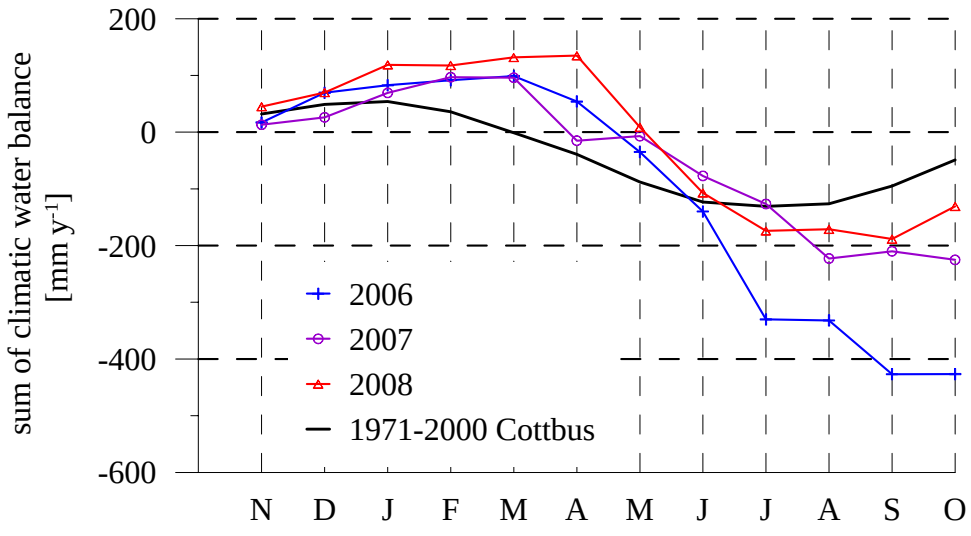

Fig. 2.6: Monthly climatic water balance from the “Chicken Creek” Catchment and long time monthly mean climatic water balance from Cottbus cumulated for hydrological years.

Fig. 2.7 shows the relative frequencies of hourly values of the wind direction in 30 degree classes for the Chicken Creek catchment. The analysis is based on 30384 hourly values sampled from September 29th, 2005 to March 18th, 2009. The results are in good agreement with the general main wind direction west-south-west for Lusatia (Gerth & Christoffer 1994).

In Fig. 2.8 are presented time series of the soil temperature for the depths 10 cm, 30 cm, 50 cm and 80 cm using the example of soil shaft C. The run of the curves shows the customary course with decreasing temperature with depth by trend in summer and increasing temperature with depth by trend in winter. The soil temperature is clearly controlled by the air temperature. The amplitudes of the air temperature fluctuations go on in a damped form with depth.

The results presented here convey a general impression of the meteorological boundary conditions since the construction of the Chicken Creek catchment. In addition, the data base provides the opportunity to analyse specific task-oriented problems in the short-term.

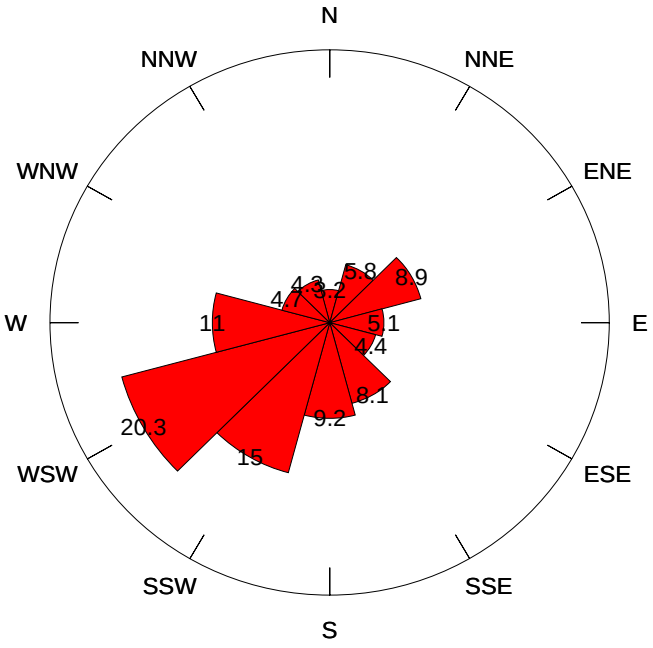

Fig. 2.7: Relative frequency of wind direction from the “Chicken Creek” Catchment.

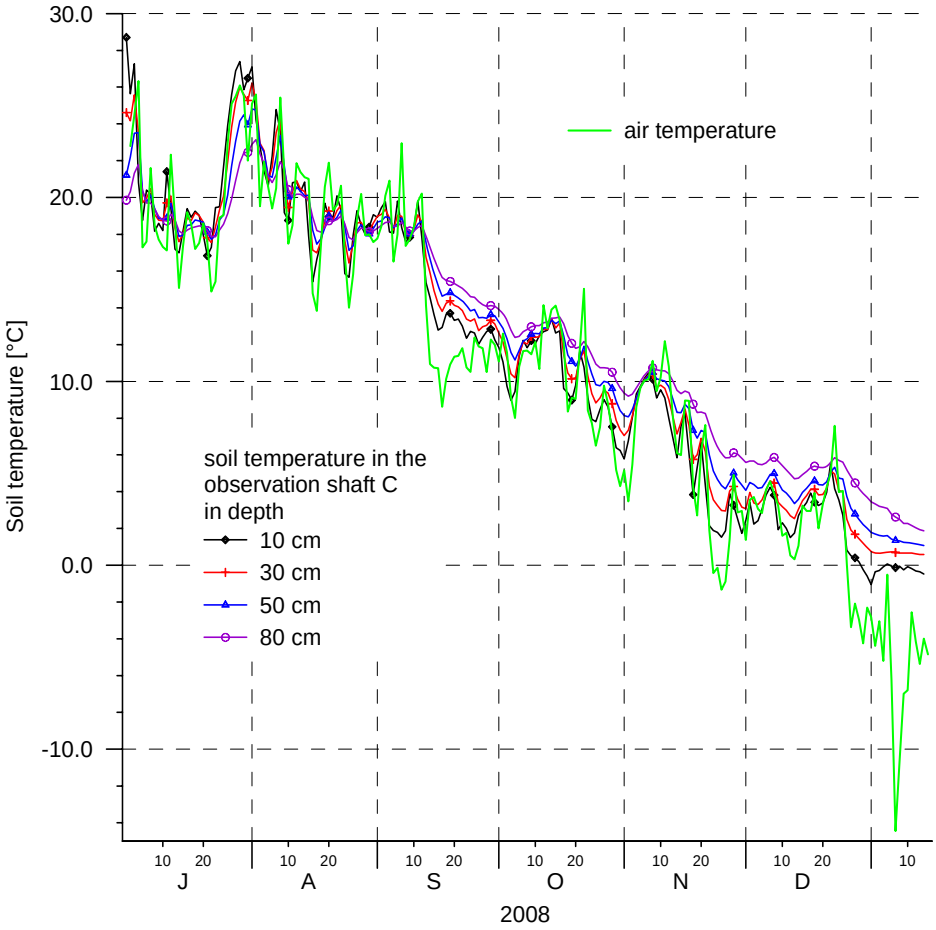

Fig. 2.8: Soil temperature courses for observation pit C.

References

Allen, R. G., Smith, M., Perrier, A. and Pereira, L., 1994: An update for definition of reference evapotranspiration. ICID Bulletin 43, No. 2, 1-34.

Böer, W., (1966): Vorschlag zur Einteilung des Territoriums der DDR in Gebiete mit einheitlichem Großklima, Z. Meteorol. 17, 267-275.

Gerth, W.-P. and Christoffer, J. (1994): Windkarten von Deutschland. Meteorologische Zeitschrift, N.F. 3, 67-77.

Gugla, G., Jankiewicz, P., Wendling, U., Klämt, A., Golf, W., Bernhofer, C., Günther, R., Menzel, L., Miegel, K. and Olbrisch, H.-D., 2001: Verdunstung in Bezug zu Landnutzung, Bewuchs und Boden. Merkblatt ATV-DVWK-M 504, ISBN 3-936514-03-8, 140 S.

Lahmer, W., Dannowski, R., Steidl, J. and Pfützner B., 2000: Flächendeckende Modellierung von Wasserhaushaltsgrößen für das Land Brandenburg. Studien und Tagungsberichte des Landes Brandenburg, Band 27, 77 S.

Grosser, K.H., 1998: Der Naturraum und seine Umgestaltung. In: Pflug, W. (Ed.): Braunkohletagebau und Rekultivierung. Springer Verlag Berlin, S. 461-474.

Heyer, E., 1993: Witterung und Klima. Teubner Verlagsgesellschaft Stuttgart, 344 S.

Heyer, E., 1962: Das Klima des Landes Brandenburg, Abh. Des Meteorol. u. Hydrol. Dienstes der DDR, Nr. 64.

Richter, D., 1995: Ergebnisse methodischer Untersuchungen zur Korrektur des systematischen Messfehlers des Hellmann-Niederschlagsmessers, Berichte des Deutschen Wetterdienstes 194, Offenbach, 93 S.

3. Atmospheric deposition

Maik Veste[1], Wolfgang Schaaf [2]

[1] Brandenburg University of Technology Cottbus, Research Center Landscape Development and Mining Landscapes

[2] Brandenburg University of Technology Cottbus, Chair of Soil Protection and Recultivation

3. 1 Introduction

Atmospheric deposition is an important input pathway for elements into ecosystems (Littmann 1994, Ihle 2001, Schaaf 2004). In initial ecosystems on quaternary material nutrient availability is a limiting factor for primary production. In this context, atmospheric input might be an important source for nutrient for the vegetation of the artificial watershed Chicken Creek. In Central and Northern Europe the high atmospheric nitrogen deposition can influence development of ecosystems. In nutrient-limited ecosystems, like dry grassland ecosystems, atmospheric nitrogen import have a large impact on primary productivity and can modify species composition, vegetation dynamics and the direction of succession (Bakker and Berendse 1999).

To provide information about the atmospheric deposition within the monitoring project, bulk deposition is sampled in a grid-design on the catchment. The gathered data will provide the annual element input into the ecosystem (Gast et al. 2001, Gast 2003, Schaaf 2004).

3. 2 Material and Methods

Sampling of bulk and dry deposition was carried out at the experimental site with 18 open bulk deposition samplers at 1 m above-ground (Fig. 3.1) located at the grid points C2, C4, C6, F2, F4, F6, I2, I4, I6, L2, L4, L6, N2, N4, N6, P2, P4, P6. Sampling started in July 2007. The samplers were made of two 2 liter receptors and collectors polyethylene bottles. The exposed area of the collector is 115 cm^2 and the collector aperture is covered by a plastic ball to prevent evaporation from the bulk sampler. The bottle is mounted in PVC pipe topped by a metal bird perch. The samples were collected at 2-weekly intervals. Samples are immediately analyzed for pH and electrical conductivity (WTW Inolab 740) and stored in a fridge at +4°C until further analysis. The samples are analyzed for concentrations of Ca^{2+}, Mg^{2+}, Na^{+}, K^{+}, Fe^{3+}, Al^{3+} (ICP-OES Unicam 701 and Thermo Scientific iCAP 6000), NO_3^{-}, SO_4^{2-}, Cl^{-} (IC Dionex 5000), NH_4^{+} (Rapid Flow Analyzer Alpkem), DOC and TOC (Shimadzu TOC-5000 and VCPH+TNM-1). Annual bulk deposition was derived from the ion concentrations and the corresponding rainfall amounts in the deposition samplers.

Fig. 3.1: Bulk deposition sampler.

3. 3 Results and discussion

The precipitation amount measured with the bulk deposition samples showed considerable differences to the rainfall amount recorded with the rainfall gauges at the weather stations (see Chapter 2). The mean precipitation in the bulk samplers during the measuring period July 10th, 2007 to December 16th, 2008 was 1145 mm, while 879 mm was recorded at weather station 1 with the automatic rain gauge. This variance can be explained by differences of the design of the used samplers, the windfield around the receptor and technical problems of the rain gauge during winter due to freezing. No distingued spatial rainfall pattern could be observed over the 18 samplers. The measured pH -values at Welzow varied between 4.1 and 6.9 and the electric conductivity between 14 and 118 µS cm^{-1} (Fig. 3.2). Major cations in the bulk deposition are K^+, Na^+, Mg^{2+} and Ca^{2+} (Fig. 3.3). The annual deposition of 2008 is shown in Tab. 3.1. The samples were analysed for Al^{3+} und Fe^{3+}, however, both elements were under the detection limits. Seasonal variations of concentration of anions (NH_4^+, NO^-, SO^{2-}, Cl^-) are shown in Fig. 3.4. Especially, the NO_3^--concentration and deposition showed a sesonal variation in 2008 and increased drasticly in summer 2008 (Fig. 3.4 C). Local agricultural sources and harvesting could be an explaination for the seasonal variation of the N-deposition (Littmann 1994). However, only a data analysis of long-term records can confirm such varitions. The caculated annual N-deposition in 2008 is 20.4 kg ha^{-1} a^{-1} (Tab. 3.1) and corresponds to other results from Brandenburg with 12 - 19 kg ha^{-1} a^{-1} (Gast 2003, Schaaf 2004) and 21 kg ha^{-1} a^{-1} (Volz 1995), respectively.

Matschullat et al. (2000) measured in the bulk deposition in the Erzgebirge at open fields NH_4^+ concentrations of 0.84 mg l^{-1} and for NO_3^- 2.67 mg l^{-1} at the end of the 1990s. The region south-east of Berlin is characterised by relative high sulphur and nitrogen deposition (Wellbrock et al. 2005). From the viewpoint of ecosystem development, the amont of nitrogen deposition is regarded as critical load for nutrient poor ecosystems like heathland ecosystems (Bakker and Berendse 1999, Ihlig 2001).

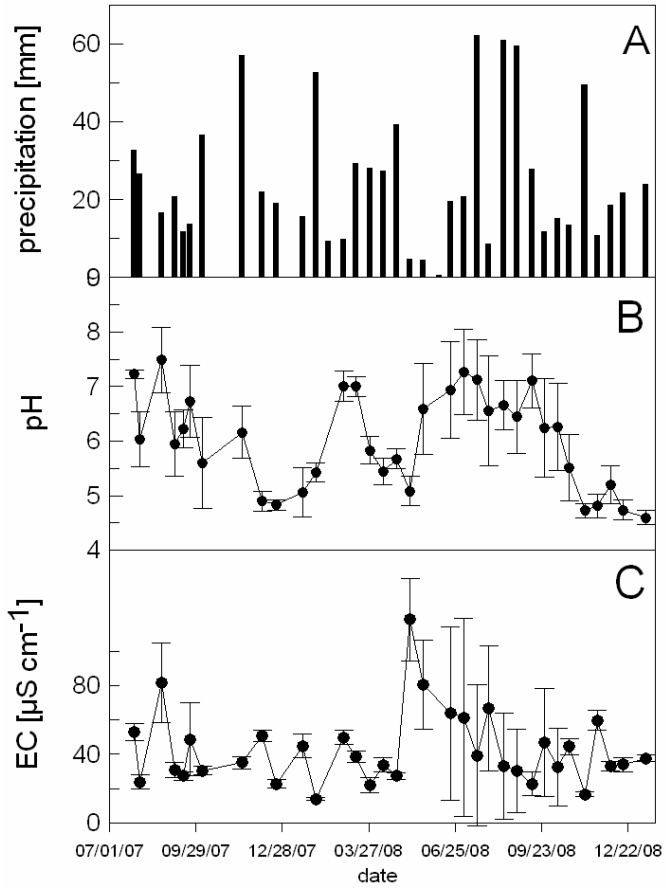

Fig. 3.2: Precipitation, pH and electric conductivity (EC) of the bulk depoition between July 10th, 2007 and December 16th, 2008.

Tab. 3.1: Median of element concentration and of annual bulk deposition at Chicken Creek in 2008.

ions	concentration [mg l^{-1}]		deposition [kg ha^{-1} a^{-1}]
Ca^{2+}	1,3	Ca	7,4
Mg^{2+}	0,2	Mg	1,2
Na^{+}	0,87	Na	5,6
K^{+}	0,18	K	2,4
Cl^{-}	1,59	Cl	7,6
NH_4^{+}	2,4	NH_4-N	11,8
NO_3^{-}	7,72	NO_3-N	8,6
SO_4^{2-}	5,6	SO_4-S	14,7
DOC	2,81	DOC	17,0
TOC	2,13	TOC	18,1

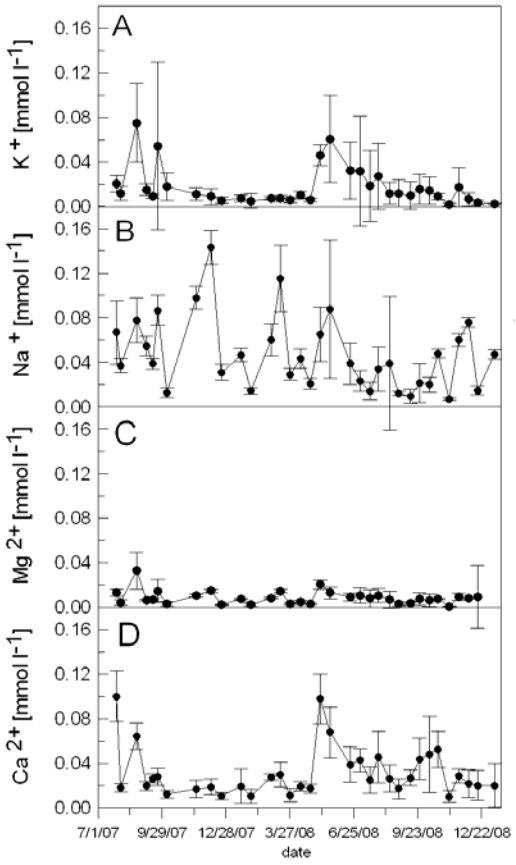

Fig 3.3: Cation concentrations in bulk deposition between July 10th, 2007 and December 16th, 2008.

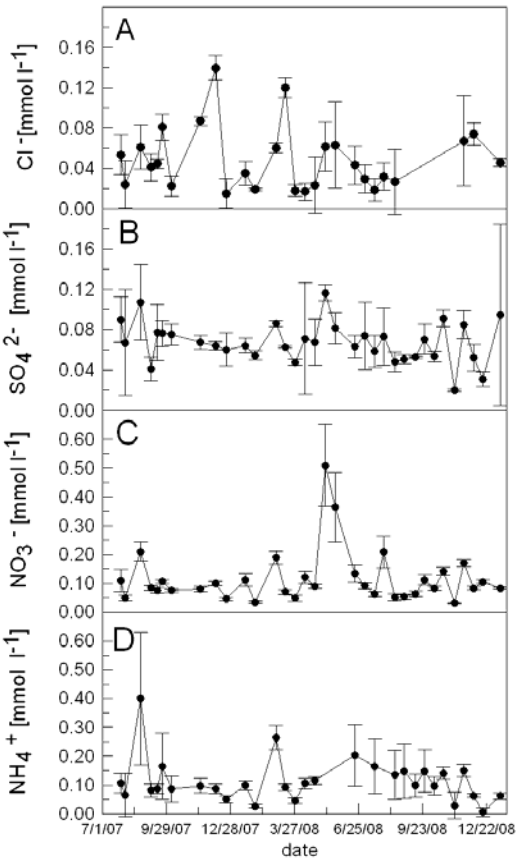

Fig.3.4: Anion concentrations in bulk deposition of between July 10th, 2007 and December 16th, 2008.

References

Bakker J. P. and Berendse, F., 1999. Constraints in the restoration of ecological diversity in grassland and heathland communities. Trends in Ecology & Evolution 14, 63-68.

Gast, M., 2003. Entwicklung des Stoffhaushalts von Kiefernökosystemen auf kohle- und pyrithaltigen Kippsubstraten des Lausitzer Braunkohlereviers. Cottbus Schriften zu Bodenschutz und Rekultivierung, Band 20.

Gast, M., Schaaf, W., Wilden, R., Scherzer, J., Schneider, B. U. and Hüttl, R. F., 2001. Water and element budgets of pine stands on lignite and pyrite containing mine soils. Journal of Geochemical Exploration 73, 63-74.

Ihle, P. (Hrsg.), 2001. Atmosphärische Deposition in der Bundesrepublik Deutschland. Teubner, Stuttgart, Leipzig, Wiesbaden.

Matschullat, J., Maenhaut, W., Zimmermann, F. And Fiebig, J., 2000. Aerosol and bulk deposition trends in the 1990s, Eastern Erzgebirge, Central Europe. Atmospheric Environment 34: 3213-3221.

Littmann, T., 1994. Immissionsbelastungen durch Schwebstaub und Spurenstoffe im ländlichen Raum Nordwestdeutschlands. Bochumer Geographische Arbeiten 59.

Schaaf, W., 2004. Development of element cycling in forest ecosystems after anthropogenic disturbances – case studies at long-term atmospheric polluted and at post-mining sites. Cottbus Schriften zu Bodenschutz und Rekultivierung, Band 24.

Volz, H.A., 1995. 10 Jahre Depositionsmessungen in deutschen Wälddern - eine Synopse. Forst und Holz 16, 483-488.

Wellbrock, N., Rick, W. and Wolff, B., 2005. Characterisation of and changes in the atmospheric deposition situation in German forest ecosystems using multivariate statistics. European Journal of Forest Research 124, 261-271.

Acknowledgements

We thank Ralph Dominik, Marin Dimitrov, Gunter Baumann and Silvio Vogt for their help with the field work. Thanks to Gabi Franke, Regina Müller, Helga Köller, Evi Müller and Anita Maletzki for the analysis of the samples together with Nonka Markova and Tzvetelina Dimitrova.

4. Hydrology and water quality

Detlef Biemelt [1], Wolfgang Schaaf [2], Kai Mazur [1]

[1] Brandenburg University of Technology Cottbus, Chair of Hydrology and Water Resource Management

[2] Brandenburg University of Technology Cottbus, Chair of Soil Protection and Recultivation

4. 1 Introduction

The site conditions at the artificial catchment Chicken Creek were designed to allow process oriented catchment modelling and multi response validation (Gerwin et al. 2009).

The conceptual model for the determination of components of the water budget for the catchment is given in Fig. 4.1. The directly measurable paths are equipped with instruments (see Chapter 4.2). Evapotranspiration, interflow and groundwater recharge are determined from state variables by using specific model conceptions. Matrix potential and soil moisture are used to determine evapotranspiration and groundwater recharge (cf. Chapter 6). Groundwater flow is determined from groundwater levels.

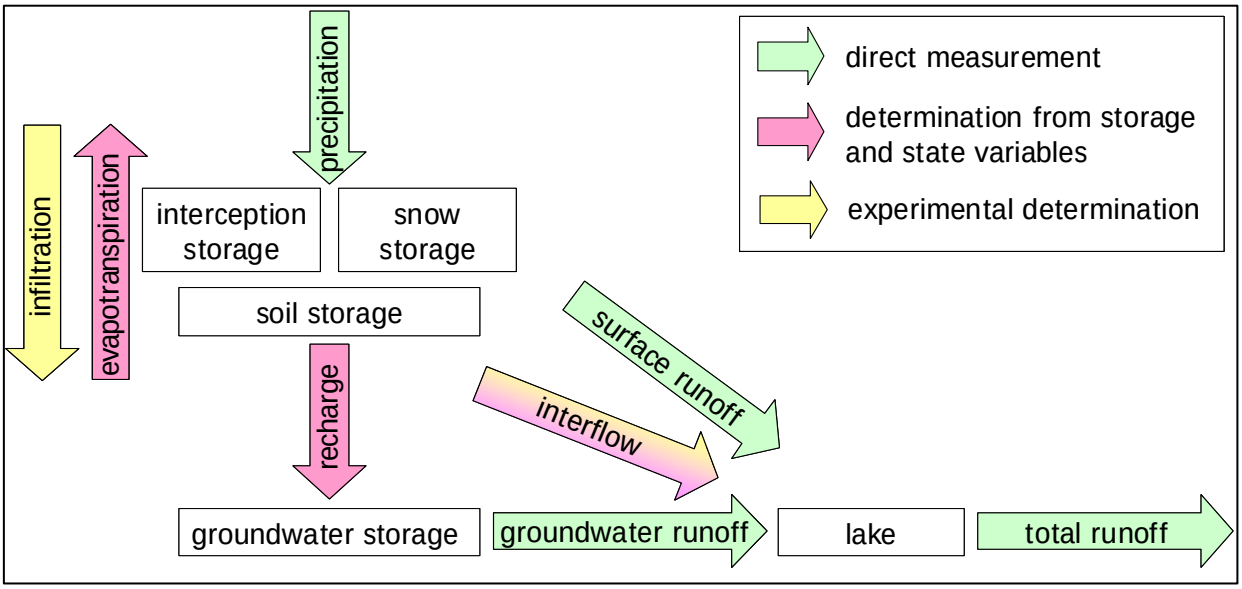

Fig. 4.1: Hydrological concept model of the catchment.

4. 2 Material and methods

The outflow of the whole catchment occurs at the outlet point of the pond. Assuming a runoff coefficient of 0.5 and a catchment size of about 6 ha, a rainfall intensity of 100 l/(s*ha) corresponds to a discharge of 300 l/s. This rainfall intensity equals to a return period of 0.5-1 year for a rainfall duration of 10 minutes, of 1-2 years for 20 min, of 10-20 years for 45 min and of 20-50 years for an event of 60 minutes (Bartels et al. 1997). About 35 m^3 of water per 1 cm water level rise are stored in the pond buffering the discharge from the catchment. The pond itself is a source area for evaporation. The outlet gauge was designed to measure discharge rates up to 250 l/s giving sufficient security to avoid uncontrolled (unmeasured) runoff from the catchment. The discharge from the Chicken Creek catchment at the outlet of the pond is the base for water budget calculation and hydrological modelling.

The streambed downstream of the pond outside the catchment was completed in September 2006. A V-notch weir was installed on September 14th, 2006. To register the discharge over a wide range with adequate accuracy, the V-notch weir was combined with a tipping bucket on March 10th, 2007. The weir (weir 2) is a combination of tipping bucket and compound weir (Fig 4.2). Because of the small difference of the water level on the both sites of the weir, a tipping bucket with flat buckets was constructed. The discharge from the pond is controlled by the water level of the pond which is automatically recorded by two pressure transducers in the pond, one at the end of the pontoon and one close to the weir (Fig. 4.2).

Fig. 4.2: Location of the two pressure transducers observing the pond level.

The tipping bucket is used to measure small fluxes. The volume of one bucket is about 1 litre. The counts are logged. If the water level reaches the two small flow pipes in the weir the measurement of discharge is started. One pipe directs water to the tipping bucket. The other one is used for water sampling. Discharge exceeding the capacity of the tipping bucket is determined by the compound weir consisting of a rectangular notch with a V-notch cut into the centre of the crest (Fig. 4.3).

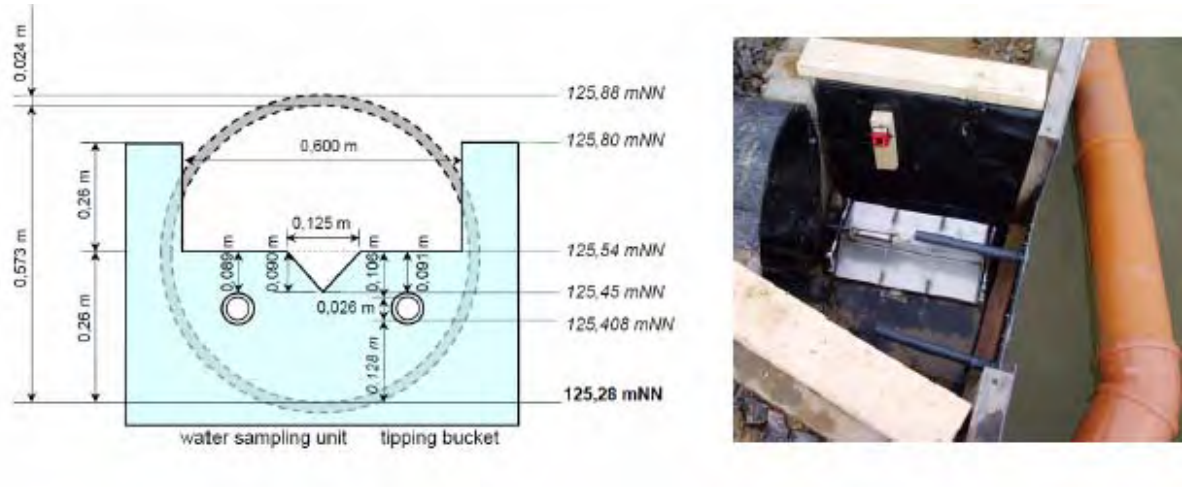

Fig. 4.3: Scheme and photo of the discharge gauge at the outlet of the pond (weir 2) with compound weir and tipping bucket.

In the lower part of the catchment, a subsurface clay wall was constructed on the clay layer surface running transversal to the assumed main flow direction. The funnel-shaped opening in this wall forms a spring where the groundwater can leak at the surface. The surface runoff from the catchment is redirected from this spring by the surface shape forming around the weir. At this point weir 1 was installed in August 2005 (Fig. 4.4).

Weir 1 is designed as a V-notch weir in a rectangle 3.0 m x 0.5 m x 0.5 m concrete channel. To avoid pollution from the concrete, the channel was faced with a stainless steel (V2A) plate. The overfall water level is registered by a pressure transducer. Because of the very low discharge at this point, weir 1 was additionally equipped with a 0.1 litre tipping bucket on January 10th, 2007.

Fig. 4.4: Groundwater spring at weir 1 after completion of the catchment surface on October 28th, 2005 (left) and detail of weir 1 (right); red lines indicate the underground clay walls.

Already the first precipitation events after the construction of the catchment showed that surface runoff is a significant fraction of the water fluxes at the poorly vegetated site (cf. Chapter 7). This resulted in the early formation of a network of erosion gullies. Two main gullies cut through the catchment surface down to the clay wall allowing groundwater exfiltration at the base of the gullies.

The main difficulties for the measurements of fast runoff components in these gullies are the unstable profile, the sediment transport with the runoff and the wide range of discharge rates. As a compromise, stainless steel (V2A) H-flumes (UGT, 2009) were installed at two gullies in the western part of the catchment (Fig 4.5). The water table is scanned by ultrasonic sensors and the level signal is logged and transformed into flow rates. Flume 1 is a 1 FT-H-flume for flow rates up to 55 l s^{-1} and flume 2 is a 2 FT-H-flume for flow rates up to 315 l s^{-1}. Unfortunately, sediment deposition in the flumes results in high service effort and affects the accuracy of the measurements.

In the central erosion gully at flume 2 a continuous base flow above the subsurface clay wall occurs. Therefore flume 2 was installed on the top of the clay wall and combined with a 0.1 litre tipping bucket. During surface runoff events the capacity of the tipping bucket is exceeded.


Fig. 4.5: Flume 1 (left) and flume 2 (right).

The second erosion gully where the groundwater leaks at the surface is in the eastern part of the catchment and has a wide profile with confluent subchannels and a high dynamic of flow rates. Here the registration of the complete range of discharge as a sum of surface runoff and base flow might only be possible by canalisation and stabilisation of the erosion channel. In order to minimise disturbance, only the continuous baseflow is measured by a subsurface drainage gutter (3.0 m x 0.5 m x 0.25 m) across the gully installed on June 17th, 2009. Water flux is registered by a 1 litre tipping bucket (Fig. 4.6).

Fig. 4.6: Drainage gutter.

Within the catchment, 21 observation wells were installed to record groundwater levels. 17 of them were installed along the grid points immediately after the completion of the Chicken Creek catchment in September 2005 (Tab. 4.1). Additional four groundwater observation pipes were installed close to the permanent soil pits in May 2008. The boreholes were drilled manually down to the clay layer by using an Eijkelkamp hand Riverside auger (Eijkelkamp 2009).

The gauges were constructed by 2" PE- pipes. The lower 1 m of the pipes are perforated with 0.3 mm slots and the lower ends were placed some centimetres into the clay layer. Both ends of the pipes were screwed with caps. The groundwater observation wells were not embedded with gravel. The five groundwater observation wells along the central row 4 and the four wells near the soil pits are equipped with water level loggers (pressure transducers). The groundwater level in the remaining wells is manually measured at least monthly.

Both weirs and one of the flumes are equipped with automated water sampling units (ISCO 6712 and ISCO 3700, Fig. 4.7). Daily water samples are taken and collected every two weeks. Sampling started in June 2007 at weirs 1 and 2 and in May 2008 at the flume. Due to technical problems sampling was interrupted at weir 1 from September 2007 to January 2008 and at weir 2 from August to October 2007.

After arriving at the laboratory, the daily samples are measured for pH (Beckmann pH34 glass electrode and WTW pH537) and electrical conductivity (EC; Hanna HI 8733 and WTW LF537). Mixed samples of the two week intervals are stored at -18°C until further analysis. The samples are analyzed for concentrations of Ca^{2+}, Mg^{2+}, Na^{+}, K^{+}, Fe^{3+}, Al^{3+} (ICP-OES Unicam 701 and Thermo Scientific iCAP 6000), NO_3^{-}, SO_4^{2-}, Cl^{-} (IC Dionex 5000), NH_4^{+} (Rapid Flow Analyzer Alpkem), DOC, TOC, TIC and TN (Shimadzu TOC-5000 and VCPH+TNM-1). Concentrations of bicarbonate (HCO_3^{-}) were calculated from total inorganic carbon (TIC).

Fig. 4.7: Automated water samplers ISCO 6712 and ISCO 3700.

4. 3 Results and discussion

The hydrological behaviour of the Chicken Creek catchment depends on internal and external factors. The development of the internal factors is influenced by the initial conditions, e. g substrate, shape, inclination, matter supply. Important external, driving forces are imposed by the weather conditions, e.g. the in- and output of water and energy.

During precipitation events rain water is separated at the catchment surface into surface runoff and infiltration depending on whether precipitation intensity exceeds the infiltration capacity of the soil or not. The water transport conditions of the substrate were initially determined by the texture itself but also by technical processes during catchment construction. As a result of surface runoff erosion occurs and changes the surface charcteristics.

The pond acts as a reservoir and constitutes an important part of the water budget. If the water level is below the discharge level, water losses only occur by evaporation. Water level rises are caused by discharge from the catchment and precipitation. The surface runoff from the catchment flows into the pond and changes the water level or induces discharge from the pond at weir 2.

Tab. 4.1: Basic data of the groundwater observation wells

Location (grid point)	date of installation	length of observation pipe [m]	top of pipe [m above soil surface]	depth of clay [m below soil surface]	water table [m below top of pipe]
C6	15.09.2005	3,53	0,64	2,86	2,72[a]
C4	15.09.2005	3,53	0,43	3,05	2,67 [a]
C2	15.09.2005	3,55	0,65	2,86	2,89 [a]
F2	14.09.2005	4,09	0,67	3,35	3,57 [a]
F4	14.09.2005	4,08	0,61	3,40	2,97 [a]
F6	15.09.2005	3,53	0,71	2,58	2,67 [a]
I6	14.09.2005	3,52	0,43	3,10	2,93 [a]
I4	14.09.2005	4,06	0,77	3,30	3,07 [a]
I2	14.09.2005	4,03	0,74	3,22	3,63 [a]
L2	15.09.2005	3,56	0,52	2,96	3,02 [a]
L4	15.09.2005	4,07	0,81	3,14	3,28 [a]
L6	15.09.2005	3,53	0,435	3,07	2,91 [a]
N6	19.09.2005	3,51	0,35	3,14	2,64 [a] *
N5	19.09.2005	3,07	0,43	2,57	1,99 [a] *
N4	19.09.2005	3,54	0,53	3,02	3,52 [a] *
N3	19.09.2005	3,07	0,185	2,78	3,05 [a] *
N2	19.09.2005	2,56	0,38	1,94	dry [a] *
B/C 5/6	13.09.2005	3,05	0,45	2,70	1,69 [b]
F 2/3	29.05.2008	4,04	0,76	3,30	2,70 [b]
I 5/6	29.05.2008	3,13	0,32	not achieved	1,71 [b]
L 2/3	29.05.2008	3,49	0,49	3,15	2,16 [b]

[a] measured on September 19th, 2005, [b] measured on Juli 3rd, 2008

* drilled and measured on the same day, no equilibrium

The transformation of water level changes to volume changes was derived from a water level/volume function of the pond (Fig. 4.8). The two graphs in Fig. 4.8 are the result of two surveys in 2006 and 2008. Differences between the two functions were caused by the better accuracy of a new GPS device (x, y, z, < 1 cm) in 2008 and by sedimentation in the pond. Unfortunately these two influences are superposed.

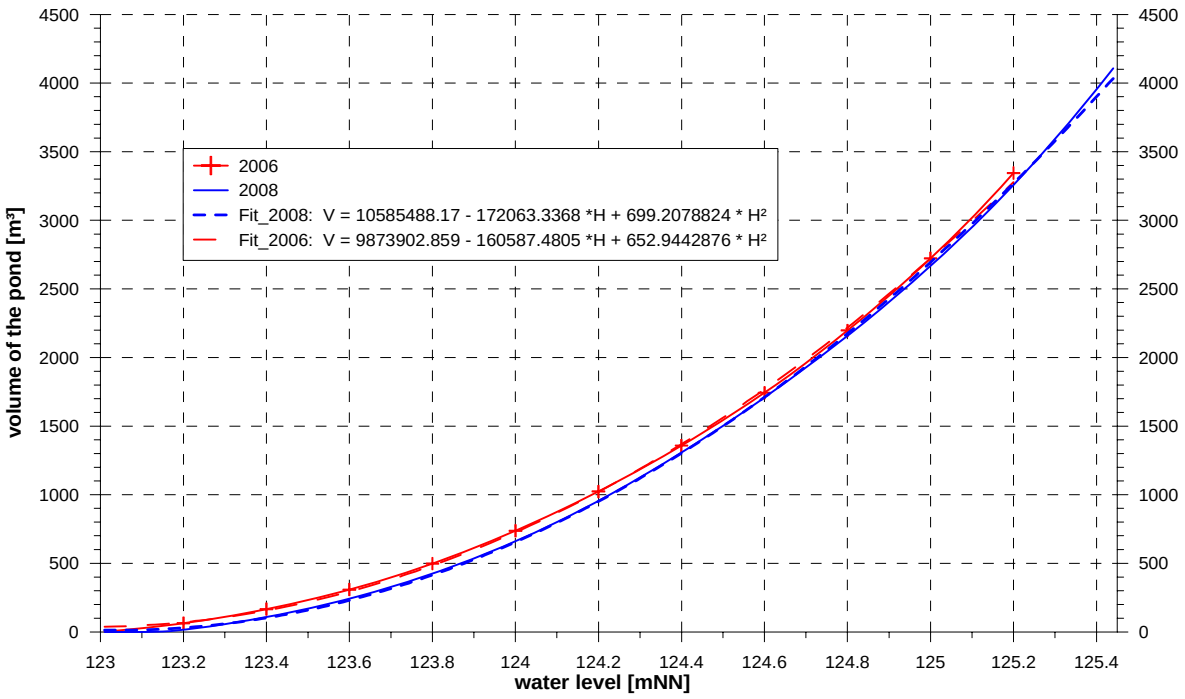

Fig. 4.8: Water level/volume function of the pond.

The special reservoir function of the pond and the geometry of weir 2 have to be taken into account when comparing modelling results and measured discharge. To analyse the real time behaviour of runoff processes from the catchment, calculated data of inflow into the pond may be more suitable.

The first complete filling of the pond occurred during a snow melt event on frozen soil at the end of January 2006 (Fig. 4.9). The region downstream of the pond was not yet finally shaped resulting in higher pond levels unteil September 2006 (cf. discharge level in Fig. 4.9).

The fast reaction of the pond level to precipitation events indicates that surface runoff is a significant fraction of the water fluxes. All water table rises and runoff from the pond at weir 2 occur during or immediately after precipitation or snow melt events. During dry periods with high evaporation, the pond level declines (Fig. 4.9, Fig 4.10) indicating that groundwater inflow during these periods is lower than evaporation losses from the pond surface. During time periods with low evaporation rates (November to March), the pond level did not fall significantly below the discharge level (Fig. 4.9, Fig. 4.10). This implies that water losses through the clay layer at the pond bottom are negligible.

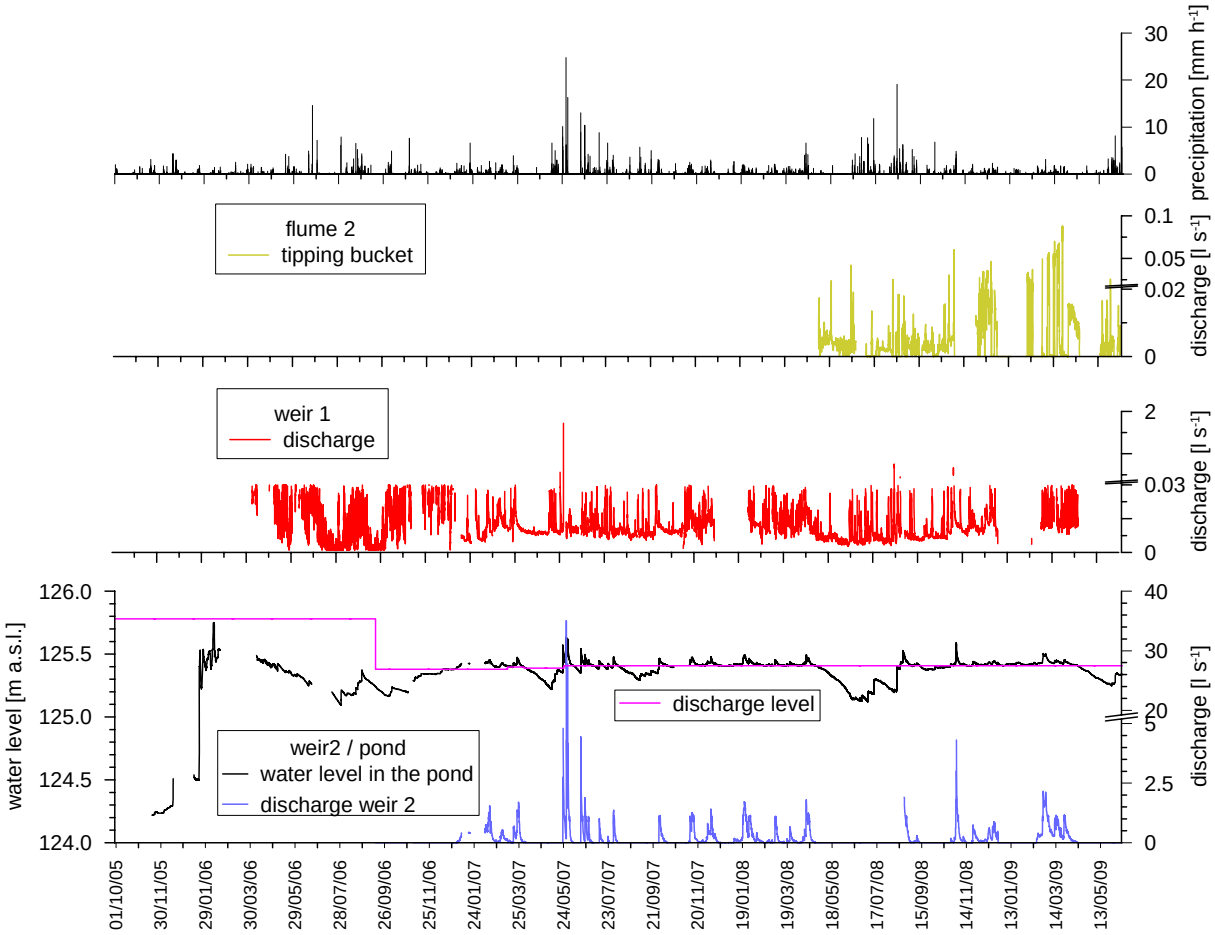

Fig. 4.9: Precipitation, discharge (weir 1, weir 2, flume 2 - tipping bucket) and pond level for the whole observation period.

The mean hourly discharge at weir 2 was 0.22 l s^{-1} in 2007 and 0.15 l s^{-1} in 2008. Calculated for the catchment area of about 6 ha discharge at weir 2 corresponds to 118 mm in 2007 and 80 mm in 2008. The maximum measured discharge at weir 2 was 35 l s^{-1} after a rain event with an intensity of 24.8 mm h^{-1} on May 27th, 2007. Especially during summer months long periods with no discharge were observed (Fig 4.9, Fig 4.10).

In contrast, water fluxes at weir 1 are recorded throughout the year except for frost periods (Fig 4.9, Fig 4.10). The mean hourly discharge of 0.015 l s^{-1} in 2007 and 0.012 l s^{-1} in 2008 is one order of magnitude smaller compared to weir 2. For the catchment area this corresponds to 8 mm discharge at weir 1 in 2007 and 6 mm in 2008. The distinct impulses caused by rain events are due to surface runoff from the area around the weir and not due to base flow.

Discharge from weir 1 shows significant differences between the periods before and after January 2007 (Fig. 4.9), which are caused by the additional installation of a tipping bucket. Obviously, the discharge is overestimated by the use of V-notch weir data alone.

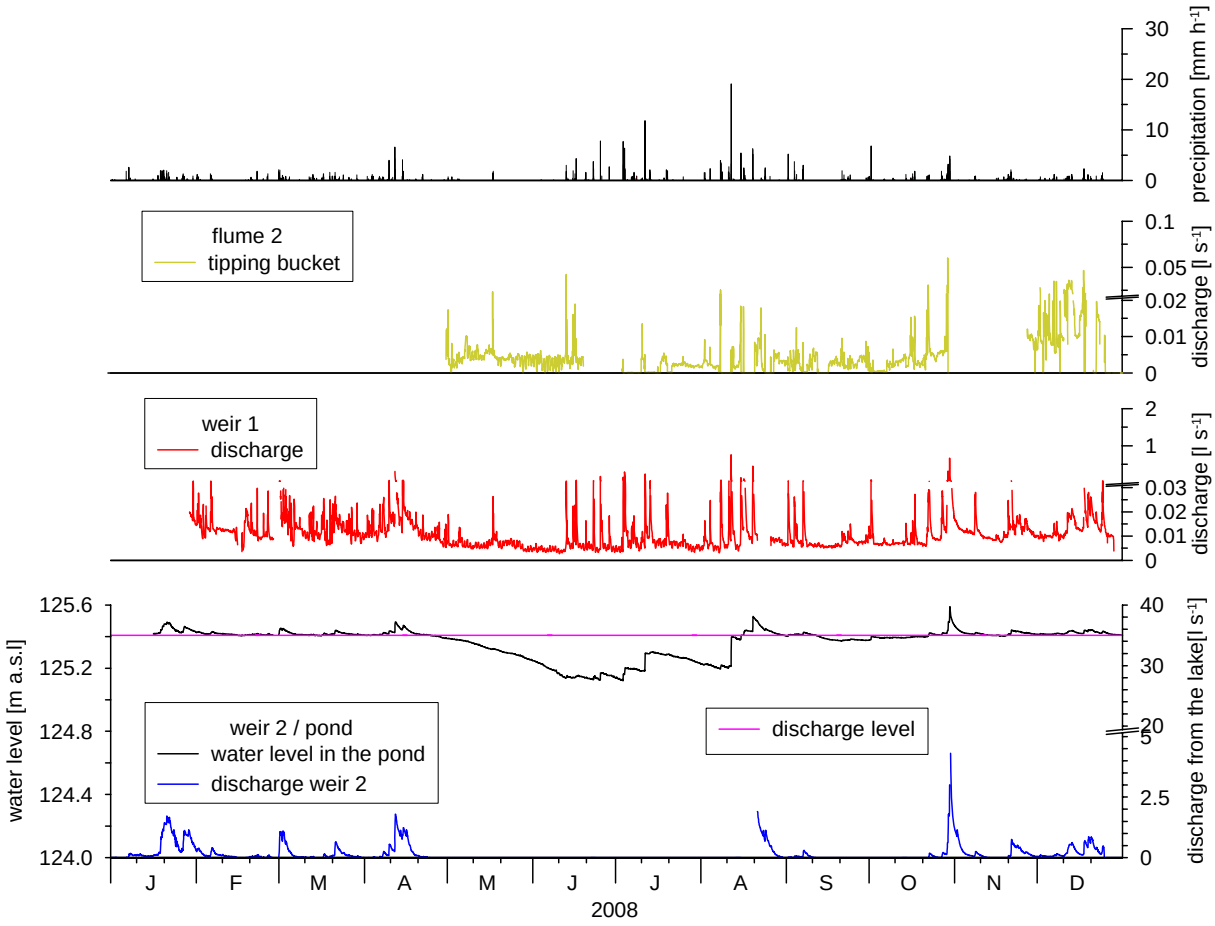

Fig. 4.10: Comparison of precipitation, discharge (weir 1, weir 2, Flume 2 (tipping bucket)) and pond level for the year 2008.

As a result of continued surface runoff the initial erosion gullies inclined deeper into the surface. Ground water building up in the substrate behind the clay walls could then discharge at the basis of the erosion gullies. Therefore, two of the main the gullies, formed by surface runoff, also became flow paths for base flow.

Flume 2 was designed to measure both surface runoff and base flow in one of the erosion gullies. Fig 4.9 and Fig 4.10 show tipping bucket data of flume 2. Missing values are due to plugging of the flume by sediment loads. Generally, the base flow at flume 2 is in a similar range compared to base flow at weir 1. Detailed analyses of the complete dataset from flume 2 have still to be done.

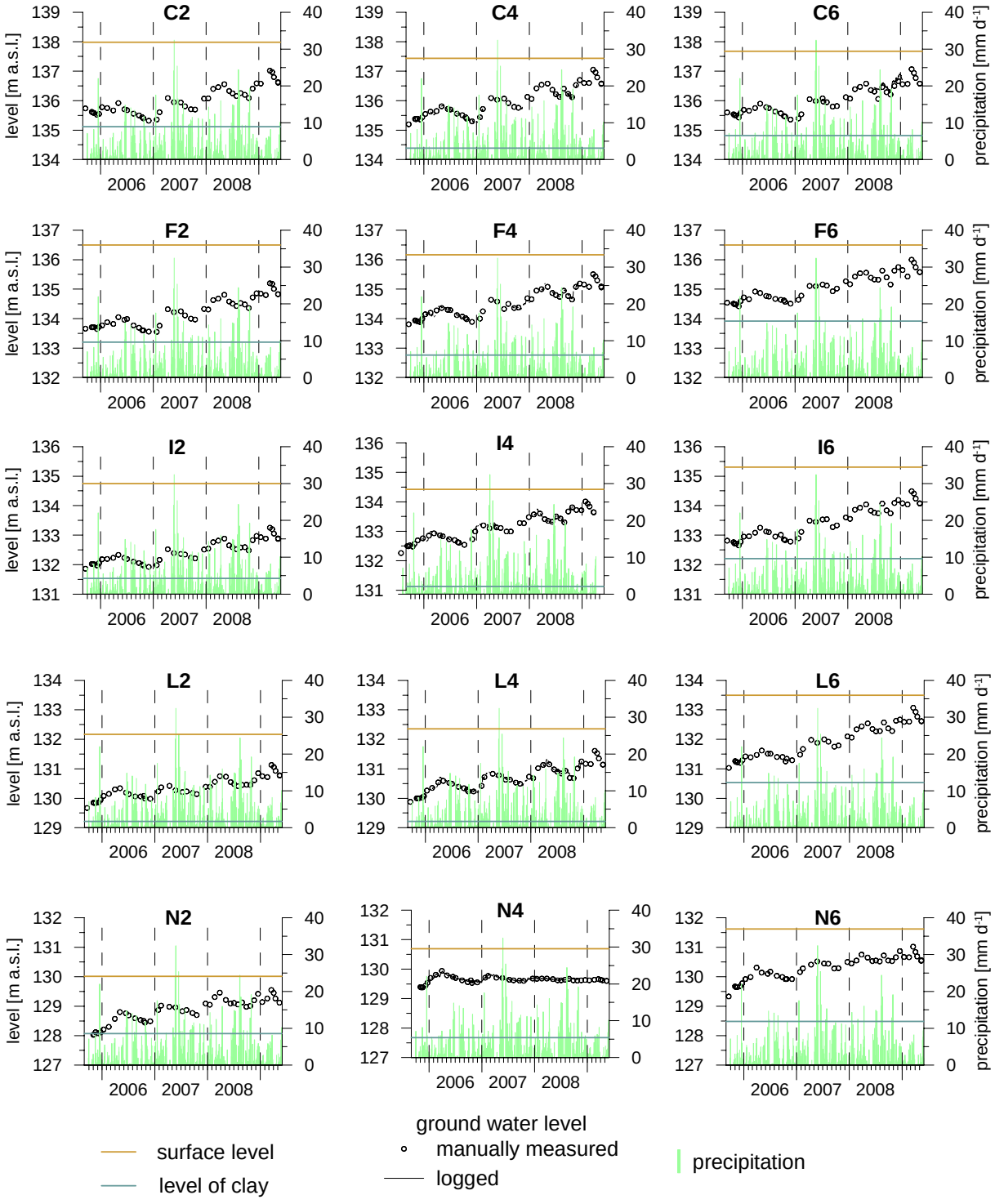

Fig.4.11: Time series of groundwater levels.

The small amount of base flow is an indication of relatively low hydraulic conductivity of the aquifer sediments. The generally increasing trend of the groundwater levels over the observation period (Fig. 4.11) indicates that groundwater recharge exceeds drainage. The highest groundwater levels during the observation period were recorded in March 2009 when groundwater levels increased up to few decimetres below the surface in some areas corresponding to up to 2 m above the clay layer.

Immediately after installation of the groundwater observation wells, groundwater levels of some decimetre were registered (Fig. 4.11). According to that a saturated zone in the substrate developed already during construction phase since spring 2004.

Despite the fact that the year 2006 was one of the driest out of the last 100 years in Lusatia (cf. Chapter 2), groundwater levels at the most of the observation wells had increased by the end of 2006. This also indicates low groundwater flow velocities within the catchment. The only exception to this observed trend was the well at grid point N4, which is located close to the central erosion gully where groundwater is discharged into the gully.

In summary, the hydrological regime at the Chicken Creek catchment is characterised by short time surface runoff events (>30 l s^{-1}, weir 2) coupled directly to precipitation events, permanent but low base flow from groundwater (mean value about 0.01 l s^{-1}), clearly higher evaporation from the pond surface compared to base flow inputs in summer and an exceedance of groundwater recharge compared to drainage.

pH values in all water samples vary between 7.0 and 8.5. Abrupt drops and increases in pH values of up to one pH unit per day can be observed (Fig. 4.12a). This is most pronounced for the flume samples, but also the weir samples follow similar trends. In general, ion concentrations in water samples from the three sampling sites are in the order flume > weir 1 > weir 2 as indicated by EC (Tab. 4.1, Fig. 4.11b). Whereas EC values at weir 2 (pond water) show only little temporal variation, considerable short-term peaks in EC of up to +/- 1500 µS cm^{-1} per day are observed in weir 1 and flume samples. EC values of weir 1 samples show typical temporal patterns with increasing values during drought periods and sharp drops after precipitation events.

Main components in all water samples are Ca^{2+}, SO_4^{2-}, Mg^{2+}, HCO_3^- and DOC (Fig. 4.12 and 4.13). These concentrations follow the order flume > weir 1 > weir 2.

Ammonium concentrations show a seasonal trend, most pronounced in the flume samples, with high values during summer months (Fig. 4.14). Also the weir samples show higher NH_4^+ concentrations in summer 2008 compared to 2007.

Concentrations of Al^{3+}, Fe^{3+} and NO_3^- were below detection limits (< 0.01 mmol L^{-1}) in all samples throughout the sampling period.

Tab. 4.1: Statistical parameters of water sample composition from the two weirs and the flume over the observation period (X = mean value, M = median, s = standard deviation, V = variation coefficient (V = S/X*100), N = number of samples)

	pH	EC	Ca^{2+}	Mg^{2+}	Na^{+}	K^{+}	NH_4^{+}	Cl^{-}	SO_4^{2-}	HCO_3^{-}	DOC
		$\mu S\ cm^{-1}$	$mmol\ L^{-1}$								
a. weir 1											
X	7,69	1149,6	6,90	1,19	0,35	0,05	0,03	0,16	6,23	3,75	1,09
M	7,78	1156,0	7,05	1,23	0,37	0,05	0,02	0,16	6,81	3,74	1,14
S	0,29	216,7	1,14	0,19	0,06	0,01	0,04	0,04	1,47	0,97	0,21
V	3,7	18,8	16,5	15,7	17,5	24,6	103,4	22,9	23,7	25,9	19,2
N	381	383	92	92	92	92	89	93	93	16	93
b. weir 2											
X	7,85	523,7	2,25	0,37	0,13	0,04	0,02	0,07	2,09	1,38	0,51
M	7,90	546,0	2,19	0,33	0,12	0,04	0,01	0,06	1,91	1,43	0,49
S	0,25	87,3	0,48	0,11	0,03	0,01	0,02	0,03	0,38	0,40	0,05
V	3,2	16,7	21,3	29,7	26,6	24,8	92,2	48,4	18,1	29,1	10,3
N	256	256	43	43	43	43	27	42	42	13	45
c. flume											
X	7,71	1828,98	9,51	1,74	0,49	0,12	0,17	0,20	10,59	3,81	1,15
M	7,87	1849,00	10,18	1,74	0,49	0,11	0,19	0,20	10,40	3,40	1,12
S	0,35	310,2	2,70	0,26	0,13	0,04	0,10	0,03	1,82	1,35	0,39
V	4,5	16,9	28,4	15,1	27,1	37,4	57,1	14,9	17,1	35,5	34,2
N	211	211	16	15	15	15	16	15	15	14	13

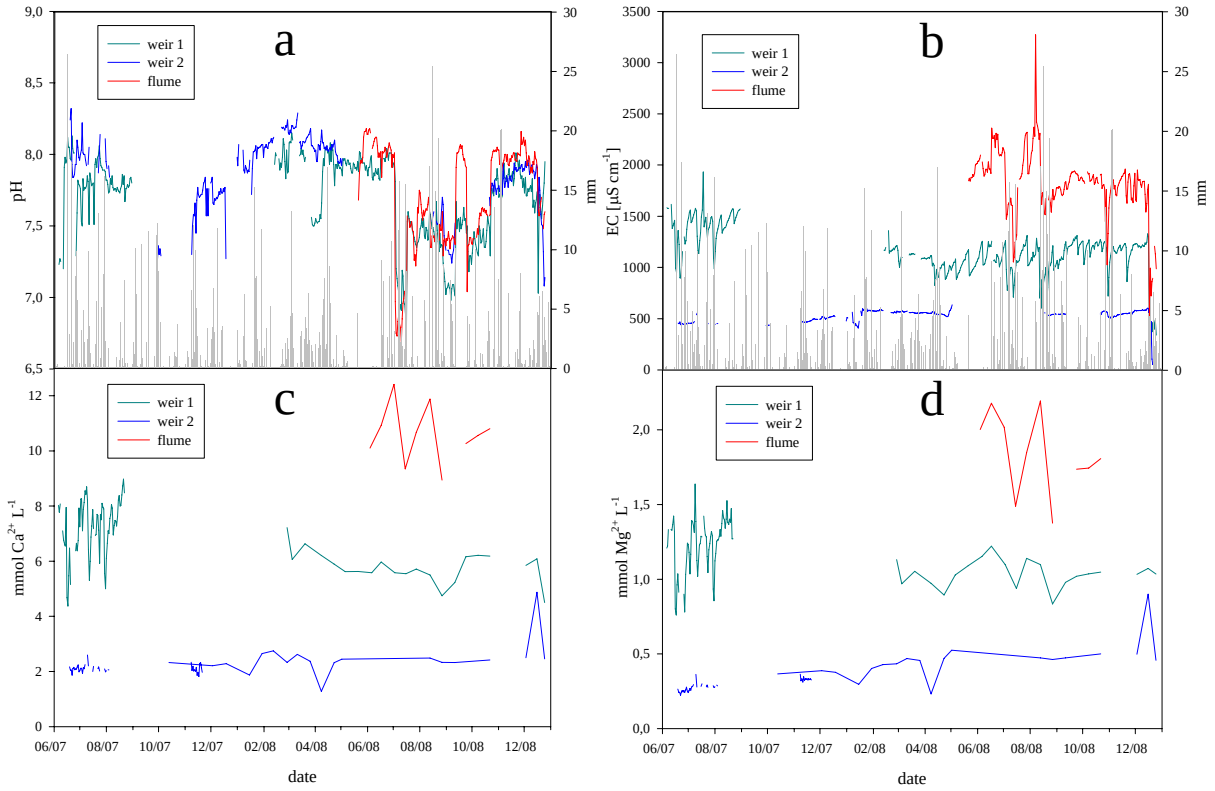

Fig. 4.12: Solution composition of water samples from weirs and flume - (a) pH, (b) EC, concentrations of (c) Ca^{2+} and (d) Mg^{2+} (included precipitation from meteorological station 1).

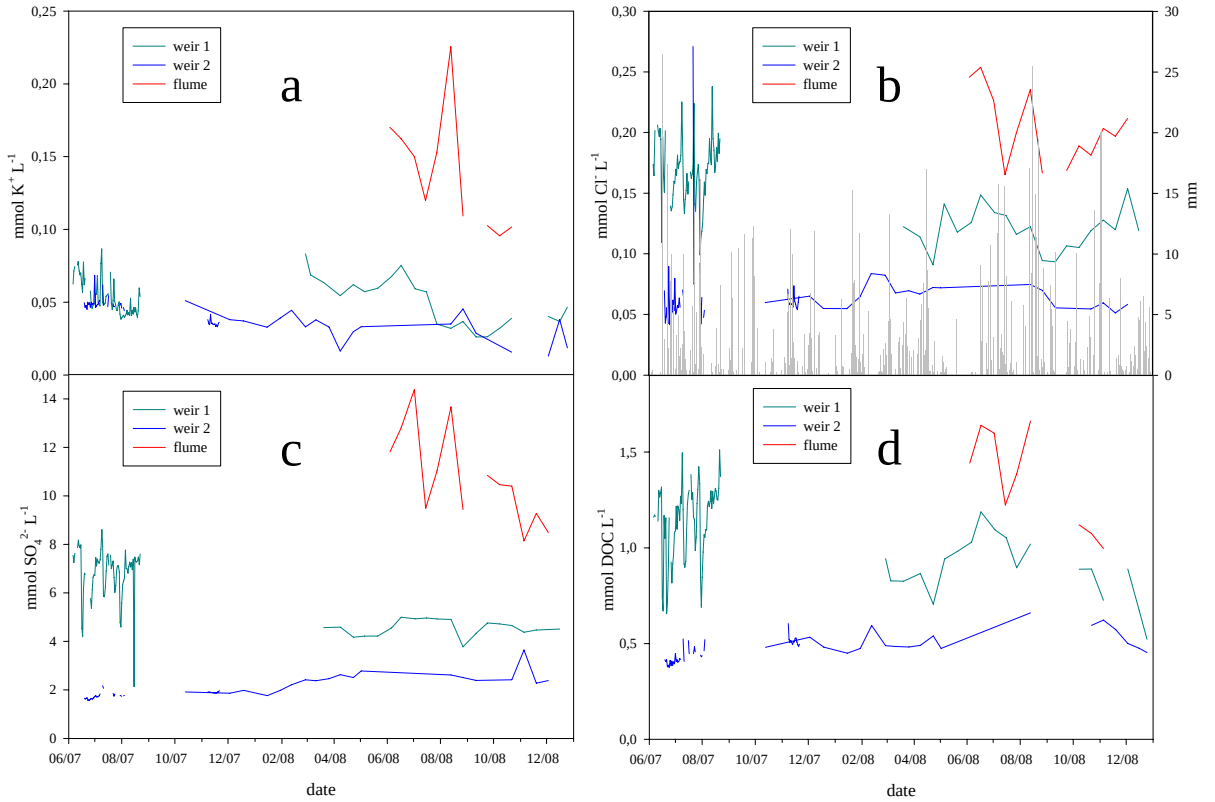

Fig. 4.13: Solution composition of water samples from weirs and flume - concentrations of (a) K^{+}, (b) Cl^{-}, (c) SO_4^{2-} and (d) DOC.

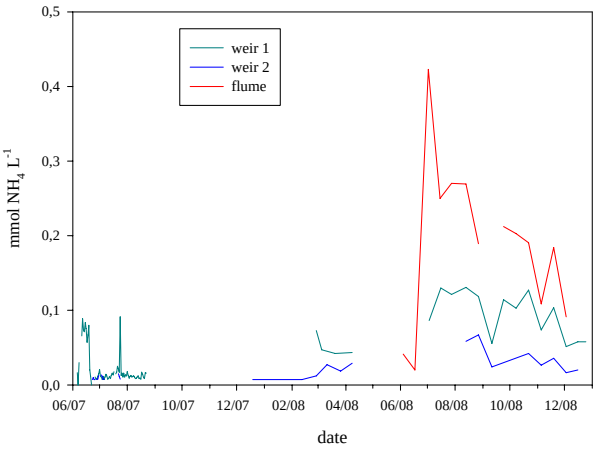

Fig. 4.14: NH_4^+ concentrations in water samples from weirs and flume.

Element fluxes were calculated from ion concentrations multiplied with the sum water fluxes per sampling period (Fig. 4.15). Fluxes are clearly governed by runoff events and amounts. Due to the relatively small water fluxes total element fluxes are low for the year 2008 (Tab. 4.2) compared to the large total volume of 117,500 m³ (Kendzia et al. 2008) and stored amounts of the catchment body.

At weir 2 which represents the outlet of the total catchment area element discharge is even more dependent on water discharge since ionic concentrations show much lower temporal variations (Fig. 4.12-4.14). For 2008 the pond discharge is about 10fold higher compared to the water fluxes recorded at weir 1. Nevertheless, element outputs are only 4-5fold higher compared to weir 1 (Tab. 4.2) showing that the pond acts as an important buffer and effective element store within the catchment. Ammonium output is only double the amount of weir 1. Calculated for the total catchment area of 6 ha, the element output rates are low in 2008 (Tab. 4.2).

Tab. 4.2: Total element fluxes with runoff at the two weirs and total output in 2008

	Ca	Mg	Na	K	NH_4-N	Cl	SO_4-S	DOC
weir 1 [kg yr^{-1}]	105.5	10.4	3.0	0.8	0.5	1.9	65.7	4.8
weir 2 [kg yr^{-1}]	437.2	47.4	14.2	4.7	1.1	10.0	345.5	26.9
total output [kg $ha^{-1}yr^{-1}$]	72.9	7.9	2.4	0.8	0.2	1.7	57.6	4.59

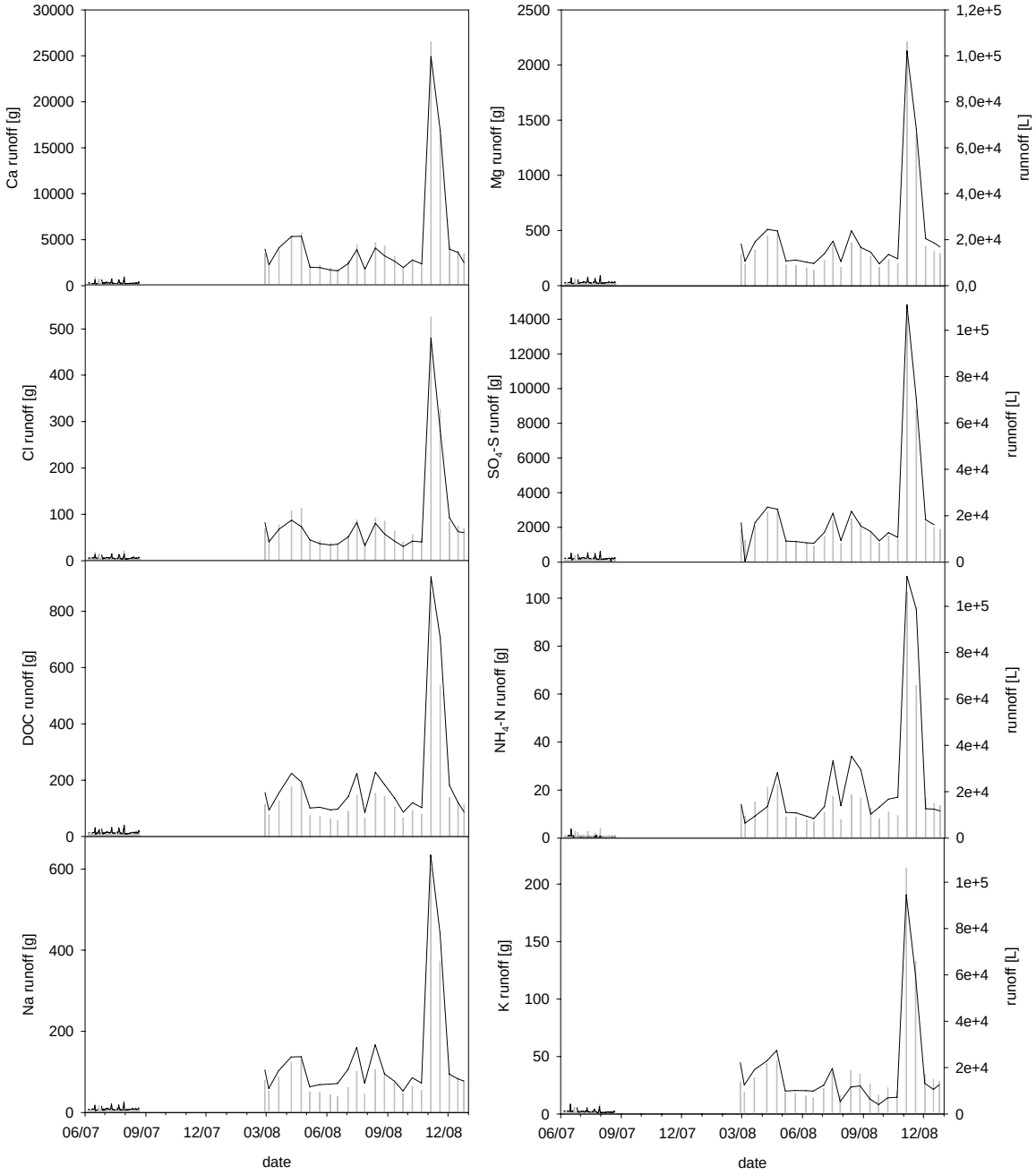

Fig. 4.15: Element fluxes with runoff at the two weirs.

References

Bartels, H., Malitz, G., Asmus S., Albrecht F. M., Dietzer B., Günther T. & Ertler, H. (1997): Starkniederschlagshöhen für Deutschland. KOSTRA- Offenbach Main, Selbstverlag des Deutschen Wetterdienstes ISBN 3-88148-325-X.

Eijkelkamp 2009: Hand auger equipment. http://www.eijkelkamp.com/Products/tabid/76/CategoryID/1/List/1/Level/a/ProductID/2/ Default.aspx?language=en-US, (25th Juni 2009).

Kendzia, G., Reißmann, R. and Neumann, T., 2008: Targeted development of wetland habitats for nature conservation fed by natural inflow in the post-mining landscape of Lusatia. World Mining 60, 88-95.

UGT, 2009. H-Flume Flow rate indicators. http://www.ugt-online.de/en/products/flow-rate-and-water-level-indicators/06-h-flume.html, (26th June 2009).

Acknowledgements

We thank our field technicians Ralph Dominik, Marin Dimitrov, Silvio Voigt and Rossen Nenov for their active help during installation of the sampling units. Together with our students Gunter Bormann and Uwe Enke they also are responsible for routine sampling and maintenance of the field equipment. We thank the lab team at the Chair of Soil Protection and Recultivation, BTU Cottbus (Gabi Franke, Regina Müller, Helga Köller, Evi Müller and Anita Maletzki) for the professional and reliable analysis of the many samples together with our student helpers Nonka Markova, Tzvetelina Dimitrova and Natasha Beltran.

5. Soil solution

Wolfgang Schaaf

Brandenburg University of Technology Cottbus, Chair of Soil Protection and Recultivation

5. 1 Introduction

Soil solution is a major medium for transport processes in soils and at the same time a reactive phase that interacts with other soil components via physical, chemical and biological processes (Schaaf et al. 1995, Schaaf 2004). Soil solution composition can be used as an indicator for soil processes (Schaaf and Hüttl 2005). Combined with water fluxes in the soil, the analysis of solutes enables the calculation of element fluxes in the soil compartment (Gast et al. 2001, Weisdorfer 1995, Schaaf 2001). Within the monitoring programme of the SFB/TRR 38 soil solution is sampled at four grid points at the catchment site. The data should provide information on the spatio-temporal development of soil solution composition.

5. 2 Material and methods

To allow permanent access for soil solution sampling four soil pits were installed in the catchment close to grid points C5, F2, I5 and L2. The pits were excavated in October 2007 down to the saturated layer in 2-2.5 m depth by hand and stabilized with a lining of PE rings with a diameter of 1 m (Fig. 5.1). From these pits boron silicate glass suction plates (∅ 10 cm) were installed into the soil. From windows in the PE tubes a metal plate was horizontally inserted 30 cm into the soil (Fig. 5.2) and the underlying soil was removed by hand. From these holes the suction plates topped with a paste made of quartz powder and deionized water were installed below the metal plate and stabilized by PE blocks and the removed soil material (Fig. 5.3). Then the metal plate was carefully removed to enable good contact between the suction plates and the surrounding soil (Fig. 5.4). Depending on the groundwater level, suction plates were installed in 2-3 depths per pit (30 cm, 80 cm and 150 cm). In the upper depth two plates each were installed in a horizontal distance of ~1 m. All plates are connected to glass sampling bottles and vacuum units (UMS VS) that provide a permanent pressure of -10 kPa (Fig. 5.5). Sampling started in November 2007 is carried out every two weeks.

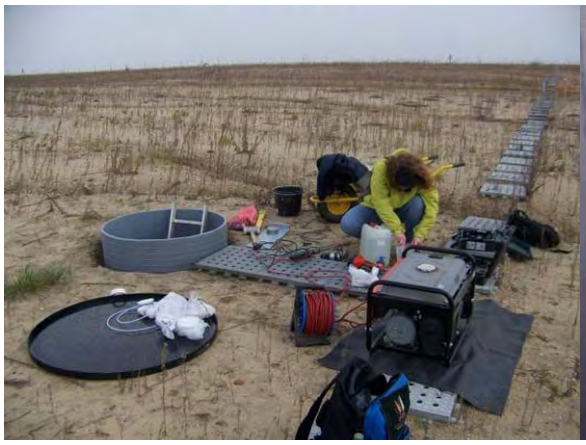

Fig. 5.1: Installation at one of the four soil pits.

Fig. 5.2: PE tube window and metal plate for suction plate installation.

After arriving at the laboratory, the soil solutions samples are measured for pH (Beckmann pH34 glass electrode and WTW pH537) and electrical conductivity (EC; Hanna HI 8733 and WTW LF537). Subsamples are stored at -18°C until further analysis. The samples are analyzed for concentrations of Ca^{2+}, Mg^{2+}, Na^{+}, K^{+}, Fe^{3+}, Al^{3+} (ICP-OES Unicam 701 and Thermo Scientific iCAP 6000), NO_3^{-}, SO_4^{2-}, Cl^{-} (IC Dionex 5000), NH_4^{+} (Rapid Flow Analyzer Alpkem), DOC, TOC, TIC and TN (Shimadzu TOC-5000 and VCPH+TNM-1).

Soil crust samples described below were analyzed for soluble SO_4^{2-} and gypsum using methods according to Reeuwijk (2002). Scanning electron microscopy (SEM Zeiss DSM 962) with EDX-detector (Oxford Instruments LINK-Pentafet-System) was used to analyze precipitation products in the crust samples.

Fig. 5.3: Suction plate topped with quartz powder.

Fig. 5.4: Suction plate installed.

Fig. 5.5: Soil pit with four suction plates and sampling bottles in three depths connected to vacuum unit.

5. 3 Results and discussion

Soil solution composition varies considerably between the four soil pits during the observation period. Compared to these spatial variations, differences in soil depth and over time are less pronounced.

Main components of all sampled soil solutions are Ca^{2+}, Mg^{2+}, HCO_3^- and SO_4^{2-} (Fig. 5.6 – 5.8). Due to the carbonate content of the substrates, mean pH values vary between 7.0 and 8.0 in all samples. Soil pit C5 shows slightly lower pH values compared to the other sampling sites. Concentrations of Al^{3+} and Fe^{3+} were below detection limits (< 0.01 mmol L^{-1}) in all soil solutions throughout the sampling period.

At 30 cm soil depth, elevated EC values at pit C5 and – to a lower extent – at L2 can be mainly explained by higher Ca^{2+}, Mg^{2+}, HCO_3^- and SO_4^{2-} concentrations in these samples (Fig. 5.6). The two parallel samples of each pit at this depth are in good agreement indicating that spatial heterogeneity is small at the scale of ~1 m.

Generally ionic concentrations increase with soil depth. At 80 cm soil depth, concentrations of Ca^{2+}, Mg^{2+} and SO_4^{2-} increase two to six fold at L2 increasing EC values to > 2500 μS cm^{-1} (Fig. 5.7). In all other pits this increase with depth is much less pronounced.

In 150 cm depth EC and ion concentrations remain elevated at L2 (Fig. 5.8).

No correlations whatsoever were found between soil solution compositions and soil parameters of the surrounding grid samples. Especially the differences between pits C5/L2 and F2/I5 are not correlated to the respective solid phase parameters. This is also true for the strong increases in Ca^{2+}, Mg^{2+}, K^+, SO_4^{2-} and DOC concentrations in 80 cm (and 150 cm, not shown) depth at pit L2.

Compared to the composition of the solid phase, the concentrations of SO_4^{2-} and DOC are surprisingly high given the very low S_t and $C_{org.}$ contents of the parent material.

During summer drought periods pale whitish precipitations were frequently observed at the vertical walls of erosions gullies (Fig. 5.9). Microscopy revealed that these precipitations form a very thin crust (<100 μm) and are composed of very small crystal grains (Fig. 5.10). Further analysis using SEM and EDX mapping showed that the particles have a size of about 5 μm and are composed of Ca and S (Fig. 5.11) indicating gypsum or anhydrite, but not showing the typical crystal structure of it. Dultz and Kühn (2005) described the occurrence of gypsum in Chernozems of Central Germany. They hypothesized the formation of gypsum in the upper 1.5 m of the profiles due to former high sulphur deposition together with low precipitation and leaching. The authors describe whitish efflorescences at the surface of aggregates. SEM images and EDX spectra of these efflorescences look exactly as in the samples from the erosion gullies (Fig. 5.11 and 5.12). Water extracts of soil samples had very low SO_4^{2-} concentrations of <0.02 mmol L^{-1}. Gypsum contents in the same samples ranged from 0.03 to 0.15 g kg^{-1}. Dultz and Kühn (2005) found gypsum contents in Czernozems of 0.1 – 2.3 g kg^{-1}. Despite the very low gypsum contents of the catchment samples, ionic concentrations in soil solutions are similar to values in water extracts given by Dultz and Kühn (2005). Therefore, it cannot be excluded that low gypsum contents in the parent material contribute to the high SO_4^{2-} concentrations in soil solutions (and in other water samples in the catchment, see Chapter 4).

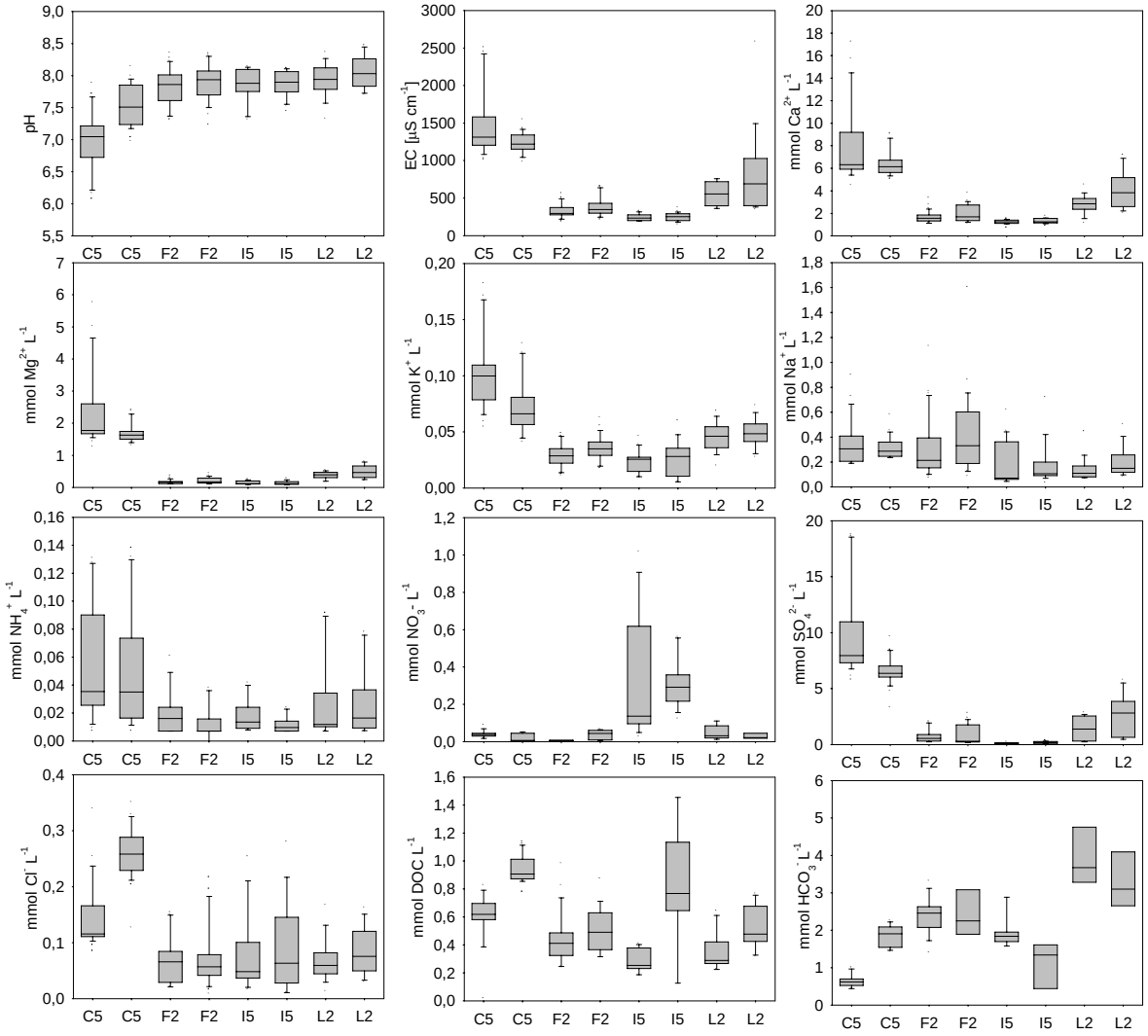

Fig. 5.6: Box plot diagrams of soil solution composition in 30 cm depth at the four soil pits.

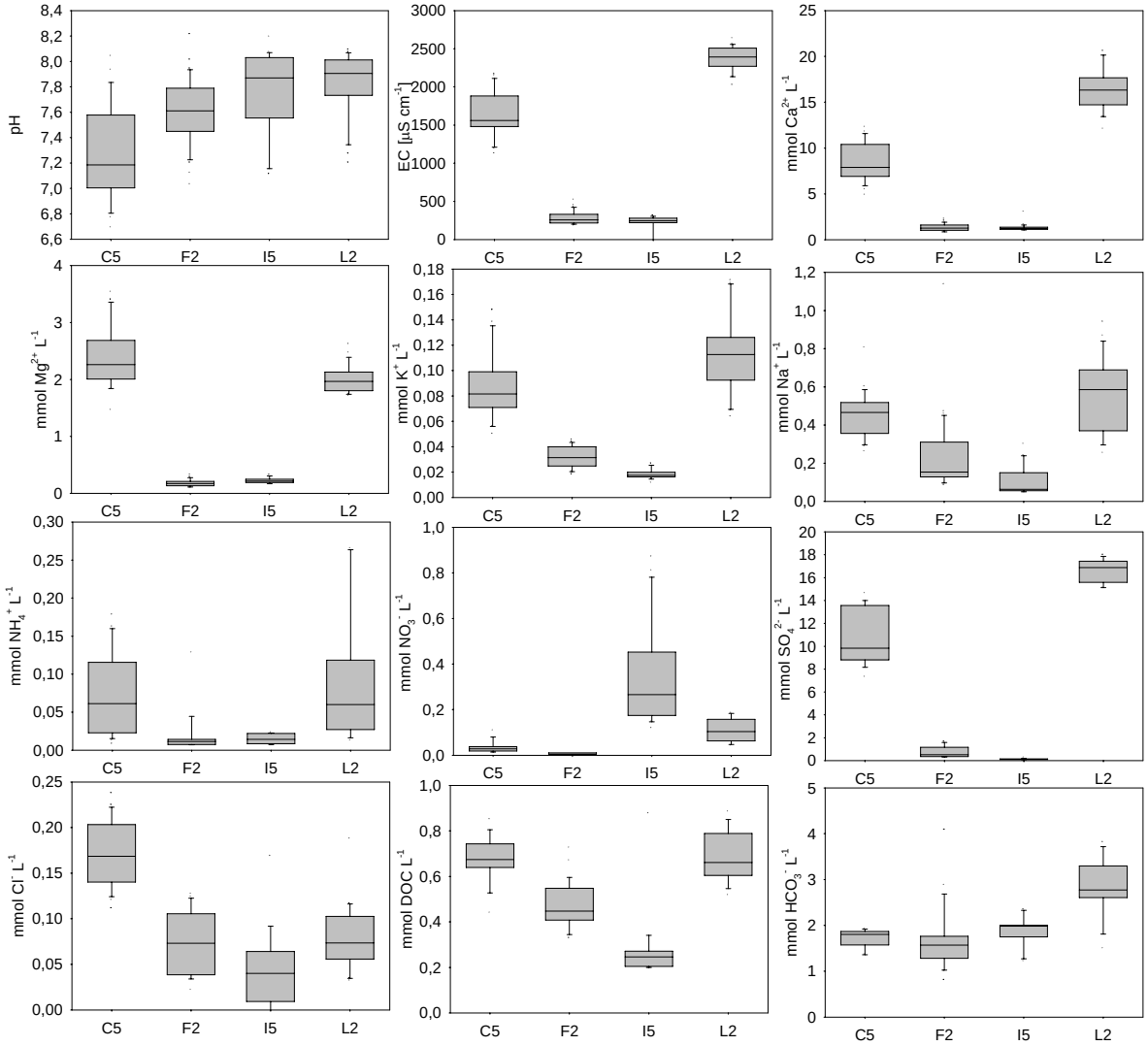

Fig. 5.7: Box plot diagrams of soil solution composition in 80 cm depth at the four soil pits.

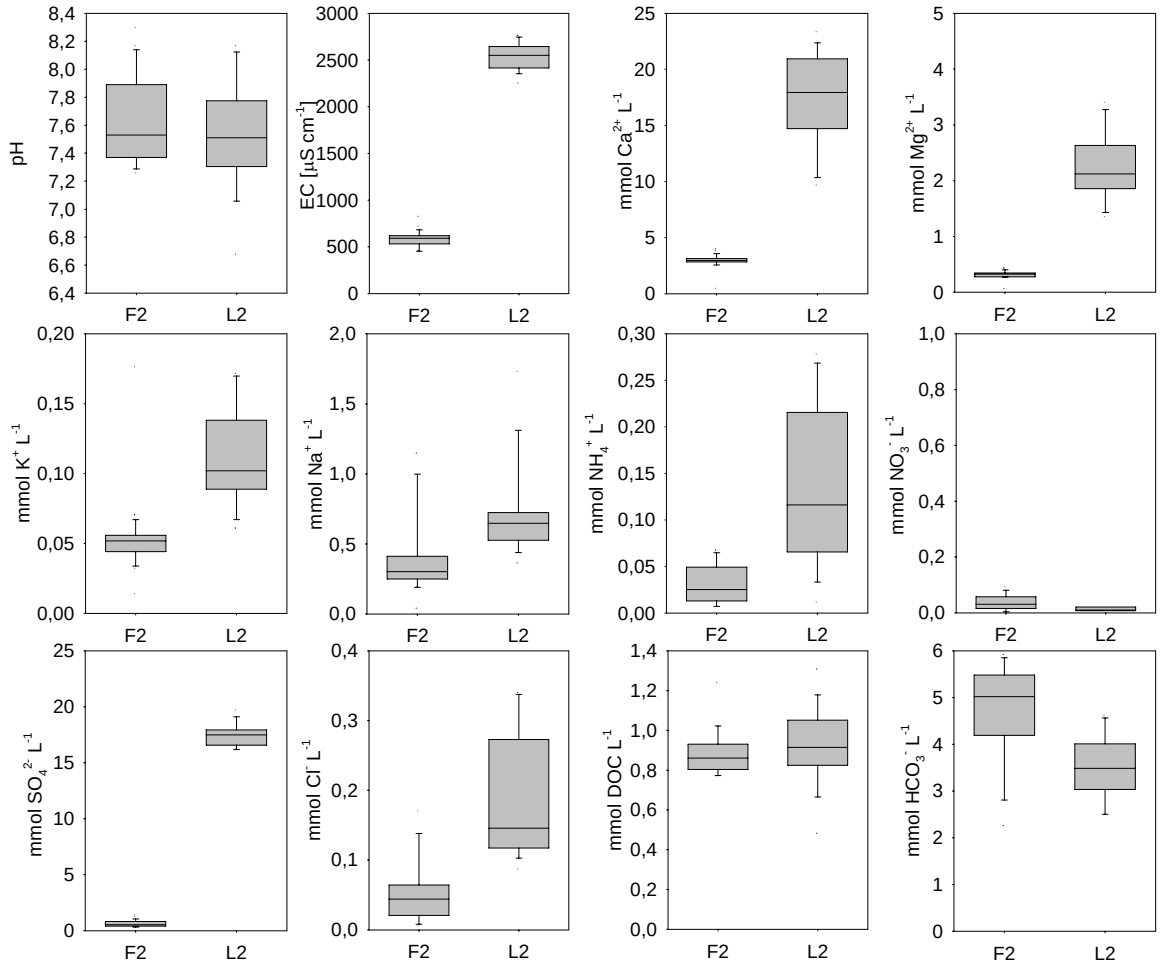

Fig. 5.8: Box plot diagrams of soil solution composition in 150 cm depth at the four soil pits.

Fig. 5.9: White soil crusts at the walls of erosion gullies developed during summer drought.

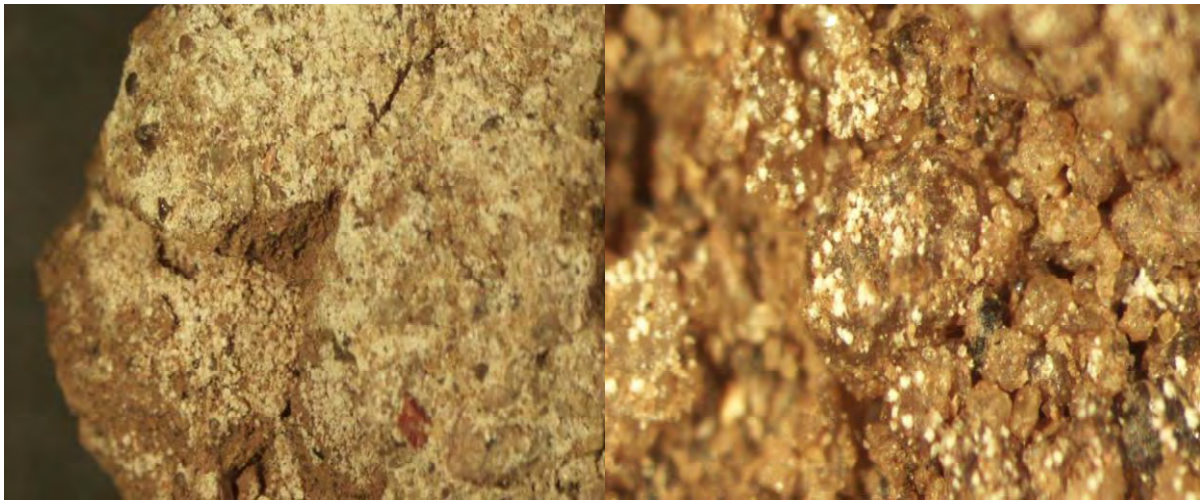

Fig. 5.10: Microscopic pictures of soil crust samples (cf. Fig. 5.9) with 6.3 times (left) and 20 times (right) magnification.

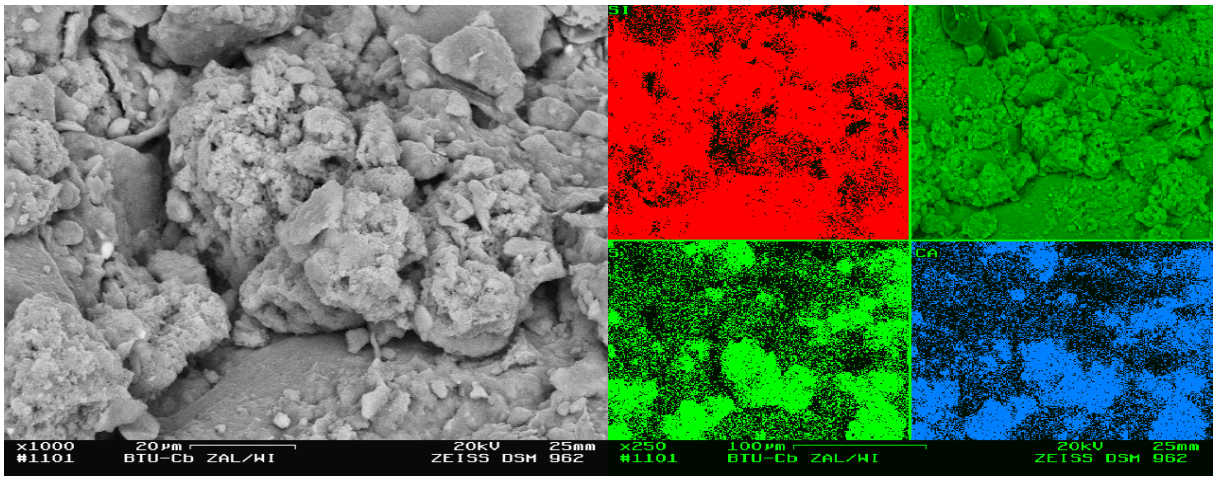

Fig. 5.11: SEM picture of a soil crust samples (left; cf. Fig. 5.9) and EDX element mapping of the same sample (right).

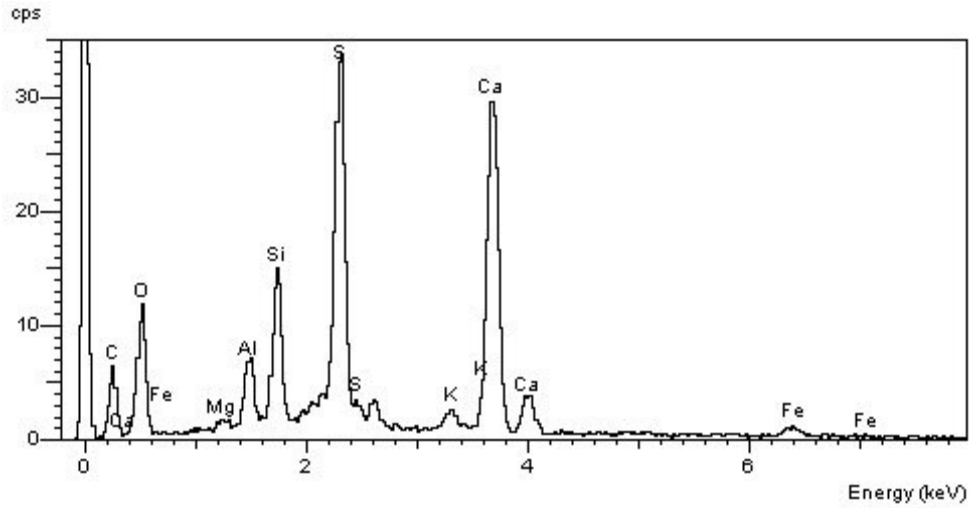

Fig. 5.12: EDX spectra of the soil crust sample in Fig. 5.11.

The temporal development of soil solution composition does not show pronounced changes of ionic composition over time (Fig. 5.13 - 5.16). The overall higher concentrations in 30 cm depth at pit C5 as indicated by EC could be due to lower water fluxes compared to other depths and pits. Also the higher concentrations of Cl^- as a conservative ion would support this explanation as mainly a concentration effect.

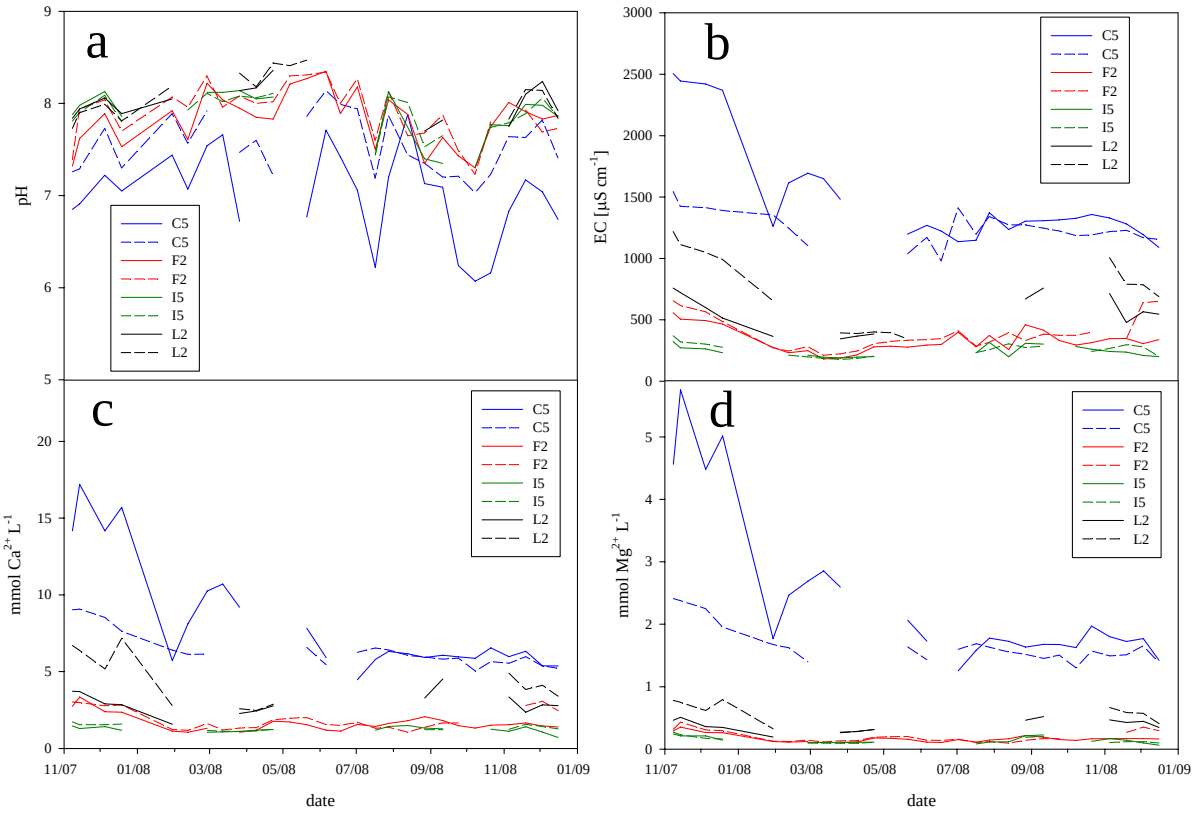

Fig. 5.13: Soil solution composition in 30 depth - (a) pH, (b) EC, concentrations of (c) Ca^{2+} and (d) Mg^{2+}.

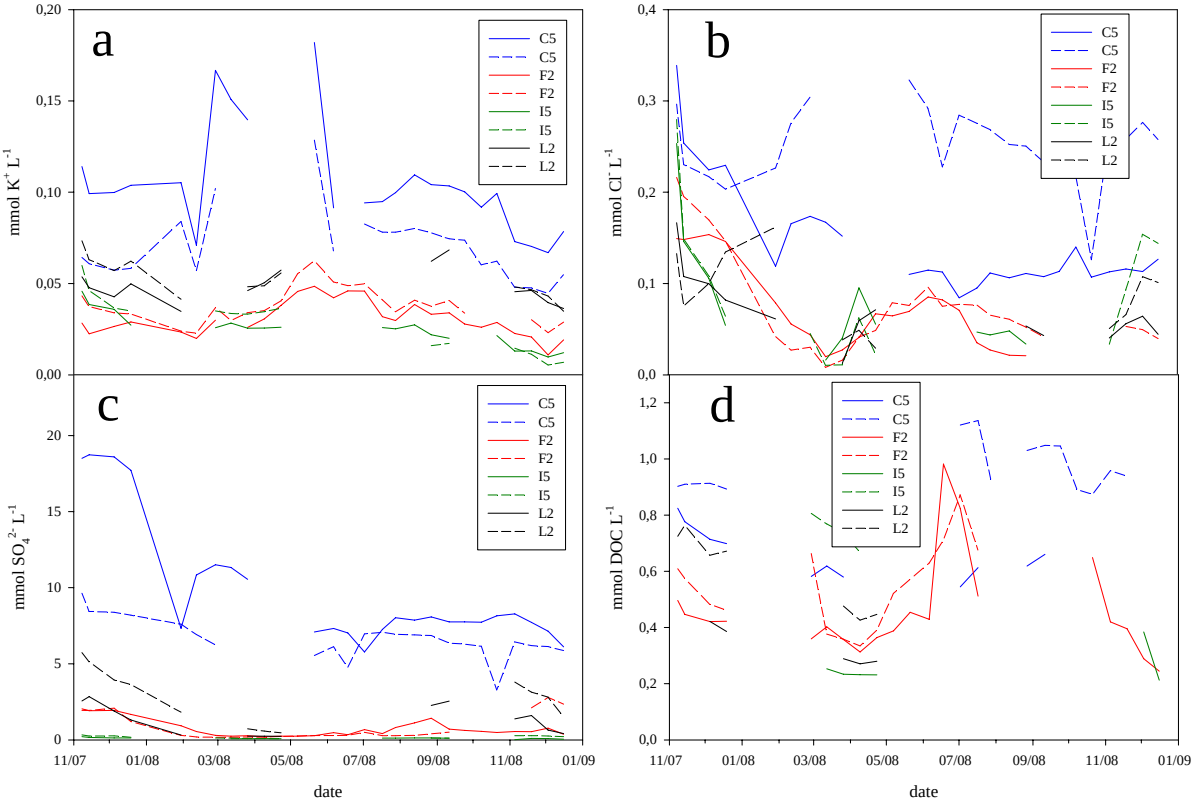

Fig. 5.14: Soil solution composition in 30 depth - concentrations of (a) K^+, (b) Cl^-, (c) SO_4^{2-} and (d) DOC.

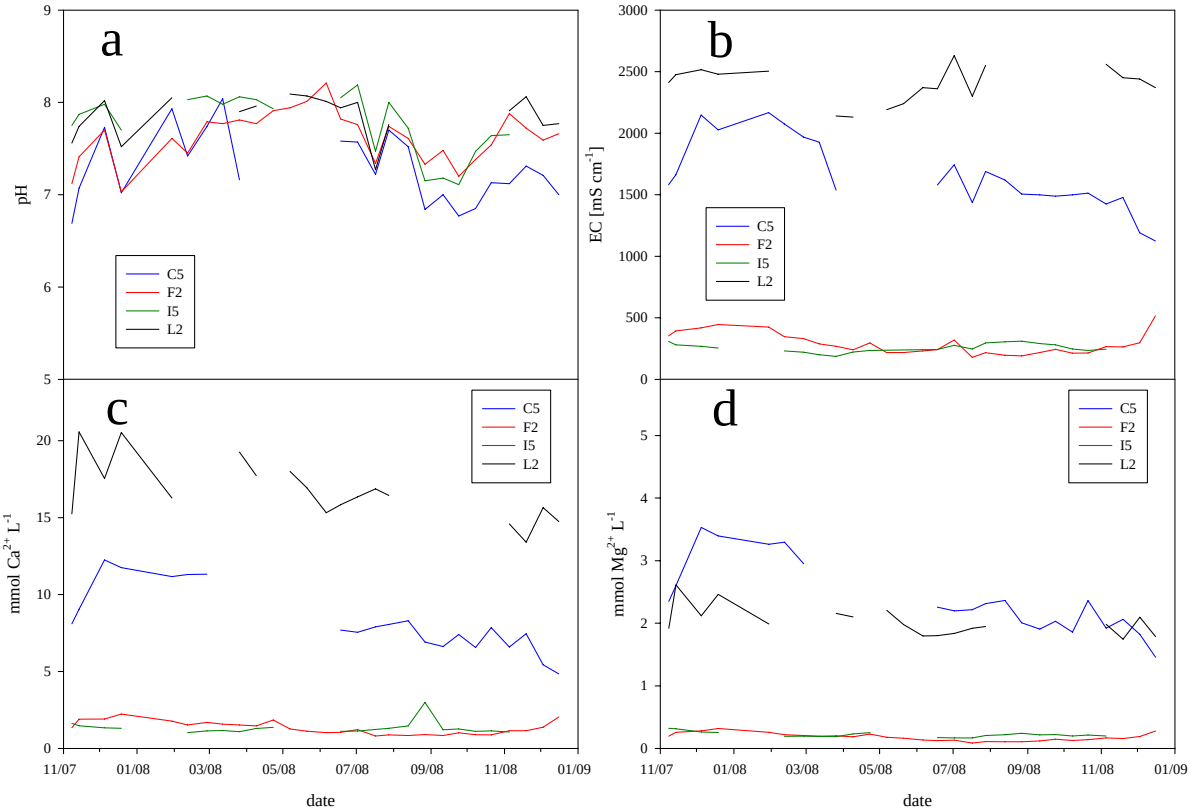

Fig. 5.15: Soil solution composition in 80 depth - (a) pH, (b) EC, concentrations of (c) Ca^{2+} and (d) Mg^{2+}.

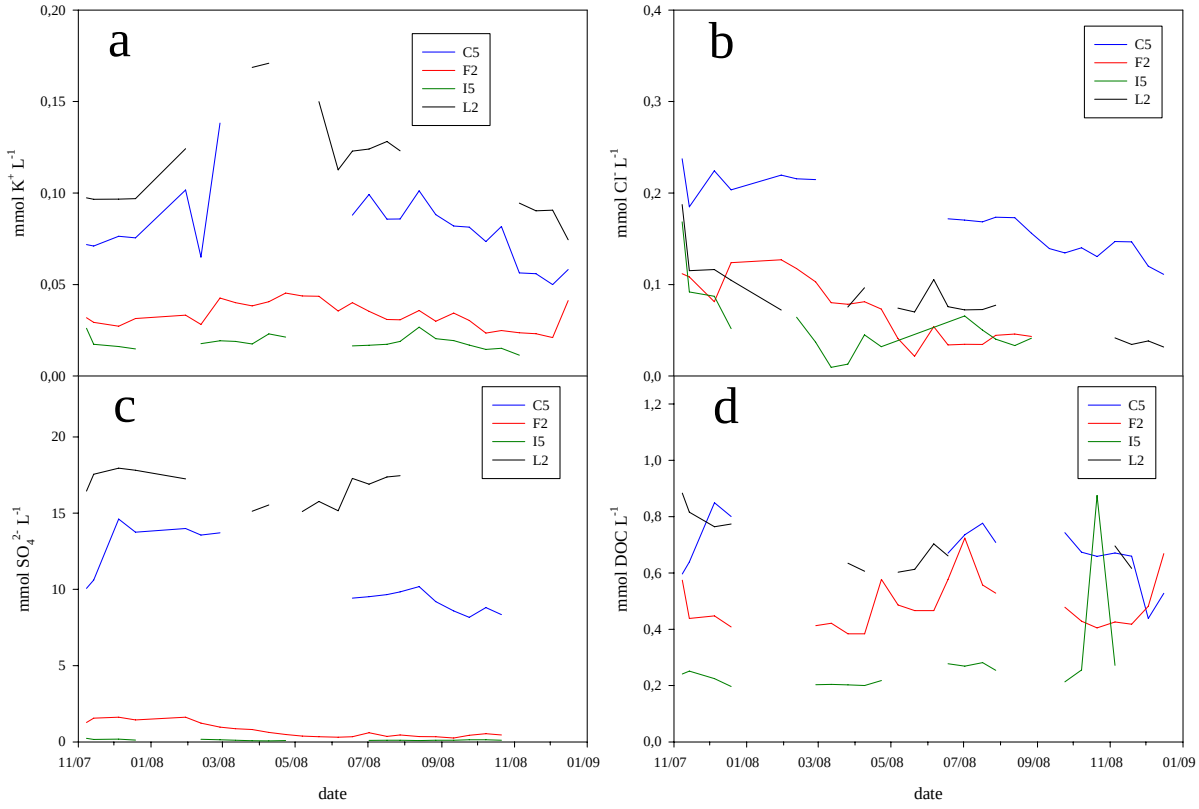

Fig. 5.16: Soil solution composition in 80 depth - concentrations of (a) K^+, (b) Cl^-, (c) SO_4^{2-} and (d) DOC.

The only seasonal effects observed in 30 and 80 cm depth are elevated NO_3^- concentrations at I5 and NH_4^+ peaks at C5 during summer 2008. In addition Na^+ concentrations in 30 cm depth at all sampling sites are elevated from May to September 2008.

References

Dultz, S. and Kühn, P., 2005: Occurrence, formation, and micromorphology of gypsum in soils from the Central-German Chernozem region. Geoderma 129, 230-250.

Gast, M., Schaaf, W., Wilden, R., Scherzer, J., Schneider, B. U. and Hüttl, R. F., 2001: Water and element budgets of pine stands on lignite and pyrite containing mine soils. Journal of Geochemical Exploration 73, 63-74.

Reeuwijk, van L.P., 2002: Procedures for Soil Analysis, Gypsum: Chap. 8, 1–2. 6th ed. International Soil Reference and Information Centre, Wageningen.

Schaaf, W., Weisdorfer M, and Hüttl, R. F., 1995: Soil solution chemistry and element budgets of three Scots pine ecosystems along a gradient in north-eastern Germany. Water, Air and Soil Pollution 85, 1197-1202.

Schaaf, W., 2004: Development of element cycling in forest ecosystems after anthropogenic disturbances - case studies at long-term atmospheric polluted and at post-mining sites. Cottbuser Schriften zu Bodenschutz und Rekultivierung, 24, 1-161.

Schaaf, W. and Hüttl, R. F., 2005: Soil chemistry and tree nutrition of restored post-mining sites. Journal of Plant Nutrition and Soil Science, 168, 483-488.

Schaaf, W., 2001: What can element budgets of false-time series tell us about ecosystem development on post-lignite mining sites? Ecological Engineering, 17, 241-252.

Schlichting, E., Blume, H. P. and Stahr, K., 1995. Bodenkundliches Praktikum. Pareys Studientexte 81.

Weisdorfer, M. 1999: Einfluss unterschiedlicher Schwefel- und Stabimmissionen in der Vergangenheit auf die chemische Entwicklung von Humusauflagen und Mineralböden in Kiefernwaldökosystemen im nordostdeutschen Tiefland. Cottbuser Schriften zu Bodenschutz und Rekultivierung 4, 214pp.

Acknowledgements

We thank our field technicians Ralph Dominik, Marin Dimitrov, Silvio Voigt and PhD student Claudia Zimmermann for their active help during excavation and installation of the soil pits and sampling units. Together with our students Gunter Bormann, Uwe Enke and Rossen Nenov they also are responsible for routine sampling and maintenance of the field equipment. We thank the lab team at the Chair of Soil Protection and Recultivation, BTU Cottbus (Gabi Franke, Regina Müller, Helga Köller, Evi Müller and Anita Maletzki) for the professional and reliable analysis of the many samples together with our student helpers Nonka Markova, Tzvetelina Dimitrova and Natasha Beltran. Microscopic and REM analyzes of the crust samples were done at the Central Analytical Lab of the Faculty of Environmental Science and Process Engineering (BTU) by Thomas Fischer and Wolfgang Wiehe.

6. Soil water

Detlef Biemelt[1], Maik Veste[2]

[1] Brandenburg University of Technology Cottbus, Chair of Hydrology and Water Resource Management

[2] Brandenburg University of Technology Cottbus, Research Center Landscape Development and Mining Landscapes

6. 1 Introduction

The main part of the Chicken Creek catchment is formed by a large water storage body composed of Quaternary sediments (Gerwin et al. 2009). The water storage capacity and water transport characteristics are important regulators of the catchment water balance. Since direct measurements of soil water fluxes are not possible, fluxes have to be calculated from matrix potential and soil moisture measurements in combination with substrate properties using soil water flux models. High temporal resolutions of the measurements allow detection of soil water changes and are important calibration and validation data for these models.

Water transport occurs in the pore system of the soil. The relations between the pore size distribution, the resulting matrix forces and the soil water content are characterized by the retention function (h-θ-diagram). Measurements of matrix potential (h) and water contents (θ) are therefore necessary to derive this function.

6. 2 Material and Methods

Four permanent soil pits (Fig. 6.1) with a diameter of 1 m were installed in the catchment close to the grid points C5 (pit C), F2 (pit F), I5 (pit I) and L2 (pit L) as described in Chapter 5. The advantage of the pit installations are the reduction of disturbances of the soil surfaces during installation and maintenance, easier installation of cables and the reduced space requirements compared to above ground installation. Furthermore, the pits ensure permanent access to the unsaturated zone.

Fig. 6.1: One of the soil pits with manual drilling for tensiomter installation.

Tensiometers of the type T4 from UMS München, Germany (von Unold 2009) are used to measure matrix potential. The tensiometers have a limited measuring range up to approx. 800 hPa due to air entry into the porous ceramic at higher pressure and can be refilled in situ. In each pit one tensiometer was installed in 30 cm, and three in 50 cm, 80 cm and 150 cm soil depth, respectively. In pit C and I no tensiometers were installed in 150 cm depth due to high ground water levels. Holes of 2 cm diameter were manually drilled carefully to minimize disturbance of the soil structure (Fig. 6.1). The tensiometers were inserted in an angle of 30º and the boreholes were refilled with the original material. The three tensiometers in the lower depths (pit C and I in 50 cm and 80 cm, and in pit F and L in 80 cm and 150 cm depth) were installed displaced along the main slope of the catchment with a distance of 100 cm (Fig. 6.2).

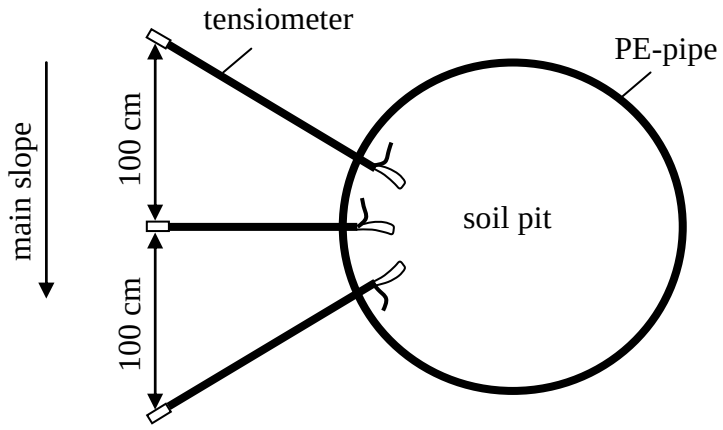

Fig. 6.2: Top view of tensiometer arrangement from pit.

Soil water content is measured with FD-probes (Theta-Probes Soil Moisture Sensor ML2x, Delta-T Devices 2009a). The antennas of the FD-probes were installed horizontally at 10, 30, 50 and 80 cm soil depth with a core drill of 5 cm diameter and 50 cm length at all four pits. The FD-probes were compressed into the sediment with a second tube (Fig. 6.3) and the core was refilled. The spaces between the sensor and the edge of the borehole in the Polyethylene shaft were closed with soft plastic. A substrate-specific calibration of the Theta-Probes was not necessary, because the substrate properties showed no specific characteristics with respects to soil organic matter, bulk density and salt content. Tests of the sensors with the four substrate samples from the pits did not improve the standard calibration setting.

Soil temperature is measured with PT-100 sensors at 10, 30, 50 and 80 cm depth in all pits.

All measured data of the tensiometers, FD-probes and soil temperatures are recorded in hourly intervals with one data-logger (DL2e, Delta T-devices 2009b) per soil pit. The sensor datasets are labeled LSSSSttt n, with

L: label of the observation pit (C, F, I, L);

SSSS: identifier for the sensor type (temperature: ("Botm", tension: "Ten", water content: "BFeu", water level, "Pegel");

ttt: soil depth in cm (10, 30, 50, 80, 150);

n: sensor number per depth (1, 2, 3) .

Fig. 6.3: Installation of FD-probes at one of the soil pits.

To cover the spatial variation of soil moisture contents PR2/6 Profile Probes (Delta-T Devices 2009c) are used in access tubes inserted into pre-augered holes. The tubes have special thin walls build from glass-fibre reinforced plastic (GRP) with an outer diameter of 28 mm, which maximise the penetration of the electromagnetic field into the surrounding soil. The probes measure simultaneously at 6 depths down to 1 m (10, 20, 30, 40, 60 and 100 cm). The accuracy is ±6 % with a generalised soil calibration in normal soils. The data are stored on a portable reading unit (HH2, Delta-T Devices 2009c) and transferred to a personal computer for further data analysis. The soil moisture data are collected at 16 grid points (C2, C4, C6, F2, F4, F6, I2, I4, I6, L2, L4, L6, N2, N6, P2, P6) in intervals of two weeks.

6. 3 Results and discussion

6. 3.1 Soil water content and matrix potential

The amplitudes of changes in soil water contents and matrix potential decrease with increasing soil depths at all four sites (Fig. 6.4 and 6.5). Rapid decreases of the tensions and rapid increase of the soil water contents are closely linked to precipitation events. Surprisingly high water availability could be observed even in the upper soil layers during the entire measuring period. This is in contrast to past experiences with soils of the post-mining landscapes in Lusatia, where tensiometer values frequently were exceeded (> 800 hPa) during summers (Scherzer 2001, Schaaf 2004). This could be not observed at the Chicken Creek catchment until August 2008. Only at soil pit L, tensions increased to several hundreds hPa in 30 cm and 50 cm depths at the beginning of July and August 2008 (Fig. 6.5 L). However, these dry periods were not reflected by the soil water contents (Fig. 6.4 L).

Only at pit C a considerable increase of the matrix potential was measured in 30 cm and 50 cm depths between end of December 2008 and the beginning of January 2009 (Fig 6.5C). At the same time an abrupt decline of the soil water content in 10 cm soil depths was recorded (Fig. 6.4). This was obviously caused by extremely low air temperatures below -10º C and the penetration of frost into the soil (cf. Chapter 2, Fig. 2.8).

Temporarily negative values of tensions (overpressure) were measured in deeper soil layers (pit F, L at 150 cm, pit C, I at 80 cm). Soil water contents rapidly increased in pits C and I at the end of October 2008 indicating a rising groundwater level.

The comparison of the time variation in sensor data from the different pits allows the detection of structural similarities or differences. Another possibility to detect of structural differences are scatter-plots of matrix potential and soil moisture values. The interpretation of these scatter-plots must take into account that the measurements are taken independently with two different sensors at close, but different locations and that under field conditions the recorded data range is small. In addition, hysteresis between drying and re-wetting has to be taken into account.

The tension curves of the three tensiometers in 30 cm and 50 cm depth at soil pit C were similar (Fig. 6.5 C), whereas in 80 cm depth differences between the three sensors could be detected. Soil moisture (Fig. 6.4 C) in 80 cm depth was lower compared to 50 cm depth at the beginning of the measurements. From October 2008 the rising ground water table caused a drastic increase of soil moisture in 80 cm depth. The tensions in 80 cm depth fluctuate around 0 hPa after October 2008, whereas the soil moisture remains permanently on a very high level. This is reflected by two separate clusters in the h-θ-diagram (Fig. 6.6 C).

The scatter-plot for the 50 cm depth data indicates substrate differences compared to 30 cm and 80 cm depth. This is supported by the texture analyses.

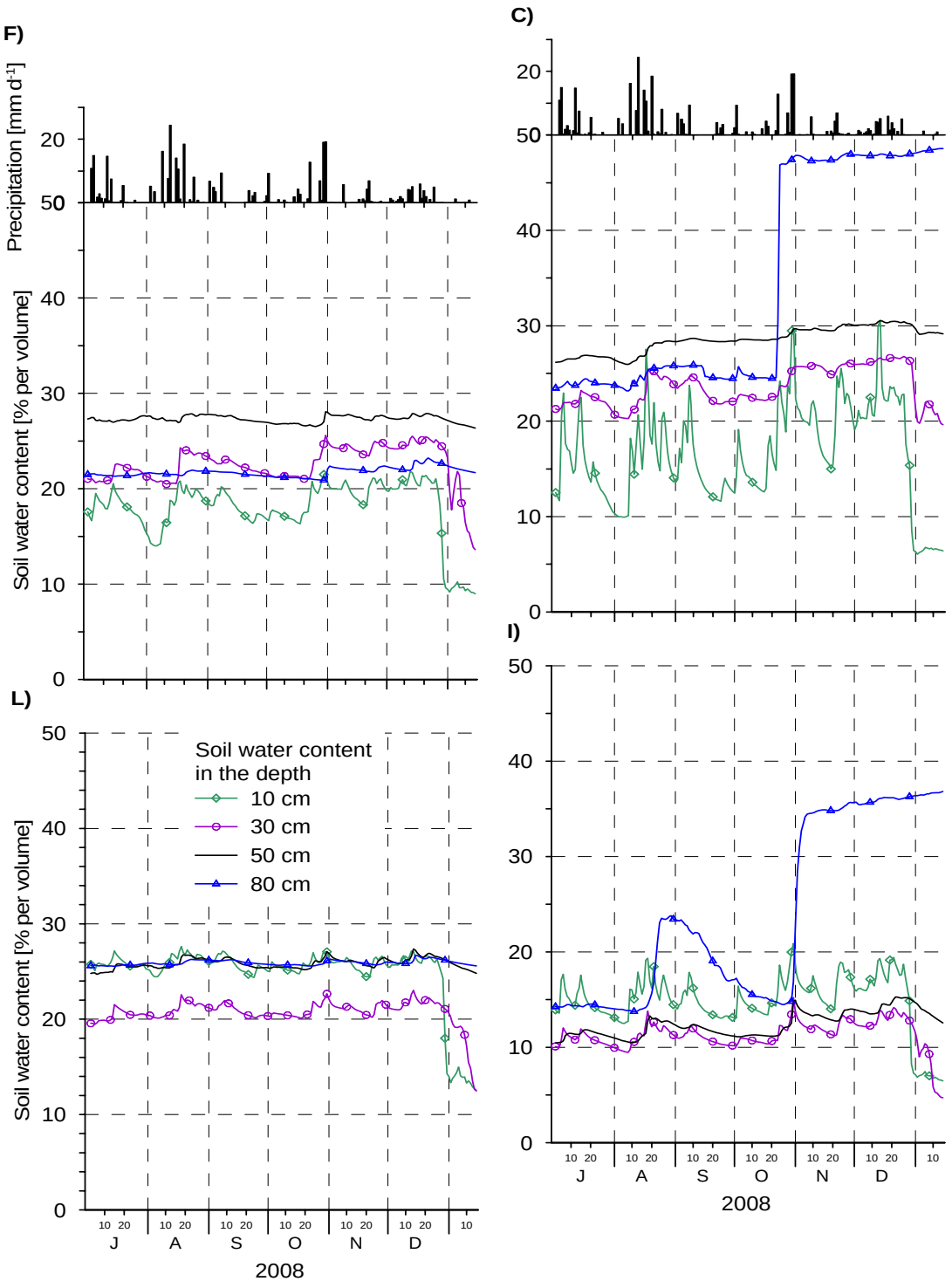

Fig. 6.4: Daily volumetric soil water contents measured at soil pits C, F, I and L. Graphs are arranged according to their position within the catchment (for location see Chapter 1, Fig. 1.2).

The soil moisture at pit F increased with increasing soil depths with the exception of 80 cm (Fig. 6.4 F), whereas the tensions decreased (Fig 6.5 F). The differences of tensions between 30 cm and 50 cm were small during the entire period. The negative tensions in 150 cm depth from mid of December 2008 until mid of January 2009 were caused by the increasing ground water table above the installation level of the tensiometers.

The h-θ-diagram (Fig. 6.6 F) shows for each soil depth a separate scatter-plot with a slight shift with depth towards higher water contents at the same tension. The data indicate a lower heterogeneity of the soil physical properties at pit F compared to pit C.

Although soil texture at pit I is characterized by the highest proportion of sand and lowest of silt compared to the other pits, the tensions showed low values. Even in 30 cm depth tensions were 60 hPa during the summer months (Fig. 6.5). According to this the soil water contents were above field capacity in all soil layers during the entire measuring period.

The sensors per depth showed very little variation and tensions decreased with increasing soil depth (Fig. 6.5 I).

Mean soil water contents generally increase with depth (Fig. 6.4 I) except for 10 cm depth. The low and negative tensions and the high water contents in 80 cm soil depths clearly indicate water saturation due to rising of the ground water from October 2008.

The h-θ-scatter plots for all soil depths are similar (Fig. 6.6 I). The data indicate relatively homogeneous soil conditions at pit I. The relative wet conditions at pit I were not expected due to the high proportion of sandy material. Apparently the sandy zone in the surrounding of pit I is affected by substrate with lower conductivity, which reduces water flow downstream and results in a high ground water table around pit I.

At pit L the tensions at 30 cm and 50 cm were in a similar range (Fig. 6.7 L) and decrease towards lower depths. Soil mositure values at 10, 50 and 80 cm were at very similar levels. Only at 30 cm depth considerably lower soil moisture values were recorded. Also the tensiometers indicate drier conditions at 30 cm and 50 cm in July and August 2008 (Fig. 6.5 L). The steep retentions curves might give an explanation for this exceptional behaviour as shown in the h-θ-scatter plot (Fig. 6.6 L). At 30 cm depth an outlier in the scatterplot indicate soil frost. The tensiometer measurements indicate relatively homogenous conditions at pit L.

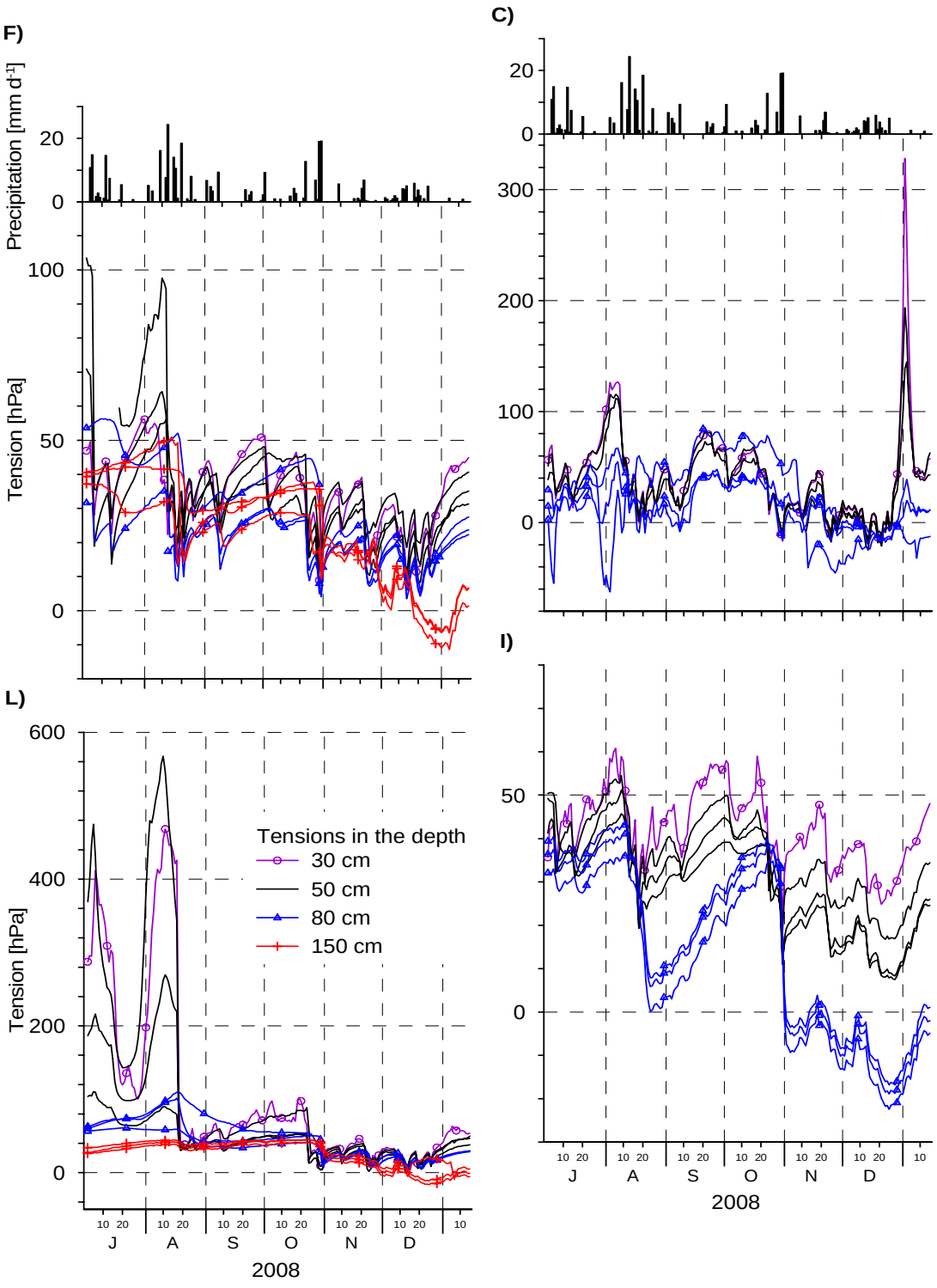

Fig. 6.5: Daily soil water tensions measured at soil pits C, F, I and L.

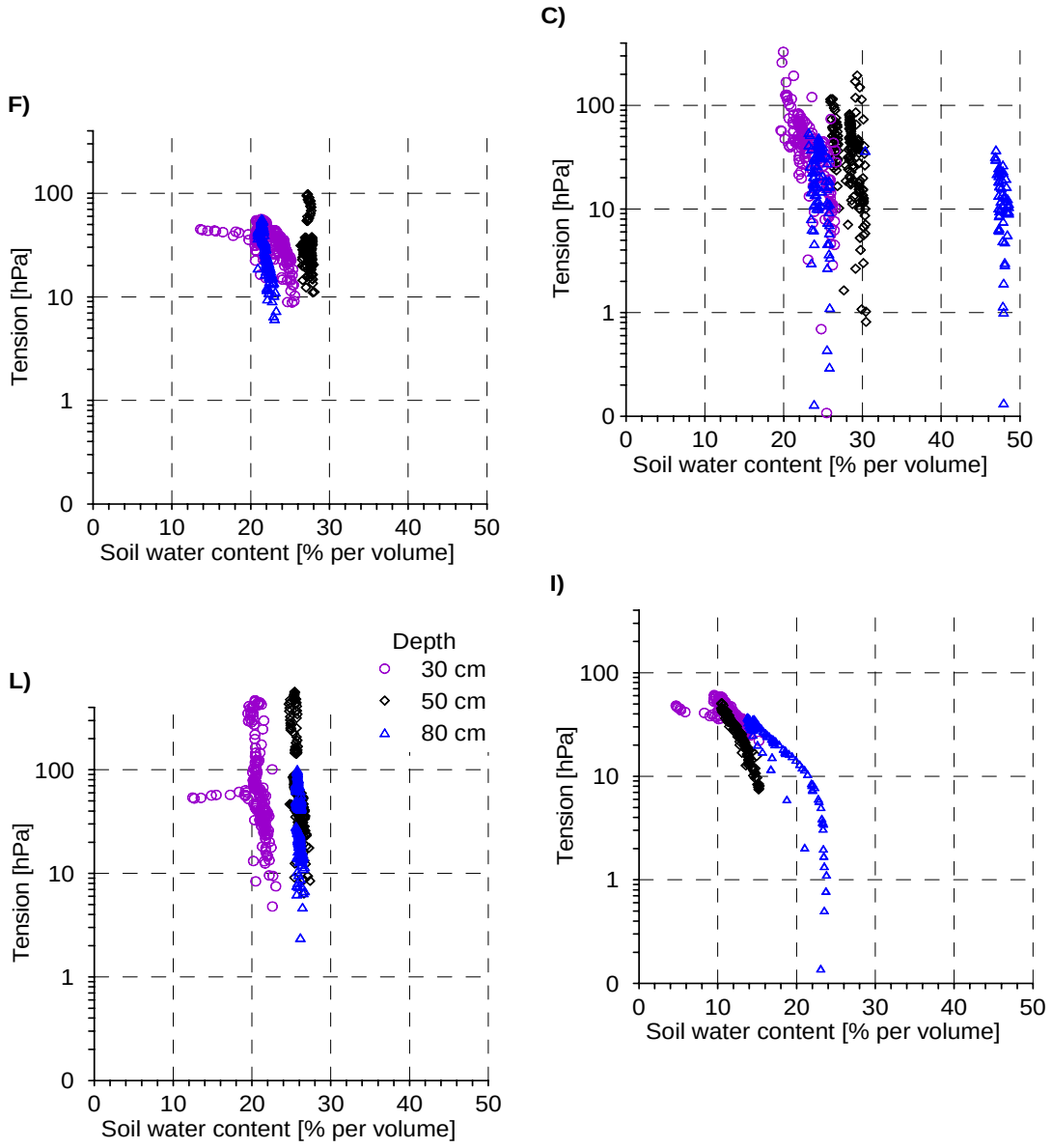

Fig. 6.6: Scatter plot of volumetric soil water contents and tensions at soil pits C, F, I and L.

6. 3.6 Relation between the soil water budget and groundwater level

The simultaneous measurements of the groundwater level and the matrix potential in the unsaturated zone allows for the characterization of the hydraulic equilibrium between the soil water and the groundwater. The distance between groundwater level and tensiometer depth is plotted versus the tension (Fig. 6.7). For pit C the tensiometer values at 50 cm and 80 cm depth were only sometimes parallel with the distance of the groundwater table. The same was found for 150 cm depth at pit F. Data from pit L indicate a hydraulic equilibrium between tension in the soil and the groundwater level during the entire measuring period in 150 cm as well as for pit I at 80 cm and partly at 50 cm.

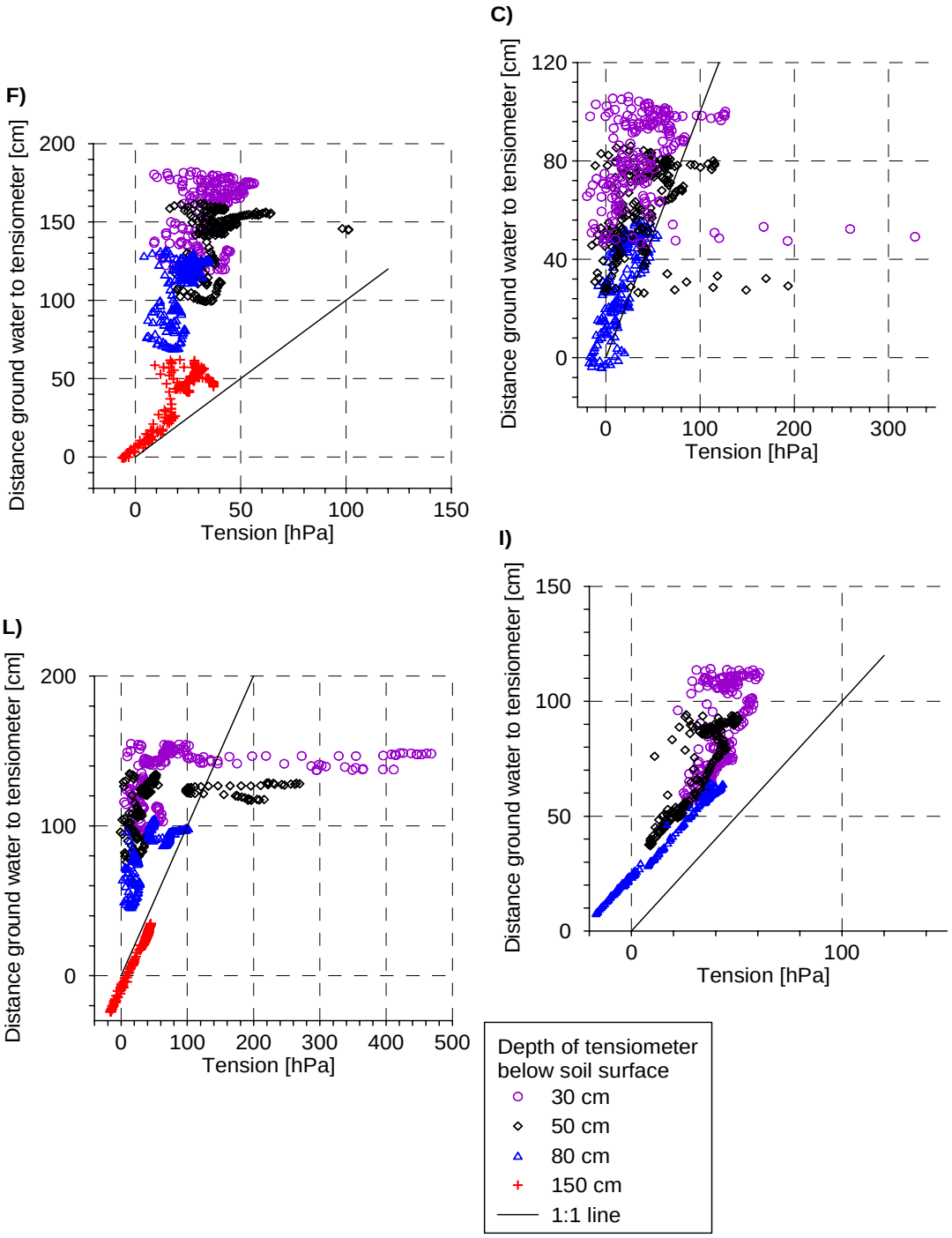

Fig. 6.7: Scatter plot of tensions and distances of groundwater levels to installation depths of tensiometers at soil pits C, F, I and L.

6. 3.7 Spatial variations of soil moisture

The spatial variations of the soil moisture content measured bi-weekly with the PR2-probes are shown in Fig. 6.8-6.10. Soil water contents increased with soil depths at all investigated sites, while amplitudes decreased. In general, the soil moisture follows the rainfall regime and indicates infiltration of precipitation into the soils. The Theta probes in the soil pits provide a more detailed time resolution of the wetting and drying processes compared to the PR2-probes. Furthermore, the lower accuracy of ±6 % of the PR2 probe limits the interpretation of spatial differences of the soil moisture regime and the comparison with the Theta-probes.

6. 4 Conclusions

The matrix potential and soil moisture data for 2008 give first information of soil water relations at the four measured soil profiles in the Chicken Creek catchment. The results show at all investigated soil depths unexpected low tension values and high water contents indicating high soil water availability for higher plants. This might be an important factor for the establishment of vegetation, pattern formation, and succession in the catchment (see also Chapter 7). Deep rooting species, especially the already established black locust trees (*Robinia pseudacacia*), might benefit from this favourable water availability and may alter the vegetation development compared to areas which are more affected by drought periods. Soil water availability was improved by high groundwater levels up <1.5 m and 0.8 m below surface in the western and in the eastern parts of the catchment, respectively. Soil moisture values above field capacity were locally observed down to greater depth during the entire observation period at the eastern site of the catchment. Clear differences of the substrate can be found in the surrounding of soil pit C. The time series can be used for the calibration of water balance models at the Chicken Creek catchment.

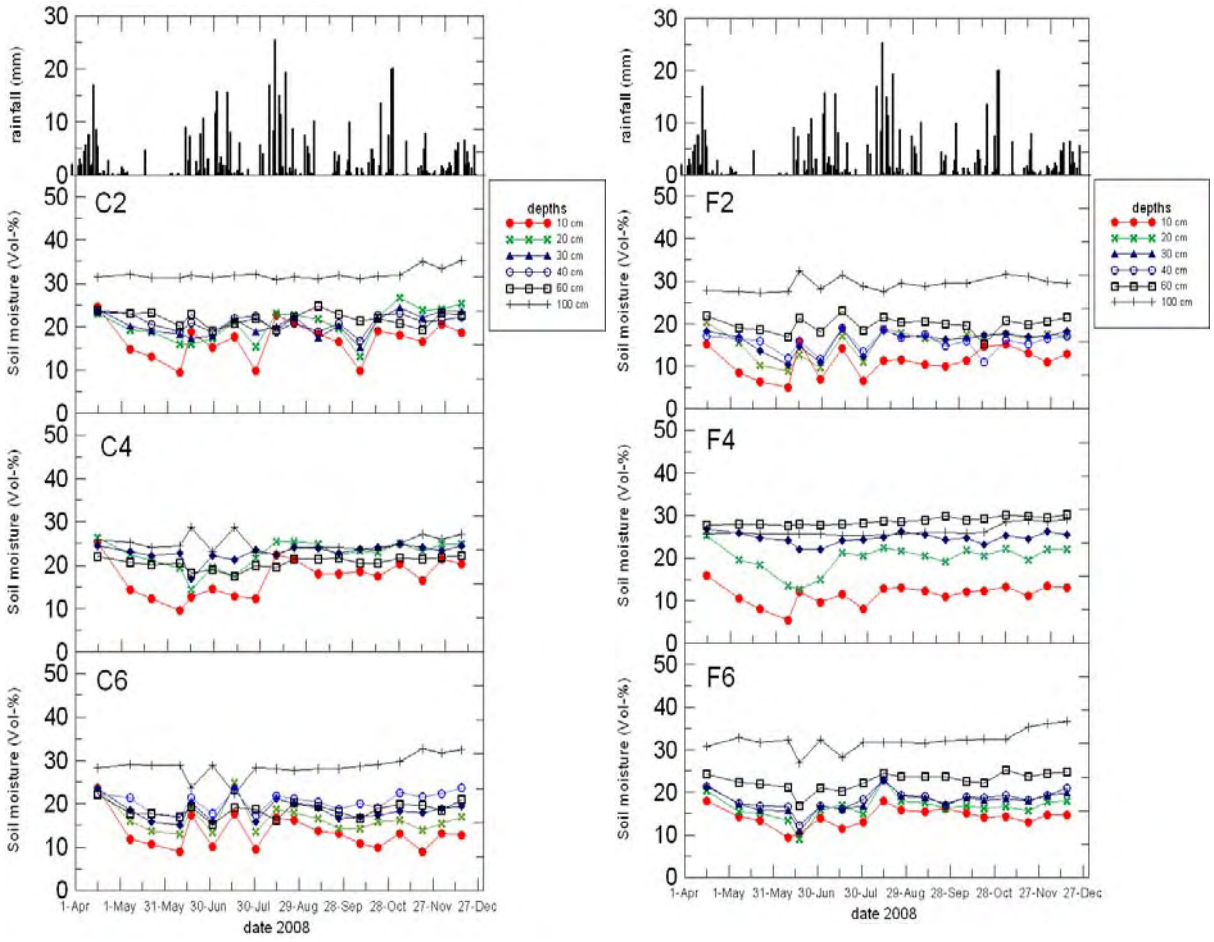

Fig. 6.8 Rainfall and soil moisture measured at grid points C2, C4, C6, F2, F4, and F6 from April 15th to December 16th, 2008 (for locations see Chapter 1, Fig. 1.2).

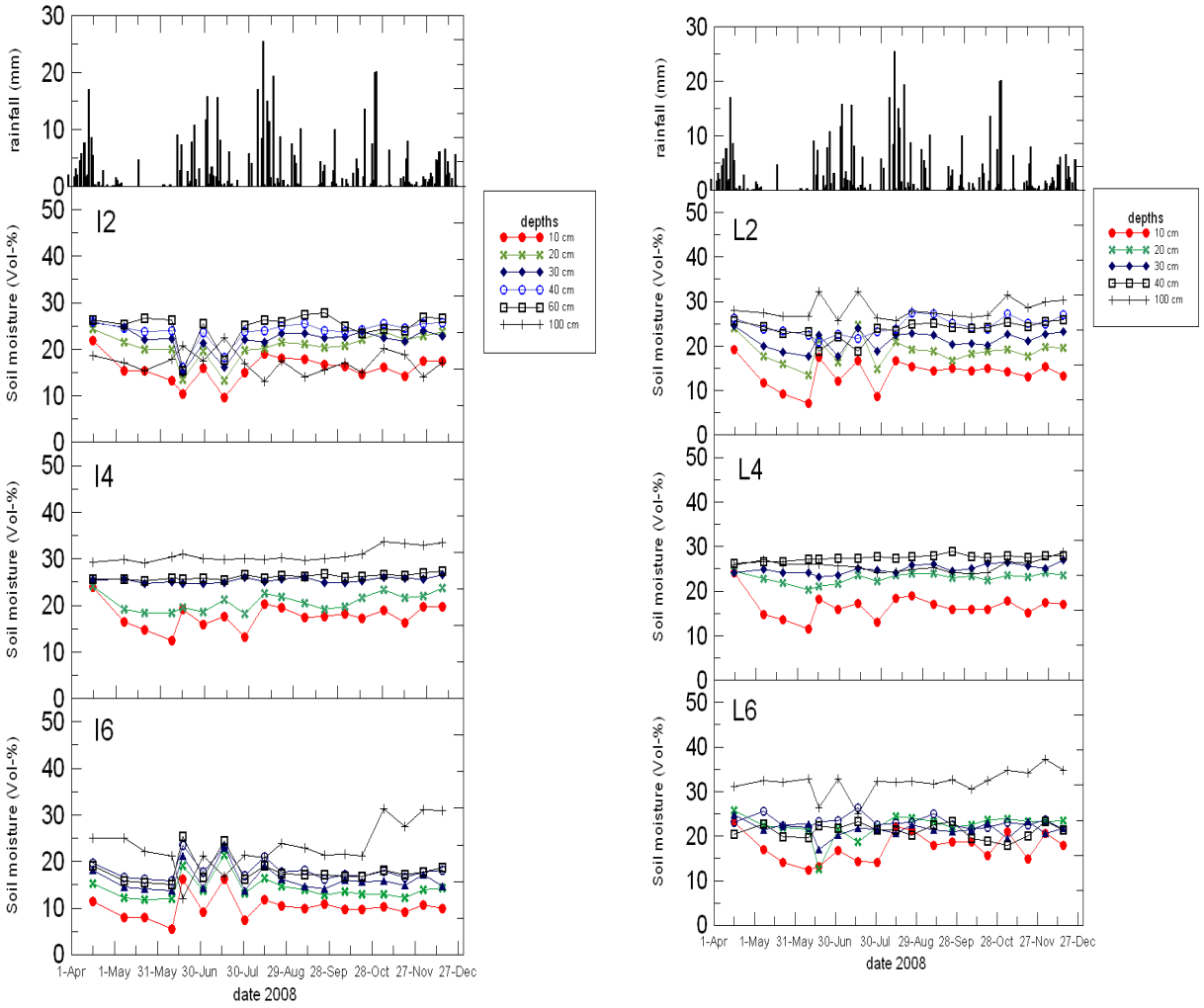

Fig. 6.9: Rainfall and soil moisture measured at grid points I2, I4, I6, L2, L4, and L6 from April 15th to December 16th, 2008 (for locations see Chapter 1, Fig. 1.2).

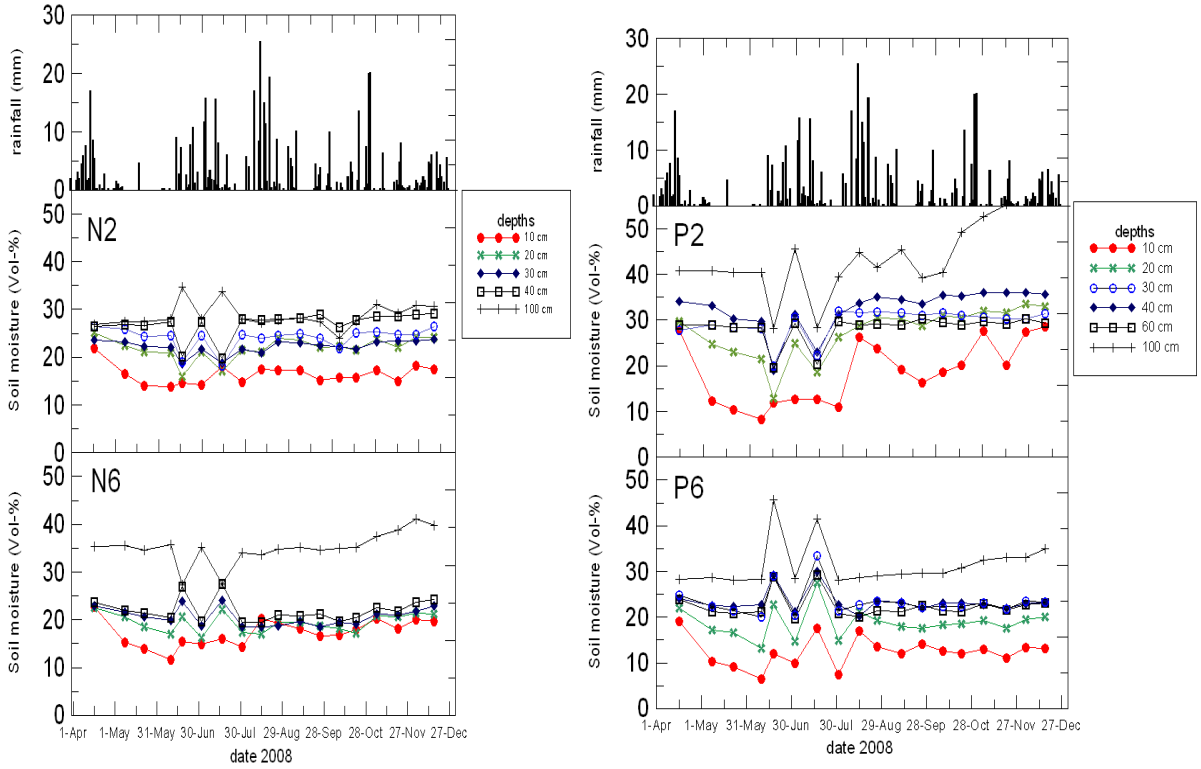

Fig. 6.10: Rainfall and soil moisture measured at grid points N2, N6, P2, and P6 from April 15th until December 16th, 2008 (location see Chapter 1, Fig. 1.2).

References

Delta-T Devices, 2009a. ThetaProbe Soil Moisture Sensor - ML2x. Internet presentation of Delta-T Ltd. Company, UK, http://www.delta-t.co.uk/products.html?product2005092818876, October 7th, 2009.

Delta-T Devics, 2009b. Data logging. Online-Publication. Internet presentation of Delta-T Ltd. Company, UK, http://www.delta-t.co.uk/data-logging.html. October 7th, 2009.

Delta-T Devics, 2009c. User Manual for the Profile Probe type PR2. Online-Publication.

Gerwin, W., Schaaf, W., Biemelt, D., Winter, S., Fischer, A., Hüttl, R.F., 2009. The artificial catchment "Chicken Creek" (Lusatia, Germany) - A landscape laboratory for interdisciplinary studies of intial ecosystem develoment. Ecological Engineering, in press, doi:10.1016/j.ecoleng.2009.09.003

Schaaf, W., 2004. Development of element cycling in forest ecosystems after anthropogenic disturbances – case studies at long-term atmospheric polluted and at post-mining sites. Cottbus Schriften zu Bodenschutz und Rekultivierung, Band 24.

Scherzer, J., 2001. Der Wasserhaushalt von Kiefernforsten auf Kippböden der Niederlausitz; Dissertation; Cottbuser Schriften zu Bodenschutz und Rekultivierung, Band 16.

von Unold, G. 2009. T4 Tensiometer. Internet presentation of UMS GmbH, München, Germany. http://www.ums-muc.de/produkte/tensiometer/t4.html, October 20th, 2009.

http://www.delta-t.co.uk/cgi-bin/attach.cgi?item=faq2005092821658. October 2nd, 2009.

7. Vegetation dynamics

Markus K. Zaplata, Anton Fischer, Susanne Winter

Technische Universität München, Department of Ecology and Ecosystem Sciences

7. 1 Introduction

After its completion in autumn 2005, the 6-ha "Chicken Creek" artificial catchment area (Brandenburg, Germany; for description of the construction see Gerwin et al., 2009) was left for unrestricted ecosystem development to investigate outcomes at the landscape scale. Concerning vegetation, an ongoing monitoring program and a succession experiment were established.

Succession models differ in respect to species establishment (Connell and Slatyer, 1977). Among the succession models, the facilitation, tolerance and inhibition models are most common. In the facilitation model of succession the change in plant species dominance over time is caused by modifications of the abiotic environment that are imposed by the developing community itself. While early successional species alter the growing conditions and the availability of resources, they "facilitate" (support) the growth of later successional species by making the environment more suitable for them. This model is appropriately used if initial conditions are rather severe and should only be applied to primary succession. In the two other models the focus lies on the mechanisms of competition: In the tolerance model of succession later successional species are able to tolerate lower resource levels. In the inhibition model of succession some early species make the habitat less suitable for the development of others, but in the long run species with longer life spans will prevail.

In this regard the following central hypotheses should be tested:

- H1: The first established individuals and species set the medium-term successional pathways. This fact implies that the initial colonization events of a progressive succession are relevant for the subsequent development. Therefore, it is important to have a detailed knowledge of the exact initial floristic situation at the very beginning of the development, at "the zero point" (approaches: analyzing the quality and quantity of an *initial* soil seed bank; seed rain analysis).
- H2: Mechanical disturbances of the vegetation cover alter the establishment and growing conditions of the plant species and will result in the vegetation returning to the initial state. We expect a patchy mosaic of regeneration niches in the catchment area to grow apart over the years. The first species that colonize will find some – possibly alternating – retreat areas, whereas progressive succession occurs in other parts (approach: analysis of developing vegetation on permanent plots).

The investigations of the vegetation comprise the analyses of (1) the soil seed bank, (2) the seed rain and (3) the vegetation development. The main research questions are:

- Soil seed bank: Was the soil completely free of diaspores at the beginning of the vegetation succession? If not, how many species and seeds formed an initial soil seed bank after completion of the catchment area?
- Seed rain: Is an input of seeds from the surroundings of the catchment area detectible? What effect does the initial seed rain have on the vegetation succession?
- Vegetation development: How does colonization proceed? Which plant species occur when, where, and to what extent? Do they form particular patterns? Regarding the patterns, are interconnections to abiotic or biotic aspects of the setting detectible, and, if so, which spatial scales are relevant?

The three aforementioned succession models will be analyzed, based on these results. Which model is able to best describe the ongoing development? Is it time for developing new models?

7. 2 Material and methods

7. 2.1 Soil seed bank analysis

Immediately after the catchment area had been constructed, a soil seed bank analysis was carried out ("seeds" in the sense of "diaspores" = "disseminules" = "generative propagules"). This fact allows an insight into the floristic potential at "the zero point" (see explanations to H1).

In October 2005, soil samples (108) were collected from a depth of 2-12 cm in a 20 m x 20 m grid (Fig. 7.1). The top 2 cm were omitted to avoid contamination by any wind-transported seeds. Each soil sample had a volume of 10 cm x 10 cm x 10 cm. Immediately after transport to the laboratory (TUM, Freising), each soil sample was spread as a thin layer on heat-sterilized sand in 28 cm x 46 cm plastic bowls. These bowls were exposed in a greenhouse in a random order which was changed randomly several times during the period of exposure to avoid heterogeneous growth conditions. The greenhouse was equipped with gauze protection to avoid infiltration of wind-transported seeds (Fig. 7.2). The samples were irrigated automatically.

New seedlings were determined as soon as possible (seedling emergence method; Fischer, 1987; Thompson, 1996) with the additional help of literature for seed determination (Csapody, 1968). Using this method, emerging seedlings indicate *viable* seeds in the analyzed soil substrate, thus, providing the ecological significance, in contrast to filtering-and-counting methods (for more details see Fischer, 1987). When species identification was impossible just after germination, the seedlings were transplanted to pots and were cultivated until the species characteristics were well-developed. Transplanting was necessary because the collected soil material as well as the sterile subsoil material of the bowls were extremely poor in nutrients, thus, putting plant survival at risk.

In order to optimize germination success, the soil samples were exposed for two vegetation periods (from October 2005 to August 2007). Some plant species essentially require either frost or a considerable temperature change to overcome dormancy. Therefore, the samples stored in plastic bags, were exposed to field climate conditions in a fenced area outside the greenhouse (6 January to 28 February 2006; 23 to 29 January 2007, both periods included several days with temperatures below 0 °C, with a minimum temperature of -13.5 °C). During the time of exposure in the greenhouse, the soil material was carefully dug several times a year to impair the establishment of bryophytes carpets and to support the seeds in getting enough radiation to start germination.

7. 2.2 Seed rain analysis

Plants use a number of different transportation facilities to spread their seeds, e.g. wind (anemochory), animals (epizoochory and endozoochory), humans (hemerochory) and water (hydrochory) (Müller-Schneider, 1983; Bonn and Poschlod, 1998; Leins and Erbar, 2008). For hydrochory running water is needed which is inapplicable for the study site, as longitudinal water transport into a catchment area is excluded by definition. Animals or humans as vectors were not analyzed. We investigated the transport by wind. A review on seed rain analysis methods is given by Fischer (1987).

We installed specific traps in order to catch wind-transported seeds. Each trap consisted of a disposable Petri dish, ca. 15 cm in diameter, with a filter paper, brushed with bag balm on the lower side, in order to attach it to the Petri dish, and on the upper side, in order to trap the diaspores. The whole trap was attached with a screw on a picket at a height of 30 cm (Fig. 7.3). Altogether there were 55 trap positions along the catchment area fence with 20 m distance between trap positions (Fig. 7.1). An exposure event was finished with the removal of the complete trap. A few traps failed, in respect that they broke or the filter paper blew away.

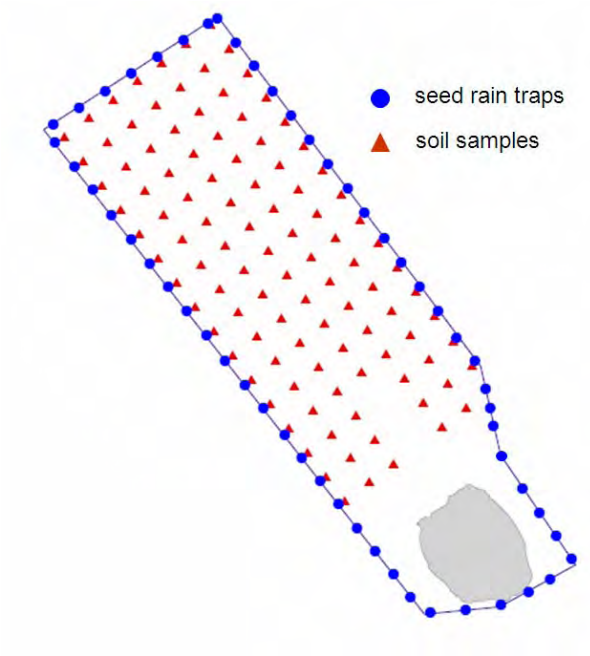

Fig. 7.1: The Chicken Creek artificial catchment area. Triangles: regular 20 m x 20 m grid to collect soil samples for analyzing the soil seed bank. At these grid points permanent plots for recording the vegetation development were also established (upper part). Circles: seed trap spots for the seed rain analysis.

Fig. 7.2: Soil seed bank analysis: collected soil samples from the Chicken Creek in a gauze-shielded greenhouse in Freising (photo: S. Winter, October 2005).

In the first campaign, we analyzed seed rain from October 2005 to September 2006, changing the seed rain traps roughly once a month. This first exposure campaign comprised 16 trap replacements. A second campaign started in August 2008 and will last for 12 months (Tab. 7.1). For seed determination we used data from the literature (Bertsch, 1941; Hanf, 1990) as well as a reference seed collection. Without a germination test it was not possible to separate living seeds from dead ones, so they were all considered as living. Seed fragments were not considered.

Tab. 7.1: Dates of the seed trap replacement. In brackets: start of exposure.

Year	Dates of seed trap replacements											
2005	(11.10)		18.10	02.11	23.11	13.12						
2006	11.01	01.02	23.02	06.04	27.04	19.05	02.06	29.06	18.07	04.08	21.08	20.09
2007	-											
2008	(01.08)		17.08	19.09	23.10	25.11	… ongoing …					

Fig. 7.3: Seed traps exposed at the edge of the Chicken Creek catchment area (photo: A. Fischer, December 2005).

7. 2.3 Plant species and growth patterns

Since 2005, the developing vegetation of the study site was recorded (Tab. 7.2). Assessment plots are assigned to the regular grid (20 m x 20 m; Fig. 7.1 for 2005, from 2006 onwards additional plots were established in the lower part). Each grid point is permanently marked by a flag denoting the centre of a quadrate plot of 25 m², with each of the four corners marked by an aluminum post (with a total height of 0.5 m, of which about 0.1 m is above ground). In addition, a plot of 1 m² was established at each corner. The monitoring program is, therefore, based on a nested plot design with one 25 m² plot at each grid point including four 1 m² plots (Fig.s 7.4 and 7.5).

For the recording of the vegetation on the 1 m² plots, we used an aluminum square meter frame, which we put over the posts during the assessment to clearly define the border lines (Fig. 7.6). In 2005, the vegetation was directly assessed, after finishing the construction works in the catchment area, but only in the 1 m² plots of the upper part.

Vegetation records included:

- the plant species for each plot;
- the cover degree for each species according to Londo (1975, modified) for each plot (Tab. 7.3);
- the individual number of each species growing on the north-eastern 1 m² plots.

Undetermined individuals were not considered. We assumed that most of them were less developed individuals of already recorded species. In our vegetation database retraceability was provided by replacement characters.

Tab. 7.2: Dates of the vegetation records and number of plots recorded.

The total number of recorded plots varied mainly due to the fluctuating water level of Chicken Creek Pond. In 2005 there are two exceptions: plots existed only in the upper part, only 1 m² plots were recorded.

Year	Time of vegetation assessment	number of 25 m² plots recorded	number of 1 m² plots recorded
2005	10. - 11.10.	0	360
2006	07. - 08.08.	119	474
2007	22. - 25.07.	120	473
2008	20. - 31.07.	119	473

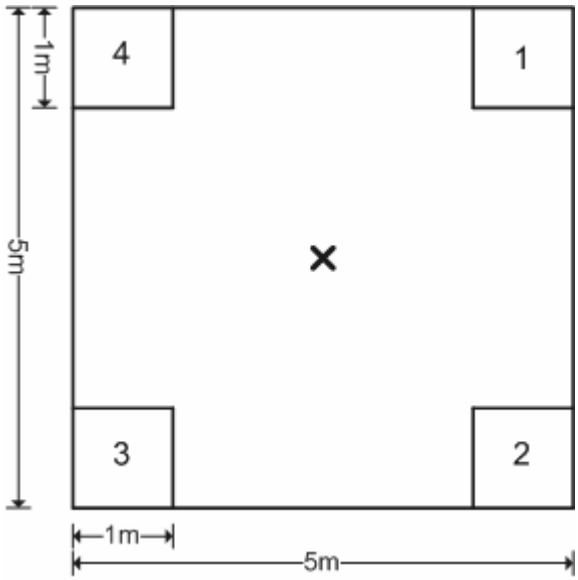

Fig. 7.4: Scheme of the nested plot design. The “x” in the centre represents the grid point; its position is marked by a metallic flag. Note the north-eastern 1 m² plot (no. 1), where the individuals of the occurring species are counted.

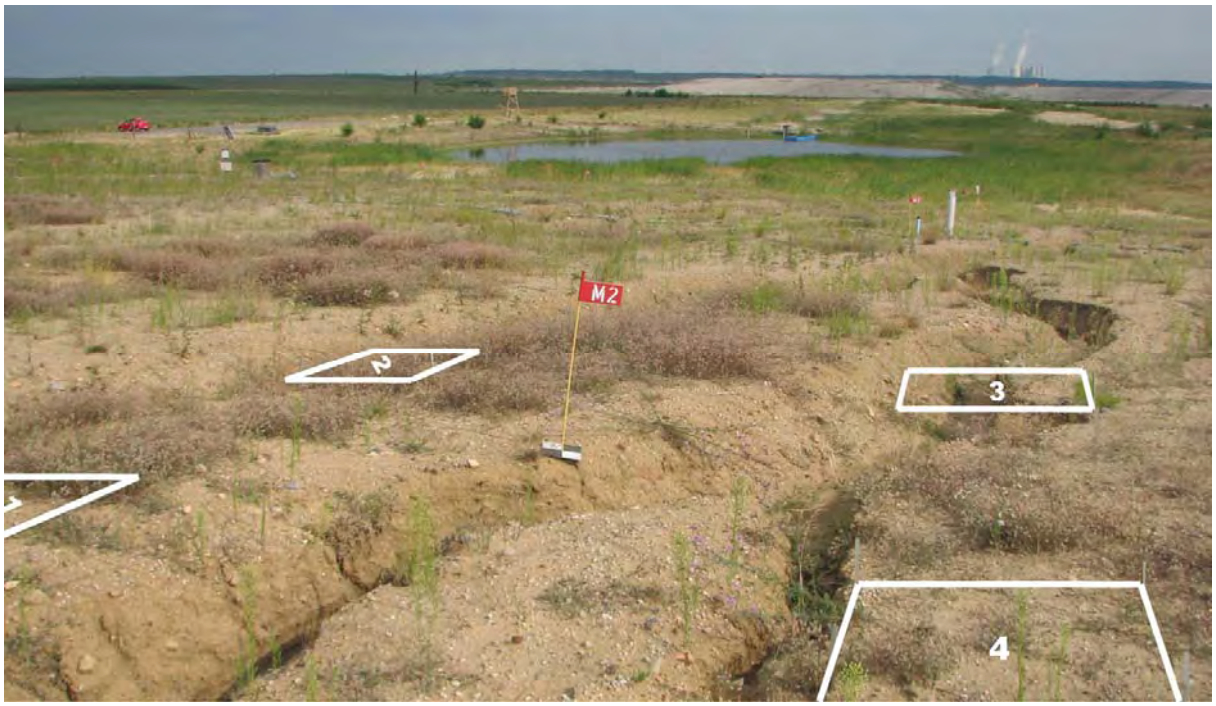

Fig. 7.5: An overview of the plots at grid point M2 (photo: M. Zaplata, July 2008). The positions of the 1 m² plots are marked (no. 1 to 4).

Fig. 7.6: Square meter frame for the vegetation record at the 1 m² plots. The sparse vegetation here consists of *Conyza canadensis* and *Filago arvensis* (photo: M. Zaplata, July 2008).

Tab. 7.3: Vegetation cover assessed by 23 distinct percentage classes following Londo (1975), modified.

-	6 %	30 %
0.1 %	7 %	40 %
0.5 %	8 %	50 %
1 %	9 %	60 %
2 %	10%	70 %
3 %	15 %	80 %
4 %	20 %	90 %
5 %	25 %	100%

7. 3 Results and discussion

7. 3.1 Soil seed bank analysis

A total of 146 seedlings emerged from the 108 soil samples (1000 cm³ each). This is equivalent to 135 seeds per m² and 10 cm soil depth (Tab. 7.4). Considering that seeds usually germinate only in the upper (undisturbed) millimetres, the germination potential was about 15 plants per m².

Because the soil nutrient content was poor (Gerwin et al. 2009), during the exposure period in the greenhouse, one-third of the emerging seedlings did not grow to a size that allowed the seedling species to be determined. Most germinated seeds (58 %) belonged to *Conyza canadensis*. Further detected species were *Fragaria vesca*, *Luzula multiflora*, and *Moehringia trinervia*. All these species were represented in the study area.

The invasive Asteraceae *Conyza canadensis* has created the principal vegetation aspect since 2006; in late 2008 it still dominated the eastern part of the Chicken Creek catchment area (see Fig. 7.11).

Tab. 7.4: Initial soil seed bank of the Chicken Creek catchment area (108 soil samples, each 10 cm x 10 cm x 10 cm).

Species	Seedlings emerged	
	total no.	no./m² (0.1 m soil thickness)
Conyza canadensis	84	77.8
Hypericum cf *perforatum*	8	7.4
Agrostis/ *Poa* ssp.	5	4.6
Luzula multiflora	4	3.7
Fragaria vesca	2	1.9
Moehringia trinervia	2	1.9
Arenaria serpyllifolia agg.	2	1.9
Cirsium arvense/ *vulgare*	2	1.9
Helichrysum arenarium or *Hierachium* spec.	2	1.9
Erigeron spec. or *Solidago* spec.	1	0.9
cf *Epilobium* spec.	1	0.9
indet	33	30.6
Total	**146**	**135.2**

7. 3.2 Seed rain analysis

Between October and December 2005, in a few (9 out of 219; 4%) traps a total of ten seeds were registered: three *Conyza canadensis*, two *Typha angustifolia*, one *Epilobium* spec., one *Calamagrostis epigejos* and three undetermined grass species (Poaceae).

Between December 2005 and mid-July 2006 a total of 16 seeds belonging to eight species were registered in 14 of the 474 intact traps collected (3%). Nearly half of the seeds belonged to *Chenopodium album* (7). The remaining diaspores belonged to *Betula pendula* (2), *C. canadensis* (1), *Crepis tectorum* (1), *Festuca* spec. (1), Poaceae (1) and two undetermined species (1 and 2).

The seed number increased strongly in 2006 between mid-July and mid-September, totalling 1996 seeds in 131 of 164 traps (80%). One seed caught in this last interval of the first exposure campaign belonged to *Betula* spec., one to *Epilobium* spec., one to a cf. Poaceae species and one to an undetermined species, while the remaining 99.8 percent all belonged to *C. canadensis.* In the last collection of the campaign (mid-August to mid-September) the seed rain reached a maximum of 922 seeds (around 18 per trap; Fig. 7.7).

The species detected and determined as wind transported diaspores are represented in the study area (except for *B. pendula*).

Seed input strongly depended on the trap position. While on the western longitudinal line 20 trap positions caught 178 seeds (mean value per trap spot 7.9, SD 7.3), at the eastern line 23 traps caught 1354 seeds (mean value per trap position 58.9, SD 34.1; factor 6.6; Fig. 7.8).

The prevalent wind-direction at the study site was west-south-west (cf. Chapter 2). The surrounding vegetation includes both recultivation areas and more or less uniformly distributed spontaneous vegetation with *Conyza canadensis*. The data suggest that the disparate seed rain is to assign to the Chicken Creek itself, so concerning *C. canadensis* the Chicken Creek already has become a seed source in the first year of plant succession.

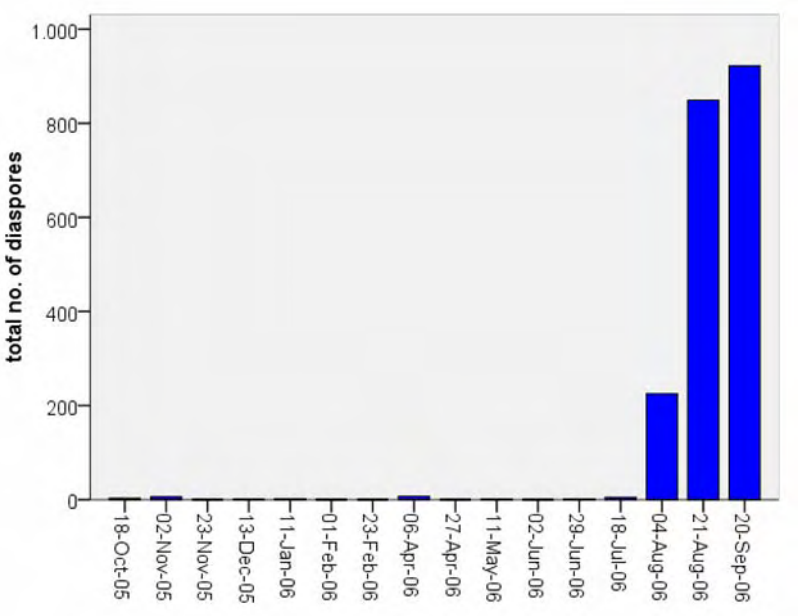

Fig. 7.7: Total number of seeds caught during the first seed trap exposure campaign.

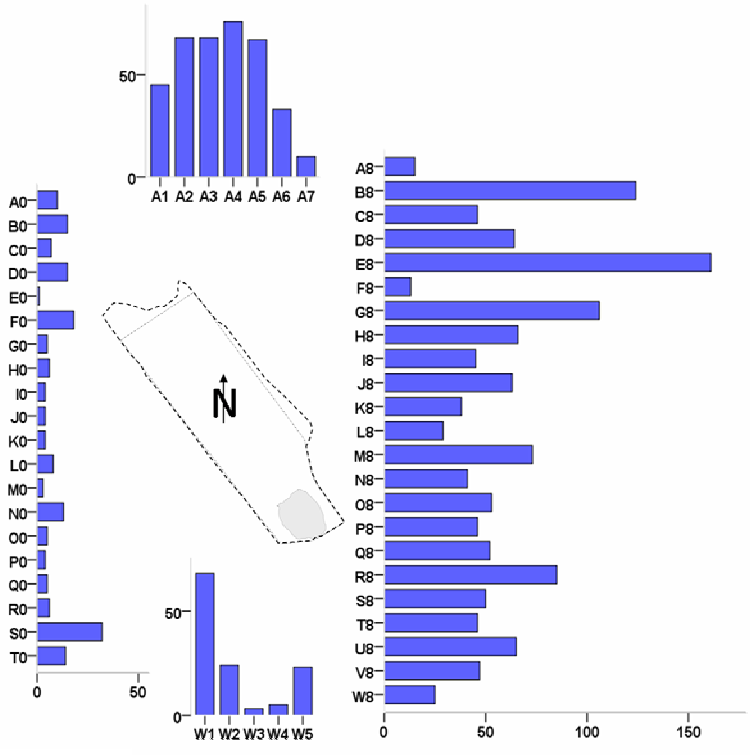

Fig. 7.8: Cumulative seed rain according to trap position.

Traps grouped according to position (A1-A7: northern edge of Chicken Creek, shown in the centre of this Fig.; A0-T0 western edge; A8-W8 eastern edge, W1-W5 southern edge). The lengths of the bars correspond to the total number of diaspores caught per trap position.

7. 3.3 Plant species and growth patterns

Since its constructural completion, a continuing strong increase of cover degree (Tab. 7.5 and Fig. 7.9) and plant species number (Tab. 7.6) has occurred in the Chicken Creek area. Within the plots in the first year (2005) 18 different species were found and in 2008 about 136 (Tab. 7.6, Tab. 7.7). In 2008, the catchment area flora included at least 13 plant species which were solely growing outside the plots: *Berteroa incana*, *Buddleja davidii*, *Campanula rotundifolia*, *Corispermum leptopterum*, *Dactylis glomerata*, *Digitaria* cf. *ischaemum*, *Epilobium angustifolium*, *Galium verum*, *Hippophaë rhamnoides*, *Hypericum humifusum*, *Populus alba*, *Sonchus oleraceus*, and *Trifolium pratense*.

Tab. 7.5: Vegetation cover for the 25 m² plots from 2005 to 2008 (vascular plant species only). For 2005, the interpolations for the 1 m² plots are shown.

Year:	Minimum	25% quartile	Median	75% quartile	Maximum
2005:	0	0	0	0.1	1.5
2006:	0.1	1.3	1.5	2.1	25.4
2007:	1.1	5.4	7.0	9.5	39.3
2008:	2.5	9.5	12.6	16.2	61.9

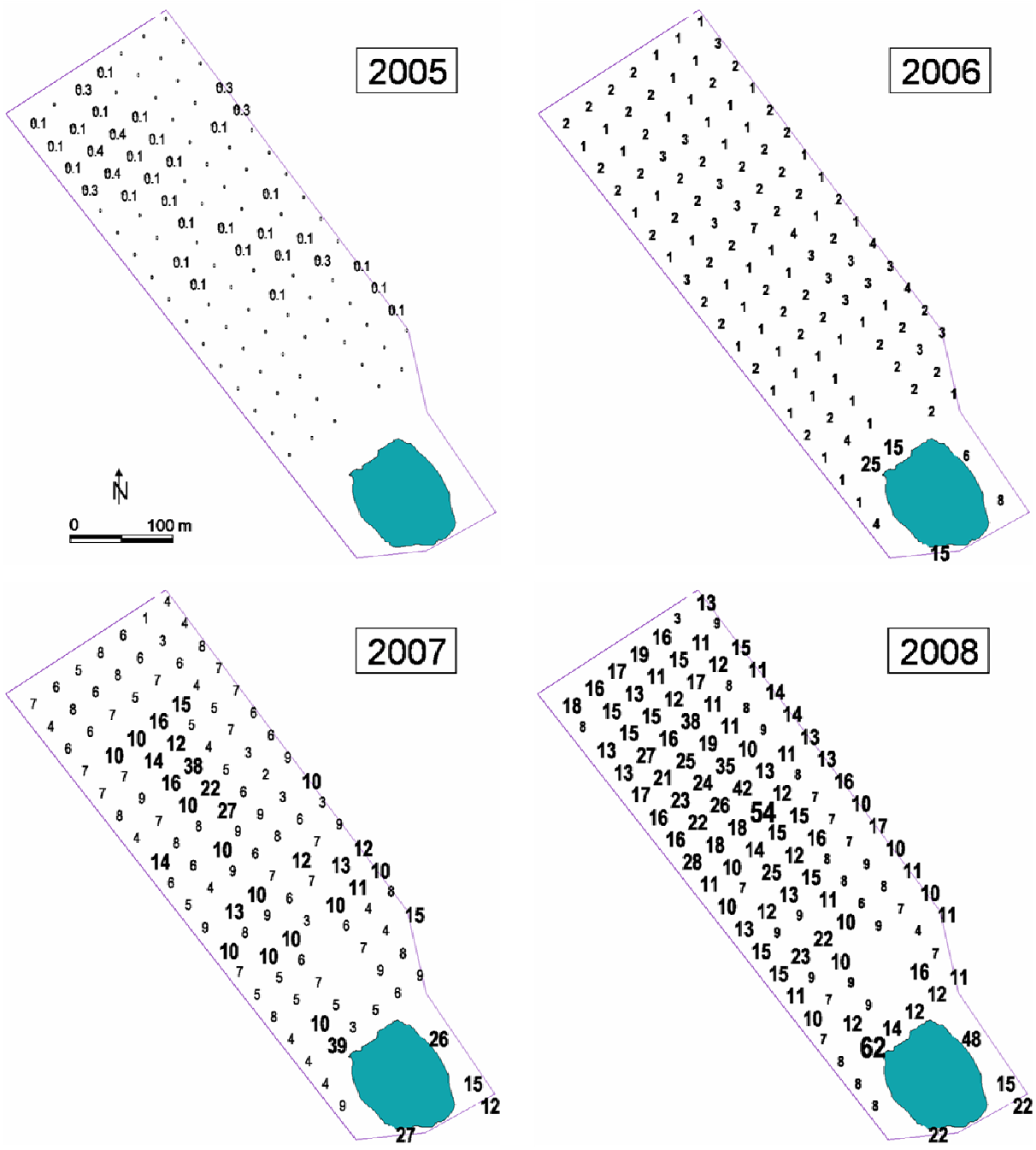

Fig. 7.9: Accumulated vegetation cover [%] for 25 m² plots, 2005–2008.

Tab. 7.6: Vascular plant species number for the 4 x 1 m² plots per grid point (number of plots Tab. 7.2) in 2005 and the 25 m² plots from 2006 to 2008.

2005:	18
2006:	88
2007:	112
2008:	136

Tab. 7.7: List of vascular plant species at the 25 m² plots in 2008 (status November 5, 2009), their lifespan, and steadiness.

The second column shows the scientific plant names according to the standard list of the German Federal Nature Conservation Agency (BfN). The third column lists the respective German plant name, the fourth column the plant families, and the fifth column the plant lifespan (a = annual, b = biennial, p = perennial, and hybrid forms), according to Rothmaler (2000). A "*" in the sixth column ("new") indicates a species with its first occurrence at the plots in Chicken Creek in 2008. In the seventh column ("steadiness"), the relative frequency of a species is given.

No.	Scientific name	German name	Family	Lifespan	New	Steadiness[%]
	Achillea pannonica	Ungarische Schafgarbe	Asteraceae	p		26
	Agrostis capillaris	Rot-Straußgras	Poaceae	p		?
	Agrostis stolonifera agg.	Weißes Straußgras	Poaceae	p		?
	Agrostis vinealis	Schmalrispiges Straußgras	Poaceae	p		16
5	*Ajuga genevensis*	Pyramiden-Günsel	Lamiaceae	p		4
	Apera spica-venti	Gemeiner Windhalm	Poaceae	a		91
	Actium minus agg.	Kleine Klette	Asteraceae	b		1
	Arenaria serpyllifolia agg.	Quendel-Sandkraut	Caryophyllaceae	a/b		74
	Artemisia vulgaris	Gemeiner Beifuß	Asteraceae	p		13
10	*Brachypodium sylvaticum*	Wald-Zwenke	Poaceae	p		40
	Bromus hordeacus	Weiche Trespe	Poaceae	a/b		23
	Bromus tectorum	Dach-Trespe	Poaceae	a		86
	Calamagrostis epigejos	Land-Reitgras	Poaceae	p		66
	Carex arenaria	Sand-Segge	Cyperaceae	p		1
15	*Carex ericetorum*	Heide-Segge	Cyperaceae	p		14
	Carex hirta	Behaarte Segge	Cyperaceae	p		4
	Carex cf. *pallescens*	Bleich-Segge	Cyperaceae	p	*	1
	Carex spicata	Sparrige Segge	Cyperaceae	p		1
	Centaurea stoebe	Rispen-Flockenblume	Asteraceae	b		8
20	*Cerastium holosteoides*	Gemeines Hornkraut	Caryophyllaceae	a		6
	Cerastium pumilum agg.	Dunkles Zwerg-Hornkraut	Caryophyllaceae	p		?
	Chenopodium album	Weißer Gänsefuß	Chenopodiaceae	a		17
	Chondrilla juncea	Großer Knorpellattich	Asteraceae	p	*	1
	Cirsium arvense	Acker-Kratzdistel	Asteraceae	p		69
25	*Cirsium palustre*	Sumpf-Kratzdistel	Asteraceae	b	*	1
	Cirsium vulgare	Lanzett-Kratzdistel	Asteraceae	b		13
	Convolvulus arvensis	Ackerwinde	Convolvulaceae	p		4
	Conyza canadensis	Kanadisches Berufkraut	Asteraceae	a		98
	Corynephorus canescens	Silbergras	Poaceae	p		23
30	*Crepis foetida*	Stink-Pippau	Asteraceae	a	*	2
	Crepis tectorum	Dach-Pippau	Asteraceae	a		97
	Danthonia decumbens	Dreizahn	Poaceae	p	*	5
	Daucus carota	Möhre	Apiaceae	b		41
	Deschampsia cespitosa	Rasen-Schmiele	Poaceae	p		3
35	*Digitaria sanguinalis*	Blutrote Fingerhirse	Poaceae	a	*	1
	Echinochloa crus-galli	Hühnerhirse	Poaceae	a		16
	Echium vulgare	Gemeiner Natternkopf	Boraginaceae	b		66
	Eleocharis cf. *palustris*	Gemeine Sumpfsimse	Cyperaceae		*	1
	Elymus repens	Gemeine Quecke	Poaceae	p		11

Tab. 7.7 cont´d

No.	Scientific name	German name	Family	Lifespan	New	Steadiness[%]
40	*Epilobium ciliatum*	Drüsiges Weidenröschen	Onagraceae	p		1
	Epilobium tetragonum	Vierkantiges Weidenröschen	Onagraceae	p		17
	Equisetum arvense	Acker-Schachtelhalm	Equisetaceae	p	*	1
	Eupatorium cannabium	Gemeiner Wasserdost	Asteraceae	p		2
	Festuca gigantea	Riesen-Schwingel	Poaceae	p	*	1
45	*Festuca ovina* agg.	Echter Schaf-Schwingel	Poaceae	p		24
	Festuca rubra agg.	Rot-Schwingel	Poaceae	p	*	13
	Filago arvensis	Acker-Filzkraut	Asteraceae	a		86
	Filago minima	Zwerg-Filzkraut	Asteraceae	a	*	?
	Fragaria vesca	Wald-Erdbeere	Rosaceae	p		4
50	*Genista pilosa*	Haar-Ginster	Fabaceae	p	*	5
	Geum urbanum	Echte Nelkenwurz	Rosaceae	p	*	3
	Gnaphalium sylvaticum	Wald-Ruhrkraut	Asteraceae	p		1
	Helichrysum arenarium	Sand-Strohblume	Asteraceae	p		4
	Helictotrichon pubescens	Flaumiger Wiesenhafer	Poaceae	p		1
55	*Herniaria glabra*	Kahles Bruchkraut	Caryophyllaceae	a/p	*	3
	Hierachium pilosella	Kleines Habichtskraut	Asteraceae	p	*	1
	Holcus lanatus	Wolliges Honiggras	Poaceae	p		5
	Holcus mollis	Weiches Honiggras	Poaceae	p		18
	Hordeum jubatum	Mähnen-Gerste	Poaceae	a		29
60	*Hordeum vulgare*	Saat-Gerste	Poaceae	p		5
	Hypericum perforatum	Tüpfel-Hartheu	Hypericaceae	p		6
	Hypochaeris radicata	Gemeines Ferkelkraut	Asteraceae	p		18
	Jasione montana	Berg-Jasione	Campanulaceae	a/b	*	1
	Juncus articulatus	Glieder-Binse	Juncaceae	p		1
65	*Juncus bufonius*	Kröten-Binse	Juncaceae	a		3
	Juncus effusus	Flatter-Binse	Juncaceae	p		1
	Juncus tenuis	Zarte Binse	Juncaceae	p	*	1
	Lactuca serriola	Kompaß-Lattich	Asteraceae	a/b		29
	Leontodon autumnalis	Herbst-Löwenzahn	Asteraceae	p		3
70	*Leontodon taraxacoides*	Nickender Löwenzahn	Asteraceae	b/p	*	5
	Lepidium ruderale	Schutt-Kresse	Brassicaceae	a/b		13
	Linaria vulgaris	Gemeines Leinkraut	Scrophulariaceae	p		1
	Lolium perenne	Deutsches Weidelgras	Poaceae	p		2
	Lotus corniculatus	Gemeiner Hornklee	Fabaceae	p		1
75	*Lupinus luteus*	Gelbe Lupine	Fabaceae	a		1
	Matricaria recutita	Echte Kamille	Asteraceae	a		7
	Medicago lupulina	Hopfenklee	Fabaceae	a/b	*	1
	Melica nutans	Nickendes Perlgras	Poaceae	p		3
	Moehringia trinervia	Dreinervige Nabelmiere	Caryophyllaceae	a/p		1
80	*Oenothera* cf. *parviflora* agg.	Kleinblütige Nachtkerze	Onagraceae	b		4
	Ornithopus perpusillus	Kleiner Vogelfuß	Fabaceae	a	*	2
	Papaver dubium	Saat-Mohn	Papaveraceae	a		2
	Petrorhagia prolifera	Sprossendes Nelkenköpfchen	Caryophyllaceae	a		23
	Phalaris arundinacea	Rohr-Glanzgras	Poaceae	p		1
85	*Phragmites australis*	Schilf	Poaceae	p		10
	Picris hieracioides	Gemeines Bitterkraut	Asteraceae	b/p	*	2
	Pinus sylvestris	Gemeine Kiefer	Pinaceae	p		9
	Plantago lanceolata	Spitz-Wegerich	Plantaginaceae	p		18
	Plantago major	Breit-Wegerich	Plantaginaceae	p		8

Tab. 7.7 cont´d

No.	Scientific name	German name	Family	Lifespan	New	Steadiness[%]
90	*Plantago major* ssp.*intermedia*	Kleiner Wegerich	Plantaginaceae	a/p	*	1
	Poa annua	Einjähriges Rispengras	Poaceae	a/p		37
	Poa compressa	Platthalm-Rispengras	Poaceae	p		47
	Poa palustris	Sumpf-Rispengras	Poaceae	p		71
	Poa pratensis agg.	Wiesen-Rispengras	Poaceae	p		5
95	*Polygonum aviculare* agg.	Vogel-Knöterich	Polygonaceae	a		5
	Populus tremula	Zitter-Pappel	Salicaceae	p		3
	Potentilla argentea	Silber-Fingerkraut	Rosaceae	p		5
	Prunella vulgaris	Gemeine Braunelle	Lamiaceae	p		10
	Prunus spec.	Traubenkirsche	Rosaceae	p		1
100	*Robinia pseudoacacia*	Robinie	Fabaceae	p		4
	Rubus fruticosus agg.	Brombeere	Rosaceae	p		8
	Rubus idaeus	Himbeere	Rosaceae	p		6
	Rumex acetosella v.*tenuifolius*	KleinerSauerampfer	Polygonaceae	p		72
	Rumex thyrsiflorus	Rispen-Sauerampfer	Polygonaceae	p		19
105	*Sagina procumbens*	Liegendes Mastkraut	Caryophyllaceae	p		1
	Salix cf. *caprea*	Sal-Weide	Salicaceae	p		2
	Salix cf. *viminalis*	Korb-Weide	Salicaceae	p	*	1
	Salix spec.	Weide	Salicaceae	p		1
	Salsola kali ssp. *ruthenica*	Ukraine-Salzkraut	Chenopodiaceae	a		11
110	*Scleranthus annuus*	EinjährigerKnäuel	Caryophyllaceae	a		16
	Scleranthus perennis	AusdauernderKnäuel	Caryophyllaceae	p		3
	Senecio vernalis	Frühlings-Greiskraut	Asteraceae	a		3
	Senecio viscosus	Klebriges Greiskraut	Asteraceae	a		1
	Senecio vulgaris	Gemeines Greiskraut	Asteraceae	a		1
115	*Setaria pumila*	Fuchsrote Borstenhirse	Poaceae	a	*	3
	Setaria cf. *viridis*	Grüne Borstenhirse	Poaceae	a		5
	Silene alba ssp. *alba*	Weiße Lichtnelke	Caryophyllaceae	p	*	4
	Sisymbrium altissimum	Hohe Rauke	Brassicaceae	a		6
	Solidago canadensis	Kanadische Goldrute	Asteraceae	p		4
120	*Sonchus arvensis*	Acker-Gänsedistel	Asteraceae	p	*	1
	Spergularia rubra	Rote Schuppenmiere	Caryophyllaceae	a		2
	Tanacetum vulgare	Rainfarn	Asteraceae	p		7
	Taraxacum officinale agg.	Gemeiner Löwenzahn	Asteraceae	p		45
	Torilis japonica	Gemeiner Klettenkerbel	Apiaceae	a/b		1
125	*Trago pogondubius*	Großer Bocksbart	Asteraceae	b		13
	Trifolium arvense	Hasen-Klee	Fabaceae	a		92
	Trifolium dubium	Kleiner Klee	Fabaceae	a	*	7
	Trifolium repens	Weiß-Klee	Fabaceae	p		8
	Tripleurospermum maritimum	Geruchlose Kamille	Asteraceae	a/b		53
130	*Tussilago farfara*	Huflattich	Asteraceae	p		34
	Typha angustifolia	Schmalblättriger Rohrkolben	Typhaceae	p	*	1
	Veronica officinalis	Echter Ehrenpreis	Scrophulariaceae	p		7
	Vicia angustifolia	SchmalblättrigeWicke	Fabaceae	a	*	2
	Vicia hirsuta	Rauhaar-Wicke	Fabaceae	a		9
135	*Vicia tetrasperma*	ViersamigeWicke	Fabaceae	a		12
	Viola canina agg.	Hunds-Veilchen	Violaceae	p		3

The distributions of several species within the Chicken Creek catchment area in the years 2005 to 2008 are exemplified below.

The annual species *Chenopodium album* (Chenopodiaceae) represents an opportunistic strategy, with a maximum at the very beginning of site development (in 2006: 4 percent at the 25 m² plot Q3) and rapidly becoming less important (Fig. 7.10).

The invasive annual to biannual *Conyza canadensis* (Asteraceae) built up the main vegetation aspect at the catchment area until 2007 when its highest cover (10 percent) was found at the 25 m² plots D5, K5, and O7 (Fig. 7.11).

The annual Fabaceae *Trifolium arvense* formed the main vegetation by far in 2008. Its highest cover (45 percent) was found at the 25 m² plot H4. T. arvense built up very dense patches especially at the western part of the study area (Fig. 7.12).

The perennial *Brachypodium sylvaticum* (Poaceae) achieves continuous growth at the western side of Chicken Creek. This is surprising for this early stage of ecosystem development because *B. sylvaticum* usually grows in semi-shaded environments (Fig. 7.13).

Robinia pseudoacacia (Fabaceae) already established in the study area (Fig. 7.14); at large 88 single individuals were recorded in 2008 (Fig. 7.15). This neophytic tree legume is used in the surroundings in short-rotation plantations for biomass production (Grünewald et al., 2009) and is also common in Lusatian forest ecosystems.

The tree species *Pinus sylvestris* (Pinaceae) achieved minor but continuous growth (Fig. 7.16).

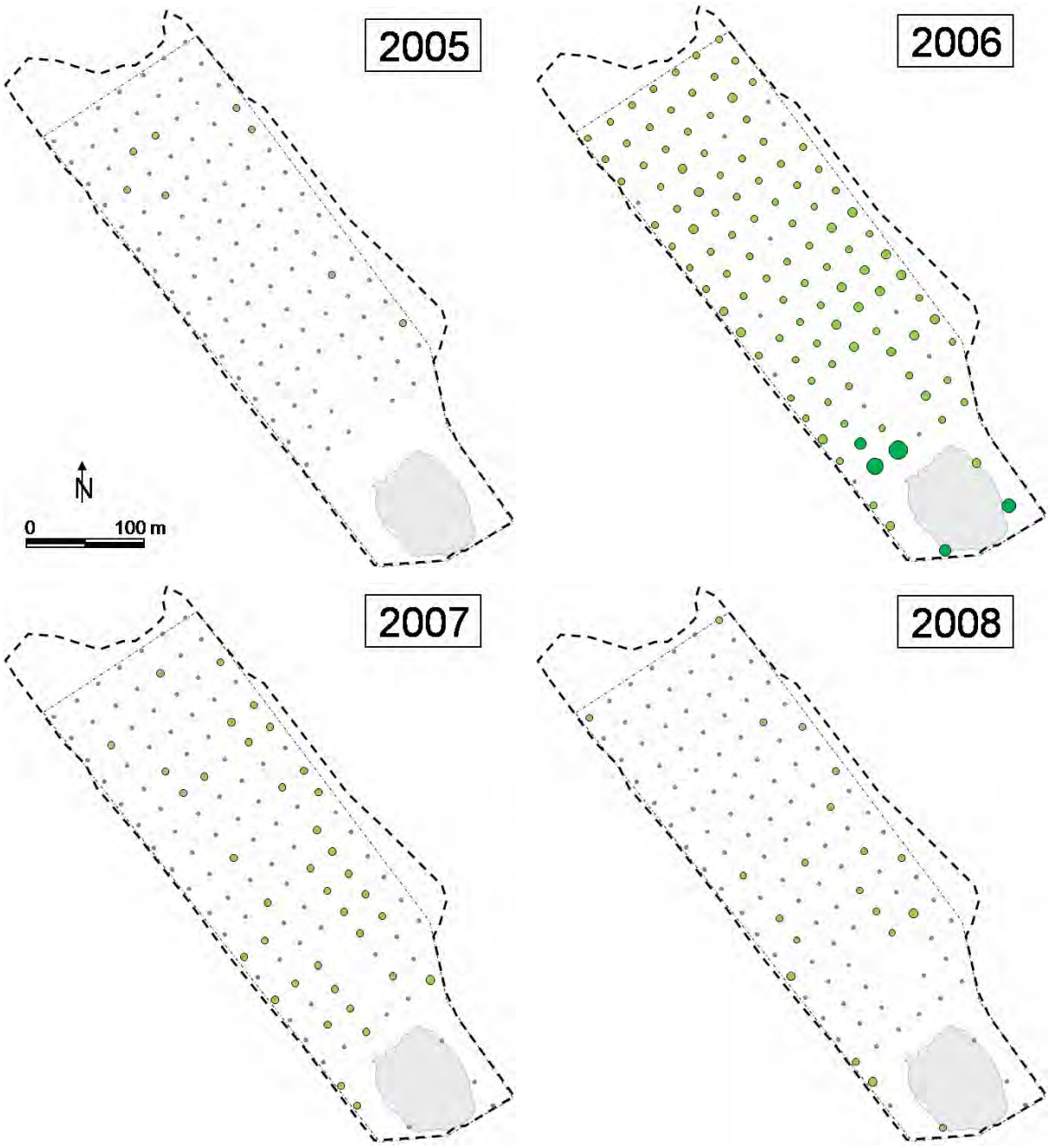

Fig. 7.10: Distribution and cover of *Chenopodium album*, 2005–2008. Light green dots (two sizes) depict covers of 0.1 and 0.5 percent, respectively. Dark green dots (four sizes) depict covers between 1 and 4 percent.

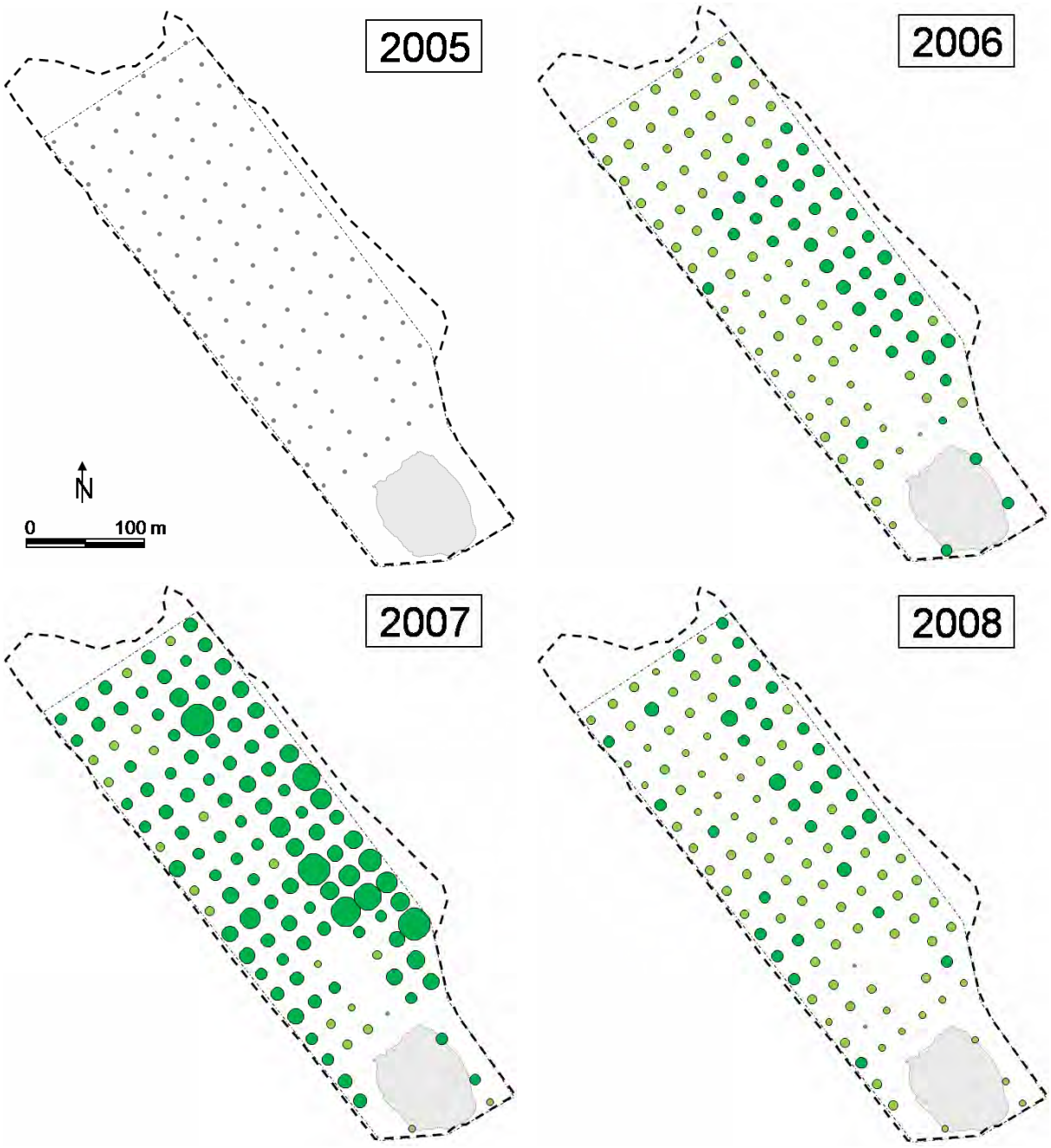

Fig. 7.11: Distribution and cover of *Conyza canadensis*, 2005–2008. Light green dots (two sizes) depict covers of 0.1 and 0.5 percent, respectively. Dark green dots (10 sizes) depict covers between 1 and 10 percent.

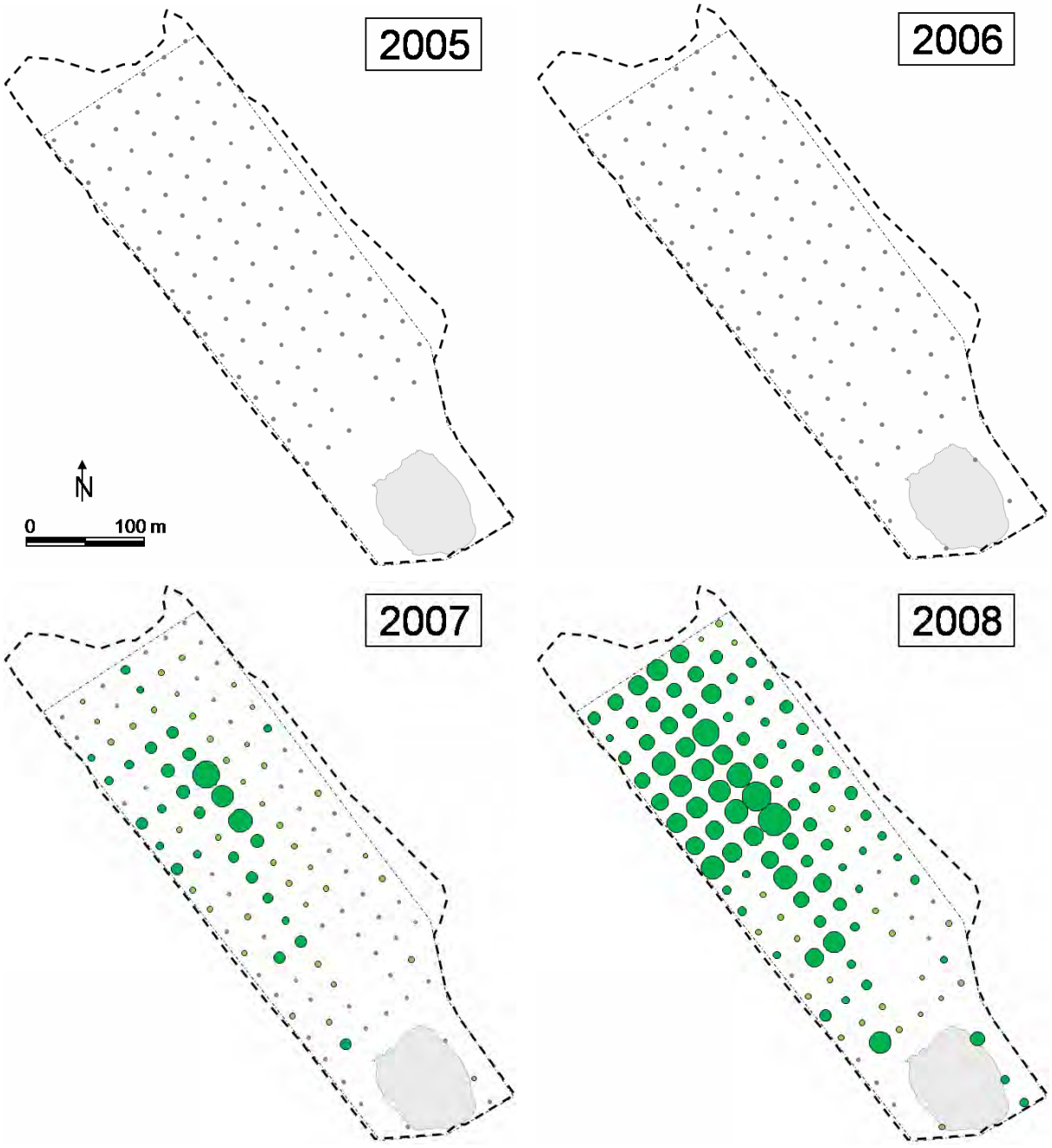

Fig. 7.12: Distribution and cover of *Trifolium arvense*, 2005–2008. Light green dots (two sizes) depict covers of 0.1 and 0.5 percent, respectively. Dark green dots (14 sizes) depict covers between 1 and 45 percent. Note that the scaling deviates from all other species shown due to a comparatively higher cover of *T. arvense*.

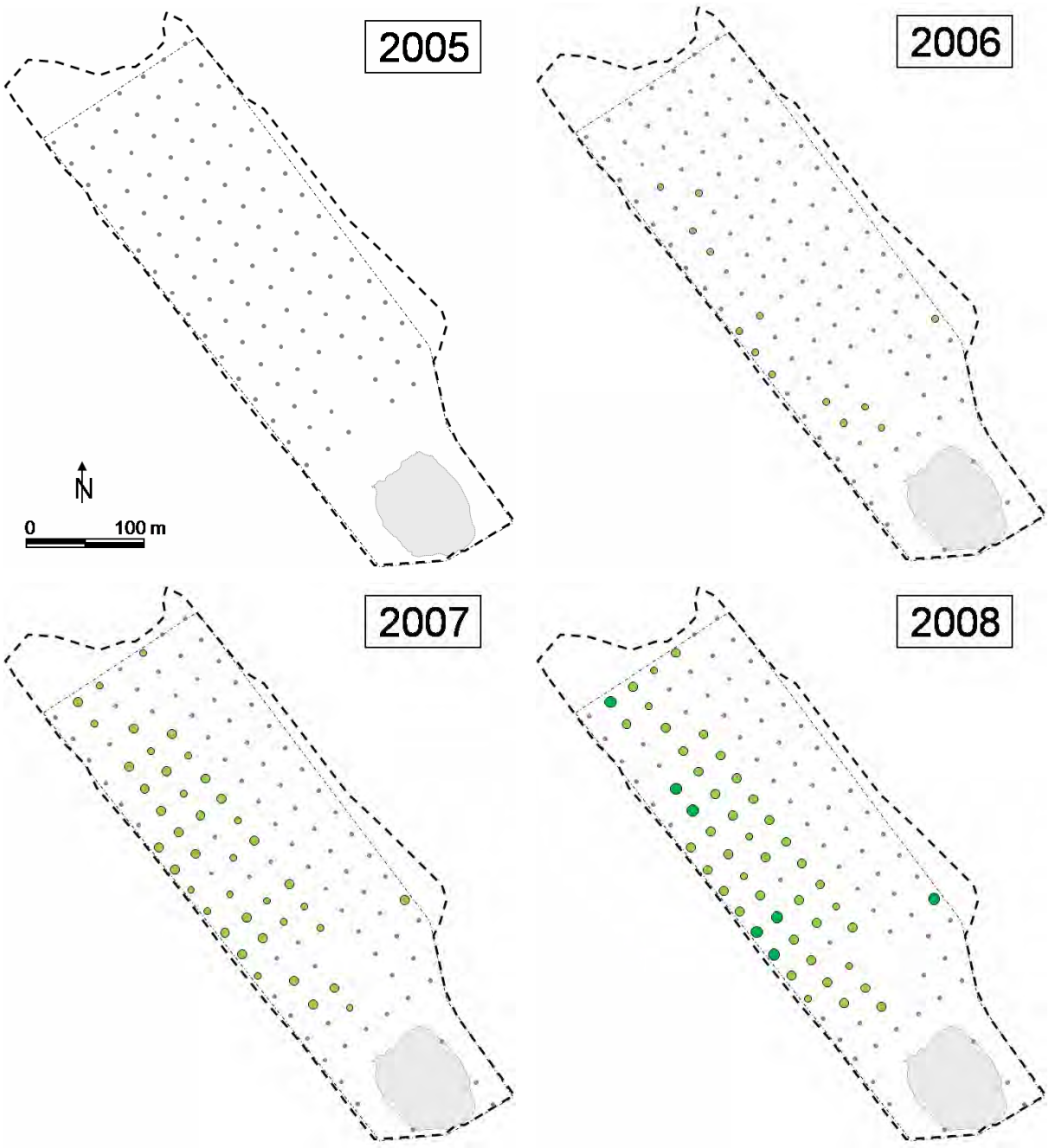

Fig. 7.13: Distribution and cover of *Brachypodium sylvaticum*, 2005–2008. Light green dots (two sizes) depict covers of 0.1 and 0.5 percent, respectively; dark green dots of 1 percent.

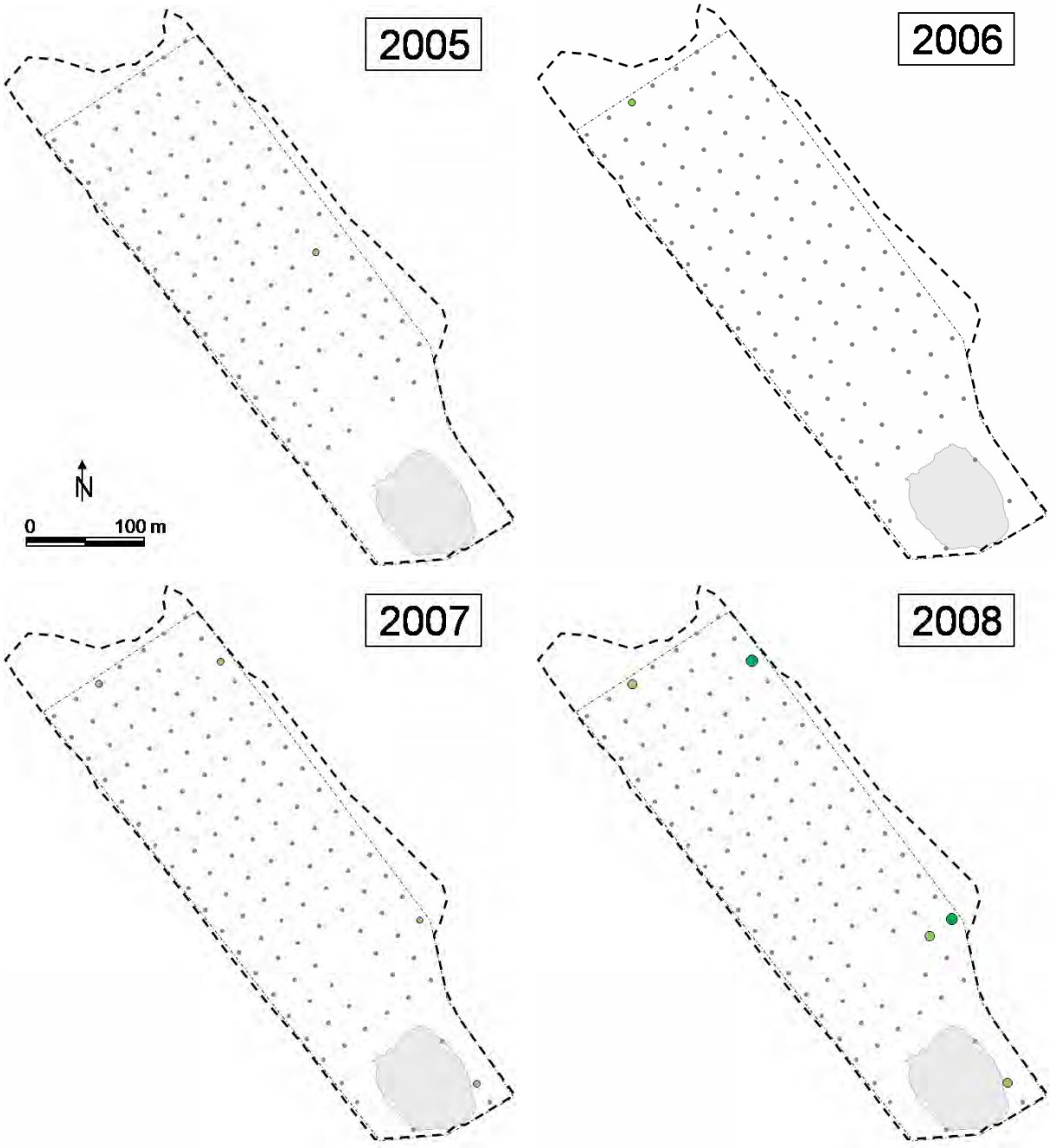

Fig. 7.14: Distribution and cover of *Robinia pseudoacacia*, 2005–2008. Light green dots (two sizes) depict covers of 0.1 and 0.5 percent, respectively; dark green dots of 1 percent.

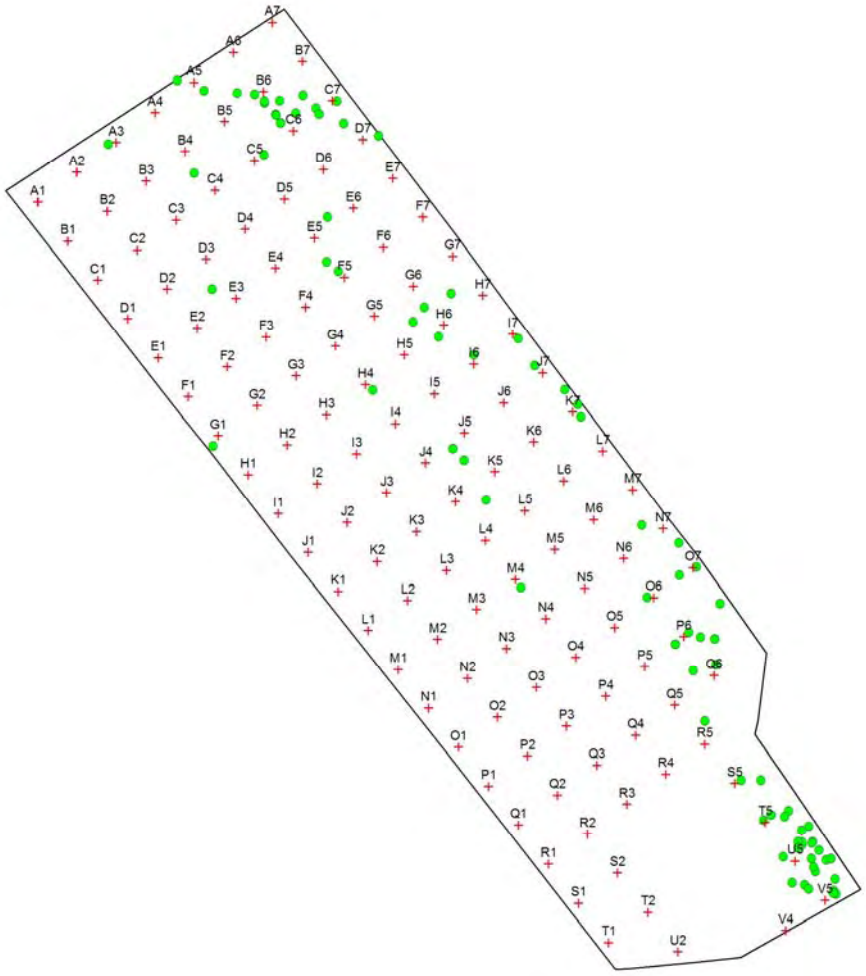

Fig. 7.15: Locations of all 88 *Robinia pseudoacacia* individuals within the catchment in 2008 (Maik Veste, pers. comm.).

These examples show that:

- both plant species number and vegetation cover increased significantly since the beginning of the catchment area development;
- the vegetation development demonstrates a high dynamic in the species cover with annuals dominating the vegetation at the beginning and perennials quickly displacing them;
- distinct spatial distribution patterns of plant species arose.

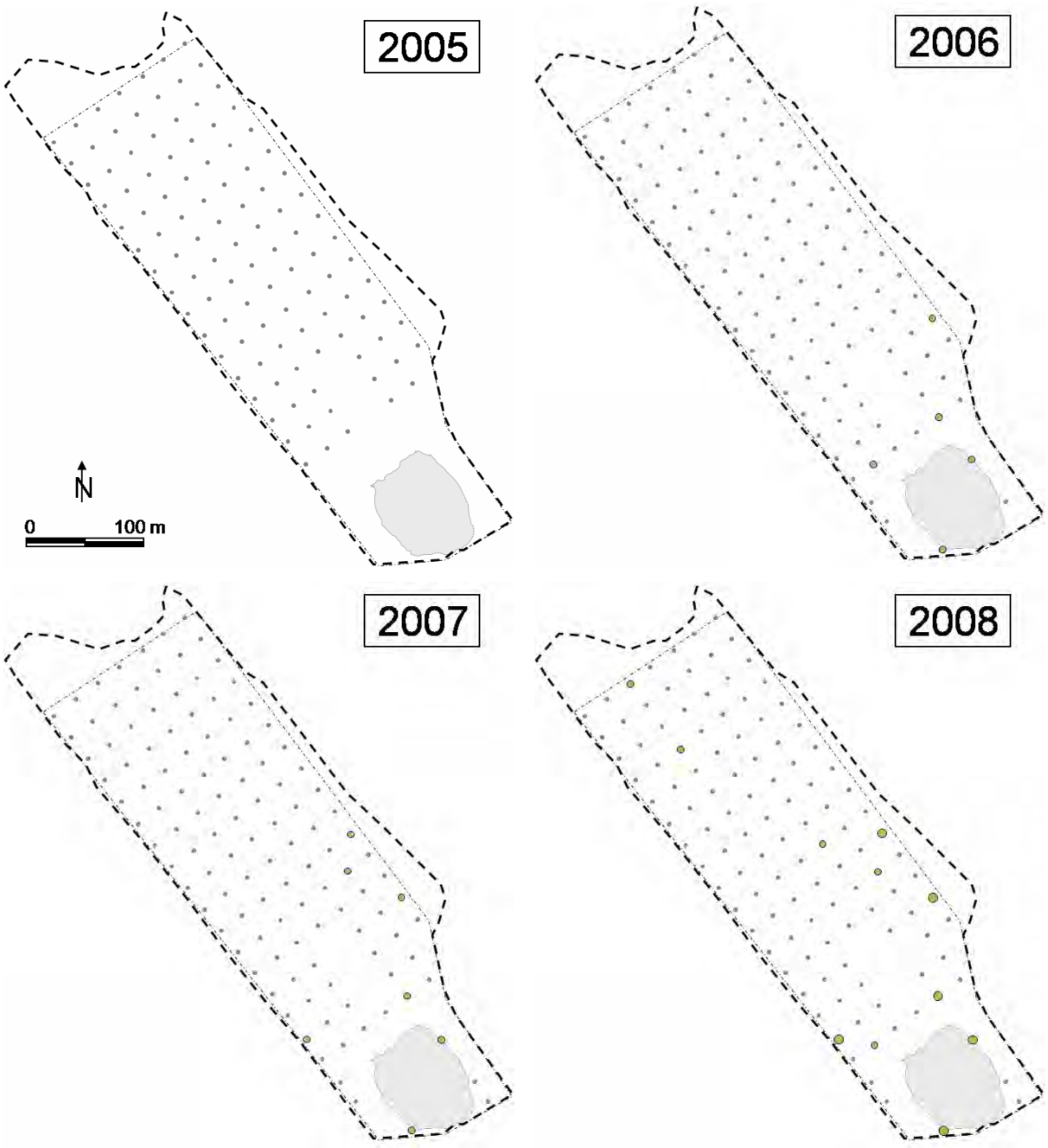

Fig. 7.16: Distribution and cover of *Pinus sylvestris*, 2005–2008. The smaller and larger green dots depict covers of 0.1 and 0.5 percent, respectively.

These early results demonstrate that the sampling design is describing well the initial vegetation development from 2005–2008. This is underlined by a) the high correlation between the plot vegetation cover estimates and the cover assessments done on the basis of aerial image analyses (cf. Chapter 11) and b) the small proportion of additional species which were not recorded on the plots (for 2008 see above). For the ongoing ecosystem development, the grid-based vegetation analyses are important. Structural heterogeneities in the catchment area (gullies, soil crusts, larger trees) will require additional approaches adapted to these differentiations, which are becoming more and more important (Denslow 1985; Felinks 2000). The continuation of the records on both, the established permanent plots and the flexible ones, aims to gain a) continued time series, b) an assessment of the specifics, and c) an assessment of the impact of the specifics and so the differentiation potential in a young developing ecosystem.

References

Bertsch, K., 1941: Früchte und Samen Ein Bestimmungsbuch zur Pflanzenkunde der vorgeschichtlichen Zeit. Handbücher der praktischen Vorgeschichtsforschung, Band 1, Ferdinand Enke Verlag, Stuttgart, 247 pp.

Bonn, S. and Poschlod, P., 1998: Ausbreitungsbiologie der Pflanzen Mitteleuropas. Grundlagen und kulturhistorische Aspekte. Quelle & Meyer Verlag Wiesbaden.

Connell, J.H. and Slatyer, R.O., 1977: Mechanisms of succession in natural communities and their role in community stability and organization. The American Naturalist, 111/982, 1119-1144.

Csapody, V., 1968: Keimlingsbestimmungsbuch der Dikotyledonen. Akadémiai Kiadó, Budapest, 286 pp.

Denslow, J.S., 1985: Disturbance-mediated coexistence of species. In Pickett, S.T.A. and White, P. (eds): The Ecology of Natural Disturbances and Patch Dynamics. Academic Press, New York, 307-324.

Felinks, B., 2000: Primärsukzession von Phytozönosen in der Niederlausitzer Bergbaufolgelandschaft. Dissertation, BTU Cottbus, 196 pp. (http://opus.kobv.de/btu/frontdoor.php?source_opus=149&la=de, last access 05 November 2009).

Fischer, A., 1987: Untersuchungen zur Populationsdynamik am Beginn von Sekundärsukzessionen Die Bedeutung von Samenbank und Samenniederschlag für die Wiederbesiedlung vegetationsfreier Flächen in Wald und Grünlandgesellschaften. Dissertationes Botanicæ, Band 110, J. Cramer, Berlin Stuttgart, 234 pp.

Gerwin, W., Schaaf, W., Biemelt, D., Fischer, A., Winter, S. and Hüttl, R.F., 2009: The artificial catchment 'Chicken Creek' (Lusatia, Germany) - a landscape laboratory for interdisciplinary studies of the initial ecosystem development. Ecological Engineering 25: 1786-1796, doi:10.1016/j.ecoleng.2009.09.003.

Grünewald, H., Böhm, C., Quinkenstein, A., Grundmann, P., Eberts, J., von Wühlisch, G., 2009: *Robinia pseudoacacia* L: A lesser known tree species for biomass. Bioenergy Research 2: 123-133.

Hanf, M., 1990: Ackerunkräuter Europas mit ihren Keimlingen und Samen. Dritte überarbeitete Auflage, BLV Verlagsgesellschaft mbH, München, 496 pp.

Leins, P. and Erbar, C., 2008: Blüte und Frucht Morphologie, Entwicklungsgeschichte, Phylogenie, Funktion, Ökologie. Schweizerbart'sche Verlagsbuchhandlung (Nägele u. Obermiller), Stuttgart, 412 pp.

Londo, G., 1975: Dezimalskala für die vegetationskundliche Aufnahme von Dauerquadraten. Berichte der Internationalen Symposien der Internationalen Vereinigung für Vegetationskunde „Sukzessionsforschung", J. Cramer, Vaduz, 613-617.

Müller-Schneider, P., 1983: Verbreitungsbiologie (Diasporologie) der Blütenpflanzen. Veröffentlichungen des Geobotanischen Institutes, Heft 61, Stiftung Rübel, 226 pp.

Rothmaler, W., 2000: Exkursionsflora von Deutschland Gefäßpflanzen: Atlasband. Band 3, 10. edition, eds: Jäger, E.J. and Werner, K., Spektrum Akademischer Verlag, Heidelberg Berlin, 753 pp.

Thompson, K., Bakker J.P. and Bekker, R.M., 1996: The soil seed banks of North West Europe Methodology, density and longevity. Cambridge University Press, 288 pp.

Acknowledgements

We thank Marin Dimitrov, Wolfgang Petrik and Maik Veste for their field and organizational assistance. Thanks to our partners at the Transregional Collaborative Research Centre (SFB/TRR 38) "Structures and processes of the initial ecosystem development phase in an artificial water catchment", the Deutsche Forschungsgemeinschaft (DFG, Bonn), and the Brandenburg Ministry of Science, Research and Culture (MWFK, Potsdam).

8. Succession of the soil faunal community during initial ecosystem development

Michael Elmer[1], Karin Hohberg[2], David Russell[2], Axel Christian[2], Hans-Jürgen Schulz[2] and Manfred Wanner[3]

[1] Brandenburg University of Technology Cottbus, Chair of Soil Protection and Recultivation, Cottbus

[2] Senckenberg Museum of Natural History, Görlitz

[3] Brandenburg University of Technology Cottbus, Chair of General Ecology, Cottbus

8. 1 Introduction

The interactions within the decomposer subsystem are of crucial importance for soil formation as well as mass and energy flow in ecosystems. In this context, the structure of the soil food web is a key driver of decomposition and mineralization processes (Walker and del Moral, 2003). Several studies have stated that the faunal contribution to nitrogen mobilization in soils is usually around one third in both natural and managed ecosystems. Further, soil food webs are highly resilient to disturbance and usually recover entirely from major disturbances such as drying, freezing and fumigation within a matter of days (Wardle, 2002).

Moreover, the soil fauna plays an important role in primary succession as it occurs immediately after exposure of new land surfaces, facilitating the establishment of other biota (Hodkinson et al., 2004, Wanner et al., 2008). On the other hand, vegetation development is important for the structure and function of the soil food web. E.g., plant species adapted for infertile soils and which grow more slowly select for decomposers that are adapted for poorer-quality litter but cycle nutrients more slowly. Plant species effects on decomposer organisms and processes are especially apparent in the course of ecosystem development (Wardle, 2002).

Changes in succession are controlled by biotic interaction, i.e. facilitation, competition and inhibition as well as tolerance. However, only few studies have investigated the interaction of vegetation and the soil food web during the initial stage of primary succession. This hold true, especially, with regard to their influence on the temporal and spatial variability of the decomposer food web components and the processes they control (Wardle, 2002, Walker and del Moral, 2003). Hence, we investigated the spatial and temporal development of several components of the soil food web during the initial stage of primary succession in the artificially created catchment “Chicken Creek”.

8. 2 Material and Methods

8. 2.1 Sampling

Regular soil faunistical sampling began in 2007 and took place at usual times of peak abundances, namely in April and October of each year (s. Fig. 8.1). Before regular zoological sampling was begun, however, two preliminary sampling periods were undertaken in October 2005 and May 2006 in order to assess initial soil-faunistical development in the catchment area. Soil-zoological sampling was always evenly distributed among the grid points, whereby attention was paid that the three regions of the catchment backslope – upper, middle, and lower – were equally sampled (s. Fig. 1.1). Additionally, pitfall traps were installed in summer 2008 in the different regions of the catchment (upper, middle, lower, semi-aquatic area around the pond) (s. Fig. 8.1).

8. 2.1.1 Sampling of endogeic soil fauna

Field sampling of the endogeic soil fauna took place via the removal of soil cores from the catchment area. At every sampling date, 27 soil cores each for mesofauna (Collembola, Acari) and microfauna (Nematoda, Tardigrada, testate amoebae) were taken. The sampling points were distributed throughout the catchment area, with 9 cores each in the upper, middle and lower region (Fig. 8.1). To prevent undue emphasis of single coordinate points, the sampled points were rotated slightly from sampling date to sampling date (see Fig. 8.1). Solely the coordinate points near the groundwater monitoring pipes (C4, I4, L4, N4) were sampled at every date to ensure direct correlations between soil fauna and hydrological or soil data.

For endogeic mesofauna, cores (6.4 cm in diameter) were taken to a depth of 5 cm. Separate cores were extracted for microfauna (3.5 cm in diameter, also to 5 cm depth). Cores for mesofauna and microfauna were always taken directly adjacent to one another to allow direct correlations between the different animal groups (Fig. 8.2). The mesofauna samples were extracted with a removable-side corer to ensure that the soil cores could be removed intact, which guarantees better extractability of the mesofauna, after which the cores were individually transferred to size-matched containers (7 cm diameter) for transportation to the laboratory (Fig. 8.3). The microfauna samples were transferred from the soil corer to plastic bags and transported to the laboratory.

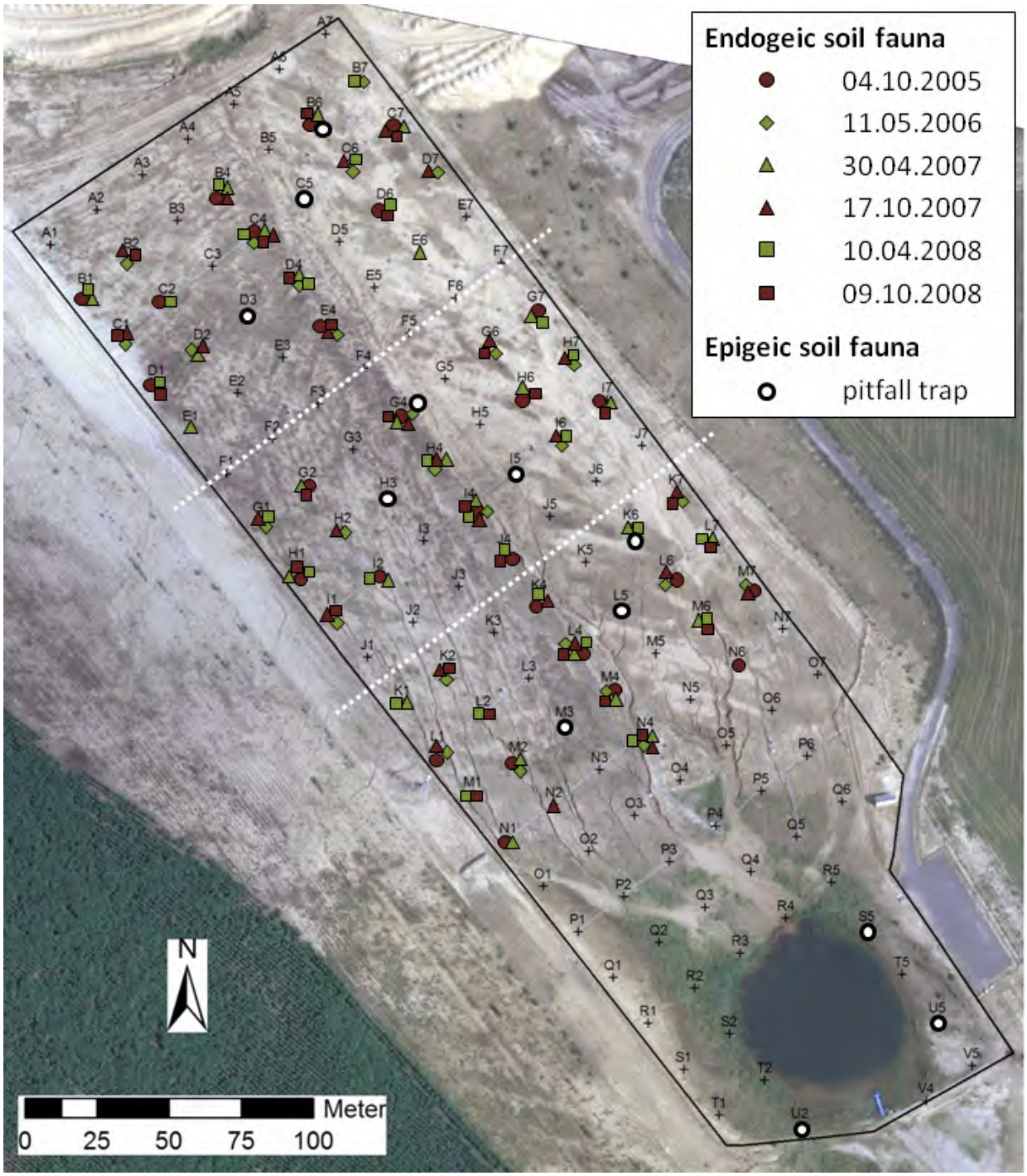

Fig. 8.1: Sample points for sampling of endogeic soil fauna and pitfall traps for epigeic soil fauna sampling at the Chicken Creek catchment area.

Fig. 8.2: Sampling points (removed cores) for mesofauna and microfauna were always directly adjacent to one another.

Fig. 8.3: Soil corer used for mesofauna soil cores.

Endogeic mesofauna was driven actively from the soil samples by means of an increasing temperature and desiccation gradient. For this, the soil cores were placed intact (within the transportation containers after removal of the lids from both sides) and inverted (with the upper surface facing downwards) onto metal nets (2 mm mesh size) above funnels in a Macfadyen-type, high-gradient extractor (Macfadyen, 1961, Bieri et al., 1978; Fig. 8.4). In the extractors, the soil cores were located between an upper heating and lower cooling chamber, which allows the development of a temperature and desiccation gradient within the cores. Extraction continued for 10-14 days, depending on climatic and moisture conditions, during which the temperature in the heating chamber was continually increased from approximately 20°C to 50°C (Fig. 8.5). Due to thermal leakage through the samples, the temperature increased in the cooling chamber as well (s. Fig. 8.5), but to a lesser degree, so that the temperature gradient within the soil cores increased from approximately 5°K to 20°K during each extraction period. Due to the inherent negative thermo- and xerotaxis and positive geotaxis of the animals, they actively migrate downwards during the extraction period, abandon the soil and fall through the funnels into 30-ml reception jars filled with a fixative and conservation medium (von-Törne mixture: 50% isopropanol with 3% glacial acetic acid and 0,3% formalin: Dunger and Fiedler, 2000).

After termination of the extraction, the collected animals were transferred sample-specifically into 70% ethanol, where they remained for approximately three weeks to allow for total fixation and conservation. The mesofauna were subsequently sorted into higher-level taxa groups (mostly at the order level) under a stereomicroscope at maximally 50× magnification and stored in 70% ethanol. The individuals of Collembola and Acari (Gamasina and Actinedida) were then further sorted into morphospecies and transferred to chambered microscopic slides in 90% lactic acid (Collembola) or cleared in a glacial acid-glycerine mixture (Gamasina) and mounted in permanent microscopic slides in a Gummi arabicum-mixture (modified after Rusek) (Gamasina) or Hoyer's medium (Actinedida).

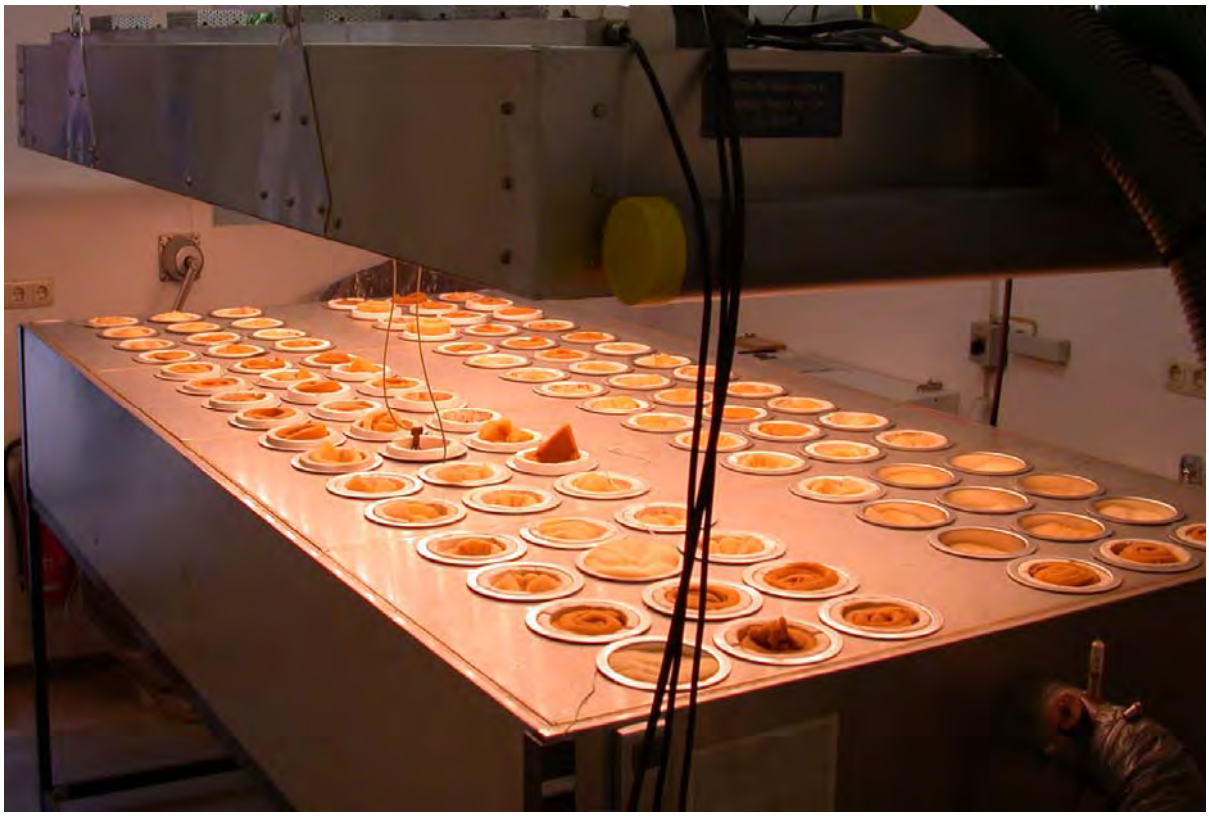

Fig. 8.4: High-gradient extractor used for expelling mesofauna from the soil cores.

All individuals were determined to species or generic level under a differential-interference microscope at up to 1000× magnification. Determination of Collembolan followed Bretfeld (1999), Fjellberg (1998, 2008), Pomorski (1990), Potapov (2001), Thibaud et al. (2004) and Zimdars and Dunger (1994), of Gamasina mainly Karg (1993) as well as original descriptions or taxonomic reviews, and of Actinedida Kethley (1990, and unpubl. manuscript), Zacharda (1978), Kazmierski (1998), Volgin (1989), Savulkina (1981) as well as original descriptions and generic and family reviews.

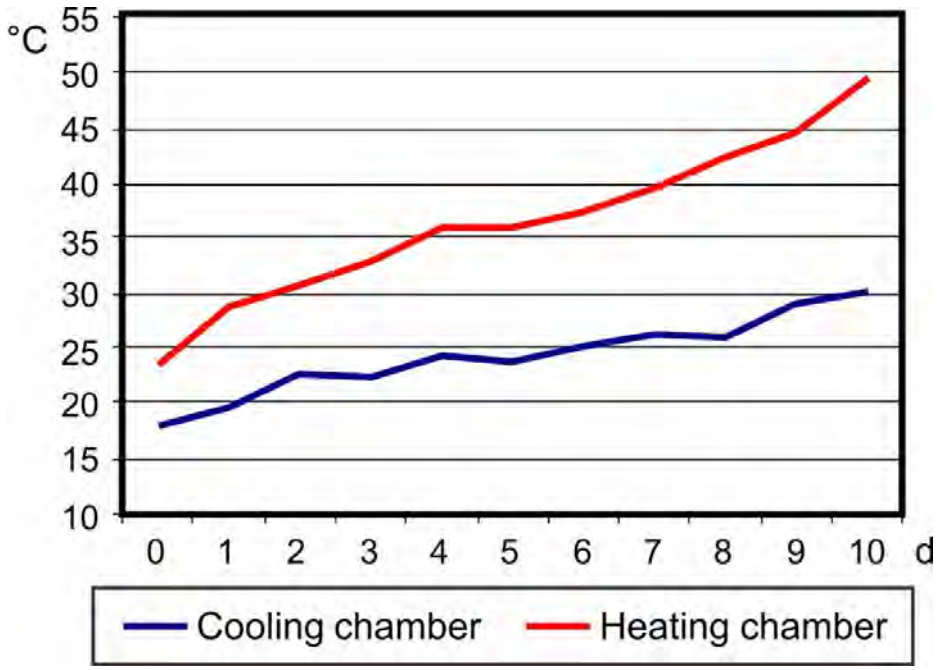

Fig. 8.5: Progression of the temperature gradient during active extraction of the mesofauna from the soil cores (data shown = averages from the actual extractions; standard errors omitted for clarity).

In contrast to the microfauna, the species of these groups have also been determined in 2005 and 2006. It was not originally planned to quantify and determine the actinedid mites. However, as their absolute dominance of the mesofauna communities became apparent in 2007, processing of this group was then undertaken. Due to this later begin and their high densities in individual samples, determination of this group has not yet been completed for the 2008 sampling periods.

Each microfauna sample was weighed and thoroughly mixed. Then, 1 g of fresh material was transferred to 8 ml formaldehyde (4% aqueous solution containing aniline blue) for conservation. Aniline blue was added to differentiate between full (living) and empty (dead) shells. Testate amoebae were determined to species level and enumerated directly with an inverted microscope using soil suspensions (30-500 mg soil per sample; for details see Wanner, 1999). Determination of testate amoebae followed e.g. Meisterfeld (2002) and numerous monographs.

The remaining substrate was placed on Baermann funnels, where nematodes and tardigrades actively migrated from the desiccating substrate downwards into a water-filled funnel and adjacent hose, from which they were removed daily, killed by heat and preserved in 4% formaldehyde. Extraction started on the day of sampling and ended with desiccation of the soil, but at the latest after five days in order to prevent increased nematode counts due to population growth. Soil moisture of the microfauna cores was determined gravimetrically (before/after total desiccation). Nematodes and tardigrades extracted from each sample were counted. Per sample hundred individuals of nematodes and of tardigrades, were identified to the species (Nematoda) or generic (Tardigrada) level under an inverted microscope. Determination of tardigrades followed Maucci (1986) and Dastych (1988), of nematodes Andrássy (1984), Brzeski (1998), Loof (1999), and numerous generic and family reviews. Additionally, individual body lengths and widths of each determined specimens were measured.

8. 2.1.2 Sampling of epigeic soil fauna

The pitfall traps were installed in summer 2008 (s. Fig. 8.1) and the plots were sampled continuously from then on. At each of the plots, a point within the larger permanent vegetation plots (excluding the smaller ones of 1 m²; s. chapter 7) was randomly selected. Each pitfall trap (diameter 12 cm) was filled with a saturated benzoic acid solution to catch epigeic invertebrates. The traps were emptied in two-weekly intervals to collect the macro-invertebrates. In the lab, the specimens were transferred to a 70% ethanol solution and preserved until determination. Up to now, the carabid beetles (Coleoptera) of six periods (until August 2008, 12 weeks) have been determined to the generic level; the specimens of the sub-family Cicindelinae have been determined to the species level.

8. 2.2 Data handling and statistics

8. 2.2.1 Mesofauna (Collembola, Acari)

The number of individuals (of total mesofauna, Collembola, Gamasina and Actinedida) as well as the number of species (Collembola, Gamasina and Actinedida) present in each sample (= extracted from each soil core) constituted the raw data for the further analysis. This data was summed into sampling-date averages in order to assess faunistical development during primary succession. Densities were determined for total mesofauna, Collembola, Gamasina as well Actinedida as sampling-date averages. For this, the average densities were calculated and standardized into individuals per m² from the total individuals of all 27 samples per sampling date through the formula

$$density\ [individuals/m^2] = x/[(\pi*0{,}032^2)*n]$$

whereby x represents the total number of individuals and n the number of soil cores (= samples) per sampling date. The soil-core radius was 3.2 cm (= 0.032 m). Total species numbers were determined as sampling-date sums for the different mesofaunal groups. In order to characterize the respective faunal communities, the community/species composition and community structure (= proportion of each species in the total community; "dominance" in %) was determined individually for Collembola, Gamasina and Actinedida.

To test for significant temporal developments in the faunal communities, the data was submitted to a variance analysis with sampling date as the main factor. Due to the non-normal distribution of soil animals, differences in the densities and species richness (individuals and species per sample, respectively) between sampling dates or years were tested for significance using a non-parametric one-way ANOVA for multiple observations (= samples) per cell (= sampling date) (modified Friedman test; Zar, 1999, Schöps and Russell, 2004). This ANOVA is based on ranked per sample data for each season and on the χ_r^2 rather than the F distribution. A post-hoc Tukey-like multiple comparison procedure for this non-parametric ANOVA (Zar 1999) tested for significant differences between sampling dates.

8. 2.2.2 Microfauna (Nematoda, Tardigrada, Testate amoebae)

Fresh weights of individual nematodes and tardigrades were calculated using the formula

$m_{nem} = l * [d^2/(1.6 * 10^6)]$ for nematodes (Andrássy, 1956) and

$m_{tar} = l * (d/2)^2 * \pi * 1.04 * 10^{-6}$ for tardigrades (Hallas and Yeates, 1972),

where l is body length, d is body width (both in micrometers), and m is individual fresh weight (in micrograms). Nematode and tardigrade biomass per sample then resulted from the average nematode/tardigrade fresh weight (measured from 100 individuals) multiplied by nematode/tardigrade counts per sample.

Nematode genera were assigned to “trophic groups” according to Yeates et al. (1993), as well as to the 1-5 “colonizer-persister (cp) scale” following Bongers (1990) and Bongers and Bongers (1998), where cp-1 consists of genera with short generation times, small eggs, high fecundity, and cp-5 of genera with longest generation times, largest body sizes, lowest fecundity, and greatest sensitivity to disturbance. Together the two classifications allow the genera to be assigned to “functional guilds” of nematodes sharing the same feeding type and cp-value (Bongers and Bongers, 1998). The weighted faunal analysis concept was applied (Ferris et al., 2001), where functional guilds of nematodes (without plant feeders) are indicators of “basal” (*b*), “structured” (*s*), and “enriched” (*e*) conditions of the soil food web. The concept uses the structure index, *SI*, and enrichment index, *EI*, to assess food web location along structure and enrichment trajectories:

$SI = 100 * (s/(s + b))$ and $EI = 100 * (e/(e + b))$,

with the basal component $b = 0.8 * (Fu_2 + Ba_2)$,

the structure component $s = 0.8 * Ca_2 + 1.8 * \Sigma(X_3) + 3.2 * \Sigma(X_4) + 5.0 * \Sigma(X_5)$,

and the enrichment component $e = 3.2 * Ba_1 + 0.8 * Fu_2$

and with Fu_2, Ba_1, etc. and $\Sigma(X_i)$ the sum of the nematode abundances within cp-class *i* (feeding types Ba, Fu, Ca and Om).

Following Ferris et al. (2001), a graphic representation of the food web condition, the “faunal profile” (for explanation, see Fig. 8.9), was produced for each sample separately. Dauerlarvae of Rhabditidae were excluded from the calculations of *EI* as they are characteristic adaptations of enrichment opportunists (cp-1) to withstand nutrient-poor situations, and as their presence, accordingly, does not indicate an actual microbial bloom (Bongers and Bongers, 1998). Additionally, algal-feeding *Ecumenicus monohystera* and *Aporcelaimellus obtusicaudatus* were excluded from the calculations of *SI* according to Hohberg (2003).

Cluster analysis of testate amoebae community development (MVSP software, Kovach Computing Services, Wales, UK) used the unweighted pair group method of average linkage (UPGMA) and Sorensen/Bray Curtis indices (considering only species inventory/species inventory and density). Redundancy analysis (RDA) was calculated and graphed using CANOCO for Windows, Version 4.5 (Microcomputer Power, Ithaca, NY, USA) to test and visualize the relationship between the environmental variables, samples and the response variables (testate amoebae species abundance).

8. 3 Results and Discussion

8. 3.1 Testate amoebae

Testate amoebae, found by regular sampling of predominantly uncovered, sandy substrate, revealed only a few species, which occurred in extremely low densities (only single shells occurred in the samples). In total, from October 2005 to April 2008, 23 samples had been analyzed, of which only 8 samples contained amoeba shells. Therefore, no abundances had been computed. However, further investigations in May 2008, which considered covered and uncovered micro-sites straight to the point, revealed an extreme assignment of testate amoebae to plant cover (cluster analysis, RDA; Wanner and Elmer, 2009). This was confirmed by a subsequent sampling in October 2008: Almost all covered sites (n = 13) revealed 100-300 specimens per gram dried soil (ind. gdm^{-1}), whereas the uncovered sites (n = 14) showed densities of 0-30 ind. gdm^{-1}.

8. 3.2 Nematoda and Tardigrada

Nematode as well as tardigrade densities and biomasses gradually increased from April 2007 to October 2008 (Fig. 8.6, 8.7), indicating a change in soil conditions and food supply. Mine-spoil sandy material presents extreme conditions for soil organisms: A general difference from natural soils is the initial lack of stratification and available organic matter, as well as a reduced binding capacity for water and nutrients.

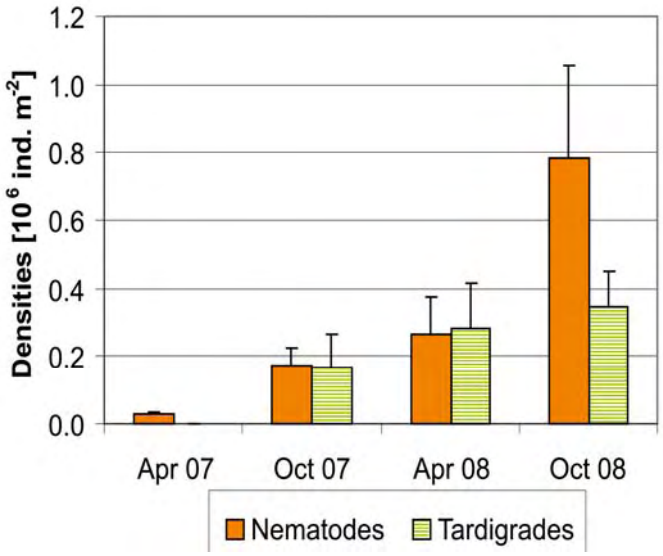

Fig. 8.6: Nematode and tardigrade densities (mean ± 1 SE, n = 27) of the artificial catchment Chicken Creek in 2007 and 2008.

The dominant genus successfully colonising Chicken Creek in April 2007 was bacterial-feeding *Acrobeloides* (83% of overall nematode numbers), a general opportunist that can withstand dehydration and food-poor conditions (Bongers and Bongers, 1998). Algal-feeding *Apodibius confusus* (99% of overall tardigrade numbers) first appeared in October 2007. Together with the large algal-feeding nematode species *Aporcelaimellus* spp. and *Ecumenicus monohystera*, *A. confusus* contributed 32.3% (October 2007), 52.5% (April 2008), and 68.1% (October 2008) of the overall tardigrade-nematode biomass.

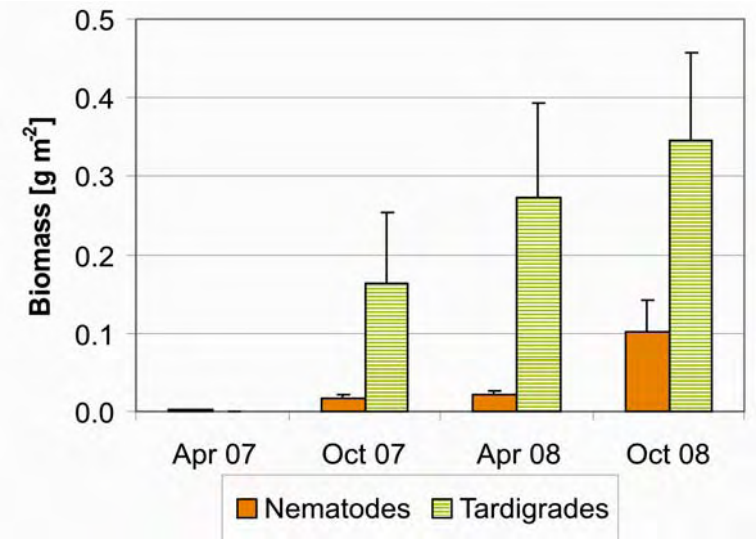

Fig. 8.7: Nematode and tardigrade biomass (mean ± 1 SE, n = 27) of the artificial catchment Chicken Creek in 2007 and 2008.

In contrast to all other trophic groups, where feeding mode is derived from potential food sources used in successful laboratory cultures, actual algal-feeders may be recognized by their green intestines. The high biomass of algal-feeders indicates that soil algae are a very important food source in these young soils. This concurs with the findings of Wanner et al. (1998) that unicellular algae are one of the first colonizers and food sources in young soils.

In contrast to the tardigrades, where algal-feeding *A. confusus* still contributed 95% of the densities in October 2008, trophic structure of nematode communities substantially changed within the 1.5 years of the present study: Whilst 96% of overall numbers were bacterial feeders in April 2007, plant root feeders gained more and more importance in the soil food web of the Chicken Creek (Fig. 8.8), and in April and October 2008 the nematode assemblages were characterized by mass occurrence of plant root feeders such as *Paratylenchus macrodorus*, which dominated three and nine, respectively, of the 27 samples. This shift clearly mirrors the increasing growth of vegetation at the Chicken Creek site.

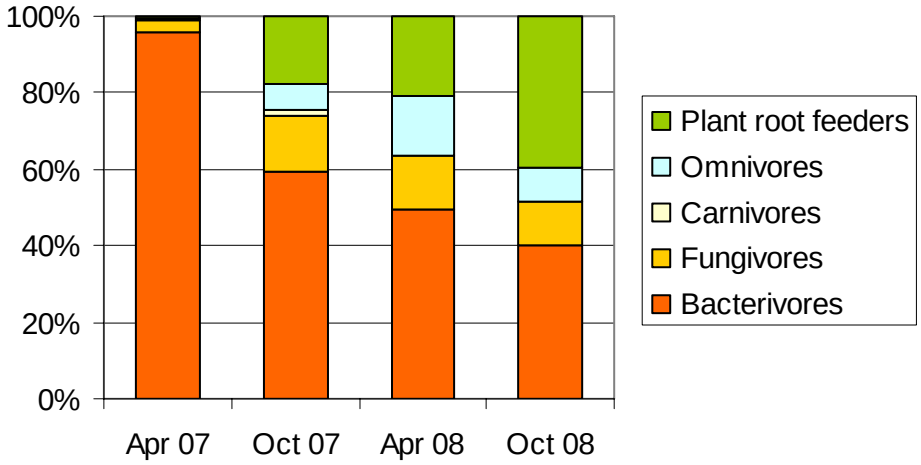

Fig. 8.8: Trophic structure of nematode communities at the Chicken Creek in 2007 and 2008.

It is expected that the food web structure should increase during early soil succession from basal food webs, where only generalists can survive and reproduce, to mature food webs with a high number of trophic links and multitrophic interactions, as demonstrated by Verhoeven (2002) and Hohberg (2003). The Chicken Creek soil food webs are located on the left side of the faunal profile, representing poorly structured food webs, far away from the status expected in natural sites (Fig. 8.9). Still, the number of trophic links within the soil food web, as indicated by the nematode community structure (structure index *SI*), was larger in October 2008 compared to April 2007. This concurs with the herbaceous plant society becoming richer and more diverse in the course of the present study, thus providing an increasing supply of niches.

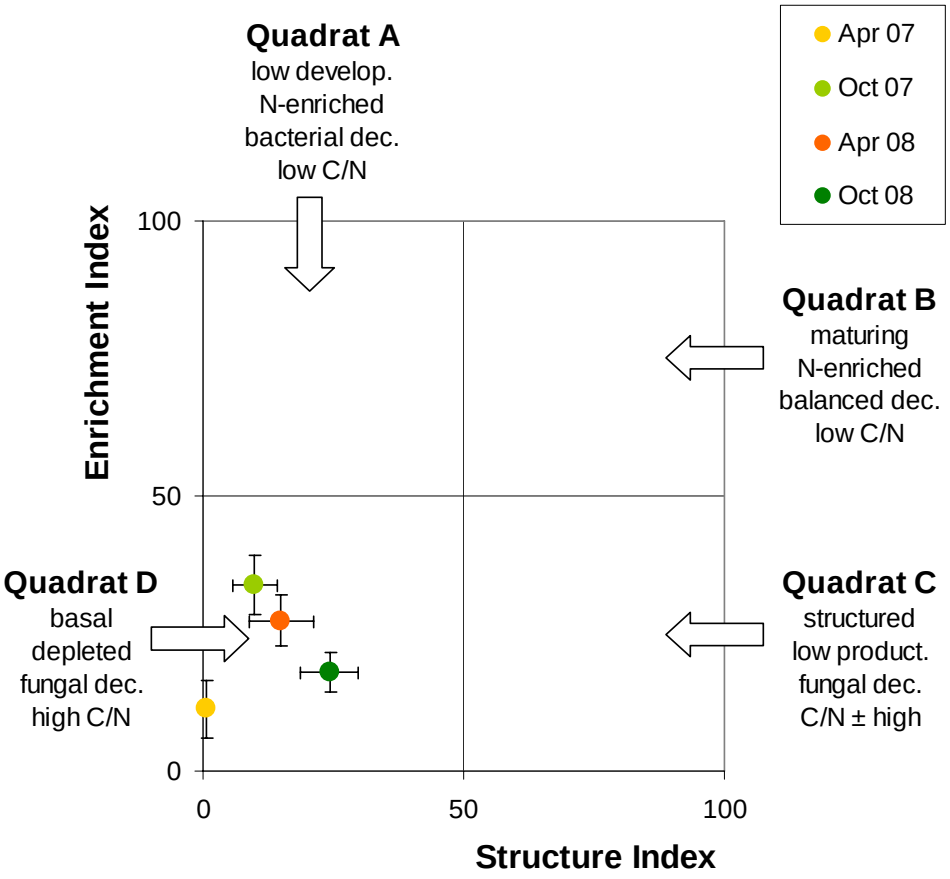

Fig. 8.9: Faunal profiles representing the soil food web condition of the Chicken Creek in relation to its structure (*SI*) and enrichment (*EI*) as indicated by the "weighted faunal analysis" (mean ± 1 SE, n = 27).

8. 3.3 Collembola and Acari

During initial development in the years 2005 and 2006 only very low densities of Collembola and Acari were observed in the catchment area (Fig. 8.10), many samples contained no mesofauna at all. Actinedid mites were the most common taxa, Collembola were found in less than 20% of the samples and then mostly as single individuals. No gamasin mites were found. Total species numbers were very low, with most individuals representing *Mesaphorura macrochaeta* (Collembola), *Nanorchestes* sp. and *Speleorchestes* sp. (both Acari, Actinedida). These species are known from sandy or newly formed soils poor in organic matter. Little is known about their feeding habits. The collembolan species is most likely microbivore (bacteria and fungal hyphae) and possibly algivore (pers. observ.), as are probably also the actinedids. Thus, in the first two years, the catchment area was only sporadically colonized by few individuals of species adapted to primary soils or nutrient-poor conditions and occupying basal positions in the soil food web.

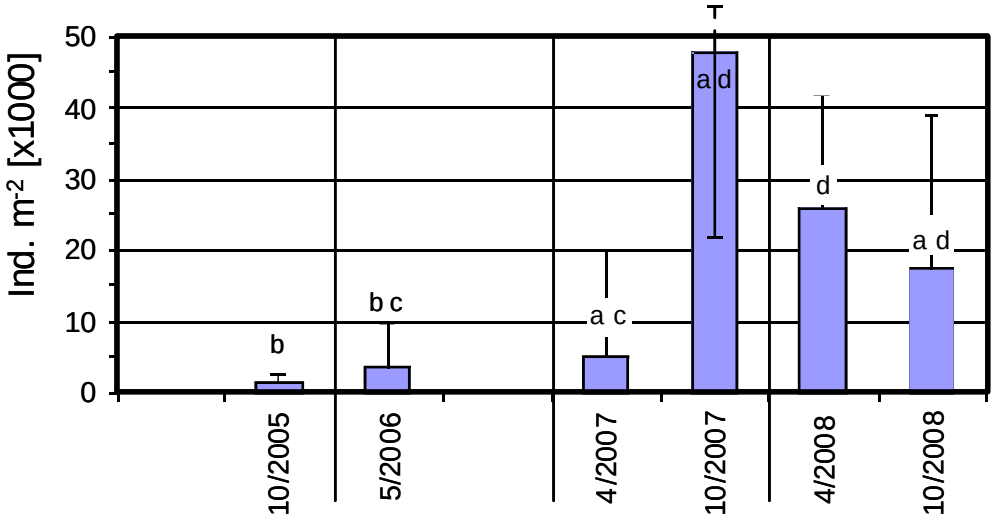

Fig. 8.10: Densities of total mesofauna (Collembola + Acari) as sampling-date averages (plus standard errors) from 2005 to 2008.

The abundances of mesofaunal arthropods increased significantly as of 2007 ($Xr^2 = 78.040$; $P < 0.001$), especially in autumn of 2007. The communities were nonetheless still strongly dominated by actinedid mites (Fig. 8.11). The variances of the abundances were very high, with many samples containing few individuals while some included many hundreds or even thousands, indicating that colonization of the soils was very heterogenic.

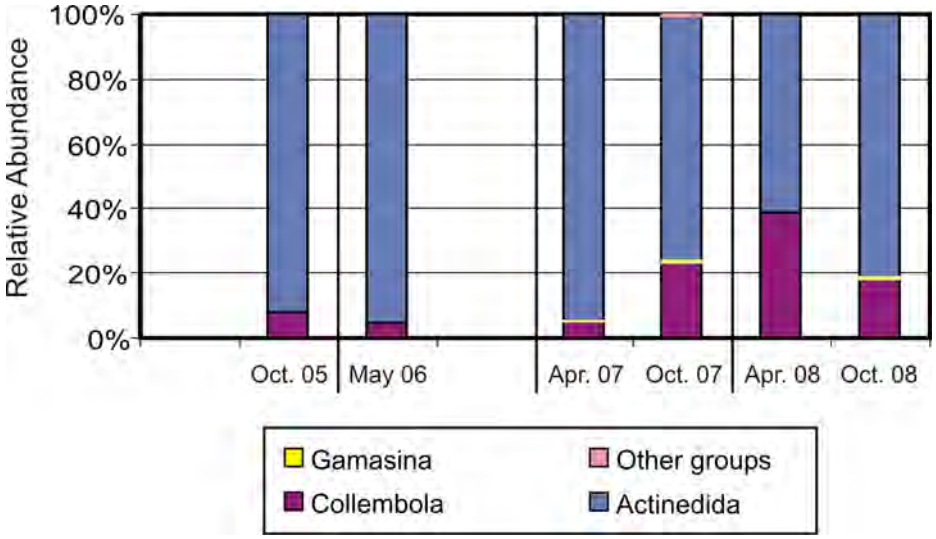

Fig. 8.11: Proportions (relative abundances) of the registered taxonomic groups within the total mesofaunal communities for each sampling date.

This sporadic individual-richness was mostly caused by strong populations of single species, e.g., *M. macrochaeta* (Collembola) and heterostigmate mite species such as *Siteroptes* sp. and *Bakerdania* sp. (Actinedida). These later species are probably microbivore (Suski, 1973, Greenslade and Cliff, 2004) and can be distributed phoretically (Rack and Vercammen-Grandjean, 1979, Masan, 1993, Kurosa, 2002), allowing strong population development if appropriate habitat and nutritional resources are found. Especially those species with the strongest population densities in autumn 2007 were reduced in 2008.

In total, species richness in the catchment area also increased in 2007 (Fig. 8.12), which was due to a strong development of the actinedid communities ($Xr^2 = 20.431$; $P < 0.001$). On the other hand, total species richness of Collembola remained fairly constant throughout the entire study period. However, their distribution within the catchment area became far more wide-spread and homogenous in 2007 and 2008, whereby the proportion of single samples containing multiple species increased significantly ($Xr^2 = 45.543$; $P < 0.001$).

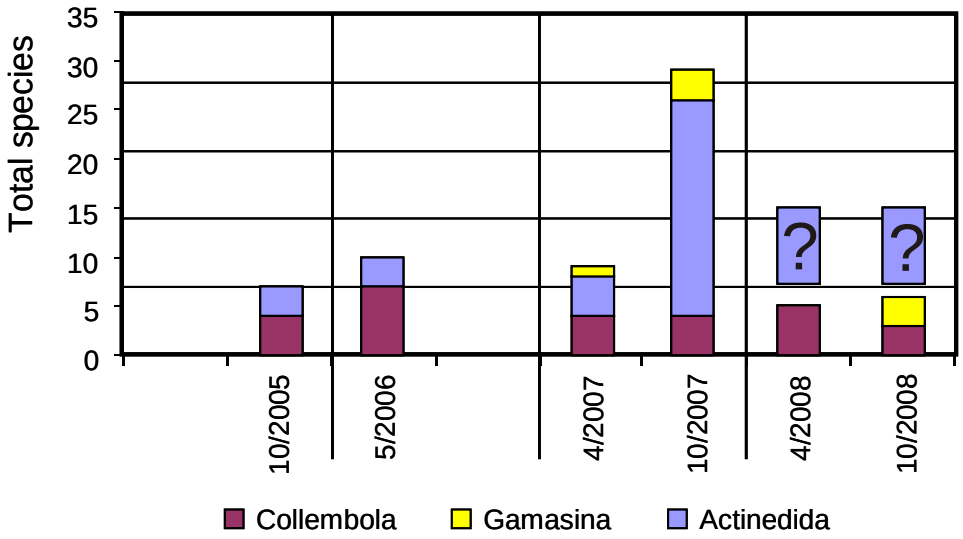

Fig. 8.12: Total species number of all mesofauna (color-separated into Collembola, Gamasina (Acari) and Actinedida (Acari) registered from 2005 to 2008.

Especially *M. macrochaeta* and *Proisotoma minuta*, the latter of which was found as single specimens as of 2005, increased steadily both in density as well as distribution throughout the entire study. They can thus be considered to have established populations in the catchment area, whereby adult specimens of *P. minuta* became abundant first in 2008. These species are common in early and middle succession stages (Potapov, 2001). Otherwise, only *Entomobrya lanuginosa* occurred throughout the study period, however only irregularly and mostly as juveniles. All other species occurred only as sporadic individuals. All registered collembolan species are widely distributed, eurytopic species (often cosmopolitan), most of which are known as pioneer species in recultivated sites (Dunger, 1968, Dunger et al., 2004).

M. macrochaeta could be shown to increase root colonization of arbuscular mycorrhiza (Cole et al., 2006).

Regarding Actinedida, the abundance and distribution of *Nanorchestes* sp. originally increased strongly from 2005 to spring of 2007. However, as many more species were found in autumn 2007, the density of this species decreased remarkably; dramatically in samples containing high densities of *Siteroptes* sp., indicating successional species replacement. Interesting was the occurrence of species such as *Cheletomimus vescus* (2006 and Oct. 2007), *Hawaiieupodes thermophilus* (Oct. 2007) and *Xerophiles ereynetoides* (2006-2007), which are very rare, most likely xero-thermophilous species probably adapted to nutrient-poor soils. Although most were only found in few individuals, the development of *X. ereynetoides* was conspicuous. Found as occasional individuals as of 2006, its density and distribution increased sharply in autumn 2007.

Within the Actinedida, the proportion of carnivorous species also increased in 2007. Whereby microbivore species (being possibly also nematophagous) represented almost 100% of the actinedid community up until April 2007, in autumn 2007 purely predaceous species accounted for approximately 25% of the species, if still less than 1% of the individuals. The state of this mite community in 2008 remains to be evaluated. First specimens of the carnivorous Gamasina were registered in 2007, however only as a few individuals in a few samples. The registered gamasin species are known from former mining spoils (Christian, 1993) and most likely immigrate through phoresy or passive wind transport. However, their only sporadic occurrence in 2007 and 2008 as well the lack of developmental stages (larvae, nymphs) are a strong indication that stable gamasin populations have not yet established themselves in the catchment area.

Thus, as of 2007, a marked development in the mesofaunal communities could be observed. Individual densities and the distribution of the different groups within the catchment area as well as the species richness of Actinedida increased strongly. This is quite possibly largely due to species that can colonize new habitats by phoresy or wind transport. Furthermore, the appearance of predaceous mesofaunal species as of 2007 – although their populations are most likely not thoroughly established – indicates a development of the soil food web beyond basal trophic levels of microbi- and algivore species, which alone were found in 2005 and 2006. A further indication of the initial status of the soil food web is that, throughout the entire sampling period, no oribatid mites were found. These detritivore and microbivore mites, one of the most common and abundant arthropod taxa in developed soils, are highly dependent on soil organic matter as a nutritional resource base. Their absence in the catchment area most likely reflects the primary-successional and nutrient-poor status of the developing soils as well as the low dispersal abilities of this mite group.

8. 3.4 Carabidae

All together, 3,187 specimens were captured within the sampling period, varying between 68 and 873 per trap. The activity-density of carabids varied between 6 and 73 individuals per trap and week (median 11.5, standard deviation 20.3), increasing significantly from the upper area to the semi-aquatic area (Fig. 8.13).

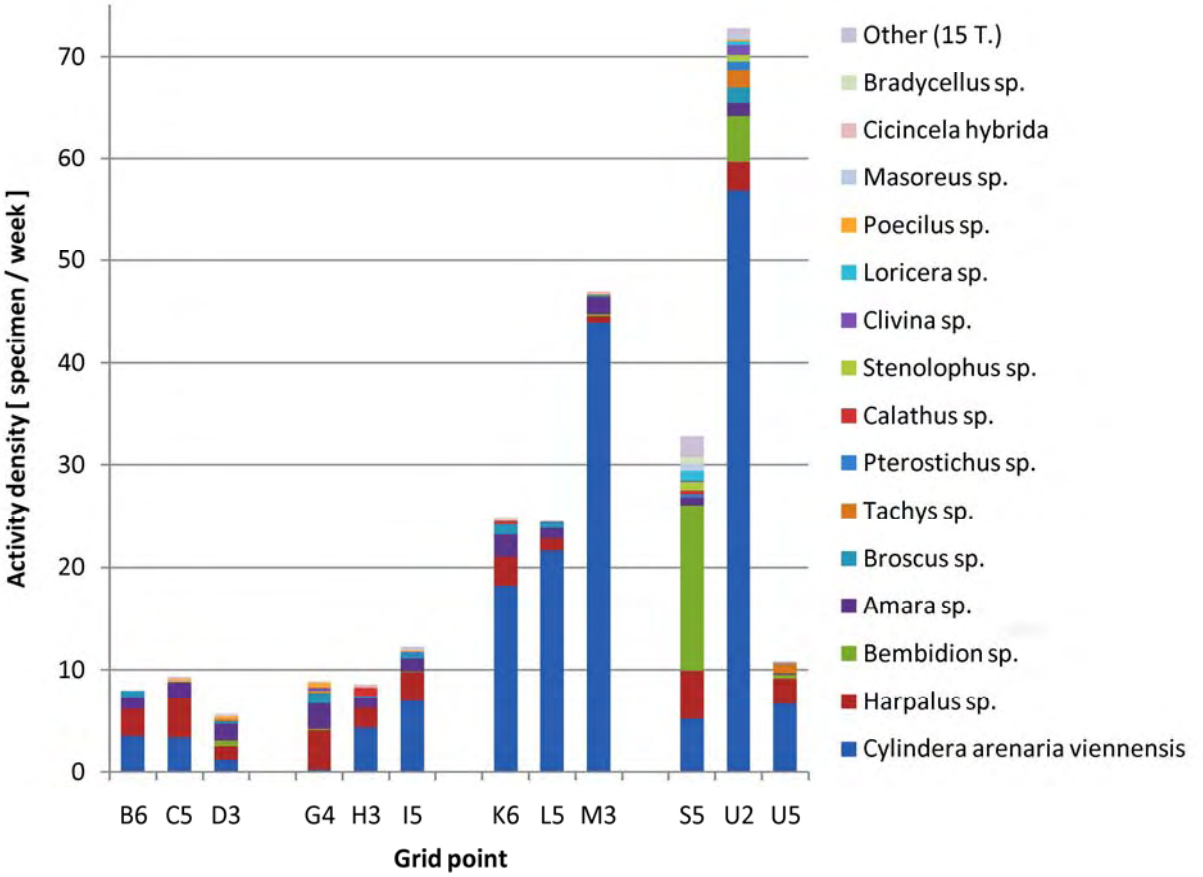

Fig. 8.13: Activity-density and dominance structure of Carabidae at the sampling points within the catchment in summer 2008.

Considering the preliminary determination, 30 taxa were observed (2 species, 28 genera). The eu-dominant species *Cylindera arenaria viennensis* (Schrank 1781) had a share of 65% in total, with increasing importance in the lower area and the semi-aquatic area (up to 93%) (Fig. 8.13). This tiger beetle is a typical pioneer species next to ponds in the post mining landscape, and is threatened by the natural succession of these habitats. In general, the carabid communities are expected to increase in diversity and density during the first ten years of primary succession. According to Brunk (2007), the key environmental parameters with regard to microscale (plot) and mesoscale (catchment) are supposed to be succession age, density and structure of the vegetation, soil moisture, and pH-value („structural diversity hypothesis“, Hamilton et al., 1964). These aspects will be addressed after species determination of all captured carabids.

8. 4 Conclusions

The spatial and temporal development of several components of the soil food web during the initial stage of primary succession in the artificially created catchment “Chicken Creek” were investigated from 2005 to 2008. Sampling of the different animal groups of the soil food web are in different stages of evaluation.

Testate amoebae up to now revealed only a few species occurring in extremely low densities. Concurrent investigations revealed an extreme dependence of testate amoebae on plant cover. Nematode as well as tardigrade densities and biomasses gradually increased from April 2007 to October 2008, indicating a change in soil conditions and food supply. In April 2007, general-opportunist, bacterial-feeding genera dominated these communities. As of October 2007, however, algal-feeding tardigrade and nematode genera contributed increasingly major proportions of the overall tardigrade-nematode biomass, indicating that soil algae are a very important food source in these young soils. Whereby algal-feeding tardigrades still constituted the vast majority of the densities in October 2008, plant root feeders gained more and more importance in the trophic structure of nematode communities, clearly mirroring the increasing growth of vegetation in the Chicken Creek site.

During initial development in the years 2005 and 2006, Collembola and Acari only sporadically colonized the catchment area, occurring in very low densities and species richness. The registered species are known from nutrient-poor soils and are most likely microbivore (bacteria, fungal hyphae) and algivore (algae), representing only basal trophic levels. Total abundances increased significantly as of 2007, but were still comparatively low and strongly dominated by actinedid mites. Colonization remained very heterogeneous. Species richness increased significantly in 2007 only for the actinedid communities. Species richness of Collembola remained fairly constant throughout the entire study period, but the distribution of dominant species became far more wide-spread and homogenous in late 2007 and 2008. All dominant collembolan and actinedid species were widely distributed, eurytopic, pioneer species, although very rare, xero-thermophilous species were observed within the actinedid mites (*Cheletomimus vescus*, *Hawaiieupodes thermophilus*, *Xerophiles ereynetoides*). Indications of successional species replacement could be observed within Actinedida already in autumn 2007.

As of 2007, the proportion of predaceous actinedid species increased and first specimens of the carnivorous Gamasina were registered. However, their densities continued to be very low. Furthermore, activity-densities and species richness of the epigeic and predaceous Carabidae were moderately high in 2008, indicating an adequate nutritional basis. They were nonetheless strongly dominated by a single, pioneer species typical for the initial stage of primary succession on sandy substrate in this region (*Cylindera arenaria viennensis*).

Thus, in general, the number of trophic links within the soil food web increased as of 2007 but especially from 2007 to 2008. This concurs with the herbaceous plant society becoming richer and more diverse, thus providing an increasing supply of nutrient resources and niches. Nonetheless, Chicken Creek soil food webs still represent poorly structured, species-poor food webs dominated by basal trophic levels, far away from the status expected of natural sites. The primary-successional and nutrient-poor status of the developing soils and the initial status of the soil food web are further indicated by the absence of oribatid mites, one of the most common and abundant arthropod taxa in developed soils. It is expected that, during soil succession, the food web structure should further increase from basal food webs, where only generalists can survive and reproduce, to mature food webs with a high number of trophic links and multitrophic interactions.

References

Andrássy, I., 1956: Die Rauminhalts- und Gewichtsbestimmung der Fadenwürmer (Nematoda). Acta Zool. 2, 1-5.

Andrássy, I., 1984: Nematoda (Ordnungen Monohysterida, Desmoscolecida, Araeolaimida, Chromadorida, Rhabditida). Akademie-Verlag, Berlin, 509 pp.

Bieri, M., Delucchi, V. and Lienhard, C., 1978: Ein abgeänderter Macfadyen-Apparat für die dynamische Extraktion von Bodenarthropoden. Bull. Soc. Ent. Suisse 51, 119-132.

Bongers, T., 1990: The maturity index: an ecological measure of environmental disturbance based on nematode species composition. Oecologia 83, 14-19.

Bongers, T. and Bongers, M., 1998: Functional diversity of nematodes. Appl. Soil Ecol. 10, 239-251.

Bretfeld, G., 1999: Synopses on Palaearctic Collembola Symphypleona. Abh. Ber. Naturkundemus. Görlitz 71 (1), 318 pp.

Brunk, I., 2007: Diversität und Sukzession von Laufkäferzönosen in gestörten Landschaften Südbrandenburgs. Dissertation BTU Cottbus, 382 pp.

Brzeski M.W., 1998: Nematodes of Tylenchina in Poland and temperate Europe. Muzeum I Instytut Zoologii Polska Akademia Nauk, Warsaw, 397 pp.

Christian, A., 1993: Untersuchungen zur Entwicklung der Raubmilbenfauna (Gamasina) der Halden des Braunkohlentagebaues Berzdorf/OL. Abh. Ber. Naturkundemus. Görlitz 67 (2), 2-64.

Cole, L., Bradford, M.A., Shaw, P.J.A. and Bardgett, R.D., 2006: The abundance, richness and functional role of the soil meso- and macrofauna in temperate grassland – A case study. Applied Soil Ecology 33, 186-198.

Dastych, H., 1988: The Tardigrada of Poland. Monografie Fauny Polski XVI. Panstwowe Wydawnictwo Naukowe, Warsaw, 255 pp.

Dunger, W., 1968: Die Entwicklung der Bodenfauna auf rekultivierten Kippen und Halden des Braunkohletagebaus. Abh. Ber. Naturkundemus. Görlitz 43, 256 pp.

Dunger, W. and Fiedler, H.J., 2000: Methoden der Bodenbiologie. Gustav Fischer Verlag, Stuttgart, 432 pp.

Dunger, W., Schulz, H.-J., Zimdars, B. and Hohberg, K., 2004: Changes in collembolan species composition in Eastern German mine sites over fifty years of primary succession. Pedobiologia 48, 503-517.

Ferris, H., Bongers, T. and de Goede, R.G.M., 2001: A framework for soil food web diagnostics: extension of the nematode faunal analysis concept. Appl. Soil Ecol. 18, 13-29.

Fjellberg, A., 1998: The Collembola of Fennoscandia and Denmark. Part I: Poduromorpha. Fauna Ent. Scand 35, 183 pp.

Fjellberg, A., 2008: The Collembola of Fennoscandia and Denmark. Part II: Entomobryomorpha and Symphypleona. Fauna Ent. Scand. 35, 264 pp.

Greenslade, P. and Clift, A., 2004: Review of pest arthropods recorded from commercial mushroom farms in Australia. Austr. Mycolog. 23, 77-93.

Hallas, T. E. and Yeates, G. W., 1972: Tardigrada of the soil and litter of a Danish beech forest. Pedobiologia 12, 287-304.

Hamilton, T.H., Barth, R.H., Jr. and Rubinoff, I., 1964: The environmental control of insular variation in bird species abundance. Proc. Nat. Acad. Sci. USA 52, 132-140.

Hodkinson, I.D., Coulson, S.J. and Webb, N.R., 2004: Invertebrate community assembly along proglacial chronosequences in the high Arctic. J Anim Ecol 73, 556–568.

Hohberg, K., 2003: Soil nematode fauna of afforested mine sites: genera distribution, trophic structure and functional guilds. Appl. Soil Ecol. 22, 113-126.

Karg, W., 1993: Acari (Acarina), Milben. Parasitiformes (Anactinochaeta). Cohors Gamasina Leach. Raubmilben. Dahl, F. (Begr.): Die Tierwelt Deutschlands und der angrenzenden Meeresteile. 59. Teil. Gustav Fischer Verlag, Jena, 523 pp.

Kazmierski, A., 1998: Tydeinae of the world: generic relationships, new and redescribed taxa and keys to all species. A revision of the subfamilies Pretydeinae and Tydeinae (Acari: Actinedida: Tydaidae) – part IV. Acta Zool. Cracov. 41, 283-455.

Kethley, J., 1990: Acarina: Prostigmata (Actinedida). In: Dindal, D.L. (ed.): Soil Biology Guide. J. Wiley & Sons, New York, 667-756.

Kurosa, K., 2002: A new genus and species of Pygmephoridae (Acari: Heterostigmata) associated with *Onthophagus* (Coleoptera: Scarabaeidae) in Japan. J. Acarol. Soc. Jpn. 11, 27-36.

Loof, P., 1999: Nematoda, Adenophorea (Dorylaimida). Spektrum Akademischer Verlag, Heidelberg, 264 pp.

Macfadyen, A., 1961: Improved funnel-type extractors for soil arthropoda. J. Anim. Ecol. 30, 71-184.

Masan, P., 1993: Mites (Acarina) associated with species of *Trox* (Coleoptera: Scarabaeidae). Eur. J. Ent. 90, 359-364.

Maucci, W., 1986: Tardigrada. Fauna d'Italia. Edizione Calderini, Bologna, 388 pp.

Meisterfeld, R., 2002: Order Arcellinida Kent, 1880. In: Lee, J.J., Leedale, G.F. and Bradbury, P. (eds.): An illustrated guide to the protozoa, 2nd edn. Society of Protozoologists, Lawrence, 827–860.

Pomorski, J., 1990: Morphological-systematic studies on the variability of pseudocelli and some morphological characters in *Onychiurus* of the "*armatus*-group" (Collembola, Onychiuridae). Part II: On synonyms within the "*armatus*-group", with special Reference to diagnostic characters. Annales Zoologici 26, 535-576.

Potapov, M., 2001: Synopses on Palaearctic Collembola Isotomidae. Abh. Ber. Naturkundemus. Görlitz 73, 630 pp.

Rack, G. and Vercammen-Grandjean, P.H., 1979: *Siteroptes* (*Siteroptoides*) *trombidiphilus* sp. n. (Acarina: Pygmephoridae) phoretisch auf einem Weibchen der Familie Trombidiidae (Acarina) aus Ostafrika. Ent. Mittl. Zool. Mus. Hamburg 6, 217-220.

Savulkina, M.M., 1981: The system, ecology and distribution of the mite family Pygmephoridae. 17 pp. (in Russian).

Schöps, F.-R. and Russell, D.J., 2004: Ein modifiziertes Friedman-Test (nicht-parametrische ANOVA) für quantitativen Auswertungen von Bodenmesofauna-Daten. Mitt. AG Bodenmesofauna 20, 31-35.

Suski, Z.W., 1973: A revision of *Siteroptes cerealium* (Kirchner) complex (Acarina, Heterostigmata, Pyemotidae). Ann. Zool. Warsz. 30, 509-535.

Thibaud, J.-M., Schulz, H.-J. and da Gama Assalino, M.M., 2004: Synopses on Palaearctic Collembola Hypogastruridae. Abh. Ber. Naturkundemus. Görlitz 75, 287 pp.

Verhoeven, R., 2002: The structure of the microtrophic system in a development series of dune soils. Pedobiologia 46, 75-98.

Volgin, V.I., 1989: Acarina of the Family Cheyletidae of the World. Brill Archive, Leiden, 532 pp.

Walker, L.R. and del Moral, R., 2003: Primary succession and ecosystem rehabilitation. Cambridge University Press, Cambridge, 442 pp.

Wanner, M., 1999: A review on the variability of testate amoebae: methodological approaches, environmental influences and taxonomical implications. Acta Protozool. 38, 15–29.

Wanner, M., Dunger, W., Schulz, H.-J. and Voigtländer, K., 1998: Soil zoological problems in central Europe. In: Pizl, V. and Tajovský, K. (eds.): Primary immigration of soil organisms on coal mined areas in Eastern Germany. Ceske Budejovice, 267-275.

Wanner, M. and Elmer, M., 2009: "Hot spots" on a new soil surface – How do testate amoebae settle down? Acta Protozool. 48, 281–289.

Wanner, M., Elmer, M., Kazda, M. and Xylander, W.E.R., 2008: Community assembly of terrestrial testate amoebae: how is the very first beginning characterised? Micr. Ecol. 56, 43-54.

Wardle, D.A., 2002: Communities and ecosystems – linking the aboveground and belowground components. Monographs in Population Biology 34, 392 pp.

Yeates, G.W., Bongers, T., de Goede, R.G.M., Freckman, D.W. and Georgieva, S.S., 1993: Feeding habits in soil nematode families and genera – an outline for soil ecologists. J. Nematol. 25, 315-331.

Zacharda, M., 1978: Soil mites of the family Rhagidiidae (Actinedida: Eupodoidea). Morphology, Systematics, Ecology. Acta Univ Carol Biol. 5-6, 489-790.

Zar, J.H., 1999: Biostatistical Analysis. 4th Edn. Prentice Hall, London, 663 pp.

Zimdars, B. and Dunger, W., 1994: Synopses on Palaearctic Collembola Tullbergiinae. Abh. Ber. Naturkundemus. Görlitz 68, 1-71.

9. Limnological development of Chicken Creek pond in the first four years

Dieter Lessmann, Rainer Deneke, Remo Ender, Brigitte Nixdorf

Department of Freshwater Conservation, Brandenburg University of Technology

9. 1 Introduction

Limnological investigations of primary colonization mechanisms and patterns in aquatic ecosystems are rare (Calderoni et al., 1992; Kalliola et al., 1991; McCormick et al., 1991; Robinson and Edgemon 1988) and mainly focused on the incidentally genesis of extreme habitats or re-colonization mechanisms after extreme disturbances (Guiral et al., 1994; Arfi et al., 1991; Elber and Schanz, 1990; Morabito and Pugnetti, 2001). Basic and general mechanisms of organism succession in ecosystems are described by Odum (1969), whereas Reynolds (1997) and Reynolds et al. (2002) discussed the strategy of planktonic colonization in aquatic ecosystems, especially in lakes. The way seasonal plankton succession is controlled by bottom-up or top-down mechanisms is shown by Sommer et al. (1986), Sommer (1991, 1993), Hehmann et al. (2001), Hubble and Harper (2001), Gobler et al. (2002). In summary, limnological investigations on control and colonization patterns of planktonic communities were carried out nearly exclusively in maturated lake ecosystems while limnological studies on newly formed standing waters are rare.

Our studies were focused on the initial limnological development of a new pond which formed the lowermost hydrological compartment of the artificial catchment area Chicken Creek with a size of 5.9 ha in the open-cast mine Welzow-Süd in the Lusatian lignite mining district. The physical and chemical development of the pond was documented as well as the biological inhabitation and processes in the pelagial with their seasonal changes. Whereas in this chapter pelagic processes are described and analyzed, the benthic development is discussed in more detail in Chapter 10.

9. 2 Material and methods

The limnological studies on Chicken Creek pond started at the very beginning of its development in 2005/2006 as occasional sampling and have been intensified from February to June 2008 as part of the preparation of a diploma thesis (Dörschel, 2009) and afterwards as part of the basic monitoring programme of the research projects of the Transregio 38 ("Structures and processes of the initial ecosystem development in an artificial catchment area"). In this report results were included until March 2009.

In 2005 and 2006 and again from September 2008, samples have been taken from a boat at the point of greatest depth of the pond and depth profiles of physical variables and fluorescence chlorophyll-a are available. From February until June 2008, sampling took place biweekly from the end of a pontoon which is located on the southern shores where water depth reached only up to 50 cm. From September 2008, it was continued as routine monthly measuring and sampling. The depth profiles of physical, chemical and biological variables were measured by using specific probes. Water samples were taken with a Limnos sampler as point samples from a depth of up to 50 cm (February – June 2008) and as mixed samples at 50 cm depth intervals, respectively.

Table 9.1 provides an overview about the routine sampling methods for in-situ investigations and chemical and biological analyses.

For sampling, conservation and analyses of the plankton following procedures were applied: All plankton samples were fixed and stored in the dark at 4°C. For phytoplankton analysis, a sub-sample of the mixed water sample was fixed with Lugol´s solution and counted later according to the method described by Utermöhl (1958). Zooplankton was enriched by filtration (mesh size 25 µm) of 20 L of the mixed sample and fixed with 3% formalin.

Bacterioplankton was taken from the mixed sample (100 ml fixed with 3% Formalin). Sub-samples were taken and fixed with formaldehyde (final concentration 1 %). Depending on expected cell densities 1-2 or 5-10 ml were filtrated through black Nuclepore PC-filters (pore size 0.2 µm). Bacterial cell numbers were counted by staining with DAPI according to the procedure of Porter and Feig (1980).

In total, the biological data comprise bacterial abundance, chlorophyll-a concentrations, phytoplankton and zooplankton taxa composition, abundance and biomass. Most biological data are only available from February 2008.

Tab. 9.1: Methods used for chemical and chlorophyll-a analyses in Chicken Creek pond

Variable	Measuring device / analytical method	DIN/EN
Temperature, electrical conductivity, pH, oxygen conc. and saturation	Hydrolab multi-parameter probe (Dataprobe 4a mini)	DIN 38404-C4 (temp.) DIN EN 27888 (el. cond.) DIN 38404-C5 (pH) DIN EN 25814 (O_2)
$K_{S4.3}$ (alkalinity)	Titration with HCl	DIN38409-H7
Total phosphorus (TP)	Flow injection analysis (FIA)	DIN EN ISO 15681-1
Dissolved inorganic phosphorus (DIP)	Segmented flow analysis (SFA)	DIN EN ISO 15681-2
NO_3^-, NO_2^-	Segmented flow analysis (SFA)	DIN EN ISO 133 95
NH_4^+	Segmented flow analysis (SFA)	DIN EN ISO 11 732
TN	Flow injection analysis (FIA)	DIN EN ISO 133 95
Si	Segmented flow analysis (SFA)	DIN 38405-D21
Ca^{2+}, Mg^{2+}, K^+, Na^+	Ion chromatography (IC)	DIN 38406
SO_4^{2-}, Cl^-	Ion chromatography (IC)	DIN EN ISO 10304-1
Fe, Al, Mn	Atomic absorption spectrometry (AAS)	DIN 38406
TIC, DIC, TOC, DOC	DIMATOC 100	DIN EN 1484, ISO 8245
Chlorophyll-a (*in-situ*)	Haardt Backscat-Fluorometer	-
Chlorophyll-a	Photometry	Nusch & Palme (1975), DIN 38412-16

9. 3 General pond development

Chicken Creek pond first formed in March 2005 when the modelled depression in the clay layer at the lowest point of the artificial catchment area Chicken Creek was filled by rain water and surface run-off. The maximum water level of 125.44 m was reached for the first time in January 2006 and the first outflow occurred.

The changes of the appearance of the pond with time have been documented by photos (Fig. 9.1 – 9.7). Besides the fast increase of the water level which was mainly due to single heavy rainfall events in 2005, major changes in the characteristics of the catchment area and especially in the close surrounding of the pond and along its shores become visible from the photos. Fast changes of the vegetation and its increasing biomass can be observed. Macrophytes, mostly reed, have been advancing more and more from the shores into the pond and its surrounding.

Fig. 9.1: Chicken Creek pond in the newly formed artificial catchment area on April 13th, 2005 (Photo: D. Lessmann).

Fig. 9.2: Chicken Creek pond on August 4th, 2005 (Photo: D. Lessmann).

Fig. 9.3: Chicken Creek pond on September 15th, 2005. The clay layer of the catchment area is now covered by sandy Quaternary sediments from the mine Welzow-Süd (Photo: R. Ender).

Fig. 9.4: Chicken Creek pond on June 20th, 2006 with pontoon and outflow weir. First vegetation appearing in the catchment area and on the shores of the pond (Photo: R. Ender).

Fig. 9.5: Chicken Creek pond on September 19th, 2007 (Photo: R. Ender).

Fig. 9.6: Chicken Creek pond on July 3rd, 2008. Shores partly covered with dense vegetation of reed (Photo: R. Ender).

Fig. 9.7: Chicken Creek pond during sampling on April 20th, 2009. Rapidly increasing vegetation around the pond and in the catchment area (Photo: R. Ender).

Right from the beginning, the new pond received eroded material from its watershed and showed a high sedimentation rate. This resulted in a decrease in pond volume (see also Chapter 10.3.2). The volume of the original pond basin was 6,483 m³ before flooding. Until 2008 pond volume decreased to 4,109 m³. Within three years the pond lost nearly 37 % of its volume. The current maximum depth is 2.4 m and the mean depth 1.1 m (Fig. 9.8, Tab. 9.2).

The water level of the pond responded very fast to precipitation due to the small catchment area, the soil layer of Quaternary sediments that covers the impermeable clay layer and the relatively low vegetation cover. On the other hand it is strongly exposed to solar irradiance and wind that lead to potentially high water losses by evaporation. In 2008, water level fluctuation reached 31 cm (Fig. 9.8), which means that the pond volume showed fluctuations of nearly 25% (see also Fig. 4.8). The minimum water level was recorded during summer in July 2008. Therefore, the maximum depth varied in reality between about 2.1 and 2.4 m.

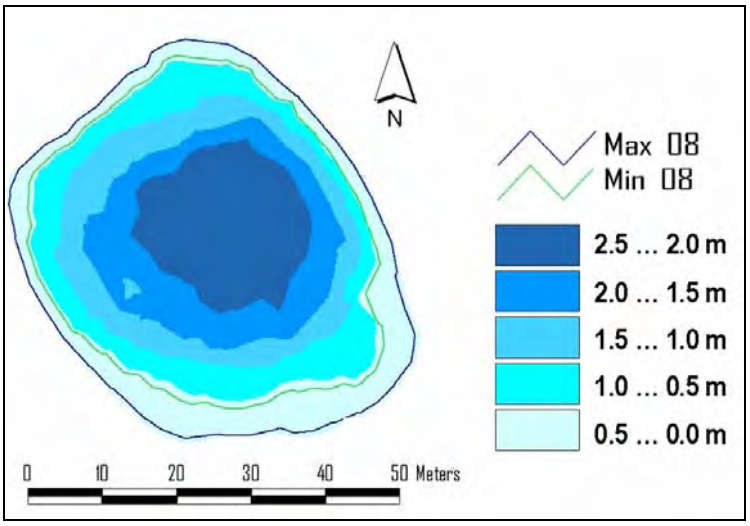

Fig. 9.8: Bathymetric map of Chicken Creek pond according to the survey from October 2008 with lowest and highest water level in 2008 (Max 08, Min 08).

Tab. 9.2: Morphometrical characteristics of Chicken Creek pond according to the pond survey from October 2008.

maximum water level		m a.s.l.	125.44
volume	V	m^3	4,109
surface area	A	m^2	3,896
maximum depth	z_{max}	m	2.4
mean depth	z_{mean}	m	1.1

9. 4 Results of the limnological monitoring

9. 4.1 Development of physical and chemical properties

Stratification and mixing

As indicated by depth profiles of water temperature and oxygen concentrations, Chicken Creek pond was polymictic. Nevertheless, periods with stratification occurred which could be observed during winter at times the pond was covered with ice, but, for example, also in April 2006 (Fig. 9.9 and 9.10). During these stratification periods, besides the temperature gradient particularly an oxygen gradient was formed which was due to the photosynthesis of phytoplankton that could be found in high abundance at certain water depths as shown by chlorophyll-a profiles (Fig. 9.19 and 9.20) and in 2008/2009 also due to the photosynthesis of macrophytes. Decomposition processes close to the bottom with their high oxygen consumption were also reflected in the oxygen profiles (Fig. 9.10).

Oxygen

In general, slight oxygen over-saturation seemed to be more typical for the pond than undersaturation. Apart from the first months of pond development when oxygen saturation reached only 84 and 96 %, in 2006 and from September 2008 the mean data from the depth profile measurements were almost continuously slightly above 100 % (Fig. 9.11). The highest oversaturation occurred in the water depth below about 1 m during periods of stratification (Fig. 9.9 and 9.10). The data from February until June 2008 represent only the oxygen concentrations in the uppermost water layer of the shallow littoral area and therefore can only be compared restrictedly with the other data.

pH and alkalinity

With values always around 8, the pH was relatively constant from the beginning until March 2009 (Fig. 9.12). According to the alkalinity (determined as acid capacity $K_{S4.3}$), with a mean of 2.2 mmol L^{-1} the pond has to be classified as hard water body. The water was well buffered by the carbonate buffering system. From 2006 to 2008 an increase of nearly 1 mmol L^{-1} occurred (Tab. 9.3).

Electrical conductivity

The data of the electrical conductivity were also relatively stable. Fluctuations occurred in the range from about 570 to 690 µS cm^{-1} in 2008/2009 and represent a medium mineralization (Fig. 9.13). Compared with 2005/2006, this means a stabilization of the mineralization of the pond water. During the filling phase the electrical conductivity varied considerably and reflected the changing composition of ions in the water and dilution of the inflow that originated mainly from surface run-off and precipitation.

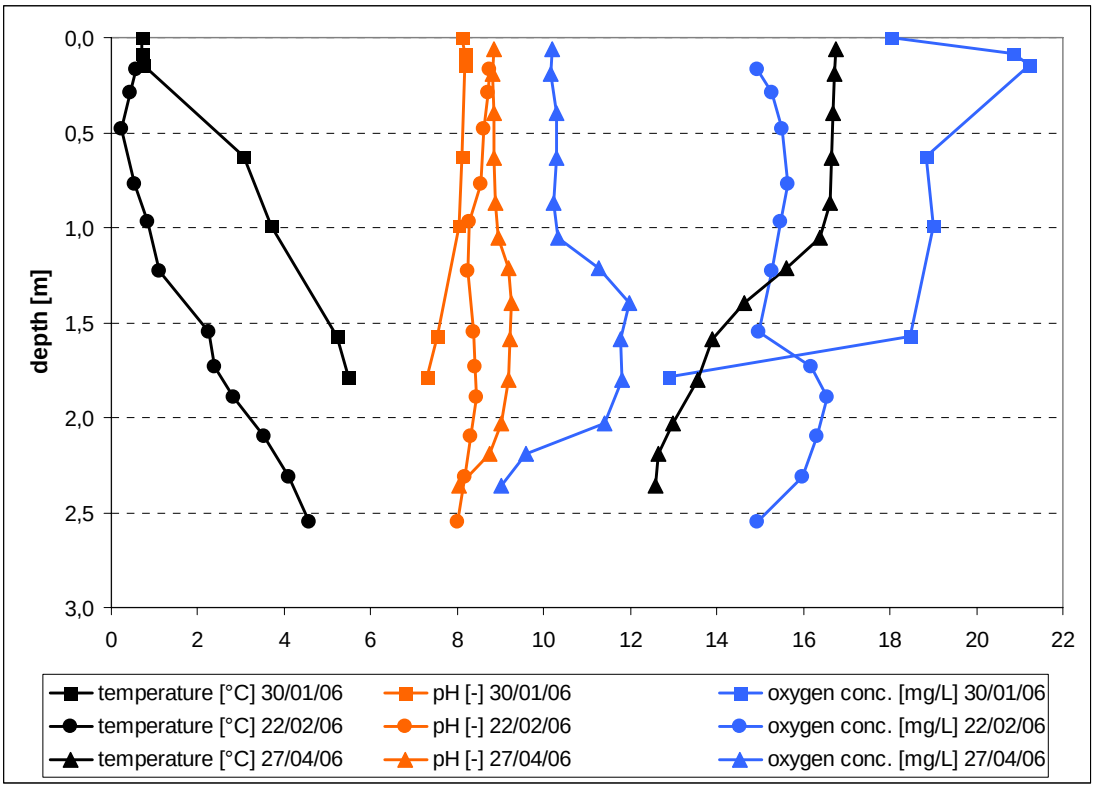

Fig. 9.9: Depth profiles of temperature, pH and oxygen concentration in Chicken Creek pond on 30 January, 22 February and 27 April 2006.

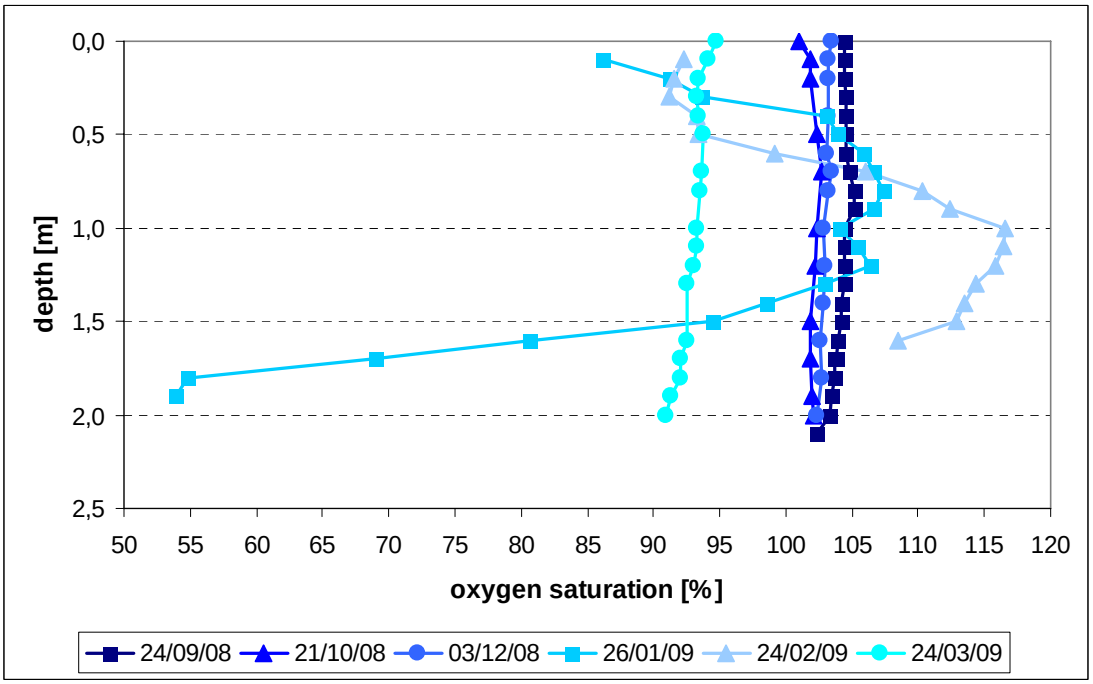

Fig. 9.10: Depth profiles of oxygen saturation in Chicken Creek pond from September 2008 until March 2009. In January and February 2009 the pond was covered with ice.

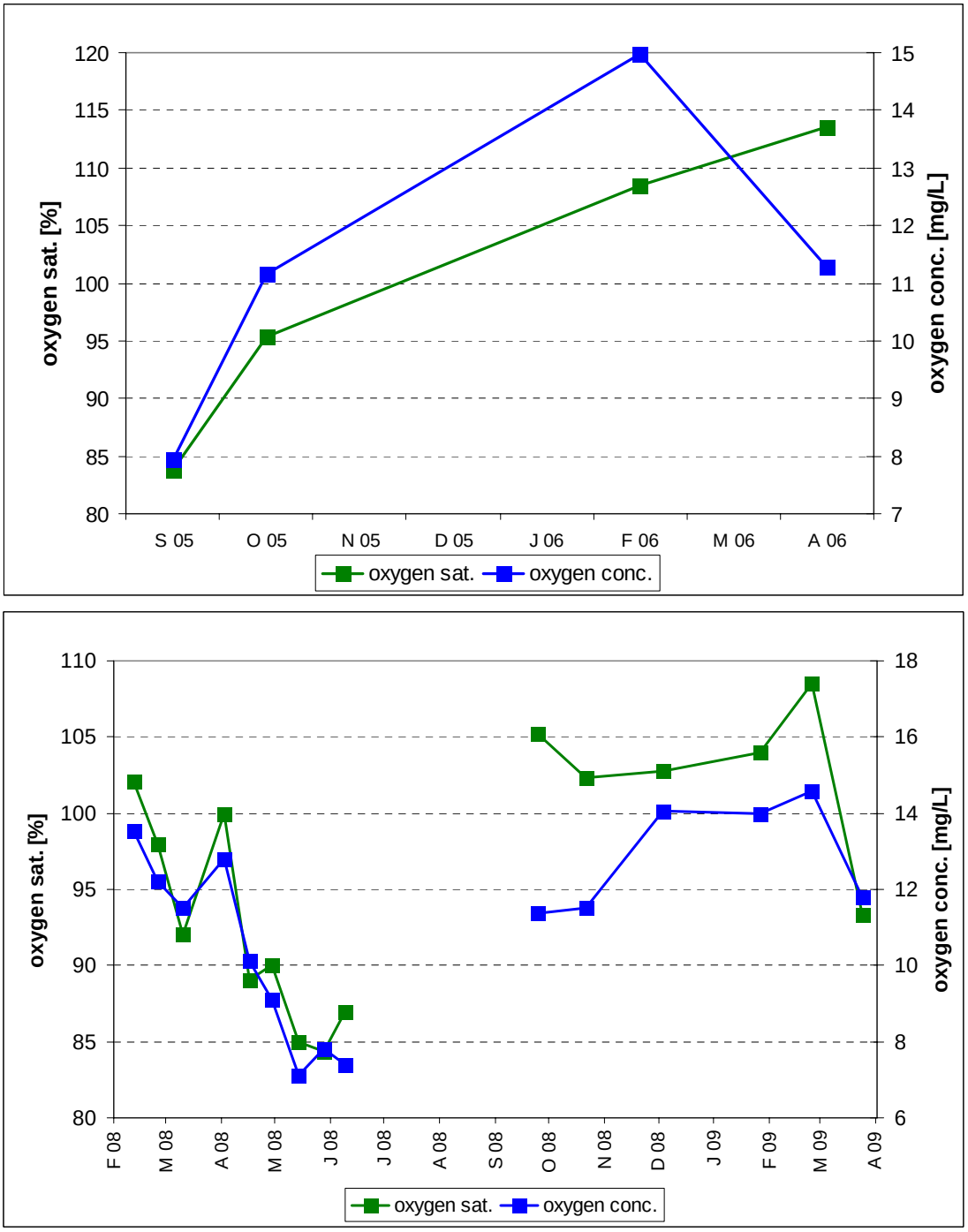

Fig. 9.11: Development of mean oxygen concentration and oxygen saturation in Chicken Creek pond within the period September 2005 until April 2006 (upper chart) and February 2008 until March 2009 (lower chart).

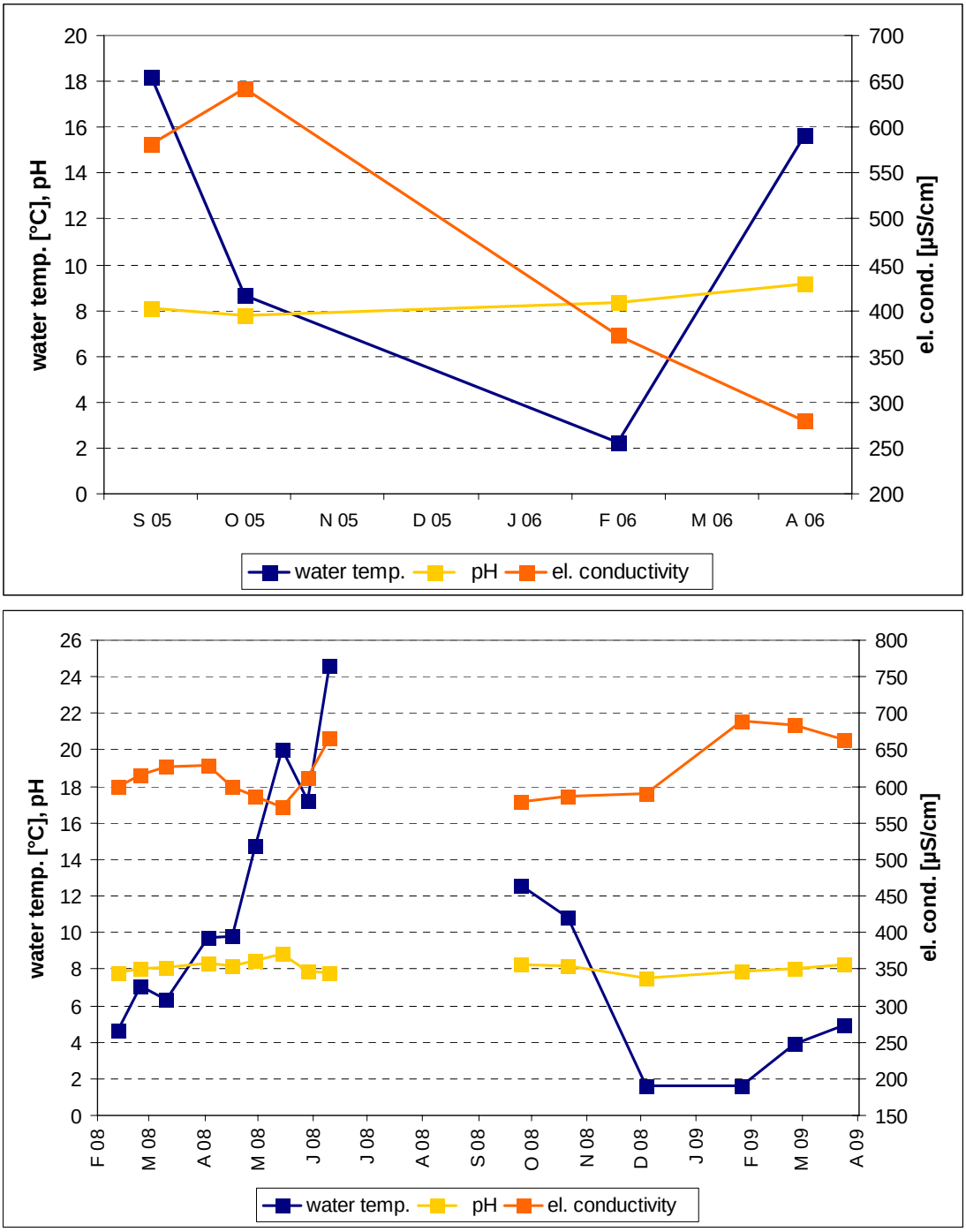

Fig. 9.12: Development of mean water temperature, pH and electrical conductivity in Chicken Creek pond within the period September 2005 until April 2006 (upper chart) and February 2008 until March 2009 (lower chart).

Tab. 9.3: Results of the chemical analyses of Chicken Creek pond. Data from 2005/2006 (n = 2 [30 January and 22 February 2006], * n = 7 with mean ± standard deviation) are compared with data from the period February 2008 until March 2009. Bicarbonate concentrations were calculated from $K_{S4.3}$ values. n: number of samples, SD: standard deviation, Min: minimum, Max: maximum.

Variable	Unit	2005/2006		2008/2009			
		Mean	n	Mean	SD	Min	Max
DOC	mg L^{-1}	-	10	9.7	2.5	5.1	13.9
TOC	mg L^{-1}	-	10	11.6	3.8	5.6	17.9
DIC	mg L^{-1}	-	10	21.7	6.0	9.7	29.3
TIC	mg L^{-1}	8.1	9	22.1	5.8	11.2	30.1
K_{S43}	mmol L^{-1}	1.3	2	2.2	-	-	-
HCO_3	mg L^{-1}	79.3	2	134	-	-	-
Ca^{2+}	mg L^{-1}	112	7	108	38.6	61.9	167
Mg^{2+}	mg L^{-1}	4.5	7	9.1	2.28	5.6	11.7
Na^{+}	mg L^{-1}	2.3	7	3.0	0.84	1.7	4.0
K^{+}	mg L^{-1}	2.1	7	0.8	0.38	0.4	1.5
SO_4^{2-}	mg L^{-1}	208	7	190	28.4	147	235
Cl^{-}	mg L^{-1}	2.6	7	2.3	1.18	1.38	4.87
Fe	mg L^{-1}	0.1	7	0.18	0.07	0.10	0.27
Al	mg L^{-1}	< 0.3	5	0.22	0.11	0.1	0.3
Mn	mg L^{-1}	< 0.05	6	0.08	0.02	0.05	0.1
NO_3^{-}	mg L^{-1}	1.4	7	0.17	0.16	<0.1	0.50
NH_4^{+}	mg L^{-1}	< 0.1	3	< 0.1	-	-	-
$N_{inorg.}$	µg L^{-1}	375 ± 515*	17	105	58	47	284
DIP	µg L^{-1}	7 ± 4*	16	5	2	1	9
TP	µg L^{-1}	47 ± 40*	17	23	8	13	40
Si	µg L^{-1}	762 ± 388*	17	280	310	39	1,313

Chemical composition

As typical for standing water bodies in the Lusatian mining district, the water was rich in sulphate. From its chemical composition it has to be characterized as calcium-sulphate-bicarbonate water (Fig. 9.13, Tab. 9.3). Besides magnesium, which was the second most important cation, all other ions contributed only in very small quantities to the total ion concentration. In general, concentrations of metals were low.

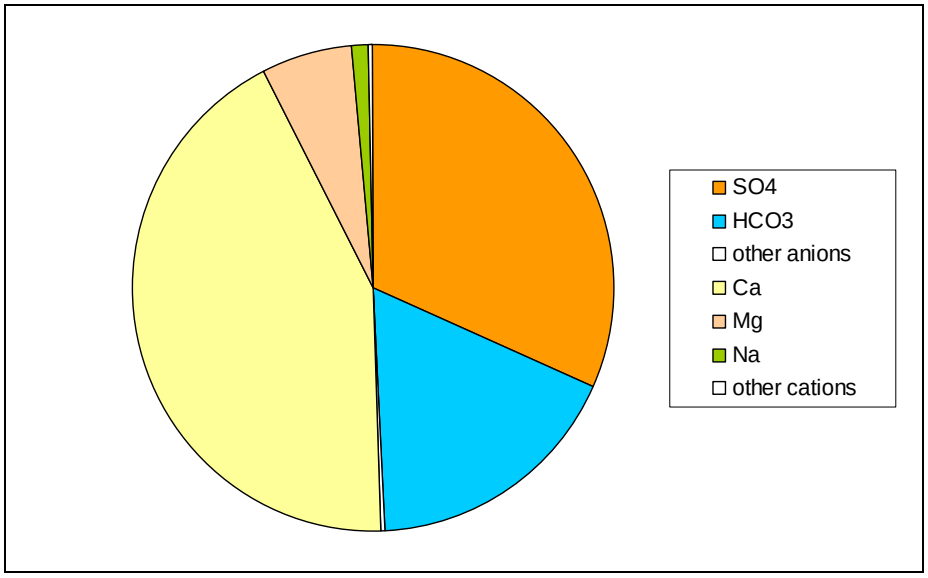

Fig. 9.13: Ionic composition of the water of Chicken Creek pond in 2008/2009. Proportion of mean ion equivalent concentrations is shown.

Nutrients

Primary production was limited by phosphorus and silica. Despite also very low nitrogen concentrations the N:P ratio was always > 16. In 2008/2009, the mean total phosphorus (TP) concentration was 23 µg L^{-1} and in a range that is typical for mesotrophic lakes (Vollenweider, 1976) (Tab. 9.3). While TP concentrations showed large fluctuations, dissolved inorganic phosphorus (DIP) concentrations were relatively stable and had a mean of 5 µg L^{-1} (Fig. 9.15). Only on the first sampling date in April 2005, DIP reached far higher concentrations of 15 µg L^{-1}. In 2005 and 2006 TP concentrations exceeded 30 µg L^{-1} several times (Fig. 9.15). It can be assumed, that TP fluctuations represented a varying phosphorus input from the catchment area, probably correlated with the variations in precipitation, run-off and sediment input into the pond. This assumption was confirmed by TP measurements during the winter 2005/2006, when at the end of the ice covering the accumulated TP content in the ice was measured: more than 600 µg L^{-1} TP were detected; a tenfold higher accumulation compared with eutrophic lakes in the Scharmützelsee region. In August 2005, when there was a TP concentration of about 130 µg L^{-1}, the water showed a yellow to brownish colour and an extremely high turbidity from suspended matter.

After larger fluctuations at the beginning of pond development, inorganic nitrogen concentrations stabilized on a low level in 2008/2009 (Fig. 9.16, Tab. 9.3). Nevertheless, because of the also relatively low phosphorus concentrations nitrogen did never control pelagic primary production.

For diatoms also silica concentrations are important. In 2005 and 2006 a continuous decrease in dissolved silica occurred from about 1,400 µg L^{-1} to less than 400 µg L^{-1} (Fig. 9.16, Tab. 9.3). In 2008, silica concentrations started on an extremely low level with less than 100 µg L^{-1} but increased from summer until January 2009. In February and March 2009 silica concentrations became much lower again. Diatoms are already controlled by silica concentrations lower than 390 µg L^{-1} (Schelske et al., 1986).

Organic carbon

For organic carbon, data are only available for the period February until June 2008 and for January and March 2009. Usually, TOC was only slightly higher than DOC with concentrations mostly between 7 and 14 mg L^{-1} (Fig. 9.14), which indicated a low biomass and a relatively low quantity of biodegradable detritus. The correlation with seasonal phytoplankton biomass succession was obvious (see Chapter 9.4.3).

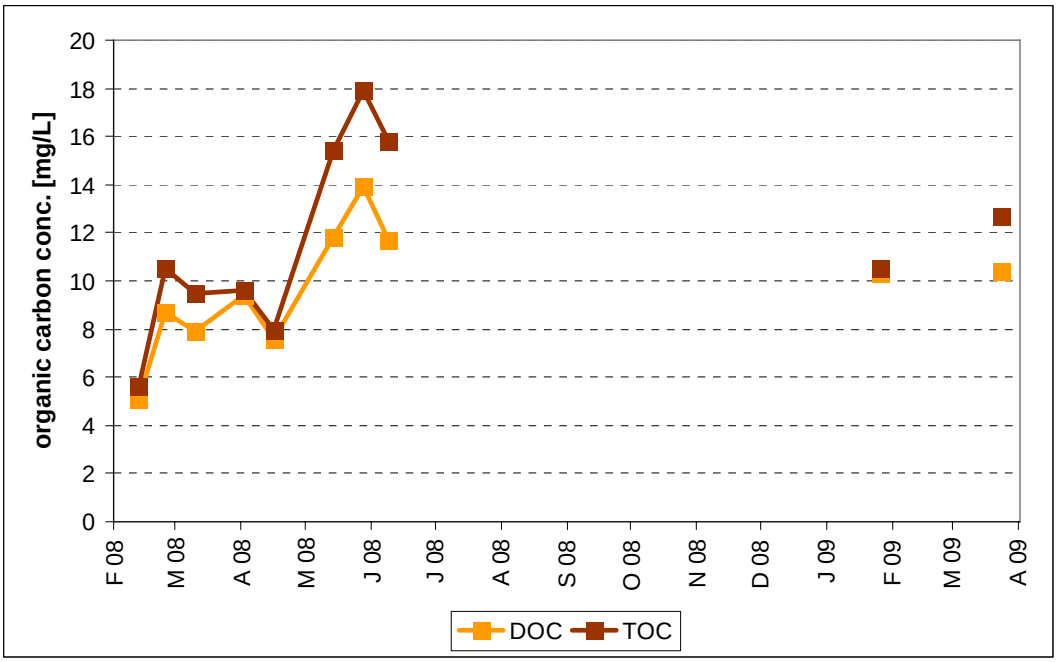

Fig. 9.14: Development of dissolved (DOC) and total organic carbon concentrations (TOC) in Chicken Creek pond within the period February 2008 until March 2009.

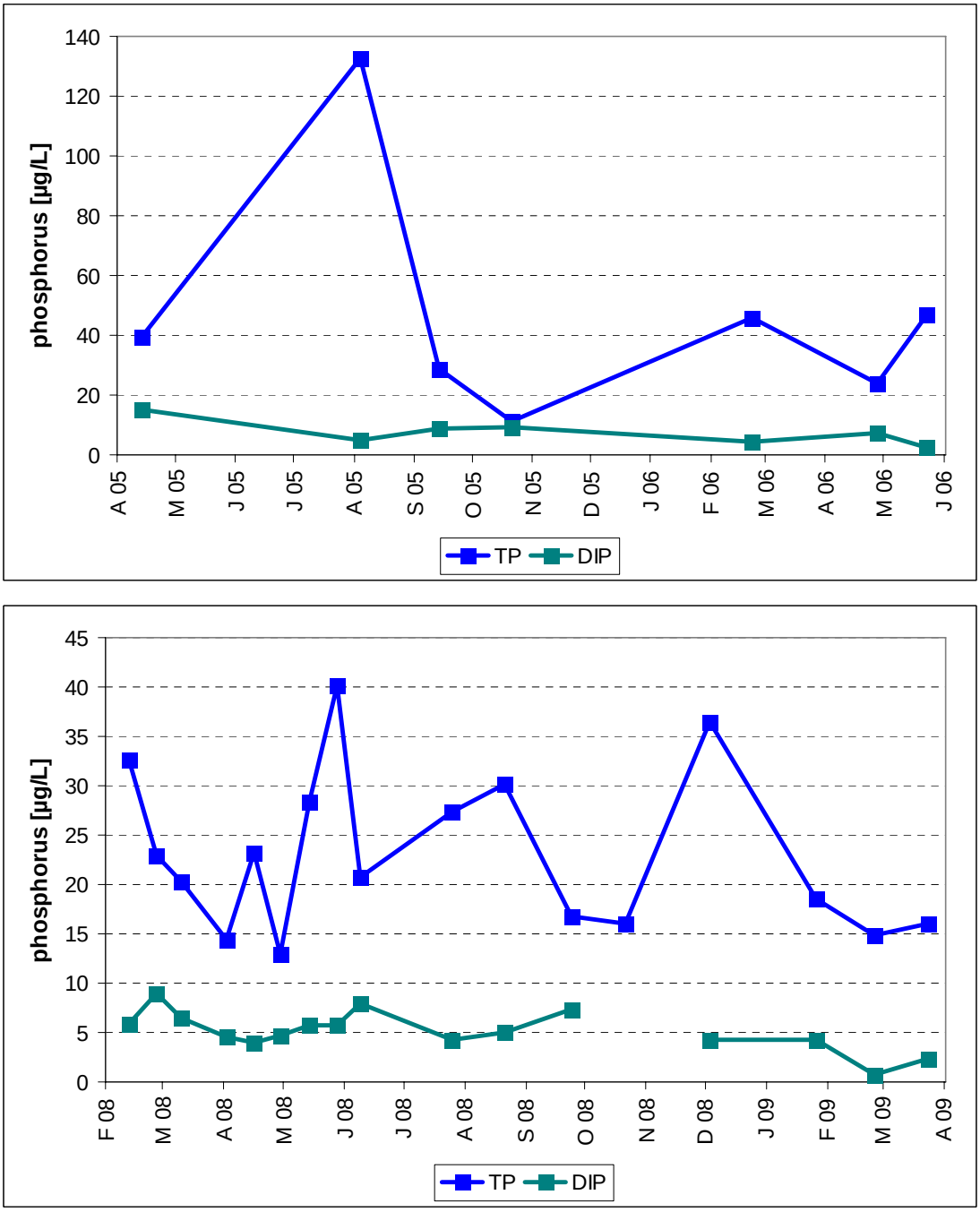

Fig. 9.15: Development of total phosphorus (TP) and dissolved inorganic phosphorus (DIP) concentrations in Chicken Creek pond within the period April 2005 until May 2006 (upper chart) and February 2008 until March 2009 (lower chart).

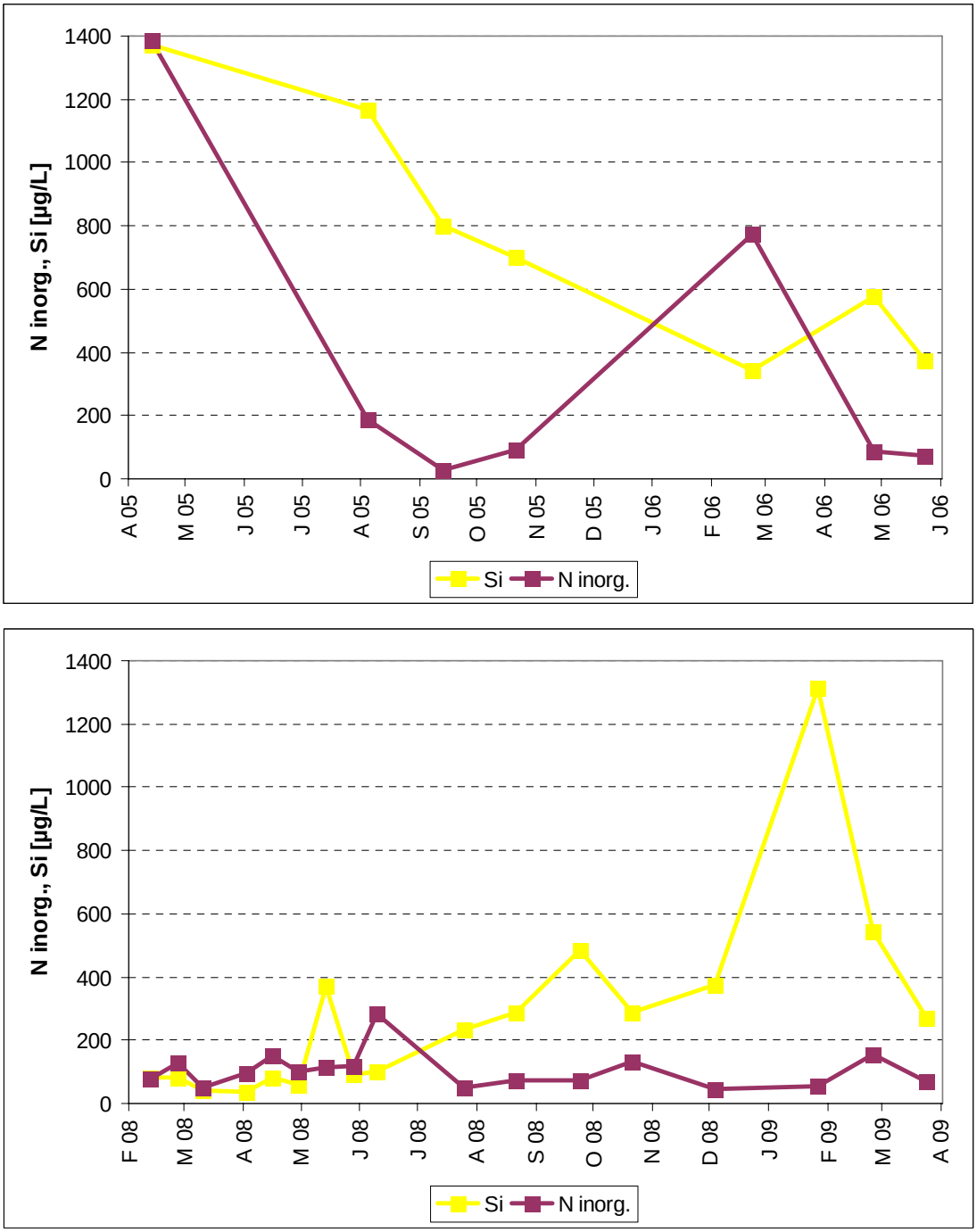

Fig. 9.16: Development of silica (Si) and inorganic nitrogen (NO_2 and NO_3) concentrations in Chicken Creek pond within the period April 2005 until May 2006 (upper chart) and February 2008 until March 2009 (lower chart).

9. 4.2 Biological development – bacterioplankton

Bacterioplankton usually forms the main heterotrophic group of organisms playing a key role in the decomposition and the re-mineralization of organic substances. Bacterial abundance of Chicken Creek pond is shown in Fig. 9.17 for the period February to June 2008. The variations were relatively low und total cell numbers were in a medium range (4.69 * 10^6 cells mL^{-1}). The low cell numbers in June 2008 (5.05 * 10^5 cells mL^{-1}) did not correspond with the general trend of high metabolic phytoplankton activity in the pelagic water at this sampling date (compare with Fig. 9.21). The sample was very turbid and seemed to be disturbed for unknown reasons.

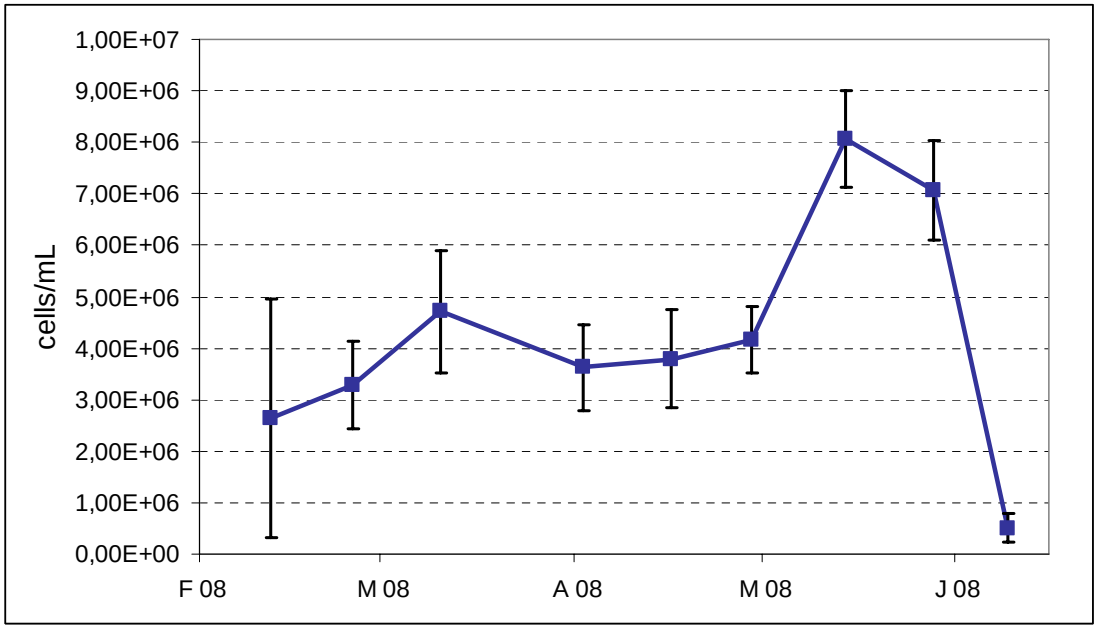

Fig. 9.17: Bacterial abundance with standard deviation of suspended and attached cells in pelagic water of Chicken Creek pond from February until June 2008.

9. 4.3 Biological development – chlorophyll-a concentration and phytoplankton

Chlorophyll-a concentration

According to the low nutrient concentrations, chlorophyll-a concentration as indicator for the biomass of the phytoplankton was also low during most times of the year. Nevertheless, some short-lasting algae "blooms" occurred in all years of the investigations in spring and summer, connected usually with high TP concentrations. At these times, the usual mean chlorophyll-a concentration of less than 5 µg L^{-1} increased to up to 20 µg L^{-1} as in June and August 2008 or even 27 µg L^{-1} as in April 2006 (Fig. 9.18).

As already proofed by temperature and oxygen depth profiles Chicken Creek pond stratified during certain periods of the year. Stratification always occurred during times when the pond was covered by ice but also with indefinite duration during other times of the year depending on the weather.

Stratification seemed to lead to a sharp increase of chlorophyll-a concentration with depth as shown by fluorescence probe data. Maximum chlorophyll-a concentration usually occurred in a depth below 1 m. For example, this becomes visible from data measured in April 2006, January and February 2009 (Fig. 9.19, 9.20). On April 27th, 2006 the highest values were recorded. Also close to the surface fluorescence chlorophyll-a concentration was about 15 µg L^{-1}. It increased in the lower 80 cm to more than 40 µg L^{-1} (Fig. 9.19). In 2008/2009, "deep" chlorophyll-a maxima reached only 5 – 10 µg L^{-1} (Fig. 9.20).

Phytoplankton

Temporal dynamics of chlorophyll-a concentration corresponded with that of phytoplankton biomass (Fig. 9.21), which was on a relatively low level (mean: 1.6 mm^3 L^{-1}) with maxima in April (3.0 mm^3 L^{-1}), June (7.8 mm^3 L^{-1}), July (2.9 mm^3 L^{-1}), and a small maximum in December 2008 (1.6 mm^3 L^{-1}). Phytoplankton cell abundances varied between 1 and $31*10^6$ cells L^{-1} in 2008/2009. The phytoplankton biovolume followed the TP concentration relatively closely (Fig. 9.15) which is a clear proof for the phosphorus limitation of primary production in Chicken Creek pond. An exception was February 2008 what may be due to harsh winter conditions that did not allow higher phytoplankton biomass.

While the absolute phytoplankton biomass maximum in June 2008 was formed by a relatively diverse group of taxa with *Pseudopedinella erkensis* (Chrysophyceae) as the most dominant one followed by *Fragilaria* sp. (diatoms) and *Euglena* sp. (Euglenophyceae), the maxima in April, July and December 2008 were mainly based on one taxon: *Dinobryon* in April, *Euglena* in July and *Dinobryon sociale* in December 2008 (Tab. 9.4).

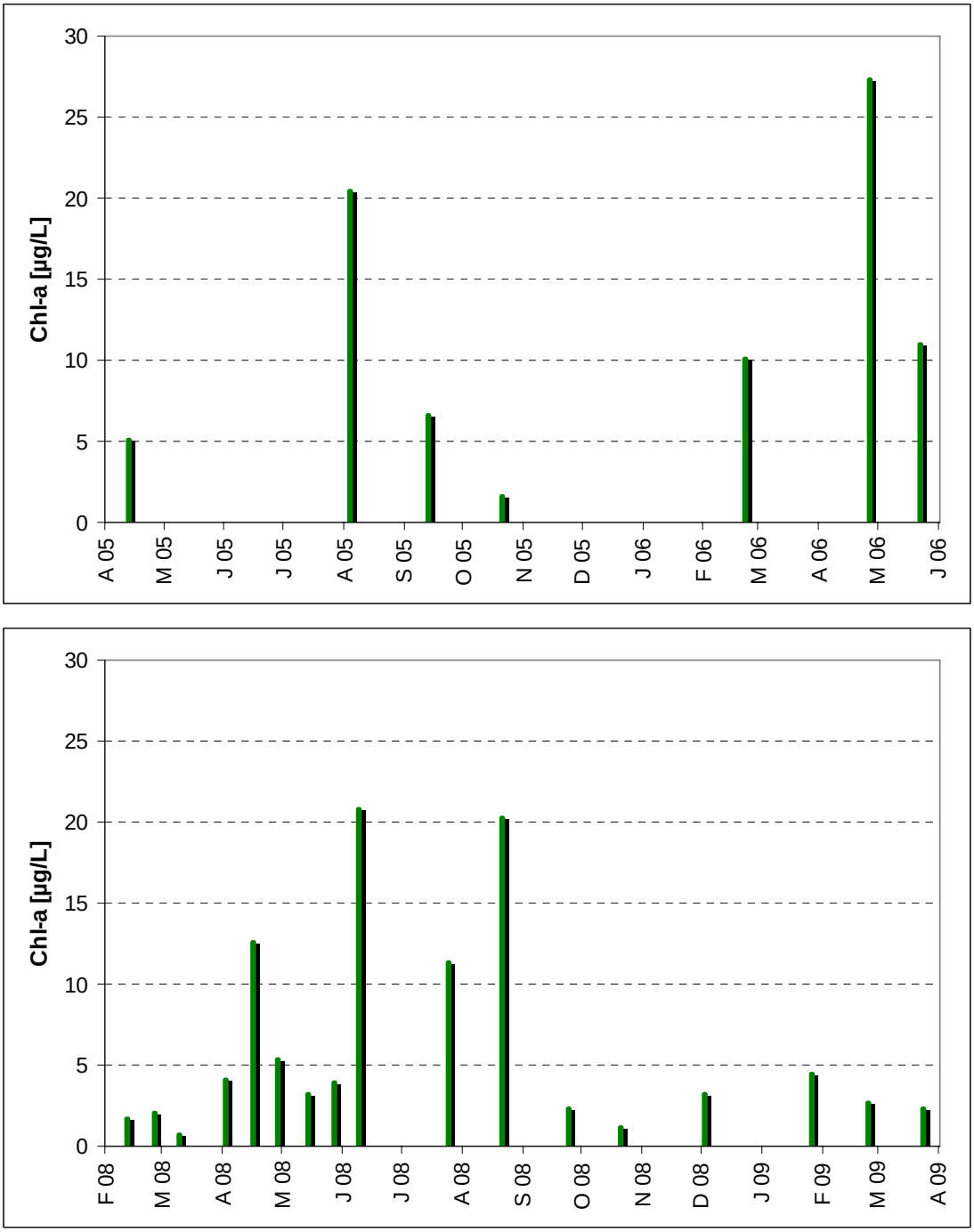

Fig. 9.18: Development of chlorophyll-a concentrations in Chicken Creek pond within the period April 2005 until May 2006 (upper chart) and February 2008 until March 2009 (lower chart).

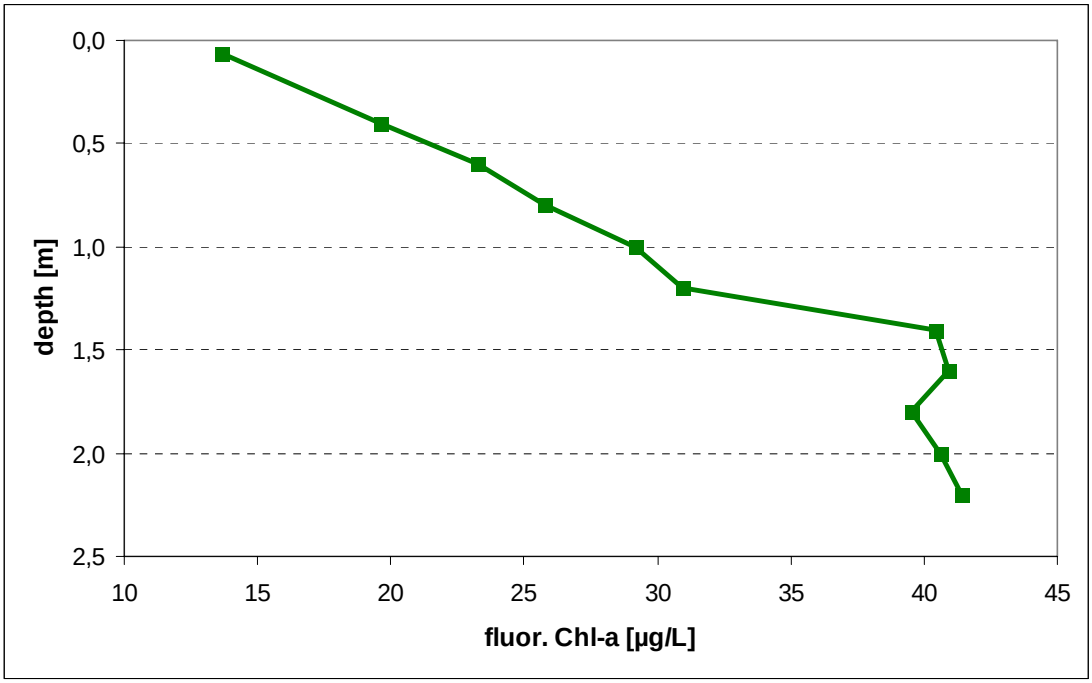

Fig. 9.19: Depth profile of chlorophyll-a concentrations measured in Chicken Creek pond by fluorescence chlorophyll-a probe on 27 April 2006.

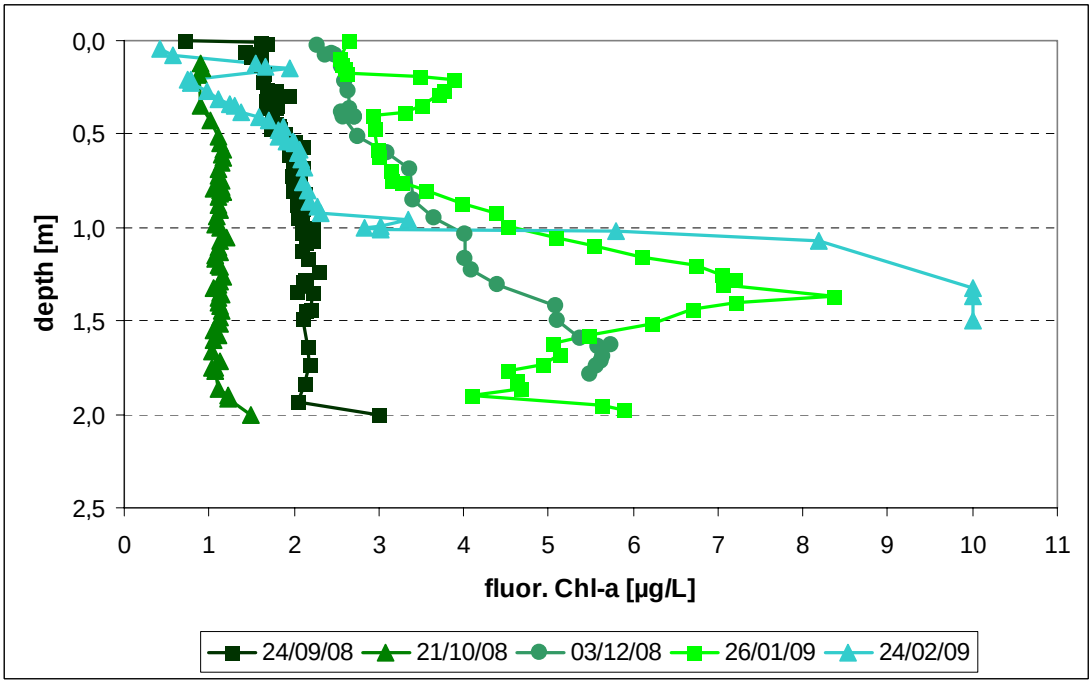

Fig. 9.20: Depth profiles of fluorescence chlorophyll-a concentrations from September 2008 until February 2009. In January and February 2009 the pond was covered with ice.

In general, dominant phytoplankton belonged to the Chrysophyceae (mean biovolume of 0.68 mm^3 L^{-1}), followed by Euglenophyceae with a mean biovolume of 0.40 mm^3 L^{-1} and Cryptophyceae with 0.18 mm^3 L^{-1}. The species with the highest biomass were *Pseudopedinella erkensis, Euglena clavata, Dinobryon sociale, D. divergens, Cryptomonas marssonii, Chromulina* sp. and *Schroederia setigera* which occurred mainly during summer with biomass maxima in June and July 2008. Cyanobacteria and diatoms, which are usually common in German lakes in the ecoregion Northern Lowlands, were rare in Chicken Creek pond. In June 2008, a peak of diatoms was recorded with *Fragilaria* sp. reaching a biomass maximum of 1.5 mm^3 L^{-1} (Tab. 9.4). This phenomenon could be explained by the silica maximum of 0.37 mg L^{-1} in May 2008, but was not repeated in autumn 2008 and winter 2009 (Fig. 9.16).

Usually, biomass of coccal Chlorophyceae, Phytomonadina, Conjugatophyceae and Dinophyceae were at a very low level with the slight exception of June 2008. Chrysophyceaen plankton which was dominated by the genus *Dinobryon* (and *Mallomonas*) is indicating soft water and/or mesotrophic conditions and is classified as association E (acc. to Reynolds, 1997) subject to the separation of *Uroglena* (association U) and nanoplanktonic species and pond populations of *Synura* in the appropriate alternative categories (associations X, W). Chicken Creek pond is a hard water body; therefore the low trophic status is the main reason for the dominance of this phytoplankton group. Reproductive survival strategies of many Chrysophyceae differ from those of most other phytoplankton species because of the formation of resting propagules at the outset of population expansion and not in response to the onset of unfavourable conditions. Chrysophyceae occur as pioneer species also in mining lakes (Nixdorf et al., 1998).

Cryptomonads are relatively small, naked bi-flagellated phytoplankton species which are widely distributed in freshwaters. *Cryptomonas* and nanoplanktonic *Rhodomonas* were the main dominant genera next to *Chilomonas*. They are ubiquitous and tend to enlarge their biomass portion in moderately nutrient enriched waters as we could detect in June 2008 under relatively high trophic conditions. Because of their motility they depend neither on mixing nor on stratification. The Cryptomonads of the association Y (acc. to Reynolds, 1997) belong to the favourite food of many zooplankton species. The high grazing pressure is one reason for the high specific productivity of these species resulting in potentially fast growing organisms. The same is apparent for the ecologically distinct, but phylogenetically mixed group of nanoplankton (2-20 µm). *Chromulina* and *Rhodomonas* belong to this association.

Pseudopedinella erkensis is used as an indicator species for alpine and pre-alpine lakes with a trophic score of 1.25 and a stenoecious factor of 1. *Euglena clavata* is not mentioned as indicator taxon but all other cited *Euglena* indicator species are classified for all lake types in the eutrophic range. *Dinobryon sociale* and *Dinobryon divergens* are characteristic taxa for mesotrophic conditions with a low stenoecious factor. *Cryptomonas marssonii* and *Schroederia setigera* indicate slightly eutrophic conditions as well as the Haptophyceaen genus *Chromulina*.

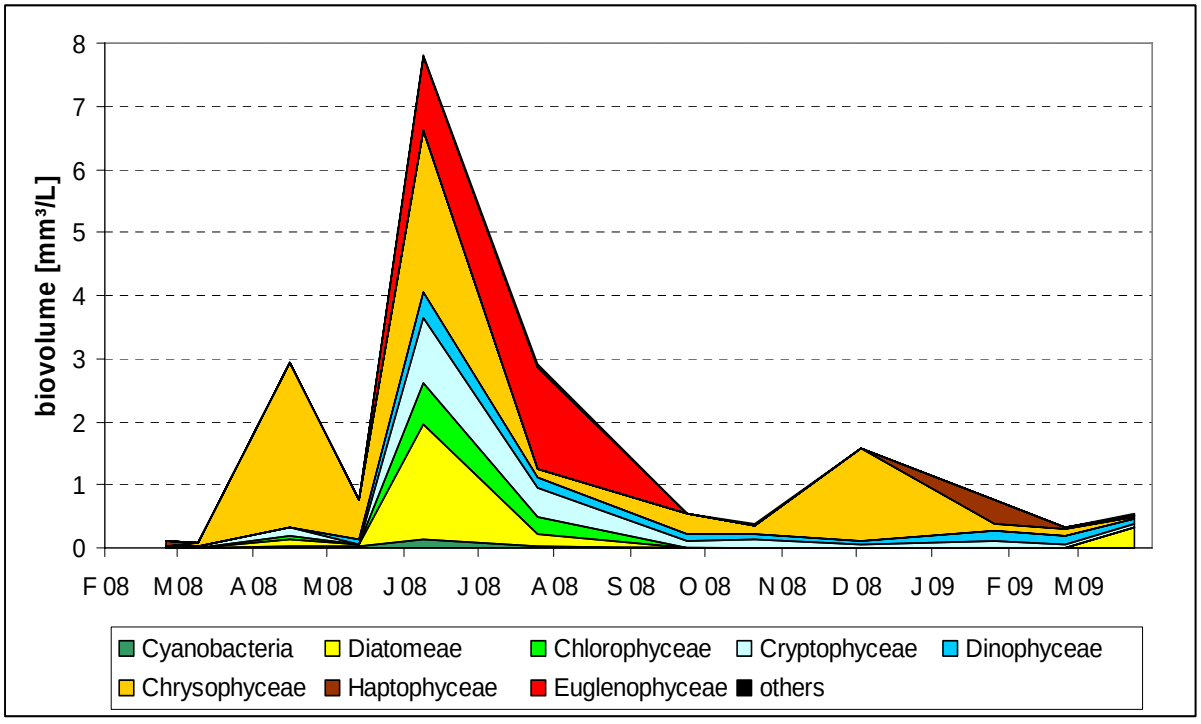

Fig. 9.21: Seasonal development of the cumulative phytoplankton biovolume and of the taxa specific biovolumes from February 2008 until March 2009.

Tab. 9.4: Abundance, biovolume and biovolume dominance of the most abundant taxa in Chicken Creek pond for selected dates in 2008.

Date	Taxon	Abundance [10^3 cells L^{-1}]	Biovolume [mm^3 L^{-1}]	Dominance [%]
16/04/2008	Dinobryon divergens	4927.7	1.189	40.4
14/05/2008	Chromulina sp.	953.9	0.491	64.7
09/06/2008	Pseudopedinella erkensis	6466.9	2.159	27.6
09/06/2008	Fragilaria sp.	1060.6	1.745	22.3
09/06/2008	Euglena clavata	129.3	1.173	15.0
09/06/2008	Cryptomonas marssonii	1681.4	0.717	9.2
09/06/2008	Schroederia setigera	1215.8	0.489	6.3
25/07/2008	Euglena clavata	181.1	1.605	55.1
03/12/2008	Dinobryon sociale	6039.8	1.331	84.8

Ecological status of Chicken Creek pond

The relation between chlorophyll-a concentration and phytoplankton biomass measured as biovolume (BV) was checked by a regression analysis (Fig. 9.22) using a data set of more than 150 lakes of the German lowlands. We found a close correlation between both parameters (Mischke & Nixdorf, 2008).

The implementation of the EU Water Framework Directive (2000) offers new assessment tools for the evaluation of the trophic properties of lakes which are indicated by phytoplankton biomass and composition. Although ponds are not considered in the system, we classified the pond according to its ecological quality element phytoplankton biomass and chlorophyll-a concentration (acc. to Nixdorf et al., 2008, Mischke and Nixdorf, 2008). In Fig. 9.22 the upper limits for the ecological status are marked according to the results of the lake assessment system for phytoplankton of very shallow lakes (lake type 11.2, see Mischke and Nixdorf, 2008) from "very good" to "bad". It is obvious, that most phytoplankton data from Chicken Creek pond are in the "very good" or "reference" state. Only the value of June 2008 is within the upper range of the "good" status.

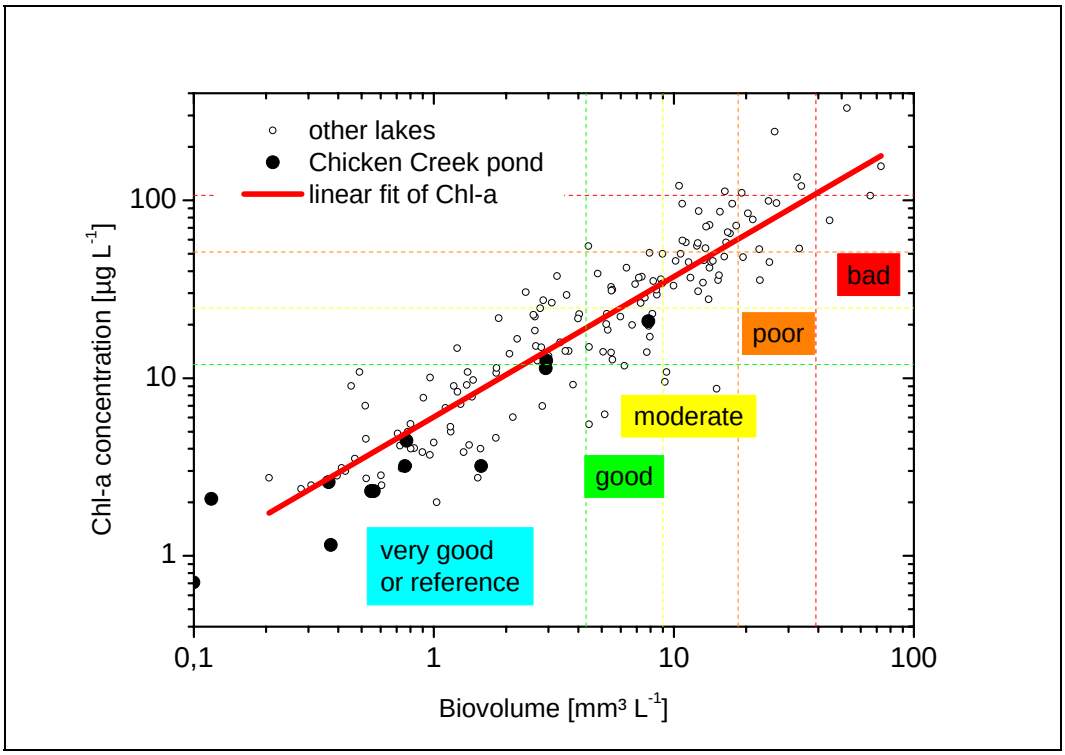

Fig. 9.22: Regression between phytoplankton biovolume and chlorophyll-a concentration of very shallow lakes of the German lowlands (lake type 11.2, mean depth <3 m) in comparison with phytoplankton data from Chicken Creek pond in 2008 and 2009. Phytoplankton parameters are classified according to their ecological qualities from "very good" to "bad" after Mischke & Nixdorf (2008).

9. 4.4 Biological development - metazooplankton

Starting from scratch several years ago the metazooplankton in Chicken Creek pond is still in a state characteristic of pioneer communities: a species poor community dominated by easily dispersing littoral and benthic taxa. Species richness was very low with a total of 27 species and a range of 5 to 13 species per sampling date. The majority were rotifers (24 species) predominated by littoral taxa from the genera *Lecane* (5), *Cephalodella* (2), *Colurella, Lepadella, Lindia* and *Squatinella.* Only three crustacean species were able to establish small populations in 2008/2009, namely, the cladoceran *Chydorus sphaericus* and two cyclopoid copepods *Acanthocyclops robustus* and *Eucyclops serrulatus*. Remarkably, no calanoid copepods or daphnids were found throughout the sampling period.

The mean biovolume of the metazooplankton was in the mesotrophic range (2.3 mm L^{-1}, Tab. 9.5). However, values of rotifer metrics were typical of much higher productive waters. Rotifers showed a pronounced seasonal fluctuation in abundance from winter to spring with a maximum in March 2008 of 18,760 Ind. L^{-1} (mainly *Keratella quadrata*), a high annual mean in abundance of 4,468 Ind. L^{-1} and a mean dominance of 80 % of the total metazooplankton biovolume. On 6 out of the 10 sampling dates the proportion of rotifers exceeded 90 % (Fig. 9.23). However, it has to be mentioned that there are no data for the summer months July and August as well as for November and December. Crustaceans became important at the time of the typical cladoceran early summer maximum in June 2008 representing 90 % of the metazooplankton biovolume. The annual mean was 20 % evenly distributed among the cladoceran *Chydorus sphaericus* and the cyclopoid copepods (Tab. 9.5). The core community consisted of four species (*Synchaeta pectinata, Keratella quadrata, Keratella cochlearis,* and *Chydorus sphaericus*), each contributing at least on two dates more than 40 % to the total biovolume.

Due to the dominance of rotifers and the small cladoceran *Chydorus sphaericus* size spectra for taxonomic groups (Fig. 9.24) show that on eight sampling dates more than 95 % of the metazooplankton biovolume was restricted to the two smallest size classes below 400 µm.

Invertebrate predation is apparently very strong in Chicken Creek pond reflected by a diverse community of predators that are able to feed on metazooplankton. In summer larvae of *Chaoborus* and Trichoptera as well as Corixidae and Hydrozoa were found in relatively high abundances and thus, they were expected to have a strong influence on the seasonal development and the size distribution of the metazooplankton. Furthermore, their presence indicates that fish predation has been of no relevance to the food web of Chicken Creek pond till now. The cyclopoid species *Acanthocyclops robustus* is an important predator within the metazooplankton food web, whereas the predatory Cladocerans *Polyphemus pediculus* or *Leptodora kindtii* are completely lacking.

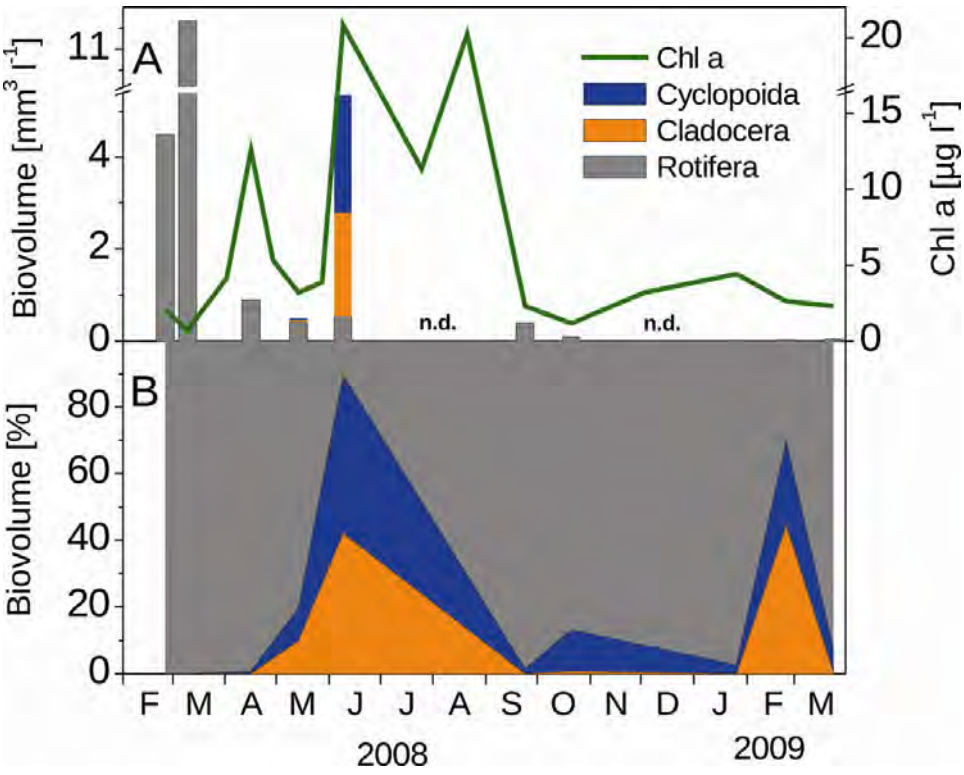

Fig. 9.23: Biovolume of metazooplankton, chlorophyll-a concentration (A) and relative share of metazooplankton groups (B) in Chicken Creek pond in 2008/2009 (n.d.: periods without zooplankton data).

Tab. 9.5: Zooplankton metrics for Chicken Creek pond in 2008/2009.

Number of samples	n	10
Species richness: total	n	27
Rotifera	n	24
Cladocera	n	1
Copepoda	n	2
Mean abundance of Rotifera	Ind. L^{-1}	4,468
Mean total biovolume	mm^3 L^{-1}	2.4
Mean % of total biovolume		
Rotifera	%	80
Cyclopoida	%	10
Calanoida	%	0
Cladocera	%	10

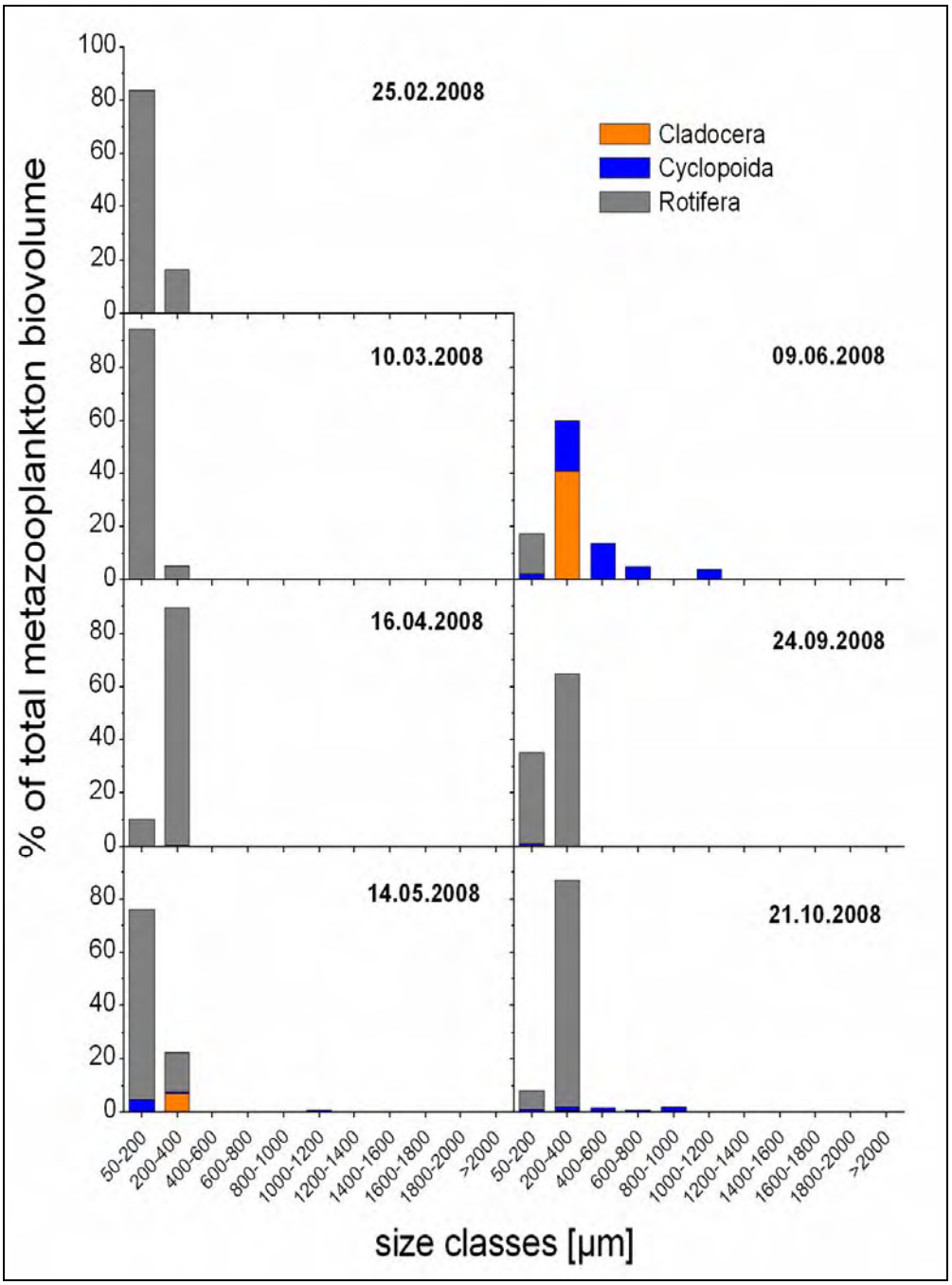

Fig. 9.24: Size spectra of metazooplankton in Chicken Creek pond for each particular sampling date in 2008/2009. Width of size classes is 200 µm, except for the class 50 – 200 µm.

9. 5 Conclusions

Chicken Creek pond is a small, shallow and polymictic standing hard water body. Ponds and small lakes differ in their morphometry, local climate, hydrology, alkalinity, nutrient loading and interactions with the catchment area and therefore they respond ecologically more sensitive to changes in abiotic conditions. This was demonstrated by fluctuations in plankton patterns which do not follow regular seasonal patterns of mesotrophic lakes. Nutrient inputs into Chicken Creek pond were coupled with precipitation and other hydrological events, which washed repeatedly high volumes of eroded material into the pond and were not regulated by phytoplankton induced retention mechanisms. Phosphorus and silica were identified as the main limiting resources for phytoplankton development. Short pulses of nutrient inputs could induce very fast and intensive response in primary production of spatial vertical segregation of phytoplankton colonization with maxima of chlorophyll-a concentration below 1 m depth. Flagellated species and pioneers with relatively high specific productivity dominated the phytoplankton indicating progress in primary colonization. Pelagic primary productivity was in an oligo- to mesotrophic range and benthic colonization of plants became of increasing importance in Chicken Creek pond.

The relative extent of macrophyte cover around and in the water body is larger compared with lakes. Main characteristics, which are important for the phytoplankton colonization patterns, are shallowness and rapid hydraulic and hydrological exchange. Whereas shallowness in general favours turbidity due to sediment (and nutrient) resuspension, changing hydrological conditions, especially water level fluctuations, prevent pelagic structuring. Rooted and attached plants have better opportunities to exploit this habitat. Only to a small extent Chicken Creek pond is influenced by sediment and nutrient resuspension (see Chapter 10). Most time, even during well mixed conditions, the water is clear and poor in nutrients resulting in low phytoplankton biomass but a high level of macrophyte colonization.

Benthic primary producers, neither macrophytes and filamentous algae nor epiphytic algae, were studied before 2009. It is expected that they contribute with a substantial fraction to carbon turnover in Chicken Creek pond.

The metazooplankton of Chicken Creek pond was characterized by a community in a state of ongoing primary colonization. Up to now few pioneer species dwell permanently in this shallow water. *Chydorus sphaericus* was a typical representative for the initial phase of colonization. The lack of other cladoceran species suggested that harsh abiotic conditions or unknown mechanisms hampered any progress towards a more diverse community. To certain extent this may be attributed to the isolation of the water body, but after more than four years of existence other reasons must be considered. Mesotrophic conditions normally provide enough food to allow a species rich zooplankton community with a moderate level of population growth. However, low species richness and fluctuating seasonal biomass in

Chicken Creek pond may indicate a very stressful environment. Biotic interactions within the food web occasionally became very intense. In March 2008, strong 'top-down' effects on phytoplankton by herbivore rotifers were suggested by a very high ratio between rotifer and phytoplankton biovolume. Later in summer 2008 'top-down' effects at higher trophic levels between invertebrate predators and metazooplankton were indicated by a very narrow size distribution of metazooplankters and high abundances of invertebrate predators. While this may explain the lack of some more sensitive pelagic filtrators, such as daphnids, other cladocerans, belonging to the Bosminidae and Chydoridae, were still not present. Rotifers having no competitors and unharmed by predation exploit food resources very efficiently and dominate metazooplankton most of the year. The high share of littoral and benthic species may be attributed to their dispersal abilities as well as to the structure of the habitat.

References

Arfi. R., Guiral, D. and Torreton, J.P., 1991: Natural recolonization of a productive tropical pond: day to day variations in the photosynthetic parameters. Aquatic Sciences 53(1), 39-54.

Calderoni, A., Mosello, R. and Ruggiu, D., 1992: The introduction of native plant species on industrial waste heaps: a test of immigration and other factors affecting primary succession. Memorie dell'Istituto Italiano di Idrobiologia 50, 201-223.

Dörschel, C., 2009: Limnologie von Kleingewässern: Pelagische Stoffumsätze und Besiedlungsmuster im Winter und Frühjahr 2008 am Beispiel Hühnerwassersee. Diploma thesis, BTU Cottbus, Department of Freshwater Conservation, 133 p. (unpubl.).

Elber, F. and Schanz, F., 1990: The influence of a flood event on phytoplankton succession. Aquatic Sciences 52(4), 330-344.

EU Water Framework Directive, 2000: Directive 2000/60/EC of the European Parliament and the Council of 23 October 2000 establishing a framework for Community action in the field of water policy. Official Journal of the European Communities L 327/1, 22/12/2000.

Gobler, C.J., Renaghan, M.J. and Buck, N.J., 2002: Impacts of nutrients and grazing mortality on the abundance of *Aureococcus anophagefferens* during a New York brown tide bloom. Limnology and Oceanography 47(1), 129-141.

Guiral, D., Arfi, R., Bouvy, M., Pagano, M. and Sainte-Jean, L., 1994: Ecological organization and succession during natural recolonization of a tropical pond. Hydrobiologia 294 (3). 229-242.

Hehmann, A., Krienitz, L. and Koschel, R., 2001: Long-term phytoplankton changes in an artificially divided, top-down manipulated humic lake. Hydrobiologia 448(1-3), 83-96.

Hubble, D.S. and Harper, D.M., 2001: Impact of light regimen and self-shading by algal cells on primary productivity in the water column of a shallow tropical lake (Lake Naivasha, Kenya). Lakes and Reservoirs Research and Management 6(2), 143-150.

Kalliola, R., Salo, J., Puhakka, M. and Rajasilta, M., 1991: New site formation and colonizing vegetation in primary succession on the western Amazon floodplains. Journal of Ecology 79(4), 877-901.

McCormick, P.V., Smith, E.P. and Cairns, J.(Jr.), 1991: The relative importance of population versus community processes in microbial primary succession. Hydrobiologia 213(2), 83-98.

Morabito, G. and Pugnetti, A., 2001: Primary productivity and related variables in the course of the trophic evolution of Lake Maggiore. Verhandlungen der Internationalen Vereinigung für Limnologie. 27, 2934-2937.

Mischke, U. and Nixdorf, B. (Hg.), 2008: Gewässerreport Nr. 10 - Bewertung von Seen mittels Phytoplankton zur Umsetzung der EU-Wasserrahmenrichtlinie. BTU Cottbus, Aktuelle Reihe 2/2008.

Nixdorf, B., Rektins, A. and Mischke, U., 2008: Standards and thresholds of the EU Water Framework Directive (WFD) - phytoplankton and lakes. In: Schmidt, M., Glasson, J., Emmelin, L. and Helbron, H. (eds.), Standards and thresholds for impact assessment series: environmental protection in the European Union. Vol. 3 (2008), Chap. 26, Springer, 301-314.

Nixdorf, B., Mischke, U. and Lessmann, D., 1998: Chrysophytes and chlamydomonads: pioneer colonists in extremely acidic mining lakes (pH < 3) in Lusatia (Germany). Hydrobiologia 369/370, 315-327.

Nusch, A. and Palme, G., 1975: Biologische Methoden für die Praxis der Gewässeruntersuchung. gwf - Wasser/Abwasser 116, 562-565.

Odum, E.P., 1969: The strategy of ecosystem development. Science 164, 262-270.

Porter, K.G. and Feig, Y.S., 1980: The use of DAPI for identifying and counting aquatic microflora. Limnology and Oceanography 25(5), 943-948.

Reynolds, C.S., 1997: Vegetation processes in the pelagic: a model for ecosystem theory. Excellence in Ecology 9, Ecology Institute Oldendorf/Luhe, Germany.

Reynolds, C., Huszar, V.L.M., Kruk, C., Naselli-Flores, L. and Melo, S., 2002: Towards a functional classification of the freshwater phytoplankton. Journal of Plankton Research. 24(5), 417-428.

Robinson, J.V. and Edgemon, M.A., 1988: An experimental evaluation of the effect of invasion history on community structure. Ecology 69(5), 1410-1417.

Schelske, C.L., Stoermer, E.F., Fahnenstiel, G.L. and Haibach, M., 1986: Phosphorus enrichment, silica utilization, and biochemical silica depletion in the Great Ponds. Canadian Journal of Fisheries and Aquatic Sciences 43, 407-415.

Sommer, U., 1991: The application of the droop-model of nutrient limitation to natural phytoplankton. Verhandlungen der Internationalen Vereinigung für Limnologie 24, 791-794.

Sommer, U., 1993: Disturbance-diversity relationships in two lakes of similar nutrient chemistry but contrasting disturbance regimes. Hydrobiologia 249, 59-65.

Sommer, U., Gliwicz, Z.M., Lampert, W. and Duncan, A., 1986: The PEG-model of seasonal succession of planktonic events in fresh waters. Archiv für Hydrobiologie 106, 433-471.

Utermöhl, H., 1958: Zur Vervollkommnung der quantitativen Phytoplankton-Methodik. Verhandlungen der Internationalen Vereinigung für Limnologie 5, 567-596.

Vollenweider, R.A., 1976: Advances in defining critical loading levels for phosphorus in pond eutrophication. Memorie dell'Istituto Italiano di Idrobiologia 33: 53-83.

Acknowledgements

The study of Chicken Creek pond for four years was only possible with the help of many people. We especially thank Ingo Henschke for his continuous efforts in field measurements and sampling and Gudrun Lippert, Ute Abel, Erwin Banscher, Christine Dörschel and Jörn Jander for chemical and biological analyses. Additional chemical analyses were provided by the Central Analytical Laboratory (ZAL) of the Faculty of Environmental Sciences and Process Engineering at BTU Cottbus. The study was part of the Transregional Collaborative Research Centre 38 "Structures and processes of initial ecosystem development in an artificial water catchment" which was financially supported by Deutsche Forschungsgemeinschaft (DFG) and Brandenburg Ministry of Science, Research and Culture (MWFK).

10. Formation and characterization of pond sediments

Andreas Kleeberg, Christiane Herzog, Sylvia Jordan and Michael Hupfer

Leibniz-Institute of Freshwater Ecology and Inland Fisheries

10. 1 Introduction

Within the artificial catchment ‘Chicken Creek’ all surface runoff and groundwater discharge is collected in a small pond at the bottom of the catchment (Gerwin et al., 2009). The pond is relatively simply structured and allows the analysis of the processes and structures during its maturation which become gradually effective and more complex in relation to its little anthropogenically influenced catchment. With incipient pond diagenesis biotic in-pond processes should become more important influencing the water and element budget to an increasing extant. Moreover, the developmental stages of the key site-typical random sucession of the catchment should be reflected in the small pond (Müller et al., 1998; Håkanson, 2005). The extent and the rates of the initial processes in the pond as influenced by the catchment should govern the pond’s further development and future system status.

Most important factor governing the trophic state of a pond is often the nutrient phosphorus (P). The extent of the input of P, its retention and particularly its present mobility (e.g. Zessner et al., 2005; Kopáček et al., 2007) in dependence on changing source and sink functions as well as biological availability play a crucial role for the rate and direction of pond development. In particular the initial dynamic of the transport as well as of the transformation and retention mechanisms of various P compounds can considerably determine the pond genesis especially of P-limited systems.

Because of its small size and depth the pond exhibits a large areal proportion of shallow littoral sediments. While profundal sediments have been studied since decades pertaining its accumulation and mobility of P, there are comparably much less studies on the littoral P dynamic (e.g. Weyhenmeyer, 1998; Güde and Gries, 1998). Beside the catchment area the littoral zone represents a highly dynamic and the most important aquatic source structure. Hence the initial pond morphology (exposition, slope), the properties of the allochthonous matters and the pioneer colonization determine, whether and to what extent which matters are translocated and therewith which P compounds are temporarily accumulated in the sediment and entrained into the water column, respectively. In addition mostly nutrient-rich system have been studied (Droppo et al., 2001).

Our contribution aimed at the characterization of the initial development of the Chicken Creek pond based on its present stage and a first sediment inventory. Of particular interest are the short history of accumulation and the initial composition of sediments including their properties in terms of the present P mobility.

10. 2 Material and Methods

10. 2.1 Study site

The small pond was created as a nearly crater-shaped pit in the bottom in 2005. The subsurface was grouted by an about 10 to 20 cm thick clay layer. The asymmetric round hollow mould (originally about 55-65 × 3 m) with quadratic bottom area was already partly filled in August 2005 and completely filled after the snowmelt in January 2006 (see Chapter 2). The morphometric characteristics are given in Tab. 10.1.

Tab. 10.1: Morphologic characteristics of the Chicken Creek pond and its catchment area (CA) Chicken Creek, Welzow-South (N 51°, 37'; E 014, 18'). MQ – mean runoff

	characteristic	unit		remarks
CA	catchment area	(ha)	5.9	approx. 450×130 m, incl. pond
	difference in height	(m)	14	
	mean slope	(%)	3	
	water level	(m a.s.l)	125.4	
	pond area	(m^2)	3805	
	pond volume	(m^3)	3992	
	maximum depth	(m)	2.4	
	mean depth	(m)	1.0	
	water retention time	(d)	289	MQ Sept. 2006 to Sept. 2008
	areal ratio CA : pond	÷	14.5	CA without the pond

Because of the small size of the pond, the system is depending on precipitation and surface runoff changing regularly it's morphometry. For example the water level varied in 2008 between 125.13 and 125.44 m a.s.l. (see Chapter 4), i.e. by 31 cm which corresponds to changes of maximal 26% in pond volume and 22.4% in pond surface area.

10. 2.2 Sampling and analysis

10. 2.2.1 Water sampling

Vertical profiles of temperature, pH, dissolved oxygen, electric conductivity and chlorophyll a were taken using a multi parameter probe (YSI 6820, Environmental Monitoring Systems) at four occasions in 2008 (August 14th and 27th, October 8th and 21st) at the deepest site of the pond.

For the determination of the concentration of total Fe (TFe) and total P (TP) unfiltered water samples were digested by H_2SO_4 and H_2O_2 (Zwirnmann et al., 1999). The digestion temperature was modified as follows: heating to 120 °C within 1 h, 120 °C for 3 h, heating to 160 °C within 0.5 h, 160 °C for 3 h, cooling to 90 °C, and further cooling to room temperature. The Fe concentration was determined by AAS (Perkin Elmer 3300, Rodgau-Juegesheim). After neutralization, the TP concentration was determined as soluble reactive P (SRP).

SRP and ammonium (NH_4^+) were photometrically determined after filtration (0.45 µm syringe filter, cellulose acetate, Whatman) by the molybdenum-blue method at λ = 880 nm (Murphy and Riley, 1962) and by a modified indophenole method at λ = 660 nm (Krom, 1980) using a segmented flow analysis (SFA, Skalar San^{plus}, Skalar Analytical B.V., De Breda). The concentration of dissolved Si (DSi) was measured (molybdate silicato complex, λ = 810 nm) by a photometer (UV2101 PC, Shimadzu; Zwirnmann et al., 1999). The concentration of the anions nitrate (NO_3^-), sulphate (SO_4^{2-}), and chloride (Cl^-) was determined after filtration (0.45 µm) by ion chromatography (System Fa. Shimadzu) (Zwirnmann et al., 1999). From an unfiltered aliquot the total organic C (TOC) and after filtration (0.45 µm) the dissolved organic C (DOC) were determined by high temperature oxidation and infralyte detection of the CO_2 formed using a TOC analyzer (Multi N/C 3100, Analytik Jena) (Zwirnmann et al., 1999).

For the chlorophyll a (Chl a) determination, sub-samples of 100-200 ml were filtered onto GF/F glass-fibre filters and stored at -80 °C for later HPLC analysis. Filters were freeze-dried and pigments were extracted by vibration shaking (2000 rpm, 1.5 hrs) with dimethylformamide and glass beads (Ø 0.75-1.0 mm). After centrifugation for 20 min (2500 g, 4 °C), pigments were separated, identified and quantified with a HPLC system (Waters, USA) (Fietz and Nicklisch, 2004).

10. 2.2.2 Sediment sampling

For the determination of the extent of accumulated sediment layer, transects were taken from inflow to the outflow (North-South transects) and crossways (West-East transects). Along each transect in a 5 to 10 m resolution sediment thickness was measured using a side marker with an accustic signal transducer. In the same spatial resolution undisturbed sediment cores (Ø 6 cm) were taken down to the bottom clay layer by means of a sediment corer with a telescope bar (UWITEC©, Mondsee, Austria). From representative cores photos were taken.

The sediment cores were sliced into layers of various thickness (0-0.5, 0.5-1, 1-2, 2-3, 3-4, 4-6, 6-8 cm etc) down to the bottom clay layer. Aliquots of sediment fresh weight (FW) were used for the determination of dry weight (DW, 105 °C, 8 hrs) and for the determination of the mean grain size distribution by wet sieving (Brenning, 1967). Out of the DW the proportion of organic matter (OM) was determined as loss on ignition (450°C, 3 hrs). TFe and TP were determined as described above. Two of the longest cores were length-wisely divided in halves and sliced according to visibly characteristic sediment layers.

One half core was used for the determination of the vertical metal distribution in 200 µm resolution by µm X-ray fluorescence (µXRF) using an ITRAX core scanner (Cox Analytical Instruments, Mölndal, Sweden). For further details see Croudace et al. (2006).

For the determination of the sedimentary P binding forms a sequential P fractionation scheme according to Psenner et al. (1984) with a few modifications according to Hupfer (1995) was applied (Tab. 10.2).

The determination of the maximal phosphate sorption capacity (PSC) was performed in duplicate using fresh sediment. The data evaluation followed in principle the procedure by Schlungbaum (1982) as well as Schulz and Herzog (2004). Briefly, following the determination of DW, FW which corresponds to 1 g DW each, was weighed and 20 ml of a defined P solution were added. On total nine P concentration ranges were dissolved both from a commercial stock solution (0-100 mg l^{-1}, MERCK p.a.) and from a weighted sample of KH_2PO_4 (250-500 mg l^{-1}). After 3 hrs incubation in an all around shaker, and centrifugation (10.060 g, 10 min) the supernatant was filtered (0.45 µm, CA membranes, Whatman), and the phosphate concentration was photometrically determined as SRP. Additionally, after centrifugation of the sediment (10.060 g, 10 min) the SRP concentration of pore water was considered in the calculation of PSC.

Tab. 10.2: Scheme of sequential fractionation of compounds of phosphorus (P) according to Psenner et al. (1984) with slight modifications following Hupfer (1995). SRP = soluble reactive P, NRP = non-reactive (organic) P, as determined as the difference between total P (TP) and SRP in the NaOH fraction.

Extraction step	time	fraction	phase extracted
0.1 M NH_4Cl	0.5 h	NH_4Cl-TP	pore-water P, loosely adsorbed onto surfaces (e.g. of Fe and $CaCO_3$), immediately available P
0.11 M bicarbonate/ dithionite (BD)	1 h	BD-SRP	redox-sensitive P, mainly bound to Fe-hydroxides, Mn-compounds
		BD-NRP	organic proportion; P of metal-associated organic matter
1 M NaOH	16 h	NaOH-SRP	P bound to metal oxides, mainly of Al and Fe, which is exchangeable against OH^-; inorganic P compounds soluble in bases
		NaOH-NRP	organic P of micro organisms and detritus; humic matter bound P
0.5 M HCl	16 h	HCl-TP	P bound to carbonates and apatite-P, traces of hydrolyzed organic P
$K_2S_2O_8$, 120 °C, pH 1	2 h	Residual P	organic and other refractory P

With the increasing ratio of the equilibrium concentration (C, mg l^{-1}) to the amount of sorbed P (SP, mg g^{-1}) the Langmuir adsorption isotherm will be expressed as a line of the type $y = ax + b$ with:

$$\frac{C}{SP} = \frac{C}{PSC} + \frac{K}{PSC} \quad (1)$$

where PSC is the maximal phosphate sorption capacity [mg g^{-1}], and K is the half saturation constant [mg l^{-1}].

Two undisturbed sediment cores (Ø 10 cm) were taken with a modified Uwitec© corer at the deepest site of the pond on October 8th. 2008. For the resuspension experiment an erosion chamber according to Gust (1990), called microcosm, was used (Fig. 10.1). The calibrated microcosm creates by a stirring disc a spatially homogeneous bottom stress (τb; Gust and Müller, 1997; Tengberg et al., 2004), expressed as shear velocity (u* = (τb/ρ)0.5 [cm s-1], where ρ is the density of the fluid).

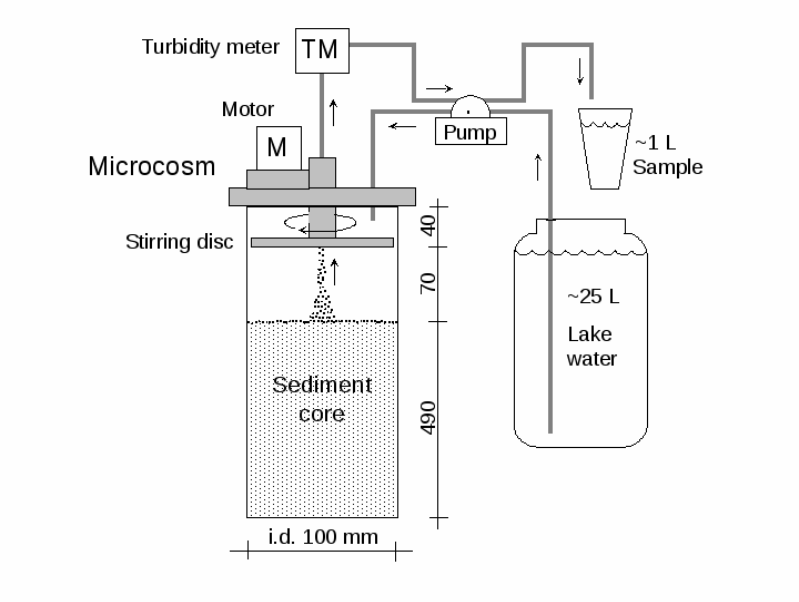

Fig. 10.1: Experimental arrangement for the resuspension experiment with intact sediment cores. To use the calibration parameters by Gust (1990) the stirring disc has to be kept 7 cm above the sediment surface. The microcosm was driven as an open system, i.e. pond water was continuously pumped through it by a peristaltic pump at a water flow of Q = 90 ± 6 ml min^{-1} (Kleeberg et al. 2008a).

In the experiment, u* was step-wisely increased every 20 min with the following 11 increments 0, 0.32, 0.56, 0.78, 0.98, 1.17, 1.35, 1.51, 1.65, 1.75 and 1.82 cm s-1. Turbidity was continuously recorded by a commercial forward scatter turbidimeter TF 10-512 (Optek-Danulat, Essen 1, Germany) with ADC-Win programmed by Labview v 5.0.

Water was sampled for chemical analyses over each and the whole u* interval. SPM was analysed in triplicate by filtering water through pre-weighed cellulose acetate filters (0.45 µm, Sartorius, Göttingen, Germany), drying at 105 ºC and weighing again. Relationship between turbidity [ppm] and SPM was used to convert the turbidity output to SPM [mg l-1]. TP out of an unfiltered sample was photometrically measured as SRP after digestion.

The entrainment rates (E) of a given component (x) were calculated in terms of a mass balance (Kleeberg et al., 2008a):

$$E_x = \sum_{i=1}^{n} \left(\frac{Out_x - In_x}{A} \right) [\text{mg m}^{-2}\ \text{h}^{-1}] \qquad (2)$$

where In_x is the input of x and Out_x is the output of x (mg h^{-1}), and A is the surface area of the microcosm (0.0079 m^2). Individual values of In_x and Out_x were calculated by multiplying the concentration of x (mg l^{-1}) with the water flow rate of the peristaltic pump (l h^{-1}).

To sample pore water from the sediment in an adequate manner, i.e. in vertical high resolution and without contact by oxygen, an *in situ* pore water sampler, called peeper, according to Hesslein (1976) was used (Fig. 10.2). Basically, the peeper consists of a dialysis sampler out of acryl glass which is mounted to an incubation base frame out of rigid PVC and metal. The dialysis membrane used is a polysulfone membran (0.2 µm HT-Tuffryn 200®, PALL GmbH, Germany).

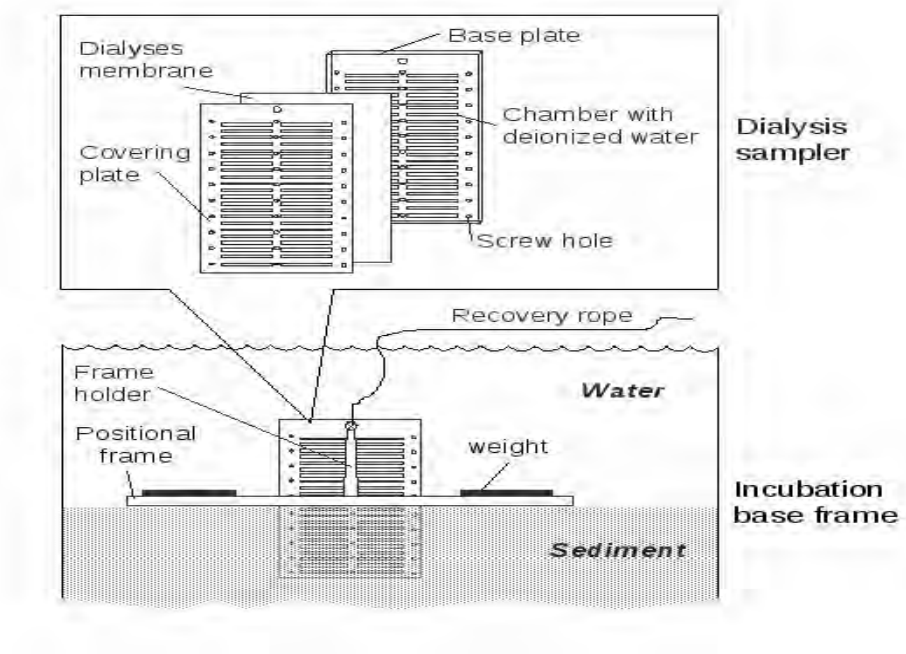

Fig. 10.2: Main components of an *in situ* pore water sampler, peeper.

Such a peeper was deployed at the inflow and outflow area of the pond for 13 days (August 14th – 27th 2008). Turnover and flux rates of SRP, (provided that PO_4^{3-} equals SRP), and of NH_4^+, were determined based on vertical concentration profiles of SRP and NH_4^+, and processed by the statistical program 'Profile 1.0' (Berg et al., 1998). Diffusion coefficients for PO_4^{3-} and NH_4^+ were drawn from the compilation of Li and Gregory (1974) and converted to the *in situ* conditions (17.4 °C, pH 8.4) according to Furrer and Wehrli (1996).

Vertical profiles of dissolved oxygen (O_2) were determined in the laboratory at undisturbed cores by a Clark type microelectrode with an outer tip diameter of 50 µm (OX50 standard, Unisense, Science Park Aarhus, Denmark), which was positioned by a motor-driven micro-manipulator with computerized depth control (see Kühl and Revsbech, 2001). Turnover and flux rate of O_2 were processed in analogy to pore water constituents.

10. 3 Results and discussion

10. 3.1 Water quality and phytoplankton composition

The pond was stratified with 20 °C at the water surface and with 18° C above the bottom in August (14th and 27th) 2008, and with 9 to 10 °C completely mixed in October (8th and 21st) 2008. The O_2 distribution at all occasions and throughout the whole water column was in the range of saturation and oversaturation (105-125%). The pH from both date to date and from the surface to the bottom was constant 8.2 to 8.4 (not shown).

The phytoplankton (31st May 2006) was characterized by the following genera: *Cryptomonas*, *Dinobryon*, *Fragilaria*, *Gymnodinium*, *Monoraphidium*, *Navicula*, *Nitzschia*, *Pseudanabaena*. At low concentrations of Chl a between 2 and 11 µg l^{-1} the pigment analysis (14th August 2008, Chl a = 10.6 µg l^{-1}) indicated a dominance of the Euglenophyta (68 %), subdominant proportions of cyanobacteria (12.5 %) as well as of Bacillariophycea and Chrysophycea (11.2 %). Concentrations of P and N were low, whereas those of SO_4^{2-} were elevated (Tab. 10.3). The latter could originate from the gypsum ($Ca[SO_4] \cdot 2H_2O$) found in small crystals in the erosion gullies (see Chapter 5).

Because mainly inorganic nutrient-poor materials have been imported the concentrations of trophy-relevant nutrients (TP, SRP, NH_4^+, NO_3^-) in the water body are very low (Tab. 10.3). Accordingly, the Chl a concentration (algal biomass) is low and the secchi depth transparency high. Lower secchi depth transparencies are only short-term and due to clay inputs. The clear water exhibits an optimal light climate for the submersed vegetation (see 10.3.7).

10. 3.2 Sediment accumulation and composition

Ponds are the most important sinks in the landscape and form a functional unit with their catchment areas (e.g. Foster and Walling, 1994). Thus, specific matter inputs should be event-related documented in the sediment of the experimental pond. This in turn should lead to a feedback of the sediment having a crucial influence on the further development of the pond. Particularly, the pond studied is at present subject to strong changes in the catchment which is characterized by a high dynamic of soil erosion out of the initial vegetation-free and still vegetation-poor slopes (Chapter 7).

Tab. 10.3: Minimum (min.) and maximum (max.) of parameter of water chemistry (August 14th – October 21st 2008, *n* = 4 occasions) of the Chicken Creek pond.

Parameter	unit	min.	max.	remarks
Sechi depth transparency	(m)	0.8	2.3	max. = bottom visibility
Conductivity	($\mu S\ cm^{-1}$)	549	581	whole water column
Total phosphorus (TP)	($\mu g\ l^{-1}$)	14	20	
Soluble reactive P (SRP)	($\mu g\ l^{-1}$)	1	2	
Ammonium (NH_4^+)	($\mu g\ l^{-1}$)	10	20	
Nitrate (NO_3^-)	($\mu g\ l^{-1}$)	20	30	
Chloride (Cl^-)	($mg\ l^{-1}$)	2.1	3.3	
Sulphate (SO_4^{2-})	($mg\ l^{-1}$)	249	256	pelagic water of peeper
Total organic carbon (TOC)	($mg\ l^{-1}$)	9.3	10.0	
Dissolved organic carbon (DOC)	($mg\ l^{-1}$	8.6	9.7	
Chlorophyll a (Chl a, probe)	($\mu g\ l^{-1}$)	1.2	11.4	whole water column
Dissolved silicate (DSi)	($mg\ l^{-1}$)	0.14		

Within only three years the bottom of the original hollow mould has been covered by a layer of sediment (Fig. 10.3) originating from an initially high surface erosion in the artificial catchment area. The thickness of the sediment layer increases with water depth and amounts to between 0.05 and 0.1 m at the shores at water depths between 0.2 und 0.4 m, and between 0.4 and 0.67 m below 2 m water depth. As favoured by the shallow western shore and due to an invading reed stand there is a layer of recent sediment which is rather developed compared to that at the steeper eastern slope (Fig. 10.3). The sediment thickness (weighed arithmetic mean) averaged to 0.30 m both in the North-South transect (*n* = 13) and the West-East transect (*n* = 17).

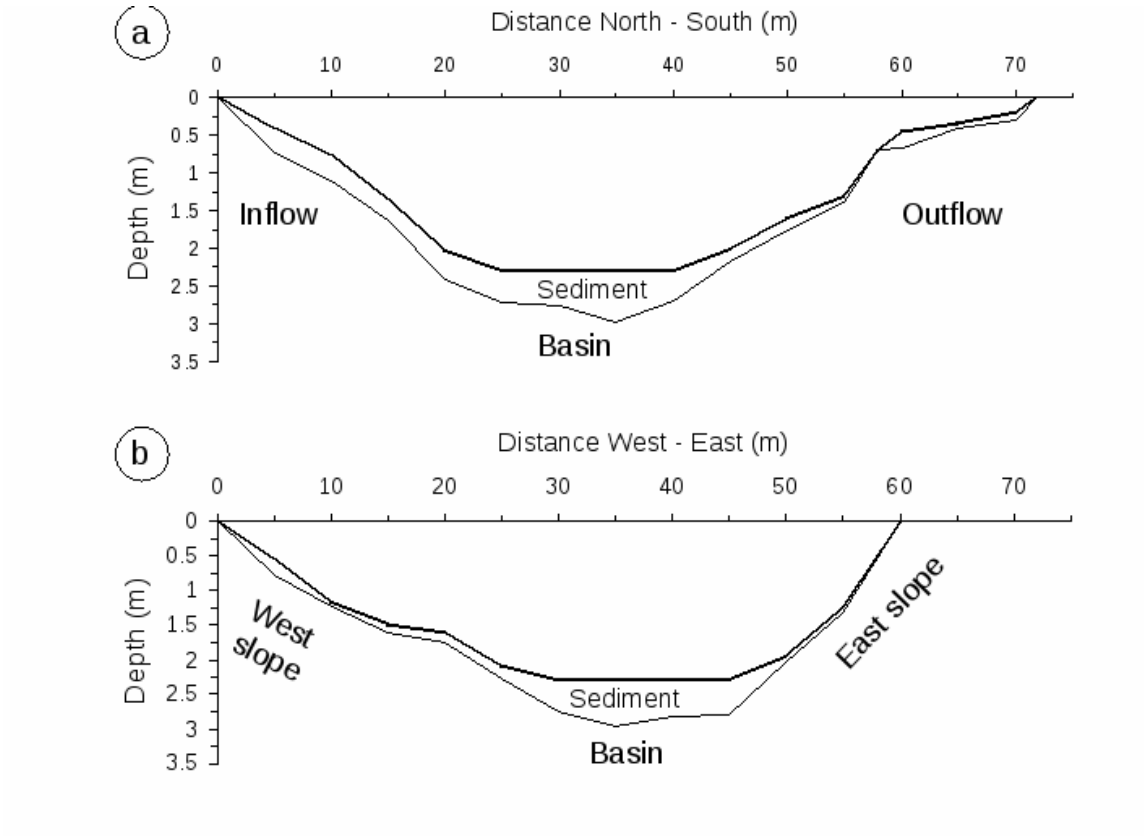

Fig. 10.3: a) Longitudinal and b) cross section of the Chicken Creek pond on August 14th 2008.

Undisturbed sediment cores of the North-South transect are shown in Fig. 10.4. The photograph clearly shows the different thicknesses of the sediment layer accumulated and differences in sediment quality above the bright clay layer at the bottom. The brown layers represent mostly inorganic material whereas darker layers are due to organic matter accumulation and/or metal sulfide formation. In the shallow area near the outflow (distance 55-70 m) periphytic algae, to be seen as a green layer, rest on the sediment surface.

Already 19.7% of the original pond volume (6483 m^3) is filled by sediment after three years. The respective sediment volume corresponds to 1280 m^3 FW. Including all 334 single samples (weighed arithmetic mean) the proportion of DW on total amounts to 56 % FW (ρ = 2.65 g cm^{-3}) and that of the organic matter amounts to 3.5 % DW (ρ = 1.4 g cm^{-3}). At a DW proportion of 56 % FW and a mean density of 1.91 g cm^{-3} the sediment accumulated corresponds to 2445 kg DW. This mass in turn, provided that it was equally imported from the total area of the catchment area (Tab. 10.1) over the three years resulted from a mean erosion rate of 13.9 kg m^{-2} a^{-1}. This erosion rate appears plausible. At a precipitation between 349 mm a^{-1} and 595 mm a^{-1} in 2006 and 2007, with maxima of 15 mm d^{-1} and 32 mm d^{-1} in 2006 and 2007, this erosion rate is comparable to other sites with similar climatic and morphological conditions. As reported by Biemelt et al. (2005) a one year study of a monitoring area (33 m^2, slope 5-15%) in the post mining landscape at Schlabendorf-North at a precipitation of 483 mm a^{-1} resulted in a mean erosion rate of 18 kg m^{-2} a^{-1}. However, particularly at short-term higher intensities of precipitation such a mean rate of 0.034 g m^{-2} min^{-1} can be considerably exceeded with rates from 1.9 to 63.4 g m^{-2} min^{-1} (Kleeberg et al., 2008b).

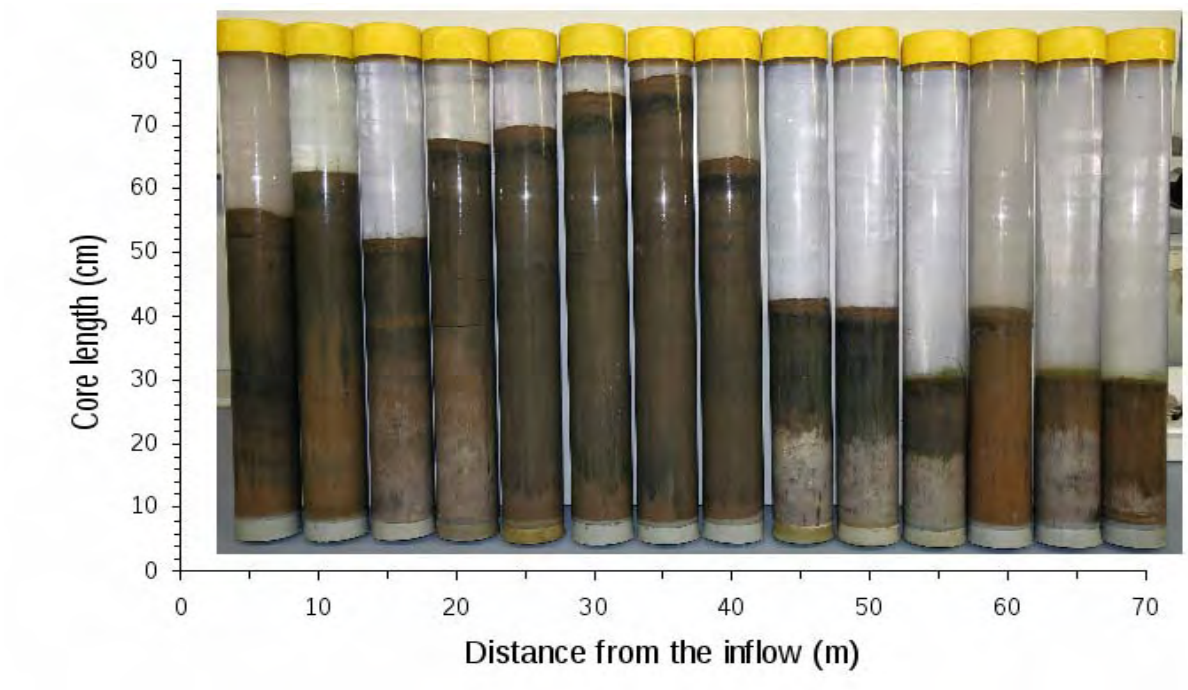

Fig. 10.4: Undisturbed sediment cores taken in a longitudinal transect every five meter from the inflow (North) to the outflow area (South) of the small experimental pond.

Considering all vertical sediment profiles and the morphometry of the pond, particularly based on the North-South transect (Fig. 10.5) different sediment qualities can be distinguished. Both in the inflow area, which is formed by an alluvial fan, and also the zone of the outflow have larger proportions of DW and lower OM proportions in a larger span. In the basin, i.e. at water depths > 2 m, a homogenous sediment with a lower DW proportion and a higher OM was accumulated.

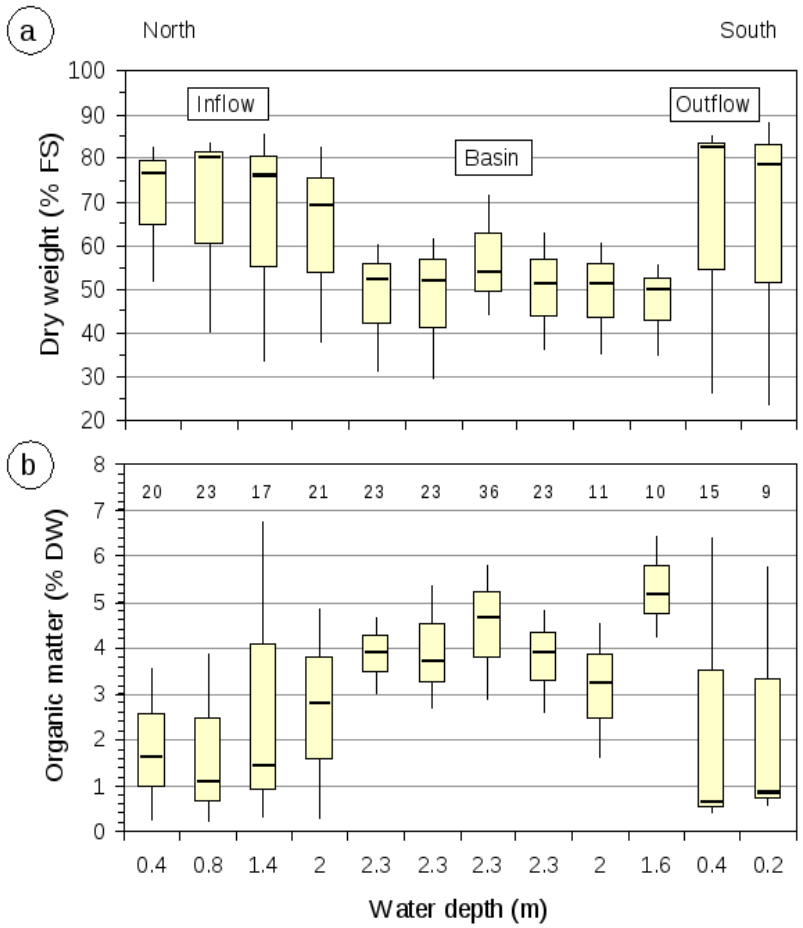

Fig. 10.5: Box plots of dry weight (a) and of organic matter (b) in a North-South transect (inflow-outflow) of the small experimental pond at the catchment area 'Chicken Creek'. Each box contains the minimum, the first (lower) quartile, the median (thick line in the box), the third (upper) quartile as well as the maximum. The numbers in panel (b) represent the number of samples analyzed.

According to the OM proportion of mostly < 5% DW the pond's deposits are a mineral sediment. According to the mean grain size silt was dominantly accumulated; in the inflow area coarse silt (0.02-0.063 mm) and in the basin and at the outflow area mean silt (0.0063-0.02 mm) which represents clastic sediment between coarser sand and finer clay.

The mean spatial and thus temporal course of DW and OM accumulation is shown in Fig. 10.6 using the cores of the basin as an example. The mean DW of the basin shows only low variations and is decreasing towards the sediment surface indicating an increasing sediment compaction with depth. In comparison, the DW is at the inflow and outflow area (< 5 cm sediment depth) about 1.5 fold higher than in the basin (not shown).

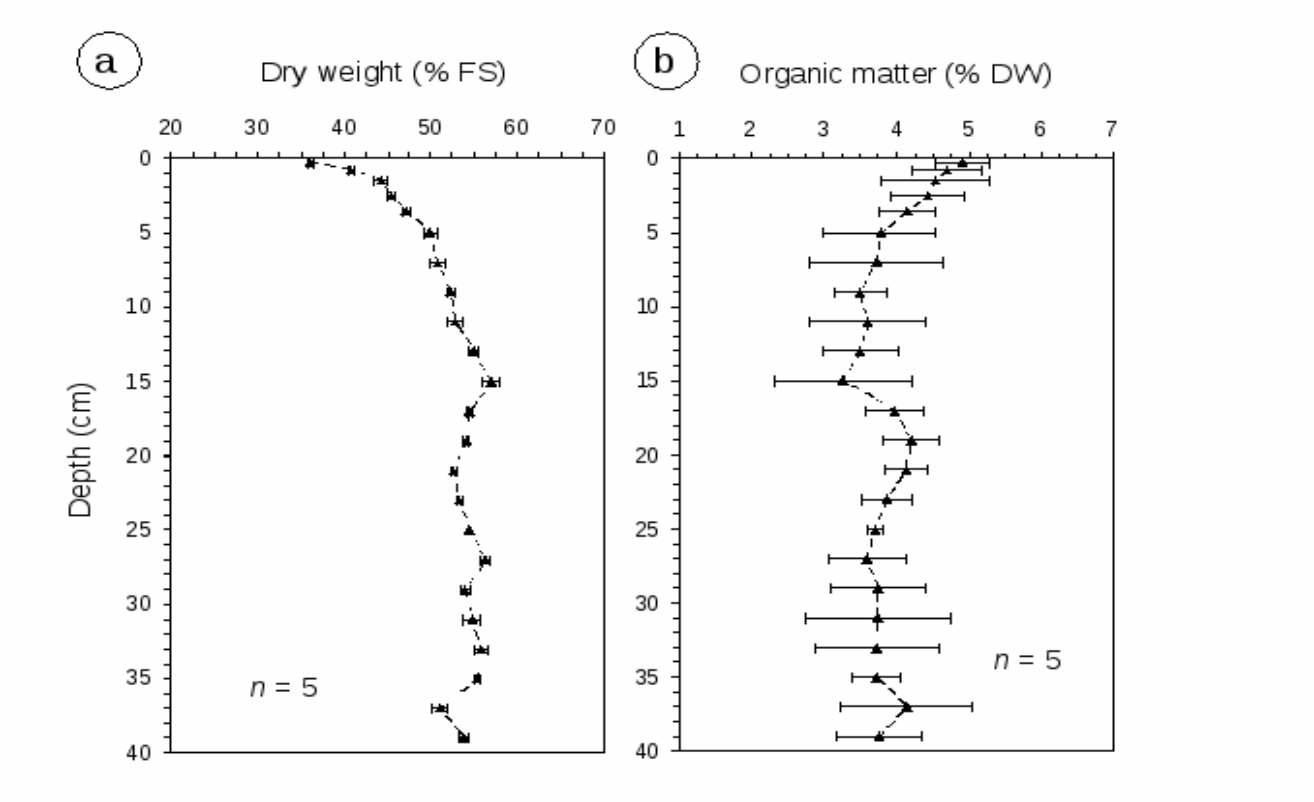

Fig. 10.6: Mean ± standard deviation (SD) of the dry weight (a) and organic matter (b) of sediment in vertical profile in the North-South transect of the basin.

The OM content with also small variations among the cores is irregularly increasing towards the sediment surface indicating its slow accumulation. Organic matter is accumulated either due to import from the catchment area or due to sediment focusing from the more shallow sites of the pond as mostly dominated by macrophytes. The vertical course of OM as described for the basin applies also for the inflow and outflow area. The OM increases in all profiles towards the sediment surface, however, is e.g. in the basin at 30-40 cm depth about 5-fold, in 5-15 cm depth ~2-fold higher as in the inflow area and similar only at the upper 2.5 cm indicating the role of macrophytes in OM accumulation (see 10.3.7)

The vertical profile from the basin represents at a high resolution the chronology of the accumulation of sediment and its constituents (Fig. 10.7). The X-radiography of the half core shows that above the bright clay layer at first thicker and brighter layers were deposited and subsequently increasingly darker and thinner layers are accumulated.

From the length of the core and the beginning of the filling of the pond form in summer 2005 until the sampling of the cores in August 2008 a mean sediment accretion rate of 200 mm a-1 can be deduced. The strong oscillating vertical distribution of Fe and Ca (Fig. 10.7) shows that the matter import in dependence on precipitation (and -intensity) and consequently the resulting soil erosion in the catchment area occurred irregularly and pulsed. The constant atomic Fe:Ca ratio with 0.8±0.2 (n = 3026) reveals that both elements behaved similarly.

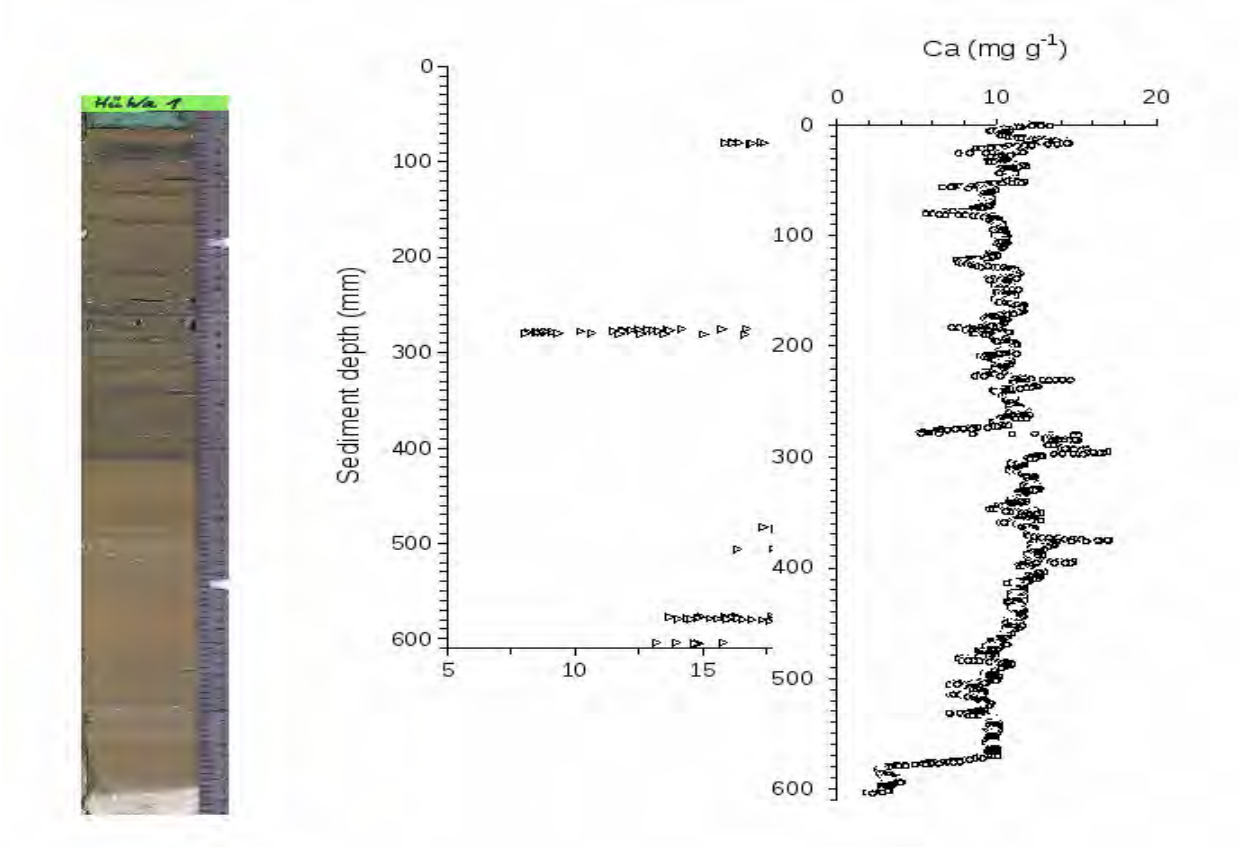

Fig. 10.7: X-ray radiography of a half core and the respective vertical profile of iron and calcium measured by an ITRAX core scanner in a 500 µm resolution. The core scanner data were calibrated with data analyzed by conventional wet digestion an elemental analysis by AAS. The core was taken at 2.3 m depth on 08 October 2008.

10. 3.3 Phosphorus binding forms and binding capacity

The example of the sequential P fractionation (Tab. 10.4) shows that the TP content of the sediment is very low.

According to the composition of the sediment (Fig. 10.5-7, Tab. 10.5), the metal-bound P forms (BD-TP and NaOH-SRP) predominate. Moreover, there is also an elevated proportion of Ca-bound P. Because of the low OM proportion the percentage of organic-bound P (NaOH-NRP) is very low. Both the predominance of metal-bound P forms and the low proportions of organic-bound P species indicate on total a currently low P mobility and consequently availability.

The sediment used for the determination of phosphate sorption capacity (PSC) is characterized in Tab. 10.5. As part of the basin the sediment used is a fine silt mineral sediment.

The Langmuir isotherm of phosphate sorption (Fig. 10.8) shows that the PSC is 2.7-fold higher that the TP of sediment (comp. Tab. 10.5). Thus, the maximal PSC determined indicates that the sediment can theoretically bind more P as currently reflected by the TP of sediment.

Tab. 10.4: Mean values (n = 2) of P bindings forms according to the sequential P fractionation (Psenner et al., 1984; Hupfer, 1995) of surface sediment (0-2 cm) from the deepest site of the pond on 31 May 2006. SRP = soluble reactive P, NRP = non-reactive (organic) P, as determined as the difference between total P (TP) and SRP in the NaOH fraction.

P form		($\mu g\ g^{-1}$)	(%TP)	specification
NH_4Cl	TP	1	0.2	pore-water P
BD	TP	88	15.5	redox-sensitive P
NaOH	SRP	237	41.6	P bound to metal oxides, mainly of Al and Fe
	NRP	14	2.5	organic P of micro organisms and detritus
HCl	TP	197	34.5	P bound to carbonates and apatite-P
Residual P	TP	33	5.8	organic and other refractory P
Sum	TP	570	100.0	P of all fractions

Tab. 10.5: Mean composition (n = 2-6) of surface sediment used for the determination of its phosphate sorption capacity of the small experimental pond (08 October 2008).

Parameter	unit	
Dry weight	(% FW)	54.4
Organic matter	(% DW)	4.3
Mean grain size	(mm)	0.0106
Fe	(mg g^{-1})	39.7
Fe:P ratio	(atomic)	22.6
Al	(mg g^{-1})	72.7
Al:P ratio	(atomic)	86.1
Ca	(mg g^{-1})	11.5
Mn	(mg g^{-1})	11.4
TP (total P)	(mg g^{-1})	0.97

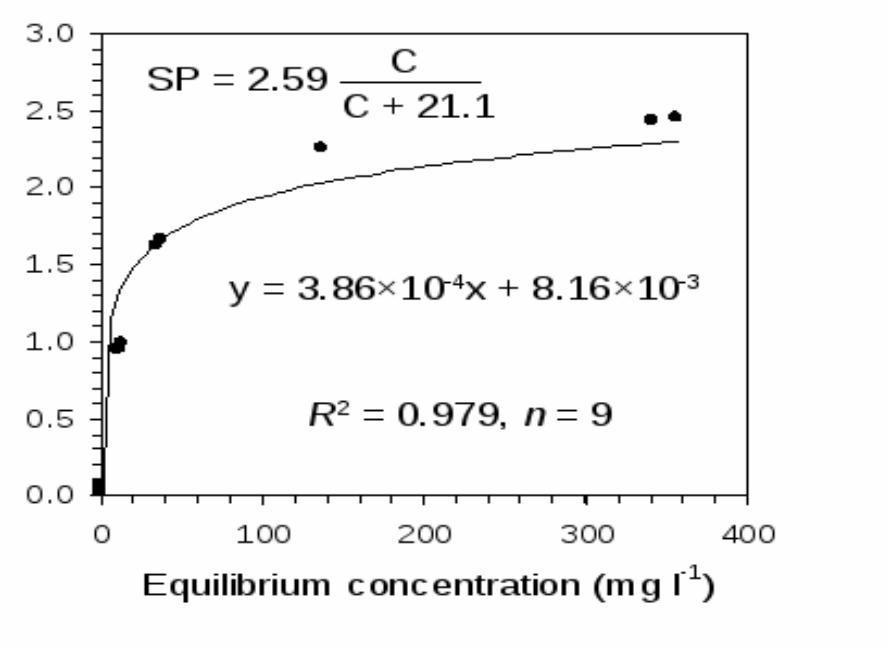

Fig. 10.8: Characteristics of phosphate sorption for surface sediment of the Chicken Creek pond (October 2008). Equilibrium concentration of phosphorus (P) in solution (C) vs. sorbed P (SP) in a logarithmic relationship. The linear equation (y = ax + b) was used fort he calculation of the Langmuir adsorption isotherm SP = PSC × C/C + K, where PSC is the maximal phosphate sorption capacity [mg g-1] and K is the half-saturation constant [mg l-1]. For the characterization of the sediment used see Tab. 10.5.

The surplus of metals for P binding as indicated by a higher atomic Fe:P and Al:P ratio favours an effective P binding and is in accordance with the results of the P fractionation (Tab. 10.4). The throughout high O_2 saturation in the real world water column and the O_2 diffusion into the sediment (see 10.3.6) favours the P binding onto oxidized Fe compounds (BD-P).

10. 3.4 Sediment resuspension

During the step-wisely increasing shear velocity *u** only the loose sediment constituents such as freshly deposited detritus was entrained from the strongly consolidated sediment (Fig. 10.9). A mass erosion following a breakup of the sediment structure did not occur.

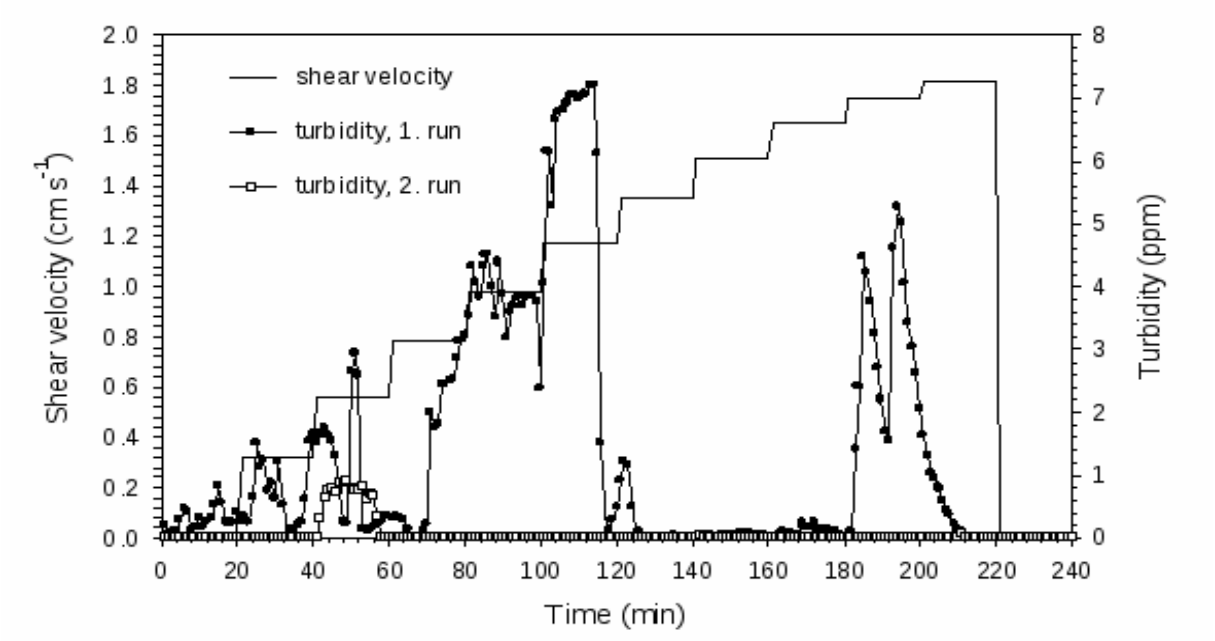

Fig. 10.9: Means of turbidity at step-wisely increases shear velocity in a resuspension experiment with undisturbed sediment cores from the basin of the small experimental pond (October 8th 2008). For the entrainment rates of parameter determined in duplicate see Tab. 10.6.

Hence, the turbidity, the concentration of SPM, TFe, TP and SRP as well as their entrainment rates E were low (Tab. 10.6). For the span of u^* 0-1.17 cm s^{-1} a non-linear significant relationship between E_{SPM} [g m^{-2} h^{-1}] and u^* [cm s^{-1}] was found: $E_{SPM} = 11.57 \times u^{*2} - 3.72 \times u^*$ ($n = 6$, $R^2 = 0.96$).

The low rates of E_{SPM} show that the present sediment surface of the basin, consisting of fine silt exhibits a high degree of consolidation and consequently a low resuspension affinity (Fig. 10. 9). Both become obvious if the E_{SPM} determined (Tab. 10.6) are compared to those of other shallow ponds with a higher productivity and nutrient-laden sediments (Tab. 10.8). It is reasonable to assume that the filling of the original hollow mould (Fig. 10.3) will lead not only to a decrease of pond volume but also to a decrease of water depth favouring the further colonization by submerged macrophytes. They are able to fix nutrients in their biomass (e.g. Barko and James, 1998) and to lower resuspension (Horppila and Nurminen, 2003). However, the increasing shallowness of the pond due to accumulation of sediments of a different quality (more OM) might coincidentally increase the resuspension affinity and could thus lead to resuspension-related nutrient and productivity pulses in the future.

Tab. 10.6: Concentration and entrainment rate with increasing shear velocity *u** in the resuspension experiment with undisturbed sediment cores from the Chicken Creek pond (October 8th 2008). The concentrations at *u** = 0 cm s^{-1} represent those of the inflowing pond water.

	Parameter	Shear velocity *u** (cm s^{-1})		
		0	0.32	1.82
Concentration	SPM (mg l^{-1})	0.30	0.69	0.38
	TFe (µg l^{-1})	32	24	100
	TP (µg l^{-1})	14	14.6	15.5
	SRP (µg l^{-1})	3	2	4
Ratio	Fe:P (atomic)	1.27	0.91	3.57
Entrainment rate	SPM (g m^{-2} h^{-1})	0	0.95	6.26
(first run)	TFe (mg m^{-2} h^{-1})	0	-19.68	163.54
	TP (mg m^{-2} h^{-1})	0	1.45	3.62

10. 3.5 Sediment pore water

Characteristic concentration gradients of SRP, Fe and sulphate (SO_4^{2-}) were found at the sediment water interface (Fig. 10.10). Both the SRP concentrations in the near bottom water (inflow: 13 µg l^{-1}, outflow: 8 µg l^{-1}) and in the pore water, with no difference between the inflow and outflow peeper (10-295 µg l^{-1}) were extremely low. Consequently, fluxes and turnover rates were negligible (Tab. 10.7) in respect to a SRP supply to the water column.

The concentration of dissolved Fe in the pore water at the inflow area with 0.34-27.7 mg l^{-1} was on average 1.6-fold higher than that of the outflow area with 0.11-8.49 mg l^{-1}. The respective flux and turnover of the inflow was about 3-fold higher than those of the outflow (Tab. 10.7). Similarly, the concentrations of Mn^{2+}, and Cl^- of the inflow peeper were about 1.6- and 1.8-fold higher than those of the outflow peeper (not shown) indicating that the catchment area represents the main source of particulate and dissolved sediment constituents. Pore water atomic Fe:P ratio varied between 7-439 (inflow area) and 10-313 (outflow area) and averaged to 117 and 114, respectively. The latter values are remarkable high and guaranty a low P mobility. The high SO_4^{2-} concentration in the water overlying the sediment decreased to minimum values between 7 and 10 mg l^{-1} at 9 cm sediment depth. The respective flux and turnover rates of SO_4^{2-} (Tab. 10.7) reveal a considerable potential of SO_4^{2-} reduction.

As calculated from the vertical profiles presented in Fig. 10.10 the fluxes (release rates directed towards the overlying water) and turnover rates of SRP and Fe were rather low (Tab. 10.7), if compared to those of nutrient-burden shallow ponds (Tab. 10.8). Hence, e.g. SRP release rate is at present of subordinate importance in supplying P to phytoplankton. Nevertheless, changes in the P mobility, at least in respect to the availability of reactive Fe compounds for the P binding (BD-P, Tab. 10.4), are to expect in future.

The SO_4^{2-} concentration in the water body (Tab. 10.3) is already relatively high, the rates of its consumption via SO_4^{2-} reduction at present still relatively low (Tab. 10.7) if compared to those reported in the literature (Tab. 10.8). However, the further accumulation of organic matter (increase of microbial available carbon proportion) will lead to an enhanced O_2 demand of the sediment (decrease in O_2 penetration depth) and at the same time to an increase of the anaerobic and obviously at present C-limited SO_4^{2-} reduction. The stimulation of the SO_4^{2-} reduction, where sulfide (HS^-) is formed which can react with ferrous Fe (Fe^{2+}) to insoluble iron sulfides (FeS_x) could contribute an immobilization of iron which is not available for a P binding (e.g. Lamers, 1998; Caraco et al., 1989).

Tab. 10.7: Flux (positive: into overlying water, negative: into sediment) and turnover rate (depth-integrated production and consumption of *n* horizons, respectively; comp. to Fig. 10.10) of soluble reactive P (SRP), dissolved Fe, and of sulphate (SO_4^{2-}) at the sediment water interface at the basin (peeper of 27 August 2008).

Parameter	unit	inflow	R^2	*n*	outflow	R^2	*n*
SRP flux	(mg m^{-2} d^{-1})	0.03			0.35		
turnover	(mg m^{-2} d^{-1})	0.16	0.99	2	0.34	0.97	4
Fe flux	(mg m^{-2} d^{-1})	20.7			6.2		
turnover	(mg m^{-2} d^{-1})	21.9	0.99	3	2.6	0.84	4
SO_4^{2-} flux	(mg m^{-2} d^{-1})	-482			-151		
turnover	(mg m^{-2} d^{-1})	477	0.98	3	156	0.99	4

10. 3.6 Dissolved oxygen at the sediment water interface

Laboratory measurements of dissolved oxygen saturation decreased from 100% (due to artificial aeration of water column) above the sediment down to zero at 2.5 mm sediment (not shown). The respective diffusive flux averaged to -549 mg m^{-2} d^{-1} and the turnover rate to 551 mg m^{-2} d^{-1}. It shows both, that the diffusion is in dependence on the sediment properties and the oxygen supply and consumption spatially restricted to the upper 2 mm. However, this can be influenced to a large extent by the filamentous green algae colonizing the surface sediment.

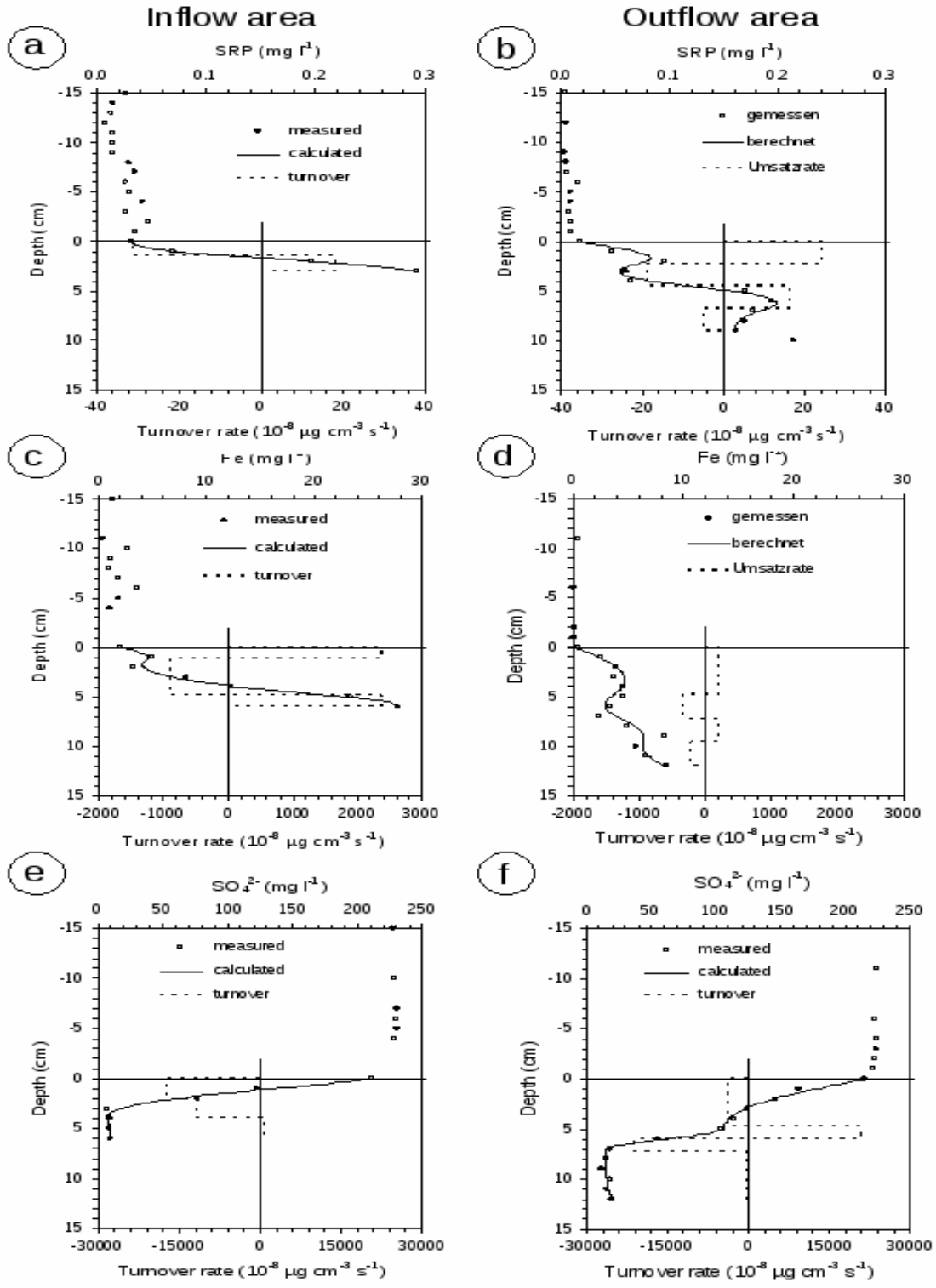

Fig. 10.10: Measured and calculated vertical profiles at the sediment water interface as well as turnover rate for different sediment horizons at the inflow and the outflow area of the pond, on August 27th 2008: a-b) soluble reactive P (SRP), c-d) dissolved Fe, and e-f) sulphate (SO_4^{2-}). For the turnover and release rates see Tab. 10.7.

Tab. 10.8: Determined parameter and rates of surface sediment (0-5 cm) of the basin of the Chicken Creek pond studied at an initial stage of development in comparison to those of sediments of comparable 'developed' polymictic eutrophic shallow ponds.

Parameter and rate	unit	pond studied	shallow lakes	source
Organic matter	(% FW)	4-5	20 – 30	Kozerski and Kleeberg (1998)
Total P	(mg g^{-1})	0.6-1.0	0.51 – 3.62	Kozerski and Kleeberg (1998)
P sorption capacity	(mg g^{-1})	2.59	1.04 – 9.52	Kozerski and Kleeberg (1998)
O_2 consumption	(mg m^{-2} d^{-1})	549.0	0.3 … 4,000	Burger et al. (2007)
Sulphate reduction	(mg m^{-2} d^{-1})	151-482	5 – 1,600	Holmer and Storkholm (2001)
Release rate SRP	(mg m^{-2} d^{-1})	0.03-0.35	1.6 – 125	Kozerski and Kleeberg (1998)
Entrainment† SPM	(g m^{-2} h^{-1})	6.3	27.8 – 54.6	Kleeberg et al. unpubl.
TFe	(mg m^{-2} h^{-1})	163.5	33.8 – 279.2	Kleeberg et al. unpubl.
TP	(mg m^{-2} h^{-1})	3.6	27.8 – 119.8	Kleeberg et al. unpubl.
Sediment accretion	(mm a^{-1})	200	0.4 – 1.8	Kozerski and Kleeberg (1998)

† at shear velocity u^* = 1.82 cm s^{-1}

10. 3.7 Vegetation and its potential impact on sediment accumulation and reactivity

A snap-shot of the vegetation in August 2008 illustrates the rapid progress of colonization and spreading of emersed and submersed macrophytes as well as of benthic algae (Fig. 10.11).

Particularly, the common reed *Phragmítes austrális* (CAV.) TRIN ex STEUD. at the western slope is able to propagate by at least 2 m long rhizomes during one vegetation period over the water surface. As favoured by the light climate ample population of the long-leaf pondweed *Potamogeton nodósus* POIRET, and scattered individuals of the Eurasian water-milfoil *Myriophyllum spicatum* L. colonized water depths up to 1 m. Predominant at the shallow areas (0.2-1 m depth) particularly at the outflow filamentous green algae such as *Rhizoclonium* and *Zygnema* spec. form extended canopies on the sediment surface. All plants either submerged or emersed can contribute to the accumulation of organic carbon at/in the surface sediment.

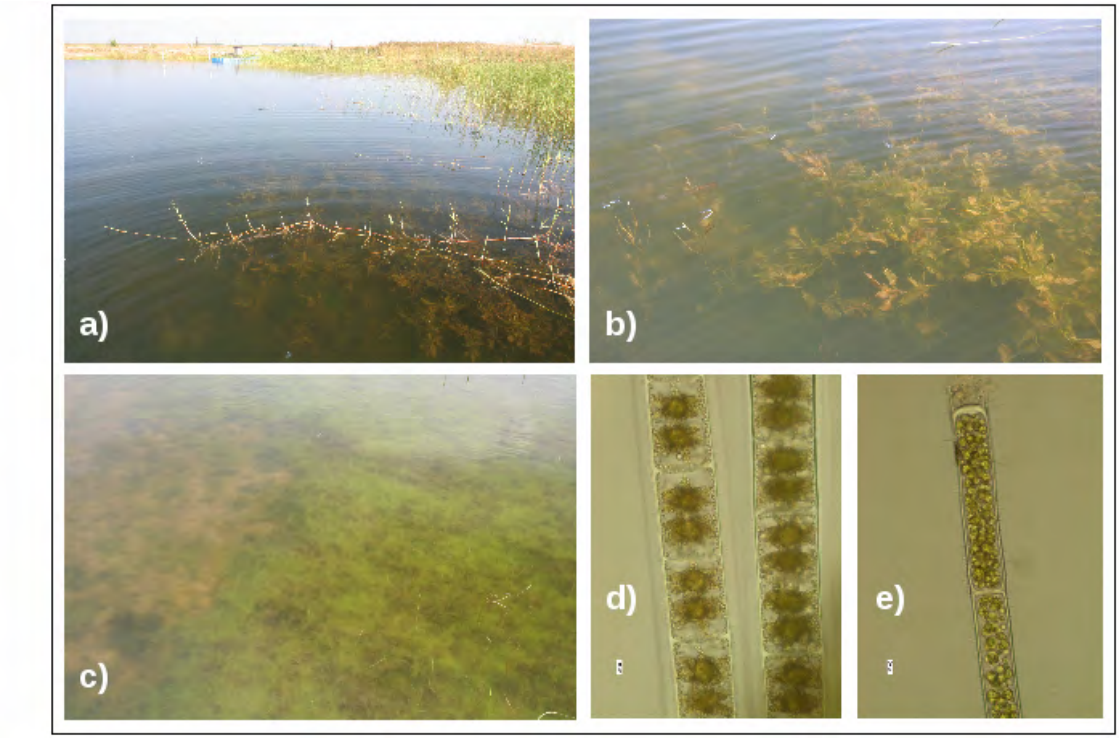

Fig. 10.11: a) View from north to the outflow area (blue landing pontoon in the back) of the Chicken Creek pond. In the foreground the submerged longleaf pondweed *Potamogeton nodósus* and the floating rhizome of the common reed (*Phragmítes austrális* are to be seen. b) Detail of *P. nodósus* at the western slope. c) Filamentous green algae on the sediment surface (periphyton) in the shallow outflow area. d) and e) microscopic photograph of the filamentous green algae *Zygnema* spec. and *Rhizoclonium* spec. The length of the small red bar corresponds to 20 µm. Photographs a) - c) were taken on August 27th 2008 nearly at the maximum of biomass at the end of vegetation period, and d) - e) on October 8th 2008.

10. 4 Conclusions

The past large accretion of sediment, spanning only 3 years, and its current composition reflect the strong interconnection between the artificial catchment and the pond. The data on sediment characteristics and reactivity presented, if compared to nutrient-burden shallow ponds representing an advanced stage of pond succession, demonstrate that the artificial pond is at an initial state. Clearly, still soil properties determine the chemical sediment characteristics (e.g. silt, metal surplus) and reactivity (e.g. low pore water fluxes). However, the results of our study also suggest that the mainly inorganic matter input due to soil erosion will decrease because topography, vegetation cover and drainage boundary conditions will change. Thus in-pond processes will become more important. Chemical sediment characteristics that govern the P retention and mobility, crucial for the future pond development, will be increasingly influenced by an increasing import of organic matter both from terrestrial and aquatic vegetation. The rate and extent to which the processes of P mobilization occur will be influenced particularly by aquatic macrophytes contributing not only to a carbon supply stimulating microbial processes but also to mobilize and translocate benthic P.

References

Barko, J. W. and James, W.F., 1998: Effects of submerged aquatic macrophytes on nutrient dynamics, sedimentation, and resuspension. In: Jeppesen, E., Sondergaard, M. and Christoffersen, K. (eds.): The structuring role of submerged macrophytes in lakes. Springer Verlag, New York, 197-215.

Berg, P., Risgaard-Petersen, N. and Rysgaard, S., 1998: Interpretation of measured concentration profiles in sediment pore water. Limnol. Oceanogr. 43, 1500-1510.

Biemelt, D., Schapp, A., Kleeberg, A. and Grünewald, U., 2005: Overland flow, erosion, and related phosphorus and iron fluxes at plot scale: a case study from a non-vegetated lignite mining dump in Lusatia. Geoderma 129, 1-18.

Brenning, U., 1967: Die Siedlungsdichte von *Arenicola marina* (L.) im Raum der Insel Langenwerder (Wismar-Bucht). Wissenschaftl. Zeitschr. Univ. Rostock [Mathemat.-Naturwiss. Reihe 9/10] 16, 1181-1192.

Burger, D.F., Hamilton, D.P., Pilditch, C.A. and Gibbs, M.M., 2007: Benthic nutrient fluxes in a eutrophic, polymictic lake. Hydrobiologia 584, 13-25.

Caraco, N.F., Cole, J.J. and Likens, G.E., 1989: Evidence for sulphate-controlled phosphorus release from sediments of aquatic systems. Nature 341, 316-318.

Croudace, I.W., Rindby, A. and Rothwell, R.G., 2006: ITRAX: description and evaluation of a new X-ray core scanner. In: Rothwell, R. G. (ed.): New ways of looking at sediment cores and core data. Geol. Soc. Spec. Publ. 267, 51-63.

Droppo, I.G., Lau, Y.L. and Mitchell, C., 2001: The effect of depositional history on contaminated bed sediment stability. Sci. Tot. Environm. 266, 7-13.

Fietz, S. and Nicklisch, A., 2004: An HPLC analysis of the summer phytoplankton assemblage in Lake Baikal. Freshw. Biol. 49, 332-345.

Foster, I.D.L. and Walling, D.E., 1994: Using reservoir deposits to reconstruct changing sediment yields and sources in the catchment of the Old Mill Reservoir, South Devon, UK, over the past 50 years. J. Hydrobiol. Sci. 39, 347-368.

Furrer, G. and Wehrli, B., 1996: Microbial reactions, chemical speciation, and multicomponent diffusion in porewaters of a eutrophic lake. Geochim. Cosmochim. Acta 60, 2333-2346.

Gerwin, W., Raab, T., Biemelt, D., Bens, O. and Hüttl, R.F., 2009: The artificial water catchment "Chicken Creek" as an observatory for critical zone processes and structures. Hydrol. Earth Syst. Sci. Discuss., 6, 1769-1795.

Güde, H., and Gries, T., 1998: Phosphorus fluxes in Lake Constance. Arch. Hydrobiol., Spec. Iss. Advanc. Limnol. 53, 505-544.

Gust, G., 1990: Method of generating precisely-defined wall shear stresses. US patent number 4,973,1651990.

Gust, G. and Müller, V., 1997: Interfacial hydrodynamics and entrainment functions of currently used erosion devices. In: Burt, N., Parker, R. and Watts, J. (eds.): Cohesive sediments. Wiley, Chichester, UK, pp. 149-174.

Håkanson, L., 2005: The importance of lake morphometry and catchment characteristics in limnology - ranking based on statistical analyses. Hydrobiologia 541, 117-137.

Hesslein, R.H., 1976: An *in situ* sampler for close interval pore water studies. Limnol. Oceanogr. 21, 912-914.

Holmer, M. and Storkholm, P., 2001: Sulphate reduction and sulphur cycling in lake sediments: a review. Freshw. Biol. 46, 431-451.

Horppila, J. and Nurminen, L., 2003: Effects of submerged macrophytes on sediment resuspension and internal phosphorus loading in Lake Hiidenvesi (southern Finland). Wat. Res. 37, 4468-4474.

Hupfer, M., 1995: Bindungsformen und Mobilität des Phosphors in Gewässersedimenten. In: Steinberg, C., Bernhardt, H. and Klapper, H. (eds.) Handbuch Angewandte Limnologie, Ecomed, Kap. IV-3.2: 1-22.

Kleeberg A., Hupfer, M. and Gust, G., 2008a: Resuspension experiments on phosphorus entrainment in a lowland river, Spree, NE Germany. Aqu. Sci. 70, 87-99.

Kleeberg, A., Schapp, A. and Biemelt, D., 2008b: Phosphorus and iron erosion from non-vegetated sites in a post-mining landscape, Lusatia, Germany: impact on aborning mining lakes. Catena 72, 315-324.

Kopáček, J., Marešová, M., Hejzlar, J. and Norton, S.A., 2007: Natural inactivation of phosphorus by aluminum in preindustrial lake sediments. Limnol. Oceanogr. 52, 1147-1155.

Kozerski, H.-P. and Kleeberg, A., 1998: The sediments and benthic-pelagic exchange in the shallow Lake Müggelsee. Internat. Rev. Hydrobiol. 83, 77-112.

Krom, M., 1980: Spectrophotometric determination of ammonia: a study of a modified Berthelot reaction using salicylate and dichloroisocyanorate. Analyst 105, 305-316.

Kühl, M. and Revsbech, N.P., 2001: Biogeochemical microsensors for boundary layer studies. In: Boudreau, B.P. and Jørgensen B.B. (eds.): The Benthic Boundary Layer. Oxford University Press, Oxford, 180-210.

Lamers, L.P.M., 1998: Sulfate-induced eutrophication and phytotoxicity in freshwater wetlands. Environ. Sci. Technol. 32, 199-205.

Li, Y.-H. and Gregory, S. 1974: Diffusion of ions in sea water and in deep-sea sediments. Geochim. Cosmochim. Acta 38, 703-714.

Murphy, J. and Riley, J.P., 1962: A modified single solution method for determination of phosphate in natural waters. Anal. Chim. Acta 27, 31-36.

Müller, B., Lotter, A.F., Sturm, M. and Ammann, A., 1998: Influence of catchment quality and altitude on the water and sediment composition of 68 small lakes in Central Europe. Aqu. Sci. 60, 316-337.

Psenner, R., Pucsko, R. and Sager, M., 1984: Die Fraktionierung organischer und anorganischer Phosphorverbindungen von Sedimenten - Versuch einer Definition ökologisch wichtiger Fraktionen. Arch. Hydrobiol./Suppl. 70, 111- 155.

Schlungbaum, G., 1982: Sedimentchemische Untersuchungen in Küstengewässern der DDR. Teil 11: Phosphatsorptionsgleichgewichte zwischen Sediment und Wasser in flachen eutrophen Küstengewässern. Acta hydrochim. Hydrobiol. 10, 135-152.

Schulz, M. and C. Herzog, C., 2004: The influence of sorption processes on the phosphorus mass balance in a eutrophic German lowland river. Wat., Air, Soil Poll. 155, 291-301.

Tengberg, A., H. Stahl H., G. Gust, V. Müller, U. Arning, H. Andersson and Hall, P.O.J., 2004: Intercalibration of benthic flux chambers I. Accuracy of flux measurements and influence of chamber hydrodynamics. Progress in Oceanography 60, 1-28.

Weyhenmeyer, G.A., 1998: Resuspension in lakes and its ecological impact - a review. Arch. Hydrobiol. Spec. Issues Advanc. Limnol. 51, 185-200.

Zessner, M., Postolache, C., Clement, A., Kovacs, A. and Strauss, P., 2005: Considerations on the influence of extreme events on the phosphorus transport from river catchments to the sea. Water Sci. Technol. 51, 193-204.

Zwirnmann, E., Krüger, A. and Gelbrecht, J., 1999: Analytik im zentralen Chemielabor. Jahresbericht des IGB (Leibniz-Institut für Gewässerökologie und Binnenfischerei) 9, 3-24.

Acknowledgements

Bernd Schütze (IGB Berlin) and Dr. Hans-Peter Kozerski (Beeskow) assisted with the fieldwork. The qualitative and quantitative analysis of phytoplankton was done by Helgard Täuscher, Barbara Meinck and Dr. Andreas Nicklisch (all IGB Berlin). The sediment analyses were considerably supported by Jan Leuschner and Hans-Jürgen Exner (IGB). Jeanette Posern (Berlin) helped with the resuspension experiment. Sabine Stahl (Univ. Bremen) did the µXRF measurements. Dr. Detlef Biemelt, Egbert Gassert and Remo Ender (all BTU Cottbus) provided pond morphology and precipitation data. Sincere thanks are given to them all.

11. Microdrone-based aerial monitoring

Maik Veste, Thomas Seiffert, Rossen Nenov

Brandenburg University of Technology, Research Center Landscpae Development and Mining Landscapes

11. 1 Introduction

For the monitoring of changes and spatial or rather temporal analysis of the highly dynamic structural development of surface structures at the artificial catchment Chicken Creek remote sensing methods a pilot study was carried out. Aerial photographs were taken for an innovative and cost efficient approach to study small-scale landforms caused by erosion. The images were taken using a microdrone-based tool by a commercial digital camera. This technique allows easy access to aerial photographs and furthermore a potentially high temporal monitoring resolution. The microdrone based aerial monitoring will allow detecting structural changes at the catchment scale (e.g. development of erosion channels, vegetation dynamics and vegetation cover).

11. 2 Materials and methods

11. 2.1 Helicopter flights

Aerial photos were taken from a helicopter on September 22nd, 2006 and June 14th, 2007 (Tab. 11.1).

Tab. 11.1: Camera types and resolutions used for the aerial photographs between 2006 and 2008

Date	Carrier	Flight height (m)	Camera type	Terrain resolution
Sep. 22nd, 2006	Helicopter	100 – 120	Olympus S700 / µ700	3 x 3 cm
Jun. 14th, 2007	Helicopter	100 – 120	Cannon EOS 400D	2 x 2 cm
Jul. 10th, 2008	Microdrone	40	Pentax Optio A30	1 x 1 cm

11. 2.2 Microdrone and image acquisition

Since spring 2008 we use for aerial monitoring a microdrone (Fig. 11.1) equipped with a digital camera that allows terrain resolution of less than 1cm/pixel depending on flying height (Veste et al. 2008). The MD4-200 microdrone is a VTOL AUMAV (VTOL = Vertical Take Off and Landing, AUMAV = Autonomous Unmanned Micro Aerial Vehicle) constructed by microdrones GmbH, Kreuztal, Germany. The microdrone is built from carbon fiber reinforced plastics. The take-off empty weight is about 585 g and approximately 900 g including the camera system and tools. The payload capacity is about 200 g and the size of the microdrone is 0.912 x 0.912 m including rotors.

The MD4-200 operates with rechargeable Lithium-polymer batteries that sustain flight times of up to 20 min. The maximum flight time certainly depends on the wind force, temperature and payload. In case of low air temperature and/or high wind speed, the battery capacity or rather the flight time is reduced accordingly. The MD4 – 200 possess four rotors and a maximum operating distance of about 2000 m depending on the flight velocity, wind force and the charging level of the batteries.

Fig. 11.1: Microdrone MD4-200.

A characteristic feature of the microdrone is the built-in GPS receiver that facilitates its use and extends its scope of application. By means of the GPS receiver the microdrone can hold its position even in the presence of wind speed up to 6 m s^{-1}. However, for precise aerial photos and to avoid crashes we use the drone only up to wind speeds of maximum 3 m s^{-1} at 2 m height above ground. Calm weather conditions are optimal for carrying out microdrone flights. The programming of the microdrone is realised by the software mdCockpit, developed by microdrones GmbH. The navigation by GPS allows way point navigation and enables to define flight plans beforehand. Depending on the size of the area that has to be photographed and the required overlap between the aerial photos, it might be necessary to execute several flights. The flight route of the microdrone over the catchment is shown in Fig. 11.2. The flight time as well as the length of the three flights on April 22nd 2009 is given in Tab. 11.2.

Due to the limited payload capacity of the micro-drone we chose the commercial, unmetric and relatively high resolution digital camera Pentax Optio A40. An absolute solution of 4000 x 3000 pixels, a pixel size of about 1,8 µm, finest detail gradations in particular in the light and shade rendition with minimum picture noise and an optomechanic image stabilizer were necessary to get good results for subsequent image interpretations.

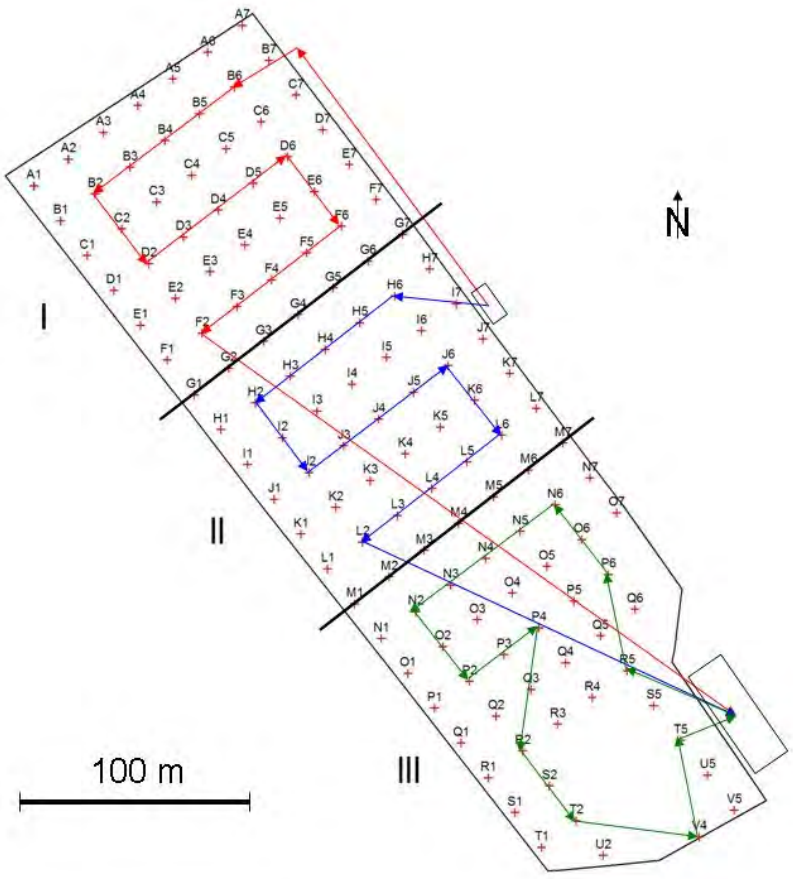

Fig. 11.2: Flight route of the microdrone with waypoints over the artificial water catchment.

Tab. 11.1: Flight distance and time of the three microdrone flights

Flight No.	Flight length (horizontal and vertical)	Flight time
1	940 m	11 min 40 sec
2	690 m	9 min 50 sec
3	665 m	10 min 30 sec

11. 2.3 Aerial image processing and analysis

The specified camera settings in combination with the defined flight plan resulted in a maximum terrain resolution of about 0.02 m per pixel (a benchmark of approximately 1:11000) depending on the defined operating altitude of 80 m. For the presented study an automatic aerial photography during a few flight stops was chosen. The activation was realised by a remote-controlled infrared system.

The complete aerial photo of the total catchment is composed by a mosaic of approx. 120 plots by 20 image blocks. Different commercial software programs are available to analyse drone based aerial photos. One of the most comprehensive software programs for this application is WGEO, a compilation of efficient GIS tools to transform and rectify space-oriented datasets. We used the module of WGEO BASIS, which possesses the functions of rectifying of grid datasets to define their existence in the terrain. In order to fit the drone based aerial pictures into a geodetic reference system as a grid dataset we used a waypoint dataset derived from a local measurement with a TRIMBLE DGPS solution. To generate these local coordinates to a geometric visualization within WGEO BASIS was helpful to find and rectify the ground control points (GCP’s) of any aerial photo (Fig. 11.3). After the manual correlation of the needed local coordinates and at least four visible GCP’s given in a single aerial photo, the trapezoid rectification tool of WGEO was required to get a new calculated, scaled, rotated and shifted image of the regarded single photograph (Fig. 11.4). After every single rectification and maybe blanking of the wanted polygon, the so originated and geo-coded pictures were saved in terms of a numeric system to facilitate easier subsequent processing. The creation of an aerial image mosaic is not licensed within WGEO BASIS. Therefore we used ArcGIS 9.3, a geographic information system software, developed by ESRI. Due to the saved geo-code of the single picture, their adjustment into blocks was possible. Finally we got a drone based aerial photo block adjustment to save it as map (Fig. 11.5).

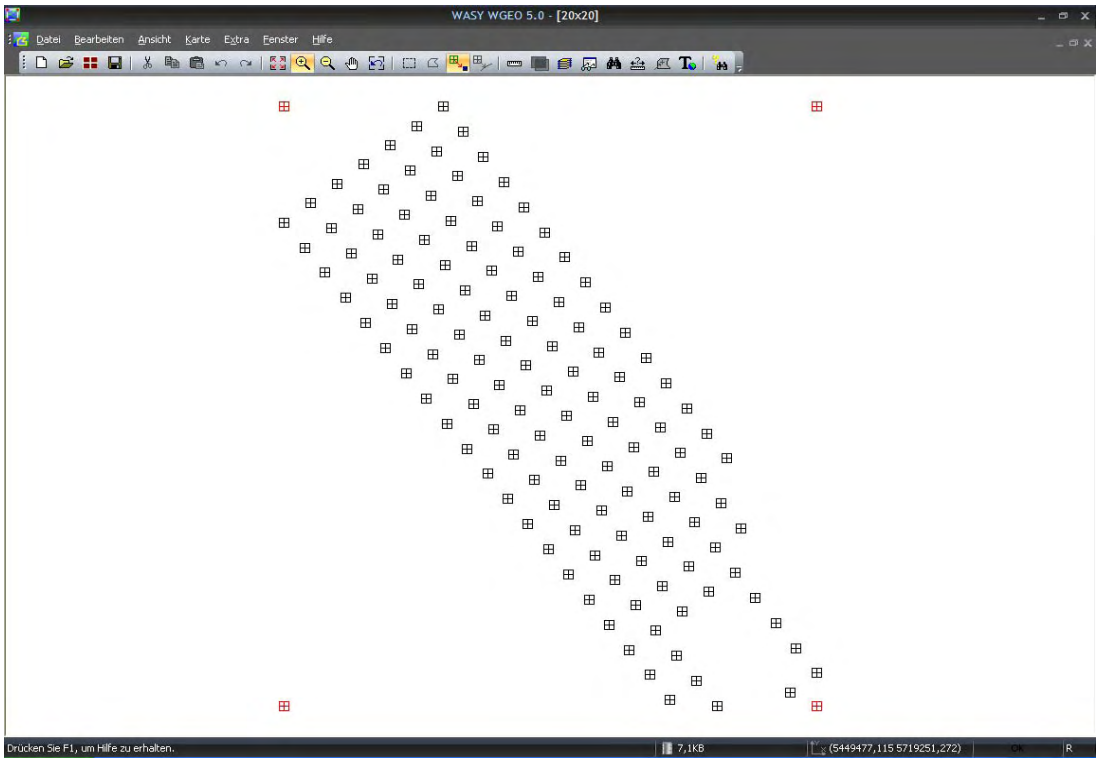

Fig. 11.3: Geometric visualization of local coordinates using WGEO 5.0.

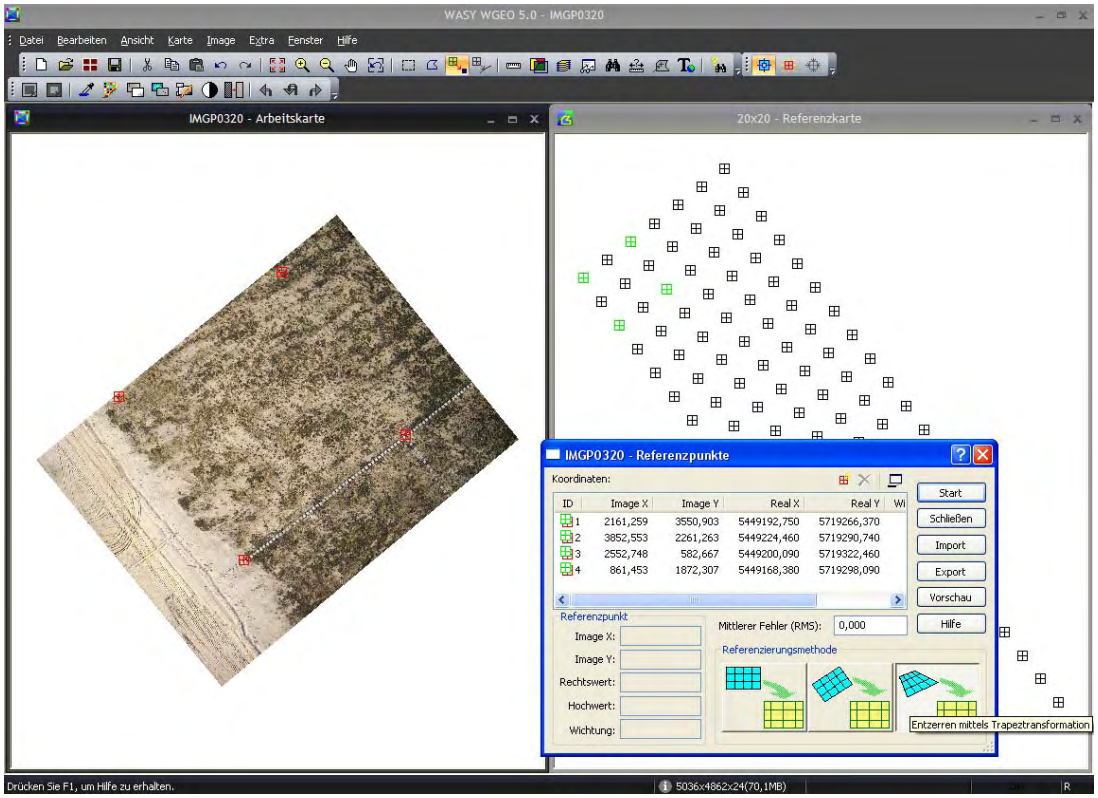

Fig. 11.4: Trapezoid rectification of a single aerial photo using WGEO 5.0.

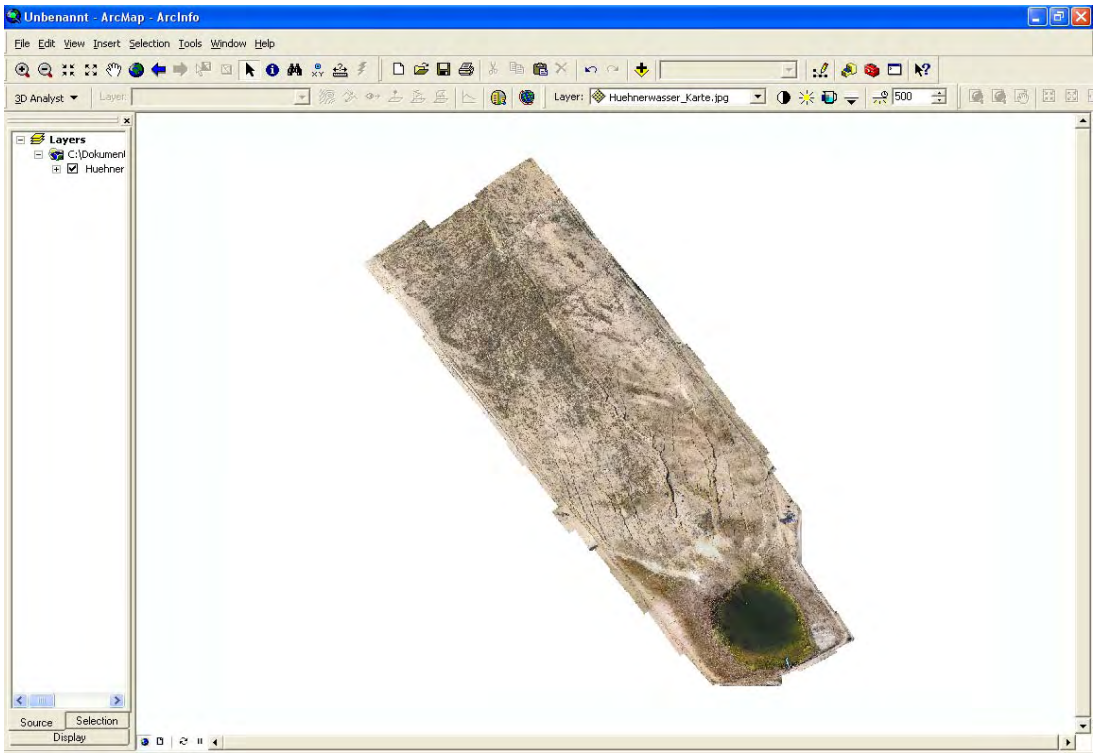

Fig. 11.5: Block adjustment saved as map using WGEO 5.0.

For monitoring of the vegetation cover from aerial photos the freeware MultiSpec was tested, developed at Purdue University, West Lafayette, IN, by David Landgrebe and Larry Biehl from the School of Electrical and Computer Engineering, ITaP and LARS (Veste et al. 2008). A supervised classification by selecting training areas for selected classes from known areas (plants, sand) was applied to identify the vegetation cover. Though only two training areas where selected to define the vegetation cover of the investigated plot.

11. 3 Results and discussion

Since 2006 three flights were carried out to cover the entire catchment (Table 11.1) and aerial photos are shown in figures 11.6-11.8. Due to technical problems the flight on July 10th 2008 covers only parts of the catchment area (Fig. 11.8).

During the investigations a few essential points became important referring to the methodology of micro-drone-based image acquisition. The relatively lightweight unmanned MD4 – 200 micro-drone and the unmetric Pentax Optio A40 digital camera we did not achieve perfect results in regard to the aspired image blocks. The acceleration and breaking of the microdrone during flight led to troubles in the flight stability of the micro-drone as carrier for the digital camera. Thus, there are different accuracies in height of every neighbouring image pair without image bundle block adjustment.

Furthermore the high wind force influenced the abidance of the accurate flight direction and according to that the correct angle of 180° of the microdrone to the route. Due to the unstable flight characteristics of the micro-drone, relative unstable sensor stability could be expected so that the calibration parameters of the digital camera changed during the flight caused by disturbances of the flight stability and a low physical stability of the camera sensor within the camera body.

A time-series from 2006 - 2008 was analysed with MultiSpec (Purdue Research Foundation. 2009). The vegetation patches of the investigated plot were detected by the program and the vegetation cover calculated (Fig. 11.9). The vegetation cover increased from 1% in 2006 to 11% in 2007 and 24% in 2008, respectively.

11. 4 Conclusions

According to the objectives and the long-term research concept of the SFB/TRR 38 disturbances within the catchment – including scientific measurements – have to be minimized. Therefore, a cost efficient remote sensing tool was tested in a pilot study. The results of this study reveal that the remote controlled MD4 – 200 microdrone is a good alternative for the monitoring of the development of surface structures (e.g. vegetation, stream network, surface properties) within the investigated artificial watershed Chicken Creek (Seiffert et al., 2009). The advantage of the microdrone in comparison to conventional airborne photos is the possibility to take close-range-like aerial photos. Due to the restricted battery charge of the carrier and with regard to the cost-efficiency, it is advisable to use the MD4-200 microdrone only for investigation areas of up to 10 ha. Wind and temperature sensitivity limits its use to calm weather conditions. Furthermore, the low payload capacity limits the use of high-resolution cameras, which are needed to improve the photo quality.

The use of an unmetric commercial digital camera for precise aerial image acquisition is a crucial factor for quality of the images due to the absence of any satisfactory camera calibration and subsequent bundle block adjustment. In our study the relative high instability of the sensor geometry of the Pentax Optio A40 was the main reason for divergences in height within an image block.

The described micro-drone-based image acquisition for later digital elevation models is a low cost method which produces relatively high-precision results, depending on the objectives. The most important advantage of this method and what makes it cutting-edge is the downright independency of any other less flexible connections of camera platforms like airplanes, helicopters and huge hot air blimps with heavy weighted digital cameras for aerial photography.

Fig. 11.6: Aerial photo of the artificial water catchment Chicken Creek September 22nd 2006.

Fig. 11.7: Aerial photo of the artificial water catchment Chicken Creek June 14th 2007.

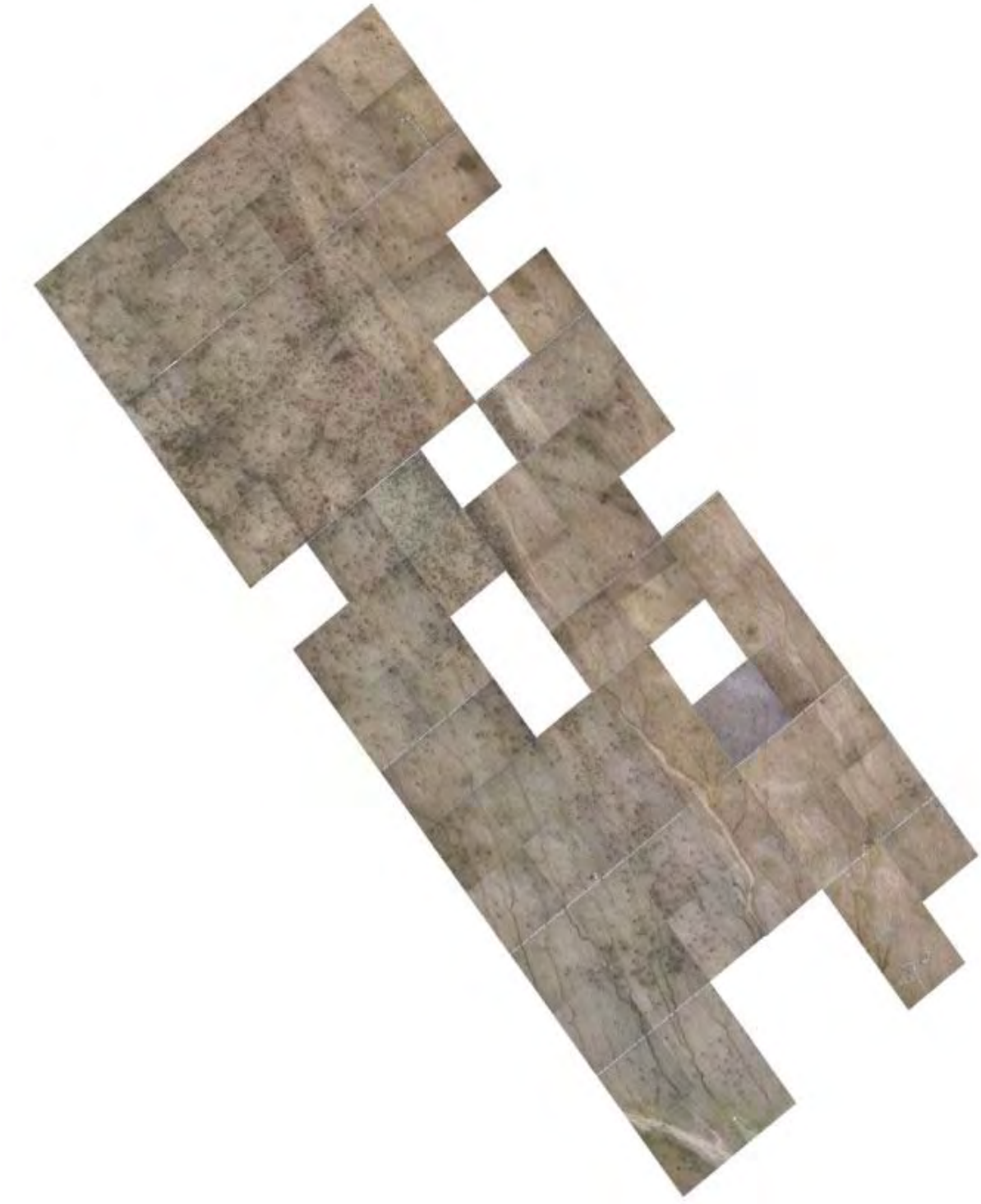

Fig. 11.8: Aerial photo of the artificial water catchment Chicken Creek July 10th 2008.

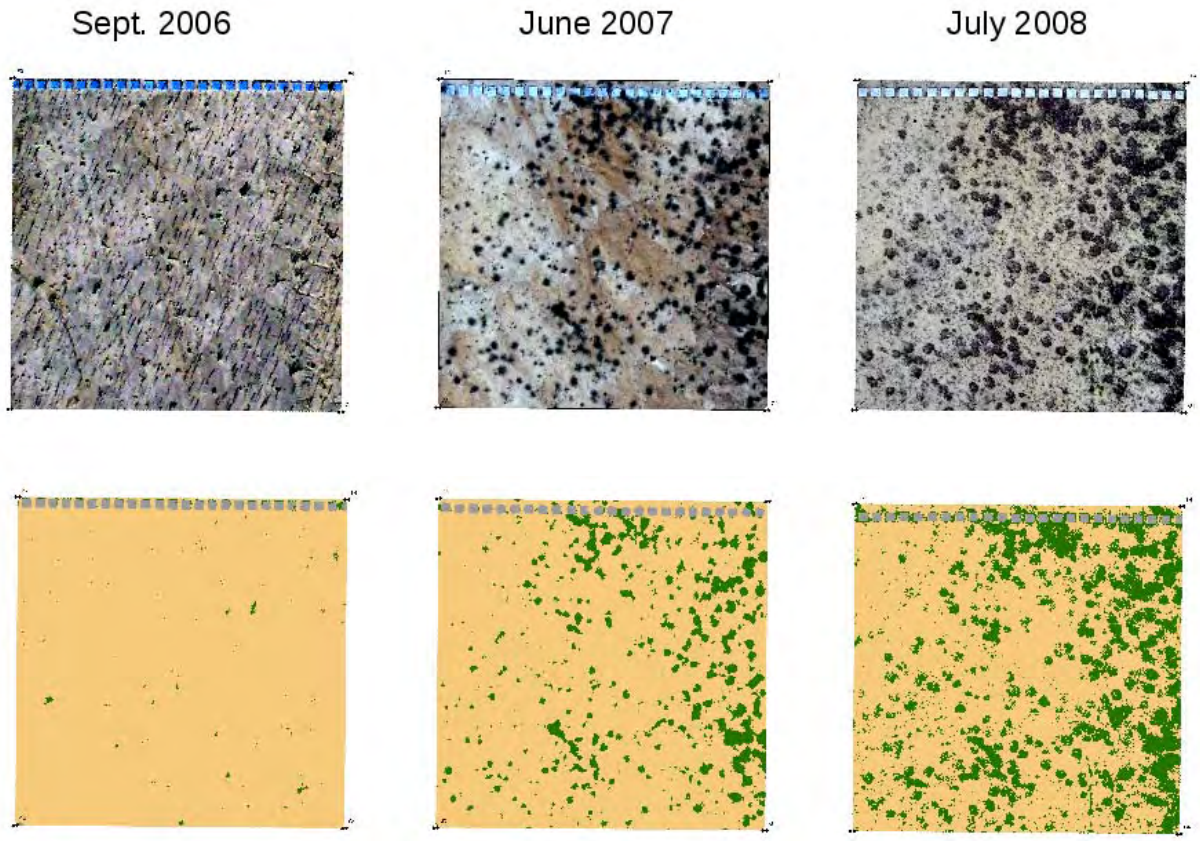

Fig. 11.9: An example of an annual survey between 2006 and 2008 of the vegetation cover in the artificial watershed using MultiSpec.

References

Purdue Research Foundation. 2009. MultiSpec©, A Freeware Multispectral Image Data Analysis System (Latest Release: 7-14-2009). http://cobweb.ecn.purdue.edu/~biehl/MultiSpec/, 30.October 2009.

Seiffert, T., Nenov, R., Mauerer, T., Gerwin, W. Veste, M. and Raab, T. (2009): Microdrone-based photogrammetry for water catchment monitoring. – In: Holzheu, S., Thies, B. (eds.): 39th Annual Conference GfÖ Dimensions of Ecology: From Global Change to Molecular Ecology, Bayreuther Forum Ökologie 115: 129-130.

Veste, M., Dominik, R., Dimitrov, M., Fischer, A., Gerwin, W. and Schaaf, W., 2008. Novel drone-based system for ecosystem monitoring – application, analysis and interpretation. Verhandlungen Gesellschaft für Ökologie 38: 820.

Acknowlegements

We thank Ralph Dominik and Marin Dimitrov for their help with the micro-drone systems.

Index of authors

Detlef Biemelt	Brandenburg University of Technology Cottbus, Chair of Hydrology and Water Resource Management, Konrad Wachsmann - Allee 6, 03046 Cottbus
Axel Christian	Senckenberg Museum of Natural History, Am Museum 1, 02826 Görlitz
Rainer Deneke	Department of Freshwater Conservation, Brandenburg University of Technology, Seestr. 45, 15526 Bad Saarow
Michael Elmer	Brandenburg University of Technology Cottbus, Chair of Soil Protection and Recultivation, Konrad-Wachsmann-Allee 6, 03046 Cottbus
Remo Ender	Department of Freshwater Conservation, Brandenburg University of Technology, Seestr. 45, 15526 Bad Saarow
Anton Fischer	Technische Universität München, Department of Ecology and Ecosystem Sciences, Emil-Ramann-Straße 2, 85354 Freising-Weihenstephan
Werner Gerwin	Brandenburg University of Technology Cottbus, Research Center Landscape Development and Mining Landscapes, Konrad-Wachsmann-Allee 6, 03046 Cottbus
Christiane Herzog	Leibniz-Institute of Freshwater Ecology and Inland Fisheries, Müggelseedamm 310, 12587 Berlin
Karin Hohberg	Senckenberg Museum of Natural History, Am Museum 1, 02826 Görlitz
Michael Hupfer	Leibniz-Institute of Freshwater Ecology and Inland Fisheries, Müggelseedamm 310, 12587 Berlin
Sylvia Jordan	Leibniz-Institute of Freshwater Ecology and Inland Fisheries, Müggelseedamm 310, 12587 Berlin
Andreas Kleeberg	Leibniz-Institute of Freshwater Ecology and Inland Fisheries, Müggelseedamm 310, 12587 Berlin

Dieter Lessmann	Department of Freshwater Conservation, Brandenburg University of Technology, Seestr. 45, 15526 Bad Saarow
Kai Mazur	Brandenburg University of Technology Cottbus, Chair of Hydrology and Water Resource Management, Konrad Wachsmann - Allee 6, 03046 Cottbus
Rossen Nenov	Brandenburg University of Technology Cottbus, Research Center Landscape Development and Mining Landscapes, Konrad-Wachsmann-Allee 6, 03046 Cottbus
Brigitte Nixdorf	Department of Freshwater Conservation, Brandenburg University of Technology, Seestr. 45, 15526 Bad Saarow
David Russell	Senckenberg Museum of Natural History, Am Museum 1, 02826 Görlitz
Wolfgang Schaaf	Brandenburg University of Technology Cottbus, Chair of Soil Protection and Recultivation, Konrad-Wachsmann-Allee 6, 03046 Cottbus
Hans-Jürgen Schulz	Senckenberg Museum of Natural History, Am Museum 1, 02826 Görlitz
Thomas Seiffert	Brandenburg University of Technology Cottbus, Research Center Landscape Development and Mining Landscapes, Konrad-Wachsmann-Allee 6, 03046 Cottbus
Maik Veste	Brandenburg University of Technology Cottbus, Research Center Landscape Development and Mining Landscapes, Konrad-Wachsmann-Allee 6, 03046 Cottbus
Manfred Wanner	Brandenburg University of Technology Cottbus, Chair of General Ecology, Siemens-Halske-Ring 8, 03046 Cottbus
Susanne Winter	Technische Universität München, Department of Ecology and Ecosystem Sciences, Emil-Ramann-Straße 2, 85354 Freising-Weihenstephan
Markus K. Zaplata	Technische Universität München, Department of Ecology and Ecosystem Sciences, Emil-Ramann-Straße 2, 85354 Freising-Weihenstephan